J Toxicol Pathol 2018; 31 (3 Suppl): 97S–214S

Nonproliferative and Proliferative Lesions of the Rat and Mouse Special Sense Organs (Ocular [eye and glands], Olfactory and Otic)

Meg Ferrell Ramos[1, a]* (Co-Chair), Julia Baker (Co-Chair)[2, a], Elke-Astrid Atzpodien[3, a], Ute Bach[4, a], Jacqueline Brassard[5, a], James Cartwright[6, a], Cynthia Farman[7, a], Cindy Fishman[8, a, b], Matt Jacobsen[6, a], Ursula Junker-Walker[9, d], Frieke Kuper[10, c], Maria Cecilia Rey Moreno[11, b], Susanne Rittinghausen[12, c], Ken Schafer[13, a, d], Kohji Tanaka[14, a], Leandro Teixeira[15, a], Katsuhiko Yoshizawa[16, a], Hui Zhang[17, a]

[a]*Member of eye subgroup*
[b]*Member of glands of the eye subgroup*
[c]*Member of olfactory subgroup*
[d]*Member of otic subgroup*
[1]*AbbVie, Inc., North Chicago, IL, USA*
[2]*Charles River Laboratories, Inc., Frederick, MD, USA*
[3]*F. Hoffman-La Roche Ltd., Basle, Switzerland*
[4]*Bayer AG, Wuppertal, Germany*
[5]*Tustin, CA, USA*
[6]*AstraZeneca, UK*
[7]*Farman Pathology, Reno, NV, USA*
[8]*GlaxoSmithKline, King of Prussia, PA, USA*
[9]*Novartis, Basel, Switzerland*
[10]*Retired; formerly The Netherlands Organization for Applied Scientific Research (TNO), Zeist, the Netherlands*
[11]*BASF SE, Ludwigshafen, Germany*
[12]*Fraunhofer Institute, Hannover, Germany*
[13]*Vet Path Services, Inc., Mason, OH, USA*
[14]*Nippon Boehringer Ingelheim, Japan*
[15]*University of Wisconsin-Madison, WI, USA*
[16]*Mukogawa Women's University, Hyogo, Osaka, Japan*
[17]*Lund, Sweden*

Introduction

The INHAND Project (International Harmonization of Nomenclature and Diagnostic Criteria for Lesions in Rats and Mice, www.toxpath.org/inhand.asp) is a joint initiative between the Societies of Toxicologic Pathology from Europe (ESTP), Great Britain (BSTP), Japan (JSTP) and North America (STP) to develop an internationally accepted nomenclature for nonproliferative and proliferative lesions in laboratory animals. The purpose of this publication is to provide a standardized nomenclature for classifying proliferative and nonproliferative lesions observed in the special sense organs (ocular, otic, and olfactory) of laboratory rodents. The standardized nomenclature presented in this document is also available electronically at the goRENI website (www.goreni.org).

This document covers the ocular, olfactory, and otic systems. The ocular system is subdivided into the eye, and the glands of the eye. The diagnostic criteria used for terms in this publication are generally those that can be seen with standard hematoxylin and eosin-stained (H&E) paraffin sections. Preferred terms for nonproliferative and proliferative lesions are presented for each tissue. Spontaneous and aging lesions, as appropriate, as well as lesions induced by exposure to test materials, are included. Although some diagnoses have synonyms provided, these terms may not be appropriate as histologic diagnoses in toxicity studies (i.e., coloboma and synechia). The nomenclature recommended here is generally descriptive rather than diagnostic.

*Address correspondence to: Meg Ferrell Ramos, DVM, PhD, AbbVie, Inc., 1 North Waukegan Rd, North Chicago, IL 60064, USA
e-mail: margaret.ramos@abbvie.com

I. Nonproliferative and Proliferative Lesions of the Rat and Mouse Eye

HISTOLOGICAL PROCESSING OF THE EYE

The eye and optic nerve are included on the core list of tissues recommended by the Society of Toxicologic Pathology for histologic examination in nonclinical repeat-dose toxicity and carcinogenicity studies.

The perfect eye section for a routine rodent toxicity study is a superior-inferior sagittal section, passing through the optic nerve head, with proper orientation and free of artifacts. Cornea should be free of clefts or folds, and corneal endothelial cells should not be vacuolated. Shattering or vacuolation of the lens should be avoided, and the lens should be correctly oriented in the globe, with the epithelium facing the cornea. Artifactual retinal separation or vacuolation is a common problem, and evaluation of photoreceptors demands sections no greater than 5 μm in thickness. Specialized ocular studies may require a different sectioning protocol, depending on the route of administration (systemic, topical intravitreal, sub-Tenon), the nature of the test article (aqueous solution, viscous depot, slow-release capsule, stem cells, subretinal device), or as a result of unusual ophthalmoscopic findings. Pathologists should be involved in determining the best protocol for a particular study.

The genesis of a good ocular section begins at necropsy. Rough handling of the eye at enucleation can induce retinal separation and optic nerve artifacts. The optic nerve should be transected at the level of the orbit to maximize the available nerve tissue. Extraocular tissues, including glands, should be trimmed off the globe prior to fixation to optimize the fixation of the retina and avoid separation; this also allows better visualization of the landmarks for subsequent trimming. Incision of the globe prior to fixation will compromise the architecture of the retina due to the reduced pressure inside the globe. Similarly, injection of fixative into the globe is not recommended, and is not necessary for rodent eyes. If orientation is critical, consider using tissue marking fluid or a suture to identify landmarks or the 12 o'clock position at time of collection, as landmarks are more difficult to see in a fixed globe. Left and right eyes should be clearly differentiated to allow correlation with clinical findings.

A variety of fixatives may be used. Perfusion fixation frequently results in artifactual spaces in the retina, and immersion fixation is probably a better option for rodent eyes. Ensure that the eye is immersed in a sufficiently large volume of fixative (at least 10x the volume of the eye) as rapidly as possible to prevent autolytic change in the retina. Submersion in 10% formalin is frequently used in toxicology studies, but retinal preservation is often compromised.

Davidson's solution gives better retinal fixation than 10% formalin, but prolonged exposure will result in artifacts associated with hardening of the lens, and clefting and pseudoedematous changes in the cornea. Rodent eyes should remain in Davidson's solution for 24 hours (no more than 48 hours). For best results, eyes should be transferred directly to ethanol on the tissue processor; consider washing and transferring to ethanol if a short delay (up to 10 days) is anticipated, but longer term archival of eyes warrants transfer to 10% formalin. Davidson's fixation is associated with artifactual vacuolation in the optic nerve due to the ethanol content, and thus a small section should be collected for fixation in 10% formalin for cross-section examination. Davidson's fixation is compatible with immunohistochemistry techniques for many antigens, and morphology is superior to that obtained with formalin fixation, but it is not suitable for electron microscopy evaluation.

Fixation with solutions containing glutaraldehyde (e.g. Karnovsky's solution) is suitable if electron microscopy is planned (Ramos et al. 2011). To improve results, submerge the globe in the fixative for 2 hours to allow initial firming of the globe and then cut a small window in one side of the globe before continuing submersion for another 2 days. This fixative tends to cause distortion of the globe due to osmolality effects, but generally gives good corneal, lens and retinal morphology. Possible artifacts include fissuring of the lens, clefting of the cornea, and vacuolation of photoreceptors.

Trimming of globes requires a very sharp blade, and should be performed with a single cut; a sawing action will result in retinal separation. Mouse eyes, or juvenile rat eyes, are best processed intact, but it is helpful to mark the globe with indelible tissue dye to allow orientation at embedding. Adult rat eyes may be oriented by making an off-center longitudinal cut, perpendicular to the long posterior ciliary artery, to remove a small (1–2 mm) calotte from one side of the globe, and then placing the eye, cut surface down, in the cassette.

If a calotte was removed prior to processing, it may be necessary to create a small window in the other side of the globe when embedding to prevent the entrapment of air bubbles. Care should also be taken to ensure that the lens is pushed firmly to the base of the cassette at embedding. Better results may be achieved by using a low-melting point paraffin with added polymers.

Sectioning artifacts may be associated with excessive time on the water bath, or with a water bath that is too hot. Adhesion may be improved by using slides that have a positive charge, slides coated with poly-L-lysine, or by adding gelatin to the water bath. Lenses may need to be softened by applying gauze soaked in acetic acid or liquid phenol to the surface of the block for some minutes prior to sectioning.

NORMAL ANATOMY AND PHYSIOLOGY OF THE EYE

Eyelids

The eyelids consist of skeletal muscle and connective tissue stroma (tarsal plate) covered by haired skin on the external surface and conjunctiva on the bulbar surface. On the eyelid margin are specialized hairs (eyelashes) and associated sebaceous glands (glands of Zeis). Additionally, Meibomian glands, specialized sebaceous glands that contribute lipid components to the tear film, have secretion pores along the inner margin of the eyelid. The comparative histology of the Meibomian gland

has been described in detail (Jester et al. 1981). The third eyelid is located in the nasal aspect of the palpebral fissure and consists of fibrous stroma supported by hyaline cartilage covered by conjunctiva (Yoshitomi and Boorman 1990). The palpebral conjunctiva covers the eyelids and the bulbar conjunctiva covers the sclera of the eye. The conjunctiva consists of a simple cuboidal epithelium with goblet cells overlying vascularized connective tissue stroma. Evaluation of the eyelid and conjunctiva macroscopically and microscopically are important components of ocular irritation/toxicity studies for topical agents.

Anterior Segment

Cornea

The tough fibrous tunic of the eye is composed of a posterior, opaque sclera and an anterior, transparent cornea. The cornea provides structural integrity for the anterior portion of the eye, serves as a primary light transmission and refractive medium, and acts as a barrier to infection. The cornea is spherical, and in most animal species, the vertical dimension is shorter than the horizontal. Transparency is attributable to salient features that include avascularity, lack of epithelial pigmentation, molecular arrangement of the stroma, and the presence of crystalline proteins in the epithelium and stromal keratocytes with properties that reduce light scatter.

The circumferential boundary between the cornea and sclera is known as the limbus. The limbus contains populations of fibroblasts, monocytes and Langerhans cells, and a reservoir of stem cells that replenish the corneal epithelium during cell turnover, or following injury. The stroma of the limbus is loose and contains a highly vascularized episcleral arterial circle that originates from the superficial branch of the anterior ciliary artery (Ramos, Attar et al. 2017). The metabolic needs of the peripheral cornea are met by arterioles from this source, which form an arcade, and by diffusion of nutrients from the aqueous humor. Capillaries may extend as far anteriorly as Bowman's membrane (see below) before looping back, or less commonly, terminate abruptly within the peripheral stroma. The avascularity of the cornea is maintained through the activity of cytokines that inhibit angiogenesis such as endostatin and thrombospondins 1 and 2, VEGFR 1 and 3 inhibitors, and tissue inhibitors of metaloproteinases, which have been identified in the cornea and are believed to prevent the encroachment of vessels beyond the limbus (Cursiefen et al. 2006).

As with most other species, the rodent cornea is composed of 5 layers (anterior to posterior): non-keratinized squamous epithelium, epithelial basement membrane, corneal stroma, Descemet's membrane, and endothelium. The rodent cornea is thicker in the central portion, and thinner in the periphery (Henriksson et al. 2009). Conflicting data regarding corneal measurements reported in the literature has resulted from use of differing techniques (*in-vivo* versus histological methods) and the rodent strain used to capture the data. Measurement of central cornea thickness (CCT) using optical low coherence reflectometer of the mouse (Balb/c) and rat (Wistar) were approximately 106 and 159 µm, respectively (Schulz et al. 2003). However, by histology, CCT for the mouse has been reported to range from ~122–160 µm (Henriksson et al. 2009; Rodriguez-Ramos Fernandez and Dubielzig 2013), and ~250 µm for the hooded rat (Massof and Chang 1972).

The corneal epithelium functions to prevent fluid loss and provide protection. In rodents, the corneal epithelium makes up approximately 30% (in contrast to other species, including humans, where the epithelium is approximately 10%) of the total corneal thickness (Henriksson et al. 2009). The epithelium is arranged in three distinct layers: superficial layer of flattened non-keratinized squamous cells; middle layer of polyhedral wing cells; and basal cells. The epithelium of the rodent cornea undergoes post-natal development and cell differentiation, with 1-2 cell layers present at birth, to 4-5 cell layers at eyelid opening, to 6-7 layers in the adult (Chung et al. 1992), although some sources put the upper limits at the central cornea closer to thirteen layers (Henriksson et al. 2009). Epithelial cells appear to derive from the basal cells of the entire cornea during early development (Chung et al. 1992; Zieske 2004). Following maturation stem cells are localized to the limbus similar to other species and are the source of epithelial cell replenishment during cell turnover, which is continuous, or recruitment following corneal injury. The integrity and function of the cornea are dependent on the division of epithelial stem cells, and the amplification and centripetal migration of the daughter cells into the cornea to populate the basal epithelium (Secker and Daniels 2009). As the cells differentiate they move horizontally towards the surface, becoming first, polyhedral suprabasal wing cells, and second, flat squamous cells at the surface, where they eventually (induced by blinking) desquamate into the tear film. The superficial squamous cells have microvilli that function to increase the cell surface and promote tear adherence (Secker and Daniels 2009).

The basal cells are anchored to a thin basal lamina, or basement membrane, by hemidesmosomes (Smith, Sundberg, and John 2002a; Smith, Sundberg, and John 2002b). Bowman's layer, an acellular, tightly interwoven meshwork of collagen fibers located subjacent to the basal lamina, does occur in rodents, but is rudimentary, and although discernable with electron microscopy, is not so using light microscopy. An amorphous membrane containing fine nerve plexi immediately adjacent to the basal epithelium has been reported using confocal microscopy (Kowalczuk et al. 2013). Unmyelinated nerve fibers occur throughout the cornea stoma of the rat (Henriksson et al. 2009).

Transparency of the cornea is primarily dependent on the arrangement of the stroma, an extracellular matrix of collagen fibrils (predominantly types I and V). The stromal matrix contains sulfated glycosaminoglycans that have a primary role in defining the hydrophilicity properties of the cornea as well as maintaining the spatial organization of the collagen fibrils - these are arranged into orthogonal lamellae which have the effect of minimizing light scatter and creating transparency (Quantock and Young 2008). The source of the stromal extracellular matrix (ECM) is derived from the keratocytes residing between the fibrils; these are modified fibroblasts with numerous interconnecting lamellapodia arranged parallel to the collagen bundles in a manner that similarly facilitates light

transmission (Hassell and Birk 2010). Keratocytes contain crystalline proteins that have properties that also reduce light scattering (Quantock and Young 2008). During embryonic development, ECM is produced at a higher rate in the central portion of the corneal stroma relative to the periphery, contributing to the curvature of the cornea. The curvature is maintained by an annulus of collagen fibers that circumferentially align the limbus. The refracting power of the cornea is dependent on the curvature of the radius of the exterior surface, which is shaped to focus an image on the visual axis.

The posterior aspect of the stroma is bordered by Descemet's membrane, a specialized basal lamina that is secreted by the corneal endothelium. Descemet's membrane is comprised of a highly ordered hexagonal array of collagen (type IV, VIII, XVIII), laminin, and fibronectin (Smith, Sundberg, and John 2002a; Jun et al. 2006). The anterior side adjacent to the stroma is present at birth; however, the endothelial cells continue to secrete the lamina throughout life such that the membrane becomes thicker with age. Descemet's membrane gradually terminates just anterior to the trabecular meshwork, although in some mice strains there is a focal thickening that is suggestive of Schwalbe's line (Smith, Sundberg, and John 2002a; Smith, Sundberg, and John 2002b). The endothelial cells (posterior epithelium) form a monolayer layer of cells that line the posterior aspect of the cornea. Cornea endothelial cells have incomplete tight junctions between cells that are permissive for movement of nutrients and other molecules from the aqueous humor into the avascular stroma. Optical clarity is achieved through active transport of fluid and ions out of the cornea to maintain a relatively dehydrated state (stromal deturgescence) through pumps and pinocytotic vesicles, and collectively, the system is referred to as a pump-leak mechanism (Bourne 2003). Proliferation of the cornea endothelial cells continues until the time of eyelid opening, whereupon they become quiescent (Zieske 2004). In the rat and rabbit, it has been demonstrated that there is a reserve of endothelial cells in the peripheral cornea/limbus that are capable of replenishing the cornea endothelium post-injury (Bredow et al. 2014; Choi et al. 2015).

Uvea & Iridocorneal Angle

The highly vascularized ocular tissues are collectively referred to as the uvea. The posterior uvea consists of the choroid, and the anterior uvea, the iris and ciliary body. The choroid and ciliary body attach to the internal surface of the sclera, while the iris arises from the anterior portion of the ciliary body. The iris extends centrally to form a circumferential diaphragm in front of the lens and modulates light penetrance by contraction of myoepithelial cells (sympathetic innervation) and smooth muscle fibers (parasympathetic innervation) that permit dilation, and constriction, respectively. Anterior ocular immune deviation ("privilege") is established though the blood-ocular barrier (BOB), which consists of the blood-aqueous barrier and blood-retinal barrier. The blood-aqueous barrier consists of tight junctions between nonpigmented epithelium in the ciliary processes, the endothelial cells of the iris vasculature, and the inner wall endothelium of the angular aqueous plexus in non-primate mammals (akin to Schlemm's canal in primates) (Coca-Prados 2014). The blood-retinal barrier is composed of non-fenestrated capillaries of the retinal circulation (inner blood-retinal barrier) and tight-junctions between retinal (pigmented) epithelial cells (outer blood-retinal barrier) preventing passage of large molecules from the choriocapillaris into the retina.

Iris

The iris originates from the anterior portion of the ciliary body. It separates the anterior from the posterior ocular chamber, allowing for communication via the pupil. The iris is divided into the anterior border layer, the stroma and sphincter inner layer, and the posterior pigmented epithelial layers which are continuous with the epithelium of the ciliary body (Ramos, Attar et al. 2017; Samuelson 2007). The anterior border is formed by a discontinuous band of fibroblasts and melanocytes. The stroma is loosely arranged and composed of collagen fibrils, fibroblasts, smooth muscle cells, and a network of nerve fibers and blood vessels. The smooth muscles of the iris control pupil diameter. The sphincter muscle is composed of bundles of smooth muscle that encircle the pupil and is under parasympathetic innervation associated with constriction of the pupil. The dilator muscle is composed of myoepithelial cells that extend radially from the iris sphincter muscle to the iris periphery in the posterior iris stroma in a spoke-like arrangement; it is under sympathetic innervation associated with pupil dilation. Pupil size and shape vary between species and state of contraction. The pupil is generally round in the rodent. The major arterial circle of the iris is furnished by anastomoses of the anterior ciliary arteries and the long posterior arteries (Riordan-Eva 2011). Stromal blood vessels are relatively thick, and allow for constant blood flow regardless of pupil constriction or dilation (Barskey 2006). Resident macrophages and dendritic cells grant immune privilege to ocular tissues of the anterior segment by modulating inflammatory reactions and establishing a deviated immune response (anterior chamber-associated immune deviation; ACAID), rather than stimulating a T-cell response that elicits delayed hypersensitivity or compliment-fixing antibodies. Deviated T-cell responses, the blood-aqueous-barrier, and immunosuppressive factors present in the aqueous collectively promote a microenvironment that spares the visual axis by minimizing inflammation in the anterior chamber that would otherwise cause potential damage to delicate ocular structures (Streilein 2003; Taylor 2009; Taylor and Kaplan 2010). The color of the iris is attributed to type and density of melanin pigment, degree of vascularization, and backscatter of incident light from stromal collagen fibers. The latter accounts for the bluish pink iris color of albino rodent species (Wilkerson et al. 1996). Pigmentation of the iris has a protective role to the retina by limiting light transmission through the pupil.

Ciliary Body

The ciliary body forms the middle component of the vascular layer of the eye (uvea), and is located between the choroid

and the iris. It is composed of smooth muscle, stroma, blood vessels, and epithelium. The external surface consists of the inner and outer leaves of the ciliary muscle, creating a cleft in which the ciliioscleral sinus resides. Ciliary processes extend from the inner surface and are covered by two layers of epithelium that are in apposition: an outer layer of low, cuboidal pigmented epithelium (non-pigmented in albino species) that is adjacent to the stroma and continuous with the RPE; and an inner layer of non-pigmented columnar epithelium that is continuous with the retina. The ciliary processes are the site of aqueous humor production, derived from the epithelium and vasculature of the ciliary body. Aqueous humor is secreted into the posterior ocular chamber and circulates through the pupil into the anterior ocular chamber. Aqueous humor exits the eye through the iridocorneal angle (ICA) at the anterior base of the iris.

The epithelium of the ciliary processes also secretes hyaluronic acid, the main constituent of the vitreous (Teixeira and Dubielzig 2013a; Teixeira and Dubielzig 2013b). The ciliary body and ciliary processes surround the coronal equator of the lens and provide a base on which ciliary (lenticular) zonules are attached. The relative tone of smooth muscle within the ciliary body controls the visual accommodation of the lens, and visual acuity is reflected in the relative amount of smooth muscle present in the ciliary body. Thus rodents, which have scant ciliary smooth muscle, have poor visual acuity.

ICA / Trabecular Meshwork

The iridocorneal angle (ICA) is formed by the base of the iris and the corneal-scleral tunic and has a critical role in maintenance of intraocular pressure (IOP), functioning as the outflow apparatus for aqueous humor. The ICA is located at the periphery of the anterior chamber (limbus), extending into the anterior ciliary body to form a recess called the ciliioscleral sinus (known as the Spaces of Fontana in primates). Broad, pectinate ligaments (iris processes or pillars) span the sinus, extending from the corneoscleral junction to the root of the iris. The trabecular meshwork (TM) is located within the sinus, posterior to the pectinate ligaments and is composed of crisscrossing cords or sheets of collagen and elastin that appear to be anterior tendinous extensions of ciliary body musculature. The TM surface is covered by a unique population of endothelial-like trabecular cells that are continuous with the endothelium of the cornea and the downstream collecting duct (Samuelson 2007).

The TM is subdivided into three layers (in order of aqueous flow): uveoscleral, or uveal meshwork (USM); corneoscleral meshwork (CSM); and juxtacanalicular, or cribriform meshwork (JCM). The corresponding intratrabecular spaces become progressively smaller, resulting in increased aqueous outflow resistance as aqueous flows through the TM, and out the JCM. Aqueous humor exits the JCM and flows into collecting ducts (Schlemm's canal; rodents are similar to humans) (Lei et al. 2011; Morrison et al. 1995), through interscleral channels, exiting the eye though episcleral and conjunctival veins. Aqueous physiology is similar across species, but dynamics may vary due to anatomical differences.

Structural differences in the ICA, ciliary body, and processes across mammalian species are related to ocular size, and the role and limitations of visual (lens) accommodation. Laboratory rodents are nocturnal mammals with relatively large eyes, and have a small ciliary body with scant smooth muscle and thus they have limited lens accommodation. The inner leaf of the ciliary body (also called the base-plate) is fibrous, and extends from the root of the iris to the ora ciliaris retina. The outer leaf, composed of smooth muscle, presses against the sclera and extends from the corneoscleral junction to the ora ciliaris retina. The sinus contains 1-2 rows of short, fine pectinate ligaments, and 2-3 layers of trabeculae, which are aligned parallel to the angle of the sinus. The ciliary processes are prominent and more numerous in rodents, a characteristic of animals with larger anterior chambers compared to other species. The blood supply to the ciliary body is derived from the two long posterior ciliary arteries (Riordan-Eva 2011). Capillaries within the ciliary body are concentrically organized. In rodents, they are less developed relative to other species that have more robust aqueous humor production (Ramos, Attar et al. 2017).

Choroid

The choroid is the layer of blood vessels and connective tissue that resides between the sclera and retina. The choroid originates from the short posterior arteries (Riordan-Eva 2011). The choroid supplies the metabolic needs of the retina, primarily through the choriocapillaris, an extensive interconnected capillary network posterior to Bruch's membrane. Bruch's membrane is a five-layered structure composed of a middle layer of elastin, bounded by a layer of collagen on either side that is juxtaposed between the basement membranes of the RPE and the choriocapillaris. Bruch's membrane selectively filters the passage of macromolecules between the retina and choriocapillaris. The capillaries have a fenestrated endothelium through which macromolecules leak into the extracellular space of the choroid. The external choroid is comprised predominantly of a venous plexus. Mid-sized anastomosing vessels and melanocytes (pigmented macrophages) reside within a pigmented reticular connective tissue mesh located between the venous plexus and the choriocapillaris; this tissue has a role in absorption of excess radiation (Ramos, Attar et al. 2017).

Lens

The vertebrate lens is a crystalline, polarized spherical structure located in the posterior chamber immediately anterior to the vitreous. The lens is suspended posterior to the iris by the ciliary zonule, a circumferential suspensory ligament composed of an elaborate system of fibers. In the rodent, these fibers adhere to the lens capsule, connecting the lens to the ciliary body (Shi et al. 2013a). The lens shares a role with the cornea for light refraction and visual acuity. The ciliary zonule transmits forces resulting from contraction or relaxation of the muscles within the ciliary body that allow for visual accommodation depending on the distance of the object. The rodent lens is round (rather than biconvex as occurs in primates, dogs, and

rabbits) and occupies approximately 75% of the ocular space (Ramos, Attar et al. 2017). The ciliary body is rudimentary in rodents, allowing for limited contraction and lens accommodation.

The lens is composed of two populations of cells. Lens epithelial cells form a monolayer sheath on the anterior surface, and secrete an extracellular protein matrix forming a capsule that surrounds the cellular elements. Posterior lens fibers are elongated, transparent, fully differentiated cells that derive from progenitor epithelial cells. Cell proliferation is restricted to progenitor epithelial cells located in the germinative layer above the lens equator (nuclear bow). Under the influence of fibroblast growth factors, progeny cells migrate, or shift posterior to the equator, where they differentiate into fiber cells. As the cells differentiate, they undergo bi-directional elongation and produce massive quantities of crystalline proteins that are arranged in complex matrices along thin filaments that compose the cytoskeleton of the fiber cell (Zampighi et al. 2011). Crytallines have a critical role in maintaining lens transparency and refractive properties. Injury to the lens may result in the formation of insoluble aggregates of crystallines, producing opacities (correlating to ophthalmically observable cataracts) that obstruct light transmission and obscure vision. As elongation progresses, the fibers become convex, and the apical tips migrate towards the anterior pole. The lens increases in size and weight as more fibers are successively incorporated into layers to form the lens mass. Older fibers (primary fibers) form the embryonic nucleus of the lens while the newer (secondary) fibers form the outer layers. Lens fibers subsequently undergo organelle degradation including nuclear loss (Dawes et al. 2014; Song et al. 2014).

Posterior Segment

Vitreous Body

The vitreous is a translucent gel-like extracellular matrix that occupies the posterior compartment of the eye. More than 95% of the vitreous gel weight is water, while the remaining balance is comprised of the structural components of collagen and proteoglycans (primarily hyaluronan, HA) (Crafoord et al. 2014). There are species and age-related differences in the relative composition of the structural components. Except for collagen and proteoglycans, the composition of the vitreous is similar to aqueous humor, and similarly is produced by the ciliary processes (Teixeira and Dubielzig 2013a), although other ocular cells (hyalocytes, Müller cells, cells of the hyaloid vessels) have been ascribed a role (Kingston et. al., 2014). Most of the soluble protein present in the vitreous is derived from plasma, and albumin and immunoglobulins represent ~80% of the protein content of the vitreous (Bishop 2014). Studies utilizing fixation and dye injection demonstrate similarity in vitreous structure between human, non-human primate, and rabbit, and likely other species (Los 2008; Worst and Los 1992). Therefore, a generalized presentation of the vitreous is provided and pertains to all species.

Vitreous collagen is arranged in fibrils with a central core of types V/XI, surrounded by type II (the predominant collagen present), all overlaid by type IX (Bishop 2014). Chondroitin sulfate chains of type IX collagen form bridges that interconnect adjacent fibrils to form sheaths, while simultaneously aid in the prevention of aggregation. Arrays of hydrophilic hyaluronan and other proteoglycans (chondroitin sulfate) are interspersed between the collagen fibrils, and appear to stabilize the fibril scaffold and control volume of the vitreous gel (Crafoord et al. 2014; Sebag 1989). The collagen fibers of the vitreous are continuous with the footplates of the Müller cells, which are thought to be a primary source of vitreous collagen (Kingston et. al., 2014).The collagen content is highest where the vitreous is a gel, and the relative proportion of gel to liquid vitreous varies among species.

Important functions for the vitreous include:

- Providing an optically clear medium through which light may pass essentially unaltered. The maintenance of the spatial configuration between fibrils by the remaining macromolecules imparts this critical function.
- Maintaining the shape of the vitreous chamber and posterior cavity, and overall shape of the ocular globe.
- Maintaining the normal positions of the lens and the retina.

Differential distribution of collagen and proteoglycans results in two basic zones (cortical and medullary) with variable densities within the vitreous. The cortical vitreous occupies the periphery of the vitreous and encases the core (medullary vitreous). The cortical vitreous is relatively more condensed and fibrillar compared to the medullary vitreous, and has the appearance of a smooth clear membrane due to the lamellar distribution of collagen fibrils and associated highly polymerized proteoglycans (primarily chondroitin sulfate). Although the cortical vitreous represents only 2% of the total vitreous volume, it is the metabolic center of the vitreous body, because it contains the hyalocytes (detailed below), which make up 90% of the cell population in the cortical vitreous; fibrocytes and glial cells make up the remaining 10%. The vitreous cortex extends anteriorly from the vitreous base to form the anterior vitreous cortex and posteriorly to form the posterior vitreous cortex. The vitreous body interfaces with a number of ocular structures through the vitreous cortex. The anterior vitreous cortex forms the posterior limits of the posterior chamber and functions in the physiologic communication between the vitreous cavity and the aqueous humor. The anterior surface of the vitreous body extends anterior and medially from the pars plana at the ora ciliaris to contact the lens posterior to the lens equator. Thus, the anterior vitreous cortex is in contact with the ciliary processes and the lens zonules, as well as the posterior lens capsule. The vitreous attaches to the lens capsule in a ring-like manner, forming the ligament of Wieger (Sebag 1992). Posterior to the ora ciliaris, bundles of vitreous fibrils attach to the internal limiting laminae (ILL) (Balazs et al. 1964). Cords of vitreous collagen insert into gaps between the neuroglia. The cortical vitreous is most firmly attached to the ILL in the area of the optic disc, the macula (in primates), and to retinal blood vessels. Retinal pathology such as neovascularization or vascular malformations occurs in the areas of

vitreous attachment to the retina. Separation of the vitreous may transmit traction to these attachments, leading to vitreous hemorrhage or retinal tears. Persistent vitreous traction on retinal tears is an important factor in the development of a retinal detachment.

The bulk of the vitreous is formed by the core, or medullary vitreous. It is essentially a cell-free mixture of collagens and hyaluronic acid (HA) existing either in a gel or a liquid state depending on the age, refraction, and condition of the eye. The exclusion of other cells and large particles from the vitreous is important for maintaining transparency. Within the medullary vitreous, the collagen fibrils generally course in an anterior posterior direction. Anteriorly, these fibrils blend with those of the basal vitreous and posteriorly they insert into the vitreous cortex.

The vitreous has, as a whole, been shown to be variable in its consistency at different ages due to differences in the proportions of gel to liquid vitreous that occur. It is generally accepted that vitreous collagen turnover is slow and perhaps nonexistent, and that the vitreous body liquefies with age. Aging and liquification is associated with loss of type IX collagen and chondroitin sulfate chains (Bishop 2014). However in many animals, including rodents, the vitreous remains in a predominantly gel state throughout life (Denlinger and Balaz 2014). Average vitreous volumes are as follows, in decreasing order: human, 4.5 mL; dog, 2.9 mL; cynomolgus macaque, 2.2 mL; rabbit, 1.6 mL, rat 0.03 mL (30 μL); mouse 0.01 mL (10 μL) (Ramos, Attar et al. 2017; Atsumi et al. 2013; Remtulla and Hallett 1985; Sha and Kwong 2006). In the adult eye, the vitreous volume is relatively fixed and permanent.

Under normal physiological conditions, a small number of hyalocytes reside in the cortical vitreous, mainly in the posterior aspect abutting the inner surface of the retina (Halfter et al. 2014). Hyalocytes are phagocytic cells that vary from oval to spindle or stellate shape, possess lysosomes, mitochondria, ribosomes, and micro-pinocytotic vesicles, and have numerous microvilli on their surface. Current literature suggests that hyalocytes play a crucial role in the formation and contraction of proliferative membranes (vitreous fibroplasia; vitreous membranes) in response to growth factors overexpressed in diseased eyes such as proliferative diabetic retinopathy (PDR) and proliferative vitreoretinopathy (PVR) (Kita et al. 2014).

Hyalocytes express cell surface antigens characteristic of monocyte/macrophage leukocyte lineage including CD45 (leukocyte common antigen), CD64 (Fc receptor I), CD11a (leukocyte-function antigen-1), and histocompatibility complex (MHC) class II antigens (Kita et al. 2014).

Hyalocytes also express F4/80, a marker common to tissue macrophages. Anterior cavity-associated immune deviation (ACAID) has been attributed to F4/80 antigen presenting cells residing in the iris and ciliary body (Masli and Vega 2011). Experimental evidence suggests that hyalocytes have a similar role in the vitreous, conferring immune deviation and modulating inflammation that occurs with delayed hypersensitivity to antigens (Kita et al. 2014; Sakamoto and Ishibashi 2011). In non-inflamed eyes, this has been coined vitreous cavity-associated immune deviation (VCAID). Immune privilege has been shown to be lost in mice with inflamed eyes, and in knockout mice deficient in natural killer T cells, a critical component of immune deviation (Sonoda et al. 2005).

Retina (Sensory Retina)

The eye is a specialized extension of the central nervous system designed for photoreception, and the conversion of light energy into graded electrical signals allowing for visual perception. The retina is a highly organized multilayered complex of photosensitive neurons and integrating and transmission neurons that initially process the visual stimulus (Rosolen et al. 2008). The retina lies internal to the retinal pigment epithelium (RPE) in the posterior compartment of the eye, extending from the optic nerve head and terminating posterior to the ciliary body. The pars plana is a continuation of non-sensory RPE, and lies anterior to the ora ciliaris as a single (most species) layer to merge with the lining epithelium of the ciliary body and apparatus. In the rodent, the retina takes up about 175º of circumference of the globe (Hebel and Stromberg 1976).

The rodent retina is very similar to that of human and of many vertebrate retinae. It is structurally divided into nine distinct layers (adapted from Ramos et al. 2011).

Photoreceptor Segments

The photoreceptors are divided into cones and rods. The nuclei of the photoreceptors reside in the outer nuclear layer (ONL) with their dendrites facing the RPE, forming the photoreceptor inner segment (PIS) and outer segments (POS). The inner segments contain large numbers of mitochondria and golgi complexes, while the outer segments is composed of stacked membranous discs containing the photosensitive pigments used in the visual cycle (rhodopsin in rods, and opsins in cones). The outer segments are ensheathed by the RPE apical processes, which facilitates phagocytosis by RPE as discs are shed continuously.

Although rods predominate in all species, the respective numbers of cones and rods and the spatial arrangement within the retina have considerable species variation.

Most animals have a region in the retina with a higher concentration of cones for increased visual acuity that is often, but not always, located at the temporal horizontal retinal. The region of cone concentration is usually referred to as the *area centralis* or visual streak, depending on its shape. In human, non-human primates and in some birds, the cone- enriched area is near the center of the retina and called the macula from its pigmented appearance. At its center is the fovea, a cone-dominated avascular region of maximal visual acuity. The rodent does not have a specialized region for visual acuity and has a much lower proportion of cones in its retina (Zeiss 2010). Diurnal rodents have a relatively high concentration of cones (30–40%), but cones are sparse in nocturnal rodents (Bobu et al. 2008; Saïdi et al. 2011). Rodents may have blue, blue/green, or green/red hybrid cones with some variable regional distribution in different species (Peichl 2005). Some mice have a preponderance of blue cones in the ventral retina, but no spe-

cialized areas such as a macula, fovea, area centralis, or visual streak is present.

External Limiting Membrane

The external limiting membrane is a dense junctional zone between Müller cells and photoreceptors. Müller cells are the primary support glial cell of the retina with processes that extend between the external and internal limiting membranes.

Outer Nuclear Layer (ONL)

The perikaryon and nucleus of the photoreceptor cell reside in the outer nuclear layer. The nuclei of rod cells are distributed throughout the layer, while nuclei of the cones form a row immediately inner to the external limiting membrane. Axons radiate inward to form synapses in the outer plexiform layer with the dendrites of second order neurons.

Outer Plexiform Layer (OPL)

The outer plexiform layer contains the synapses between the axon terminals of the photoreceptor cells and bipolar cell dendrites, which may have synaptic relationships with multiple receptors. Bipolar cells transfer visual signals to ganglion cells through synapses formed in the inner plexiform layer, while horizontal cells form connections between groups of rods and cones through lateral synapses.

Inner Nuclear Layer (INL)

The nuclei of second order neurons (bipolar cells, horizontal cells, amacrine cells, and interplexiform cells) and Müller cells (retinal glial cells) reside in the inner nuclear layer (Wässle and Boycott 1991; Masland 2001; Boycott and Wässle 1999). Bipolar cells have two processes that separately extend inward and outward connecting to ganglion cells and photoreceptors. Bipolar cells receive synaptic input from either rods (rod bipolars) or cones (cone bipolars) and transmit signals to ganglion cells. Horizontal cells are less frequent and often lie in the outer part of INL. These GABAergic inhibitory interneurons help integrate and regulate the input from multiple photoreceptor cells, optimizing vision under both bright and dim light conditions. Amacrine cells are numerous and often lie in the inner aspect of the INL. These are also inhibitory interneurons that interact with bipolar cells and ganglion cells to regulate neuronal impulses allowing one area of the retina to influence the activity of another. Müller cells are specialized glial cells that provide structural and functional support to the retina. These cells also maintain the stability of the retinal extracellular environment through the uptake of neurotransmitters, removal of cellular debris, and storage of glycogen for energy. Their nuclei are located in the INL and their long processes stretch radially across the thickness of the retina contacting the outer and inner limiting membranes. Müller cells have a close spatial relationship to pericytes of the retinal blood vessels and contribute to the maintenance of the blood-retinal barrier. Cells in the INL can be quantified and identified by special stains (Jeon et al. 1998).

Inner Plexiform Layer

Synapses between bipolar cell, amacrine, and interplexiform cells integrate and refine the signals from the photoreceptors in the inner plexiform layer (Protti et al. 2005). Axons from these cells in turn synapse with dendrites from the ganglion cells.

Ganglion Cell Layer

Ganglion cell nuclei and perikarya reside near the inner surface of the retina forming the ganglion cell layer. Ganglion cells are third order neurons that receive integrated visual signal from second order neurons. Axons from the ganglion cells form the optic nerve. Astrocytes and displaced amacrine cells may also be present in the ganglion cell layer.

Nerve Fiber Layer

Axons from the ganglion cells reside in the nerve fiber layer at the inner surface of the retina to converge at the optic disk, collectively exiting the eye as the optic nerve. The vision impulse traverses the optic nerve to reach the brain. Fibers are interspersed with astrocytes and other retinal glial cells.

Internal Limiting Membrane

The internal limiting membrane is a basement membrane secreted by the terminal footplates of the Müller cells. It separates the bases of the Müller cells (and retina) from the adherent vitreous body.

The thickness of the sensory retina decreases towards the periphery. Examples of the thickness of the various layers in the central retina of a rat are as follows: 28-30 μm (POS), 14-15 μm (PIS), 52 μm (ONL), 12 μm (OPL) and 28-29 μm (INL) (Hebel and Stromberg 1976).

Optic Nerve

The optic nerve (cranial nerve II) begins at the optic disc (optic papilla, optic nerve head) and courses from the posterior aspect of the globe to the brain. The optic nerve is composed primarily of the axons from ganglion cells (GC), which extend from the inner retina, traversing posteriorly and centripetally within the inner nerve fiber layer to converge into bundles at the optic disc forming the nerve. The central area of the optic disc is depressed (meniscus of Kuhnt), and is supported by a thickening of the retinal inner limiting membrane. Ganglion cell axons and axon bundles are surrounded by astrocytes at the surface of the optic disc. As the nerve passes through the scleral canal it crosses an open meshwork of collagenous beams or plates continuous with the sclera (termed the lamina cribrosa). This connective tissue meshwork also contains elastin and lends support for the nerve tissue. The lamina cribosa is composed of sparse connective tissue in both rats and mice, and is less distinct compared to other laboratory species (Greaves 2000; Rubin 1974). In most species including rodents, the axons are myelinated distal to the lamina cribrosa, so that on funduscopy, the optic disc is poorly demarcated from the surrounding tissue, and thus does not have a white appearance. In pigmented rats the optic disc may appear gray. Myelination

is provided by the cell processes of oligodendroglia, which form sheaths around the ganglion cell axons. Myelin in the optic nerve stains positive with Luxol fast blue stain (LFB).

The bulbar portion of the optic nerve (orbital optic nerve) crosses the space between the globe and the optic foramen (retrobulbar optic nerve), continuing to the optic canal to become the intracranial optic nerve between the optic foramen and the optic chiasm. The optic nerve between the globe and the optic chiasm of the rat is long (11.7-12.3 mm) with most (three-quarters) of the length contained within the intraorbital space (Hebel and Stromberg 1976). The optic nerve is an extension of the brain and is surrounded by dura, arachnoid, and pia maters, the later of which intimately surrounds and sends septae into the nerve. The optic nerve normally contains a small population of microglia, the phagocytes of the nervous system. The blood source of the optic nerve is derived from the internal ophthalmic artery, which lies inferior to the optic nerve. In rodents, the ophthalmic artery trifurcates posterior to the globe into the central retinal artery, and nasal and temporal posterior ciliary arteries, which supply the optic disc in addition to the retina and anterior uvea (Morrison et al. 1999). Four to eight arterioles and venules, equidistant from each other, extend and branch dichotomously from the center of the disc (Rubin 1974).

Retinal blood circulation

There are two vascular systems that supply the rodent retina, similar to human and many other species. The rodent retinal vasculature has a holangiotic pattern (fully vascularized). The ophthalmic artery enters the eye through the optic nerve and divides into several branches that service the entire retina. Retinal vessels form a multilayered network between the OPL and IPL to nourish the cells of the inner layers of the retina. The choroid blood system posterior to the retina supplies the outer retina (particularly the photoreceptors) through diffusion. Venous outflow from the eye is primarily via the vortex veins and the central retinal vein.

Retinal vascular structure in rodents is of interest, as it is used as a model for studying angiogenesis and microvascular pathology (Stahl et al. 2010). Microvascular lesions and angiogenesis can be visualized in living animals by using different imaging tools (Ruggeri et al. 2007). The retinal vasculature in rodents can also be isolated from the retina for analysis of capillary lesions (Agardh et al. 1997).

Retinal Pigment Epithelium

The retinal pigment epithelium (RPE) is a monolayer of non-sensory cuboidal cells that exteriorly line the retina. The RPE and retina originate from different portions of the optic vesicle during embryonic development and are attached by an extracellular matrix specialized to enable interaction between the RPE and POS. Retinal disease or toxicological insult may result in loss of adhesion between the retina and RPE, resulting in retinal detachment and formation of a subretinal space (Mecklenburg and Schraermeyer 2007). Pathological retinal detachment must be differentiated from artifact detachment, which is readily induced during processing of ocular tissues. RPE has critical roles in the support and viability of the photoreceptors with functions that include absorption of stray light, adhesion of the sensory retina to the choroid, secretion of growth factors, maintenance of the interphotoreceptor matrix (IPM), photoreceptor membrane turnover, and retinoid metabolism (Bok 1993; Marmor 1998). The apical membrane of RPE cells have numerous, long microvilli that interdigitate with the outer segments of the photoreceptors, allowing for efficient turnover of discs as they are shed from the photoreceptors. The accumulation of inclusion bodies (see lysosomal accumulations, below) containing photoreceptor outer segment membranes can be observed in aging RPE and are associated with RPE degeneration that can lead to blindness (Marmor 1998). The basal membrane of the RPE has large infoldings and an association with Bruch's membrane. Tight junctions between RPE form an important component of the blood retinal barrier (BRB) necessary for the maintenance of immune deviation in the posterior segment of the eye. They also prevent leakage of blood constituents from the choriocapillaris, and create osmotic pressure that assists in drawing fluid out of the retina through cellular mechanisms. Transcellular movement of glucose, retinol, amino acids and other nutrients into the retina, and that of metabolic wastes out, is regulated by receptors, ion channels and exchangers, and cytoplasmic organelles. These have a polar distribution in RPE, and the regulated movement of ions through the cell and IPM creates ionic gradients that maintain photoreceptor excitability and permits electrical transmission of light stimulus (Hughs 1998).

RPE have a critical role in the visual cycle of vitamin A, the generation of 11-cis-retinaldehyde, and subsequent formation of pigments essential for vision. RPE acquire vitamin A from the blood (choriocapillaris) via membrane receptors, from photoreceptors following light bleaching and subsequent release, or from shed photoreceptors. Subsequent processing through multiple enzymatic pathways converts vitamin A to analogues for storage and/or use in visual function (Palczewski 2014). Aging and photo-oxidative stress can disrupt these pathways and lead to visual impairment and retinal degeneration.

In most mammalian species, RPE contain melanosomes, elliptical-shaped granules of melanin pigment found in the apical and mid-portion cytoplasm of the cell. Melanin enhances object discrimination in bright light conditions by absorbing scattered light. In rodents, melanosomes tend to be rounder and fewer in number commensurate with the low-light conditions of their visual needs. Albino species have melanosomes, but lack melanin granules. Melanin tends to diminish and fuse with lipofuscin in RPE with aging. Some pharmacological agents, particularly substances with cationic properties (Boulton 1988) bind to melanin and induce pigmentary changes that may be observed on fundic examination. Melanin binding can unintentionally result in drug sequestration, prolonged drug exposure to sensitive ocular tissues, enhance free-radical injury, and can cause retinal toxicity through impaired RPE function. Age-related changes in melanin content, lipofuscin accumulation, and the formation of conjugates (melanolipofuscin) impairs light absorption, enhances oxidative stress, and

results in RPE degeneration.

RPE produce growth factors and cytokines that contribute to retinal homeostasis and an anti-inflammatory environment that can conversely have adverse roles in ocular disease. Cellular transdifferentiation, migration, and proliferation of RPE are associated with the production of sub-retinal fibroplasia (membranes) observed in macular degeneration, and may have a role in fibroplasia at the retinal surface (retinal or epiretinal fibroplasia) (Kita et al. 2014; Mehta et al. 2014; Zhao et al. 2013).

Sclera

The posterior compartment of the eye is ensheathed in a tough, outer spherical tunic composed of bundles of fibroelastic connective tissue arranged concentrically to the ocular surface. The sclera begins at the limbus, transitioning from regular corneal lamellae to irregular scleral lamellae that branch and interweave. The sclera merges with the surrounding dura mater posteriorly and is penetrated by the optic nerve at the posterior margins of the globe. The sclera has roles in protecting the eye from injury, maintaining ocular shape and IOP during movement of the eye, and in aiding visual acuity while reducing back-scatter from light. The sclera is covered by a fibroelastic membrane, the Tenon capsule, which forms a sleeve around the attachment of the ocular muscles to the sclera. The Tenon capsule fuses with the conjunctiva posterior to the limbus, and extends posterior to fuse with connective tissue surrounding the optic nerve. The sub-Tenon space is a site that can be potentially exploited in some species for drug administration. The rat does have a Tenon, however in the mouse it is poorly defined.

The sclera has a rich nerve supply but lacks a specific vascular bed, which renders the eye vulnerable to particularly painful or prolonged inflammation. Systemic connective tissue disease often has a scleral component. Inflammation occurring within the sclera may culminate in necrosis because of the sluggish removal of inflammatory debris and slow cell turnover (Ramos, Attar et al. 2017).

TERMINOLOGY AND DESCRIPTIONS

Nonproliferative Lesions of the Rat and Mouse Eye General Terms

Apoptosis (N) Eye

Species
Mouse; Rat.

Other Term(s) Used
None.

Pathogenesis/cell of origin
Cell origin varies with tissue type (see individual section).
Programmed cell death.

Diagnostic Features
- Cell shrinkage and convolution.
- Cytoplasmic condensation (hypereosinophilia).
- Chromatin condensation (pyknosis) and peripheralization in early apoptosis.
- Karyorrhexis with fragmentation of condensed chromatin.
- Intact cell membrane.
- Formation of blebs to produce apoptotic bodies.
- Cytoplasm retained in apoptotic bodies.
- Phagocytosis of apoptotic bodies by tissue macrophages or other adjacent cells.
- Lack of inflammation.

Special Techniques for Diagnostics
- Terminal TdT-mediated dUTP-Nick-End Labelling (TUNEL) assay, staining for caspases or ultrastructural evaluation can be used to specify apoptosis.

Differential Diagnoses
Necrosis, single-cell
Cell necrosis is differentiated from apoptosis by the combination of cell and nuclear swelling, karyolysis, karyorrhexis, minimal nuclear pyknosis, loss of cellular detail, cellular debris, and inflammation.

Comment
Diagnostic nomenclature should follow recommendations from the INHAND Apoptosis/Necrosis Working Group (Elmore et. al., 2016). It may be difficult to differentiate apoptosis from single cell necrosis in ocular tissues without special stains. A diagnosis of apoptosis/single cell necrosis may be appropriate if there is no need to separate individual diagnoses, if there is uncertainity regarding separate diagnoses, or if both processes are present.

Atrophy (N) Eye

Species
Mouse; Rat.

Other Term(s) Used
Varies with tissue type (see individual section).

Pathogenesis/cell of origin
Cell origin varies with tissue type (see individual section).

Diagnostic Features
- Decreased size of tissue or organ structure.
- Associated with decreased numbers of cells and/or cell layers.
- Distortion of adjacent/attached tissue structures.

Comment
With few exceptions (e.g. cornea epithelium, ocular muscles) atrophy of ocular structures is not reversible.

***Fibroplasia (N)* Eye**

Species
Mouse; Rat.

Other Term(s) Used
Membranes; varies with tissue type (see individual section).

Pathogenesis/cell of origin
Cellular transdifferentiation of an endogenous ocular cell population to cells with a fibroblastic phenotype that subsequently proliferate, migrate and organize into membranes.

Diagnostic Features
- Transdifferentiated cells generally have slender, fusiform profiles reminiscent of fibroblasts, produce collagens, and form dynamic linear arrays. Fibroblastic membranes resemble the fibrotic process that occurs in wound healing.
- Membranes can form under the retina, on the surface of the retina, and within the vitreous or aqueous humor.
- When mature, contraction can place tension on attached structures, resulting in possible retinal detachments, optic nerve prolapse, lens displacement, and iridal-cornea adhesion or iridal-limbal adhesion (synechia).

Differential Diagnoses
Varies with tissue type (see individual section). Fibroplasia, defined by the type and location, is the preferred diagnostic terminology. Fibrosis should be reserved for chronic lesions that contain mature collagen.

Neovascularization
- Vascular proliferation with associated collagen production.

Comment
Fibroblastic membranes can occur in absence of tissue injury or be part of a disease process. Fibroplasia is induced by a change in cytokine mileau that favors cellular- transdifferentiation and may occur spontaneously as an aging or degenerative disease process, as a sequel to an inflammatory process, or following tissue injury as a reparative process. TGFβ has been implicated in the pathogenesis of fibroplasia in ocular tissues (Masli and Vega 2011) where it tends to be progressive. Cell populations identified in fibroblastic membranes include corneal endothelial cells, spindle cells that are associated with zonule fibers that attach to the lens, hyalocytes, retinal glial cells, Müller cells, and RPE (Joshi, Agrawal et al. 2013). Fibroblasts may also have a role.

***Fibrosis (N)* Eye**

Species
Mouse; Rat.

Other Term(s) Used
None.

Pathogenesis/cell of origin
Recruited fibroblasts in response to tissue injury, or endogenous ocular cells that have undergone cellular transformation and assumed a fibroblastic phenotype.

Diagnostic Features
- Linear arrays of fibroblastic cell types and mature collagen.
- Often associated with tissue injury and subsequent wound healing similar to that observed in systemic reactions.

Differential Diagnoses
Fibroplasia
See above.

Comment
Fibrosis should be reserved for findings that include mature collagen. Mature collagen is most often associated with tissue injury and typical wound healing. However, fibroblastic membranes associated with cellular transformation due to spontaneous disease or inflammation can contain mature collagen and appear quiescent, rather than active, on histopathology.

***Infiltrate, inflammatory cell (N)* Eye**

Species
Mouse; Rat.

Other Term(s) Used
Infiltration; varies with tissue type (see individual section).

Pathogenesis/cell of origin
Leukocytes recruited from the systemic circulation. The pathogenesis is uncertain, but presumably leukocyte infiltrates are a self-limiting response designed for immune surveillance and minor tissue repair activities.

Diagnostic Features
- Foci of a single inflammatory cell population or a mixture of different cell types without other features of inflammation.

Differential Diagnoses
Inflammation
- Inflammatory cellular infiltrate associated with features of inflammation that include edema, congestion, hemorrhage, and/or necrosis.

Comment
'Infiltrate' is the preferred term, followed by the predominant cell type (neutrophilic, eosinophilic, lymphocytic, plasmacytic or histiocytic) or mixture of different cell

types (mixed). Infiltrates resolve without residual damage to the intraocular tissues, and with re-establishment of the blood-ocular barriers. Infiltrates or aggregates of lymphocytes occur spontaneously in many structures of the eye, including the ocular glands, eyelids, conjunctiva, cilary body, choroid, and surrounding the optic nerve where it exists the eye.

***Inflammation (N)* Eye**

Species
Mouse; Rat.

Other Term(s) Used
Varies with tissue type (see individual section).

Pathogenesis/cell of origin
Leukocytes recruited from the systemic circulation.

Diagnostic Features
- Cell lineage varies with inciting cause.
- Leukocyte infiltrates or aggregations, associated with adjacent tissue damage, and may be accompanied by necrosis, vascular inflammation, and hemorrhage.

Differential Diagnosis
Infiltrate, inflammatory cell
- Leukocyte infiltrates without other indications of inflammation or tissue injury.

Comment
Inflammation should only be used diagnostically when tissue injury or other indicators of inflammation are present, in addition to leukocytes. Intraocular inflammation is an indication that a breach in the blood-ocular barrier has occurred. This is associated with loss of immune deviation ("immune privilege"), and a conversion from the ocular homeostasis immune suppressive environment to one that is pro-inflammatory. Intraocular proteins, normally sequestered from the immune system (preventing establishment of tolerance to self-antigens), may come under immune surveillance and generate a delayed hypersensitivity response, resulting in additional ocular injury. Modifiers should be used to designate cell lineage, and locators to identify tissue type.

***Mitosis, increased number (N)* Eye**

Species
Mouse; Rat.

Other Term(s) Used
Mitotic figures, increased

Pathogenesis/cell of origin
Varies with cell type and location.

Diagnostic Features
- Chromatin in varying stages of division.
- Cells are typically enlarged as they are for cell division.

Differential Diagnosis
Neoplasia

Comment
Increased numbers of mitotic figures are commonly observed as a reparative or regenerative process following tissue injury. Mitotic figures are normally observed in the cornea, which has a high rate of epithelial turn-over. An increase in incidence occurs following phototoxicity or administration of tubulin inhibitors. Mitosis can also be observed in the endothelial cells of the vasculature, epithelial cells of the uvea, and occasionally in cells within the retina.

***Necrosis; Necrosis, single-cell (N)* Eye**

Species
Mouse; Rat.

Other Term(s) Used
None

Diagnostic Features
- Often contiguous cells.
- Cell and organelle swelling.
- Pyknosis (nuclear condensation; minor component).
- Karyorrhexis (nuclear fragmentation).
- Karyolysis (degradation of nuclear material).
- Cytoplasmic blebs.
- Plasma membrane rupture.
- Intracellular contents released into surrounding tissue.
- Inflammation may be present.

Differential Diagnoses
Apoptosis

Comment
Diagnostic nomenclature should follow recommendations from the INHAND Apoptosis/Necrosis Working Group (Elmore et. al., 2016).

***Neovascularization (N)* Eye**

Species
Mouse; Rat.

Other Term(s) Used
New blood vessels; angiogenesis

Pathogenesis/cell of origin
Neovascularization is characterized by the outgrowth of pre-existing blood vessels within a region into adjacent ocular tissue that generally is avascular. Typical regions of the eye subject to neovascularization are the cornea (cor-

neal neovascularization) and retina (retina neovascularization). Choroidal neovascularization involves the expansion of choroidal vessels into the retina and is observed in spontaneous disease of humans with macular degeneration, and in some animal models. Primary drivers of neovascularization are conditions that promote anoxia, inflammation, or diseases that have a cytokine milieu (e.g. metalloproteinases, VEGF, Ang-2) that favors angiogenesis.

Diagnostic Features
- Extension of a blood vessel into a region that should be avascular.
- May be blind ended (cornea).
- Evidence of vascular leakage (edema, inflammation). Unlike normal vessels, vessels produced under these conditions do not have adequate tight junctions.
- Associated with other elements of primary disease specific to region.

Special Techniques for Diagnostics
- Immunohistochemistry for endothelial cells, pericytes, smooth muscle.
- Fluorescein angiography in-vivo.

Differential Diagnoses

Angioma; angiosarcoma

Proliferation of capillary channels (capillary hemangioma) of the retina and optic nerve have been reported in humans. Local ocular vascular tumors are rare in animals, and there are no reports in rodents.

Vascular hamartomas

Local proliferation of well-formed, non-neoplastic, but redundant blood vessels within a tissue that is normally vascularized. Vascular harmatomas are considered to be an embryological malformation. There are no reports in the eyes of rodents.

Vascular hyperplasia

Local nodular benign proliferation of blood vessels limited to their point of origin. Not reported for ocular tissues.

Telangiectasia

Dilated blood vessels; may potentially be observed in the conjunctiva.

Comment

Neovasularization is a unique phenomenon that results in the sprouting of new blood vessels from a pre-existing blood supply to an adjacent tissue (e.g. conjunctiva, retina, optic nerve, choroid). It is driven by a number of local cytokine and metalloproteinases influences that are upregulated by diseases that result in anoxia or inflammation within ocular tissues that do not have their own blood supply. New blood vessels have poorly formed or inadequate tight junctions and thus leak plasma and proteins into the tissue, severely compromising vision. Neovascularization can potentially be reversed by removing the inciting cause, and through treatment with VEGF antagonists, which have proven to be efficacious in clinical use.

Eyelid

Infiltrate, inflammatory cell, eyelid (N) Eyelid

Species

Mouse; Rat.

Other Term(s) Used

None.

Diagnositic Features
- Leukocyte infiltrates without other indications of inflammation (see general terminology, above).

Differential Diagnosis

Inflammation
- Leukocyte infiltrates with features of inflammation (see general terminology, above).

Comment

Infiltrates are not uncommon at the eyelid dermal or conjunctival margins. Infiltrates may also be associated with adnexa in the dermis.

Inflammation, eyelid (N) Eyelid

Species

Mouse; Rat.

Other Term(s) Used

Blepharitis; blepharoconjunctivitis.

Diagnostic Features
- Leukocyte infiltrates associated with other indications of inflammation (see general definition above).

Differential Diagnosis

Infiltrate, inflammatory cell
- Leukocyte infiltrates without other features of inflammation.

Comment

Inflammation is macroscopically characterized by excessive sebum or keratin debris adherent to the eyelid margin and eyelashes. Some inbred mouse strains are affected by blepharoconjunctivitis (Smith, Montagutelli, and Sundberg 1996a). Secondary bacterial infection is common in affected mice and periorbital abscesses have been reported. Inflammation of epidermis and adnexal structures of the eyelid as well as common diseases of rodent skin are covered in the manuscript on Integument (see Introduction, Mecklenburg et al. 2013). For information on inflammation of the dermis and stroma of the eyelid, the reader is referred to the manuscript on Soft Tissue (see Introduction,

Greaves et al. 2013).

Atrophy, Meibomian gland (N) **Eyelid**

Species
Mouse; Rat.

Other Term(s) Used
None

Pathogenesis/cell of origin
Acinar and/or ductal epithelial cells.

Diagnostic Features
- Irregularly shaped tubules or acini with dilated or reduced lumina.
- Lined by cuboidal or flattened epithelium.
- Loss of normal vacuolated cytoplasmic appearance.
- Interstitial fibrosis may be present.
- The lumina of the tubules may be filled with desquamated cells and accumulated sebaceous material.

Comment
Atrophy of the Meibomian gland has been reported with deficiency/inhibition of enzymes involved in fatty acid synthesis (Miyazaki et al. 2001).

Infiltrate, inflammatory cell, Meibomian gland (N) **Eyelid**

Species
Mouse; Rat.

Other Term(s) Used
None

Pathogenesis/cell of origin
Acini and/or ducts and interstitial tissue.

Diagnostic Features
- Foci of a single inflammatory cell population or a mixture of different cell types without other features of inflammation.

Comment
Minimal to mild infiltrates of neutrophils and lymphocytes are normally present in the meibomian gland (Yoshitomi and Boorman 1990).

Inflammation, Meibomian gland (N) **Eyelid**

Species
Mouse; Rat.

Other Term(s) Used
None

Pathogenesis/cell of origin
Acini and/or ducts and associated interstitial tissue.

Diagnostic Features
- Focal or multifocal areas of single or mixed inflammatory cellular types.
- Interstitial edema and/or vascular congestion with other indications of inflammation (see general terminology above).
- May be associated with squamous metaplasia of acinar/ductal epithelium or interstitial fibrosis in chronic conditions.
- Granulomatous or pyogranulomatous inflammation can be observed.

Differential Diagnoses
Infiltrate, inflammatory cell, Meibomian gland:
- Foci of single or mixed inflammatory cell types without other features of inflammation.

Comment
Modifiers are recommended in relation to the predominant inflammatory cellular type (neutrophilic, eosinophilic, lymphocytic, plasmacytic or histiocytic) or mixture of different cellular types (mixed). Viral infections tend to result in multilobular inflammation and may have inclusions present.

Inflammation, Granulomatous, Meibomian gland (N) **Eyelid**

Species
Mouse; Rat.

Other Term(s) Used
Foreign body inflammation; stye; chalazion.

Pathogenesis/cell of origin
Alveoli/ ducts; often spontaneous and/or age-related.

Diagnostic Features
- Granulomatous reaction composed of epithelioid macrophages, multinucleated giant cells, lymphocytes and plasma cells.
- Foreign body may be present (lipid secretions, released secondary to blocked ducts).

Comment
Granulomatous inflammatory reactions of the eyelid margin secondary to released lipid secretions of sebaceous glands of Zeis or Meibomian glands are clinically referred to as stye and chalazion, respectively.

Cornea / Conjunctiva

Atrophy, epithelium (N) (Figure 1) **Cornea: Conjunctiva**

Species
Mouse; Rat.

Other Term(s) Used
Decreased number of epithelial cells, or decreased cell layers (cornea). Attenuation is a specific change observed on spectral microscopy for the corneal endothelium (see below) and should not be used in place of atrophy for the cornea epithelium.

Pathogenesis/cell of origin
Corneal or conjunctival epithelial cell; may be drug-induced or incidental.

Diagnostic Features
- Decreased number of cells, and/or cell layers.
- May be associated with secondary changes, such as edema.

Differential Diagnoses
Epithelium, regeneration:
- Reparative phase following erosion/ulceration (flattened cells covering ulcerated/eroded area); enlarged epithelial cells with mitotic figures are present.

Artifact:
- Associated with removal of epithelium or endothelium during tissue processing.

Comment
Inhibition of mitosis (such as by chemotherapeutic agents) causes an inability of basal cells or limbal stem cells to proliferate, leading to decreased numbers of epithelial cells/layers. The epithelial cells remaining may appear enlarged and/or disorganized in compensation for fewer cells present. Atrophy does not occur in the endothelium of the cornea, which consists of a single layer.

Attenuation, endothelium (N) **Cornea**

Species
Mouse; Rat.

Other Term(s) Used
None.

Pathogenesis/cell of origin
Cornea endothelial cells, in regions where cell loss has occurred.

Diagnostic Features
- Individual endothelial cells flatten and spread out to cover spatial defects created by endothelial cell loss. This change may not be appreciated on light microscopy, and is best visualized using spectral microscopy.
- On cross section, cells are flattened in profile, and appear smaller on histological examination.
- Endothelial cell layer may have evidence of cell drop-out.

Differential Diagnoses
Decreased numbers of endothelial cells.
Cell loss without compensatory attenuation; cornea homeostasis is compromised and thus there is associated corneal edema in regions of spatial defects. Inflammation may occur secondarily.

Comment
When endothelial cells are lost due to trauma, disease, or other reasons, the adjacent cells spread out in an attempt to cover the resulting defect and maintain cornea homeostasis. Attenuation is commonly observed on the peripheral margins of the cornea, although it may be difficult to appreciate on histological examination of cross sections. Attenuation and generalized loss of corneal endothelial cells are best observed on clinical examination using spectral microscopy. Attenuation is seen in rats administered the phototoxic agent, 8-methoxypsoralen, followed by exposure to UV radiation.

Cyst, inclusion (N) **Cornea; Conjunctiva**

Species
Mouse; Rat.

Other Term(s) Used
None

Pathogenesis/cell of origin
Corneal epithelial cells, organized to form a small cystic structure.

Diagnostic Features
- Cystic space that is lined by well-differentiated epithelial cells within the cornea.
- Epithelial cells may be keratinized.
- Cyst may contain fluid.
- Leukocyte infitrates or inflammation may be present.

Differential Diagnoses
Neoplastic lesions (see Papilloma, squamous cell and Carcinoma, squamous cell).

Comment
Pathogenesis has not been determined – may either be congenital or the result of trauma, followed by disorganized healing (Geiss and Yoshitomi 1999).

Edema (N) (Figures 2, 3) **Cornea; Conjunctiva**

Species
Mouse; Rat.

Other Term(s) Used
None

Pathogenesis/cell of origin

Injury or functional failure of either the endothelium or epithelium of the cornea; barriers may be intact, or a spatial defect may be evident**.**

Diagnostic Features

- Paleness of the stroma on H&E staining, and irregular expansion of the collagen fibers.
- Separation of epithelium or endothelium from the basal lamina.
- Clear spaces or vacuoles within epithelial cells, or clefts between epithelial cells (fluid-filled, but may not be evident following tissue processing).
- Edema appears as corneal opacification macroscopically.

Differential Diagnoses

Artifact splitting of collagen fibers:

- Varying degrees of hydration of the sectioned tissues can result in variable appearance on the slide, leading to incorrect diagnosis of edema in some instances.

Comment

Edema often occurs from a functional failure of the corneal endothelium homeostasis mechanisms, resulting in altered stromal fluid and electrolyte balance. Fluid may accumulate in both the stroma (altering the arrangement of the collagen bundles) and in the epithelium. Edema may occur with trauma, developmental abnormalities, or degenerative age changes. Similar to other species, rodents lose endothelial cells with age, which may result in osmotic decompensation. Regardless of cause, corneal edema occurs due to insufficient endothelial pumping mechanisms.

Erosion/ulcer (N) (Figure 4) **Cornea; Conjunctiva**

Species

Mouse; Rat.

Other Term(s) Used

None

Pathogenesis/cell of origin

Corneal/conjunctival epithelium. Associated with trauma, reduced tear production resulting in dry eyes, topical or gas/vapor caustic agents, and corneal mineralization. Unregulated, energy independent, passive cell death with leakage of cytoplasm into surrounding tissue and subsequent inflammatory reaction.

Diagnostic Features

- Incomplete loss (erosion) or focal deficit (ulcer) of the surface epithelium.
- Histologically, the outer epithelial layer is eroded. Abrasions may be associated with inflammatory infiltrates and necrosis.
- Chronic conditions may be associated with corneal neovascularization.
- Fluorescein positive when examined in-vivo.

Differential Diagnoses

Inflammation (Keratitis):

- Inflammation of the corneal epithelium and stroma without loss of the epithelium. Inflammation may facilitate artifact epithelial separation from the stroma during processing.

artifact:

- Processing artifacts, such as separation of the cornea epithelium from the stroma, are common in the eye. A diagnosis of ulcer should be associated with expectant concurrent findings in the stroma and/or epithelium (e.g. inflammation, edema).

Mineralization (Corneal dystrophy):

- Dystrophy is the clinical term for accumulation of abnormal material in the cornea; mineral is most often seen in the rodent. Corneal mineralization may be associated with inflammation, edema and neovascularization. Mineralization is most often observed in aged rats.

Comment

Abrasions may be incidental in rodents, often related to caging conditions or environmental irritants. Topical acid or alkali burns, gases/vapors, dust or other foreign particles contacting the eye, and desiccation are all possible causes or erosion/ulceration. Erosion and necrosis of conjunctival epithelium may be associated with ocular irritants (Maurer et al. 1998; Maurer and Parker 1996).

Fibroplasia (N) (Figure 5) **Cornea**

Species

Mouse; Rat.

Other Term(s) Used

Retrocorneal membrane.

Pathogenesis/cell of origin

Stromal keratocytes or corneal endothelial cells that have undergone cellular transdifferentiation (metaplasia) assuming a fibroblast phenotype. Fibroplasia occurs as a reparative process following injury to the cornea endothelium, and from the failure of adjacent endothelial cells to adequately cover subsequent spatial defects.

Diagnostic Features

- Localized layers of elongated to spindle-shaped cells overlying the inner surface of the cornea.
- May be associated with adjacent focal changes to the stroma, such as edema or inflammation.

Comment

Corneal endothelial cells do not regenerate in most species. Corneal fibroplasia is more likely to occur when there

is loss of enough cells to the point that the endothelium cannot respond adequately to cover a defect.

Fibrosis, stroma (N) (Figure 9) **Cornea**

Species
Mouse; Rat.

Other Term(s) Used
Corneal scar.

Pathogenesis/cell of origin
Activated keratocytes.

Diagnostic Features
- Area within the corneal stroma that microscopically appears as dense collagenous stroma.
- Fibrosis may correspond macroscopically to corneal opacity.

Comment
Keratocytes are activated following corneal injury and may proliferate to fill in wound gaps. Activated keratocytes contain smooth muscle actin and may phenotypically behave similar to myofibroblasts. In these cases high levels of collagen are produced that lack the organized lattice-like structure that is typical of the translucent cornea, instead forming an opaque extracellular matrix (ECM) within the defect. Transparency can be restored through cell turn-over, and replacement with fibroblasts that are capable of producing ECM that contains sulfated glycosaminoglycans (Hassell and Birk 2010).

Hypertrophy, Descemet's membrane (N) (Figure 6) **Cornea**

Species
Mouse; Rat.

Other Term(s) Used
Increased thickness, Descemet's membrane.

Pathogenesis/cell of origin
Spontaneous accumulation of collagen within Descemet's membrane adjacent to the corneal endothelium.

Diagnostic Features
- Focal thickenings of Descemet's membrane, consisting of accumulations of unbanded collagen subjacent to the corneal endothelium.

Differential Diagnoses

Fuch's Dystrophy (reported in humans):
- Focal thickenings of Descemet's membranes associated with endothelial cell loss.

Baned collagen fibers:
- Secreted by corneal endothelial cells as a sequela to injury or a disease process. Banded collagen can be differentiated from unbanded collagen using electron microscopy.

Comment
Hypertrophy of Descemet's membrane is occasionally observed in aging mice (Jun, Chakravarti et al. 2006).

Infiltrate, inflammatory cell, conjunctiva (N) (Figure 11) **Cornea; Conjunctiva**

Species
Mouse; Rat.

Diagnostic Features
- Foci of a single inflammatory cell type or a mixture of different cell types without other features of inflammation.

Differential Diagnosis
Inflammation
- Infiltrates of leukocytes associated with inflammatory features such as edema, hemorrhage and necrosis.

Comment
Infiltrates of lymphocytes, sometimes with lymphoid follicle formation, are normally present in the conjunctiva (Yoshitomi and Boorman 1990). Infiltrates may be seen at the periperhal margins but are not normally observed within the cornea.

Inflammation (N) (Figures 2, 3, 6) **Cornea; Conjunctiva**

Species
Mouse; Rat.

Other Term(s) Used
Keratitis (corneal inflammation); Conjunctivitis (conjunctival inflammation).

Pathogenesis/cell of origin
Inflammatory response due to a variety of possible causes, including injury, infection (SDAV, Staphylococcus, others), photosensitization, or necrosis. Type of leukocyte response varies with inciting cause.

Diagnostic Features
- Inflammatory cellular infiltrate with associated edema, congestion, hemorrhage and/or necrosis.
- May be associated with neovascularization, degenerative or hyperplastic alterations of the epithelium, fibrosis, or mineralization.

Differential Diagnoses
Infiltrate, inflammatory cell, conjunctiva:
- Foci of a single population or mixed inflammatory cell types without other features of inflammation.

Comment

Modifiers are recommended in relation to the predominant inflammatory cellular type (neutrophilic, eosinophilic, lymphocytic, plasmacytic or histiocytic) or mixture of different cellular types (mixed). Ocular irritation is a common clinical feature (Maurer et al. 1998) and while inflammation may originate in either the conjunctiva or cornea, it generally extends to both areas. Inflammation of the conjunctiva or cornea is associated with submucosal or stromal edema respectively, and may result in erosion/ulceration, and subsequent regeneration of the epithelium.

Keratinization (N) (Figures 3, 5, 10) **Cornea**

Species

Mouse; Rat.

Other Term(s) Used

Cornification; dyskeratosis.

Pathogenesis/cell of origin

Superficial keratocytes that become cornified with chronic injury.

Diagnostic Features

- Focal regions of the cornea that contain superficial layers of keratin.

Comment

Keratocytes become progressively flattened as they migrate towards the corneal surface for removal. Chronic injury is associated with the production of keratin. Defective tear production and vitamin A deficiency are reported causes of corneal keratinization.

Mineralization (N) (Figures 7, 8, 9) **Cornea**

Species

Mouse; Rat.

Other Term(s) Used

Corneal dystrophy; calcific band keratopathies; dystrophic calcification.

Pathogenesis/cell of origin

Mineralization of the cornea generally occurs secondary to focal injury, but can also occur with metastatic mineralization. Mineralization can develop due to incomplete eyelid closure, and subsequent chronic irritation of the cornea. Mineral formation has also been associated with high ammonia levels due to urease-positive bacteria in the bedding. Subepithelial mineralization has been reported in numerous mouse strains (Swiss, BALB/C, C2H, DBA/2, C57BL/6) and rats (Sprague-Dawley, F344, Wistar).

Diagnostic Features

- Mineralization occurs in the subepithelial region or in the anterior stroma and has a basophilic, extracellular granular to globular appearance on H&E similar to mineralization elsewhere. Mineralization may be confirmed with von Kossa stain, if present in sufficient quantity.
- May be associated with epithelial necrosis, foreign body reaction and scarring.

Differential Diagnoses

Sequestrum

- Focal region of divitalized stromal or epithelial tissue surrounded by vital tissue. Sequestrum has been reported in several species, but the occurrence in rodents is uncertain.

Comment

Mineralization appears as punctate opacities in the cornea grossly. Mineralization may be related to changes in the corneal microenvironment causing calcium to precipitate. When present in rodents, careful histologic examination of all major organs should be conducted to see if there is evidence of systemic mineralization. Most instances of mineralization in rodents do not fit the true definition of corneal dystrophy, described as spontaneous, non-inflammatory, bilateral changes with no associated systemic disease. Mouse strains with true corneal dystrophies include C57BL/10ChPr, Rhino and OEL (Van Winkle 1991).

Neovascularization (H) (Figures 3, 5, 10) **Cornea**

Species

Mouse; Rat.

Other Term(s) Used

New blood vessels, cornea.

Pathogenesis/cell of origin

Neovascularization generally occurs secondary to corneal damage and is often associated with inflammatory mediators. Blood vessels originate from extension/proliferation of endothelial cells from the limbal vessels into the peripheral margins of the corneal stroma and extend centrally into the normally avascular cornea.

Diagnostic Features

- Blood vessels within normally avascular corneal stroma.
- May be associated with corneal stromal edema and inflammation as well as conjunctival congestion.

Differential Diagnoses

Corneal nerves:

- Special stains or IHC to differentiate corneal nerves from non-perfused blood vessels may be necessary.

Comment

Neovascularization may occur spontaneously in older animals; the finding has been reported in nude (*Foxl*^{nu}) and hairless (*hr*) mice (Smith, Sundberg, and John 2002b; Smith, Hawes et al. 1996b). Vessels may persist as nonper-

fused ghost vessels visible on ophthalmic exam as linear opacities. Neovascularization can be related to deficiencies of tryptophan, riboflavin, Vitamin A and zinc. In some species, corneal vessels may extend normally beyond the limbus, and may/may not be perfused.

Pigment (N) **Cornea; Conjunctiva**

Species
Mouse; Rat.

Pathogenesis/cell of origin
Extracellular granular or amorphous material deposited within the stroma or epithelium of the cornea or conjunctiva. Increased pigmentation also occurs from an increase in number of melanocytes within the tissue, or an increase in intracellular pigment within the resident epithelial cells.

Diagnostic Features
- Variably sized, shaped and colored aggregates of material, either cytoplasmic or extracellular.

Differential Diagnoses
Mineralization
See above.

Comment
Pigment may be endogenous (e.g. melanin), occur from hemorrhage (hemosiderin, hemoglobin), or derive from exogenous sources (e.g.foreign body). Increased pigmentation associated with an increase in melanin granules can occur with chronic irritation or trauma. Melanin granules can be found intracellular within intraepithelial melanocytes (which may increase in number following injury) or corneal epithelial cells (thought to acquire melanin from melanocytes), or as extracellular deposits (McCracken and Klintworth 1976). Extracellular deposits of brown-colored metabolic intermediates in the cornea epithelium or stroma occurred with administration of chlorpromazine and other phenothiazine deritives, and pigment changes have been reported with exposure to gold, mercury and analine dyes (Hogan and Zimmerman 1962). Potential vision effects vary with severity and location; pigmentation within the perilimbal region has no impact to vision, and pigmentation in the central cornea may go unnoticed to the patient if minimal. Pigmentation resolves over time with removal of the stimulus and when intracellular, with cell turnover.

Vacuolation, epithelium or endothelium (N) (Figures 11, 12) **Cornea**

Species
Mouse; Rat.

Other Term(s) Used
Lipidosis; phospholipidosis.

Pathogenesis/cell of origin
Lysosomal accumulation of lipid or other substances (including glycosaminoglycans, mucopolysaccharides and others) within the cytoplasm of epithelial cells, endothelial cells, or keratocytes. These are generally removed during tissue processing, resulting in the appearance of clear vacuolated spaces on light microscopy.

Diagnostic Features
- Clear cytoplasmic vacuoles following tissue processing.
- Phospholipidosis causes lipid-like vacuoles in corneal epithelial cells and keratocytes; bluish granules may be observed on H&E staining.

Special Techniques for Diagnostics
- Semi-thin sections followed by Toluidine Blue staining: irregular cytoplasmic inclusions are seen with phospholipidosis.
- Electron microscopy: typical lamellar and crystalline inclusions of phospholipidosis.

Differential Diagnoses
Artifact vacuolation
Vacuolation resulting from edema (see above; Figure 2)

Comment
Vacuolation may be drug-induced. Some cationic amphiphilic drugs can cause phospholipidosis of the corneal epithelium and/or corneal endothelium. Tilorone can cause phospholipidosis and mucopolysaccharidosis (MPS) in rats. Lysosomal storage diseases result in the abnormal accumulation of substances, most often glycosaminoglycans, within cells. MPS VII, caused by a deficiency in B-glucuronidase, is an autosomal recessive mutation reported to occur in homozygous mice (gus^{mps}/gus^{mps}) (Smith, Sundberg, and John 2002b). Lysosomal accumulation may result in corneal opacities that are grossly visible on ophthalmic examination.

Filtration Angle/Trabecular Meshwork

Congenital

Malformation, filtration angle (N) **FA/TM**

Species
Mouse; Rat.

Other Term(s) Used
Pectinate ligament dysplasia; mesodermal dysgenesis, goniodysgenesis.

Pathogenesis/cell of origin
Malformation occurs from a failure in development of the spaces forming the trabecular meshwork.

Diagnostic Features

- Disorganization or complete absence of the structures of the drainage angle and/or trabecular meshwork.

Differential Diagnoses

SECONDARY ALTERATIONS of the drainage angle:

- Due to iridal-trabecular adhesion, trabecular collapse, trabecular fibrosis, or proliferation of the cells that line the trabecular meshwork.

Comment

Malformation of the filtration angle significantly impacts aqueous fluid outflow, and can result in glaucoma. Abnormalities of the aqueous plexus and the trabecular meshwork occur in Foxc1 and Foxc2 mutant mice (Smith, Sundberg, and John 2002b).

Acquired

***Narrowed filtration angle (N)* FA/TM**

Species

Mouse; Rat.

Other Term(s) Used

Compaction of trabecular beams; collapse, trabecular meshwork.

Pathogenesis/cell of origin

Displacement, compression or collapse of the trabecular beams, reducing or obliterating the spaces between the beams.

Diagnostic Features

- Reduced space between the trabeculae, compaction of trabecular beams, and partial or complete obliteration of aqueous plexus.
- The presence of cells and/or material within the drainage angle/trabecular meshwork.
- Enlargement and/or distortion of the eye if aqueous flow is sufficiently impaired.

Differential Diagnoses

MALFORMATION, FILTRATION ANGLE

- Malformations are best observed on ophthalmoscopy.

Comment

A narrow filtration angle is associated with increased resistance in aqueous humour outflow and IOP, clinically causing glaucoma. Glaucoma is more commonly observed spontaneously in larger species, but can be induced experimentally in rodents. The trabecular meshwork is scant in rodents and spontaneous collapse apparently is rare. However, iridal-cornea adhesion can block the outflow of aqueous humor to a degree that the filtration angle collapses on itself. Following laser photocoagulation, the iris may scar to the angle over the meshwork (iridal-trabecular adhesion), and hyphema of the anterior chamber or atrophy of the ciliary body may occur (Levkovitch-Verbin, Quigley et al. 2002). Collapse of the trabecular meshwork may be experimentally induced in animal glaucoma models (i.e. laser photocoagulation) (Ueda, Sawaguchi et al. 1998, Levkovitch-Verbin, Quigley et al. 2002). Substances such as cells (red blood cells and leukocytes), free pigment, melanocytes or macrophages containing pigment, or test material that has been administered into the aqueous or vitreous humour may become lodged within the meshwork and impede aqueous flow.

Inflammation (N) (Figure 12) **Anterior Chamber; Aqueous Humor**

Species

Mouse; Rat.

Other Term(s) Used

Inflammation, anterior segment; uveitis

Pathogenesis/cell of origin

Recruitment of leukocytes originating from the systemic circulation.

Diagnostic Features

- The presence of leukocytes of single or mixed cell type in the anterior chamber.
- Generally associated with increased protein in the aqueous appearing as eosinophilic fluid.
- Severe inflammation may appear as flocculent fluid and/or contain beads or strands of fibrin.

Differential Diagnoses

None

Comment

Leukocytes are not found in the anterior chamber without inflammation in some other part of the eye, e.g. the cornea, uvea, or vitreous. However on occasion it may be possible to observe residual inflammatory cells following an inflammatory insult that have yet to be cleared from the anterior chamber, or that have migrated from the posterior to the anterior chamber.

Proteineous fluid (N) (Figures 12, 21) **Anterior Chamber; Aqueous Humor**

Species

Mouse; Rat.

Other Term(s) Used

Increased protein

Pathogenesis/cell of origin

Vascular compromise within the uveal tissues of the anterior segment.

Diagnostic Features
- Generally associated with increased protein in the aqueous appearing as eosinophilic fluid.
- Lack of other inflammatory features.
- Aqueous may contain beads or strands of fibrin.

Differential Diagnoses
None

Comment
The aqueous normally has a low protein content and increases are generally associated with an inflammatory process within the uveal tissues of the anterior segment (ciliary body, iris). However, on occasion an increase in protein may be observed in the eye without other indications of inflammation (drug administration, needle insertion). Increased protein is diagnosed as 'flare' on ophthalmoscopy.

Uvea, Iris and Ciliary Body

Congenital

Adhesion, iris (N) (Figures 13, 14, 16) **Uvea: Iris and Ciliary Body**

Species
Mouse; Rat.

Other Term(s) Used
Iridocorneal fibroplasia or strands; iridal-corneal adhesion. Adhesions may be congenital or acquired.

Pathogenesis/cell of origin
Adhesions between the anterior edge of the iris and the endothelium of the cornea (anterior synechia) or the posterior edge of the iris and the anterior surface of the lens (posterior synechia).

Diagnostic Features
- Adherence of the iris to the cornea or lens (on ophthalmoscopy observed as anterior and posterior synechia, respectively). Anterior adhesions to the cornea can potentially block the outflow of the aqueous humor through the filtration angle causing increased intraocular pressure and glaucoma (Ramos, Attar, et al. 2017).
- Peripheral anterior synechia refers to a condition in which the iris adheres to the angle. Failure of aqueous drainage may result from peripheral anterior adhesions in conditions such as uveitis (Williams 2007).
- Pigment on the anterior lens capsule suggests prior occurrence of posterior adhesions.
- Adhesions may cause opacities in either the cornea or lens (Foster 1958).

Differential Diagnosis
Artifact
- Artifacts associated with tissue processing can result in displacement of the iris; pigment on the anterior lens capsule or corneal endothelium may also occur as an artifact of processing.

Comment
Adhesions can be detected on examination through topical instillation of a mydriatic agent; distortion of the pupil occurs upon pupil dilation. Acquired adhesions are most often observed as a sequela to anterior uveitis, but may also occur with trauma, or can be experimentally induced by laser photocoagulation (Ueda, Sawaguchi et al. 1998). Spontaneous adhesions are observed in SD rats (Taradach and Greaves 1984), but are rare in the mouse. Adhesions in older mice are usually a sequela of inflammation in the anterior segment. Posterior adhesions in mice are often associated with cataracts (Geiss and Yoshitomi 1999). The etiology of congenital adhesions is not well understood. Synechia is a clinical ophthalmic term, and should not be used as a histological diagnosis.

Hypoplasia, ciliary body (N) **Uvea: Iris and Ciliary Body**

Species
Mouse; Rat.

Other Term(s) Used
Reduced size, ciliary body

Pathogenesis/cell of origin
Myofibrils of the ciliary body; dysgenesis associated with defects in Fibrillin-2 (Fbn2) gene.

Diagnostic Features
- Decreased size of ciliary body – often segmental.
- Associated with a decreased number of folds on EM examination.

Differential Diagnosis
Atrophy, Ciliary Body
Degeneration, Ciliary Body
- In either atrophy or degeneration, a loss of tissue mass occurs secondary to traumatic or inflammatory injury, or to another disease process.

Comment
Reported in Fbn2 $^{-/-}$ mice (Shi, Tu et al. 2013b). Hypoplasia of the ciliary body is associated with anatomical defects in the iris.

Malformation, iris (N) **Uvea: Iris and Cilary Body**

Species
Mouse; Rat.

Other Term(s) Used
Coloboma (iris, or posterior); dyscoria.

Pathogenesis/cell of origin
Failure of closure in the optic fissure can cause malformations resulting in small holes, spatial defects, or other irregularities to the iris.

Diagnostic Features
- The rodent iris contains scant stroma and has a narrow-curved profile on cross section. Malformations can appear as irregular expansions of the stroma, or as blunting or folding at the inner margin. Spatial defects may be recognized as irregularities in either the posterior or anterior surface on histopathology; differentiation from tissue processing artifact is facilitated by advanced knowledge of clinical findings.
- Posterior or choroidal coloboma is a spatial defect of the choroidal blood vessels near the optic nerve, and may occur simultaneously with iris malformation in congenital cases. In these occurrences, the regional sensory retina and RPE are not developed, and the retina vasculature is distorted.

Differential Diagnoses
Abnormalities in pupil shape:
- Associated with inflammation of the anterior uvea.

Comment
Iridal malformations in young rodents (especially mice) appear as an abnormality in pupil shape (spatial defect in the iris), and is clinically diagnosed as pupillary dyscoria (Rubin and Daly 1982). Careful sectioning is important to capture spatial defects histologically. Coloboma is a clinical term, and should not be used as a histological diagnosis. Localized developmental errors may lead to spatial defects/holes in other specific ocular structures such as the choroid and optic nerve. They can occur in association with microphthalmia (Geiss and Yoshitomi 1999; Williams 2002).

***Persistent pupillary membrane (N)* Uvea: Iris and Ciliary Body**

Species
Mouse; Rat.

Other Term(s) Used
Persistent pupillary strands; iridal fetal membrane.

Pathogenesis/cell of origin
Vessels and mesenchyme of the pupillary membrane.

Diagnostic Features
- Collagenous or membranous strand of tissues found in the anterior or posterior chamber, or spanning across the pupillary opening (Heywood 1973).
- Strands of tissue may appear on cross section as free-floating, or can be tethered at one or more places to the iris, lens, or cornea.

Differential Diagnoses
Persistent embryonic lens vasculature:
- A more likely diagnosis if associated with the presence of blood in the anterior segment.

iridal fibroplasia

Comment
Persistent pupillary membranes are remnant vascular strands of the developing iris that fail to undergo postnatal atrophy; they are best diagnosed on ophthalmoscopy. Membranes may be free-floating, bridge the iris, or extend from the iris to the lens or cornea where they are associated with focal opacity of the lens, or corneal opacity, respectively (Taradach, Regnier et al. 1981). They may be observed in Sprague-Dawley rats, Crj:CD (SD) rats, and in mice, and individuals with this finding should be excluded from ocular studies. Persistent pupillary membranes may block the filtration angle, impair aqueous drainage, and cause pupil-block glaucoma (Young et al. 1974; Williams 2007).

Degenerative

***Atrophy, iris (N)* Uvea: Iris and Ciliary Body**

Species
Mouse; Rat.

Other Term(s) Used
Degeneration, iris

Pathogenesis/cell of origin
Iris stroma.

Diagnostic Features
- Decreased size of iris associated with reduction in stroma and blood vessels.
- Iris may appear irregular in size or shape circumferentially on cross section.
- Irregular contours may suggest the presence of spatial defects within the stroma.
- Enlarged posterior epithelial cells containing prominent pigment granules.
- Pupillary sphincter and ciliary processes appear hypertrophic.

Comment
Iris atrophy is best diagnosed on ophthalmic examination and can readily be recognized due to distortions of the pupil size and shape and poor response to miotics. As the iris atrophies, small holes in the stroma appear initially, followed by coalescence, and the stroma appears increasingly disorganized as mesodermal tissue and blood vessels regress. Iris atrophy occurs in the (C57L X A/He) F1 mouse (Geiss and Yoshitomi 1999), and may occur in association with glaucoma in aging DBA/2J mice (Smith, Sundberg, and John 2002b).

Atrophy, ciliary body (N) **Uvea: Iris and Ciliary Body**

Species
Mouse; Rat.

Other Term(s) Used
Degeneration, ciliary body

Pathogenesis/cell of origin
Ciliary body myofibrils.

Diagnositic Features
- Decreased size and/or decreased numbers of myofibrils within the ciliary body.
- Fragmentation of myofibrils and detachment of the sarcoplasma may be observed on electron microscopy.

Comment
Atrophy of the ciliary body muscle has been described in aged Wistar rats (Eiben and Liebich 1989) and may occur in other rodents. Atrophy of the ciliary muscle may result in distortions of the iris, and pupil size and shape.

Acquired

Congestion (N) (figure 12) **Uvea: Iris and Ciliary Body**

Species
Mouse; Rat.

Other Term(s) Used
None

Pathogenesis/cell of origin
Microvasculature of the iris.

Diagnostic Features
- Dilated vessels with the presence of erythrocytes (congestion as a histological diagnosis should be avoided due to the common occurrence of postmortem pooling of blood within the microvasculature).

Differential Diagnoses
Vascular dilation:
- Associated with inflammation.

Artifact of postmortem blood pooling

Comment
Iridal blood circulation is best assessed on clinical examination using ophthalmoscopy. Dilation of iridal vessels, with or without the presence of erythrocytes, can occur irrespective of physiological status of the eye at time of euthanasia. Iritis is a clinical term associated with vascular congestion observed on ophthalmoscopy irrespective of the presence of inflammation, and should not be used as a histological diagnosis.

Infiltrate, inflammatory cell (N) (Figure 15) **Uvea: Iris and Ciliary Body**

Species
Mouse; Rat.

Other Term(s) Used
None

Pathogenesis/cell of origin
Leukocytes that have entered the eye via the uveal vessels of the ciliary body and iris.

Diagnostic Features
- Infiltrates of leukocytes in the ciliary body or processes, and iris stroma and/or epithelium.
- Inflammatory features are not present.

Comment
Mononuclear cells, including lymphocyte aggregates, are found spontaneously in uveal tissues.

Inflammation (N) (Figures 12, 14, 16) **Uvea: Iris and Ciliary Body**

Species
Mouse; Rat.

Other Term(s) Used
None

Pathogenesis/cell of origin
Leukocytes that have entered the eye via the uveal vessels of the ciliary body and iris. Cell lineage varies with inciting cause.

Diagnostic Features
- Infiltrates of leukocytes in the ciliary body or processed, and iris stroma and/or epithelium.
- Inflammatory features such as edema and expansion of the stroma, hemorrhage, and/or necrosis are present.
- Vascular involvement is usually evident with inflammation (activated endothelia, damage to vascular walls, perivascular infiltrates).

Comment
Inflammation is the preferred diagnostic term used with appropriate modifiers as to cell type when features of inflammation are present. Inflammation of the iris or ciliary body may be associated with aqueous leukocytes and protein, which appear as irregular regions of eosinophilic, amorphous fluid in the anterior compartment of the eye. Leakage of protein into the aqueous is diagnosed as 'flare' on ophthalmic examination. Inflammation of the iris indicates a breach in the blood-ocular barrier, and a possible loss of immune deviation. Uveitis is a clinical term and should not be used as a histological diagnosis.

Pigment, increased/decreased, iris (N) **Uvea: Iris and Ciliary Body**

Species
Mouse; Rat.

Other Term(s) Used
Discoloration, iris; alteration in iris color

Pathogenesis/cell of origin
Change in the number of melanocytes within the stroma, or the quantity of pigment granules within the melanocytes. Only relevant in pigmented species or strains.

Diagnostic Features
- Increased numbers or size of melanocytes in the iris stroma.
- If decreased pigmentation, decreased number of melanocytes or decreased amount of pigment within melanocytes.

Differential Diagnoses
Sequel to hemorrhage (hemosiderin).

Comment
Pigment changes can occur following administration of compounds (for example urethane in neonatal hooded rats; Roe, Millican et al. 1963). Decreased pigmentation may be associated with inflammation, edema, and aging. Pigment changes can also be congenital (Schafer and Render 2013b). Increased pigment deposition occurs in DBA/2J mice homozygous for iris pigment dispersion or iris stromal atrophy (Smith, Sundberg, and John 2002b). Increased pigment and/or a change in pigment may also occur with topical application of prostanoid compounds such as latanoprost.

Vacuolation, cytoplasmic, epithelial (N) (Figure 17) **Uvea: Iris and Ciliary body**

Species
Mouse; Rat.

Other Term(s) Used
Lysosomal storage disease, varies with cause (e.g., phospholipidosis).

Pathogenesis/cell of origin
Epithelium of the iris or ciliary body processes. Metabolic defect leading to accumulation of molecules within the epithelial cells of iris, ciliary body processes, or ciliary muscle.

Dianostic Features
- Vacuolated spaces within the cytoplasm of the epithelial cells of the iris or ciliary processes, or within the ciliary muscle.

Comment
Cystine crystal accumulation has been reported in the ciliary body stroma and process epithelium of CTNS $^{-/-}$ mice, an animal model for cystinosis lysosomal storage disease (Kalatzis, Serratrice et al. 2007).

Lens

Degeneration, lens fiber (N) (Figures 12, 14, 18–21, 23) **Lens**

Species
Mouse; Rat.

Other Term(s) Used
Lens fiber swelling; lens fiber fragmentation; Morgagnian globule; bladder cells; liquefaction; cleft formation; cataract.

Pathogenesis/cell of origin
Degeneration results from biochemical changes that alter the homeostasis of the lens, denature the proteins of the lens, and/or disrupt the integrity of the lens fiber. The initial biochemical change is often acidification, whereupon fibers lose fluid, shrink, and fluid collects in clefts between fibers. With other pathogeneses, such as with osmotic changes, the fibers will instead swell and become globular ('Morgagnian globules'). Degeneration is a diagnostic term that encompasses many of the specific terms listed below.

Diagnostic Features
- Clefts - spaces form between lens fibers, which have a rounded profile, with accumulation of fluid with variable amounts of protein. Lens fibers may fragment if the lesion progresses.
- Fragmentation – swollen, membrane-bound fragments; rounded globules (Morgagnian globules).
- Liquefaction – collection of proteinaceous fluid within the lens cortex as small pockets or larger areas, in place of lens fibers.
- In severe cases, may be associated with dystrophic mineralization.

Differential Diagnoses
Artifact:
- It is important to recognize artifact lens fiber fragmentation due to fixation, which is often angular, and may result in cleft formation (this is most notable in nonhuman primate eyes fixed with modified Davidson's fluid). Careful comparison to concurrent controls is necessary.

Autolysis

Vacuolation
- See below

Comment

'Degeneration' may be used as an aggregate diagnostic term to include many of the nonspecific changes observed in the lens fibers, while more specific changes are best described as comments. In advanced disease the cortical fibers are completely liquefied and lost, and the nucleus of the lens is free floating in the lens capsule. Cataract is a clinical diagnostic term used to describe opacities visualized on ophthalmic examination, and should not be used as a histological diagnosis.

Dislocation, lens, anterior or posterior (N) (Figures 19, 20) **Lens**

Species

Mouse; Rat.

Other Term(s) Used

Lens luxation; lens displacement.

Pathogenesis

Rupture of zonular fibers (suspensory ligament of the lens) that suspend the lens behind the iris. Primary occurrence may be related to hereditary zonulary weakness. Spontaneous occurrence may be secondary to trauma, glaucoma, inflammation, and neoplasia.

Diagnostic Features

- On histology, the lens is displaced either into the anterior chamber (anterior luxation) or posterior compartment (posterior luxation).
- Chronic dislocation may be associated with secondary changes, such as inflammation, vitreal fibroplasia, and iridal-lens adhesions.

Differential Diagnoses

Artifact:

- Associated with processing, particularly trimming.

Comment

Posterior luxation may be associated with secondary trauma to the retina and cataract formation. Anterior luxation may be associated with adhesions between the anterior lens and posterior iris (synechia) or with the corneal endothelium. Fibroblastic transdifferentiation (metaplasia) of the anterior lens epithelial cells may occur as a sequela (Tanaka, Inagaki et al. 1995). Due to the frequent occurrence of artifact displacement of the lens during tissue processing, this diagnosis should be made with caution.

Fibroplasia, lens epithelium (N) (Figure 19) **Lens**

Species

Mouse; Rat.

Other Term(s) Used

Metaplasia, fibrous, or cellular-transdifferentiation, lens epithelium.

Pathogenesis/cell of origin

Injury to the lens and subsequent cellular transdifferentiation (metaplasia) of the anterior lenticular epithelium.

Diagnostic Features

- Spindloid cells and an eosinophilic collagenous matrix in place of the lens epithelium and subjacent lens fibers.
- Linear arrays of collagen.

Differential Diagnosis

Hyperplasia, Lens epithelium

- See below. (Figures 18, 56)

Fibrosis

- If mature collagen is present.

Comment

Following injury, the anterior lens epithelium assumes a myofibroblast-like phenotype that produces type I and type III collagen and glycosaminoglycans, forming fibrous tissue. Fibroplasia often occurs in association with hyperplasia of the anterior lenticular epithelium. A new lens capsule may be secreted over the fibrotic region following maturation.

Hypertrophy, lens capsule (N) **Lens**

Species

Mouse; Rat.

Other Term(s) Used

Increased size, lens capsule.

Pathogenesis/cell of origin

Anterior lenticular epithelium.

Diagnostic Features

- Increased thickness of lens capsule.
- May be uniform (age-related) or focal (possible response to injury).

Comment

The anterior lenticular epithelium continues to produce lens capsule material for the life of the animal, i.e., the anterior lens capsule will continue to thicken with age in the animal, while the posterior lens capsule does not.

Hypertrophy, lens epithelium (N) **Lens**

Species

Mouse; Rat.

Other Term(s) Used

Increased size, lens epithelium.

Pathogenesis/cell of origin

Injury to the anterior lenticular epithelium.

Diagnostic Features
- Enlarged or swollen cell profile.
- Often associated with adjacent swollen, pale lens fiber.

Differential Diagnosis
- Vacuolation, associated with inclusions.

Comment
Swollen lens fibers are most commonly seen in the area of the nuclear bow, particularly in association with damage caused by exposure to phototoxicants and UVA light. Bright eosinophilic spherical globules of denatured proteins (Morgagnian globules), may be present.

Hypertrophy, lens fiber (N) **Lens**

Species
Mouse; Rat.

Other Term(s) Used
Increased size/swelling of lens fiber; degeneration of lens fiber; 'bladder cells'.

Pathogenesis/cell of origin
Fluid intake by lens fibers most often occurs due to hyperosmotic conditions.

Diagnostic Features
- Swelling of lens fiber can vary from scattered individual fiber profiles that are increased in size, to numerous, enlarged fusiform cells with foamy cytoplasm ('bladder cells').
- Variable eosinophilic staining.

Differential Diagnosis
Degeneration
- See above

Comment
Increased glucose or other simple sugars, among other agents, can promote fluid intake resulting in swollen fibers. Swollen lens fibers may not produce opacities identifiable on ophthalmic examination, and may potentially be reversible. Simple sugars passively diffuse into the lens fibers, but once inside, they are actively reduced by aldose reductase (AR), which has high activity in the lens fibers. Glucose is converted to sorbitol, which does not readily diffuse out of the lens fiber. Significant accumulation of sorbitol within the fiber creates a hyperosmotic environment that results in passive diffusion of fluid into the fiber. Swelling may be irreversible with agents that are not metabolized by the lens fiber. Degeneration results (see above) if the change progresses and there is denaturation and coagulation of crystalline proteins, or if breaks occur in the fiber membrane.

Inflammation, lens (N) **Lens**

Species
Mouse; Rat.

Other Term(s) Used
Phacoclastic uveitis.

Pathogenesis/cell of origin
Leukocyte infiltrates (neutrophilic and/or granulomatous) within the lens.

Diagnostic Features
- Accumulation of neutrophils and/or macrophages into and around the lens.
- Lens fibers associated with the inflammatory cells are often liquefied or fragmented.

Comment
Leukocyte infitrates into the lens are generally not innocuous, and thus invariably imply the presence of inflammation. Infectious processes are common causes. Injury to the lens can result in inflammation but more often results in proliferation of the anterior lens capsule. Phacoclastic uveitis is a clinical term associated with rupture of the lens and inflammation.

Mineralization, lens fiber (N) (Figures 14, 21) **Lens**

Species
Mouse; Rat.

Other Term(s) Used
Calcification; dystrophic mineralization/calcification.

Pathogenesis/cell of origin
Injury to, or degeneration of, lens fibers resulting in mineral deposition, or calcification of the damaged tissue.

Diagnostic Features
- Lens fibers have intensely basophilic granules or crystalline material.

Comments
Mineral deposition or calcification is not an uncommon sequela to degenerative changes of the lens, particularly those that result in devitalization of the tissue.

Necrosis, lens epithelium (N) **Lens**

Species
Mouse; Rat.

Pathogenesis/cell of origin
Anterior lenticular epithelium toxicant or inflammatory injury.

Diagnostic Features
- See features of single cell necrosis described above.

- Focal, multifocal, or diffuse loss of anterior lenticular epithelium may occur.

Comment
Antineoplastics and radiomimetics can cause necrosis (or apoptosis) of the anterior lenticular epithelium.

Rupture, lens capsule (N) (Figures 22, 23) **Lens**

Species
Mouse; Rat.

Other Term(s) Used:
None

Pathogenesis/cell of origin
Posterior lens capsule.

Diagnostic Features
- Extruded lens fibers (into the vitreous) from the posterior aspect of the lens.
- Spatial defect or break in posterior lens capsule evident on histopathology.
- Free ends of the lens fibers tend to coil away from the site of the break.
- Adjacent lens fibers tend to have degenerative features.

Differential Diagnoses
Artifact

Comment
Spontaneous rupture of the lens capsule can occur in rodents as early as 10 weeks of age and is usually in the posterior portion of the lens since it is thinner than the anterior lens capsule (Tanaka, Inagaki et al. 1996). Rupture may also occur in association with cataracts or trauma. Rupture of the capsule can be associated with a significant inflammatory response in the vitreous and lens.

Vacuolation, lens epithelium or lens fiber (N) **Lens**

Species
Mouse; Rat.

Other Term(s) Used
Phospholipidosis.

Pathogenesis/cell of origin
Vacuolation of lens epithelium or fibers is associated with cytoplasmic inclusions that generally represent lysomal accumulation of molecules.

Diagnostic Features
- Foamy vacuolation of the cytoplasm of the anterior lens epithelium.
- Vacuoles are non-staining or contain lightly amphiphilic material.

Differential Diagnoses
Hypertrophy, Lens epithelium or Hypertrophy, Lens fiberlens Fiber liquification

Comment
Definitive diagnosis may require electron microscopy to demonstrate the presence of electron-dense lamellar inclusions within lysosomes. Several drugs are known to cause phospholipidosis resulting in lysomal accumulation of both the drug and cationic amphiphilic molecules in either the lens epithelium or lens fibers.

Vitreous

Agenesis, vitreous (N) (Figure 24) **Vitreous**

Species
Mouse; Rat.

Other Term(s) Used
Development anomaly; absent vitreous

Pathogenesis/cell of origin
Agenesis of the vitreous is associated with other ocular development disorders that result in microphthalmia.

Diagnostic Features
- The eye is markedly smaller then normal (microphthalmia).
- Internal structures are malformed, rudimentary, or absent.

Comment
Development of the vitreous is closely associated with that of the lens, retina, and retinal vasculature and thus development abnormalties in any one structure are reflected in the other structures, including the vitreous (Kingston et. al., 2014). Mutations in Pax6, Mitf, Cat4 and other genes have been implicated in the occurance in mice (Smith et al, 1994; Smith, John, and Nishina 2002; Collinson et al, 2000). While failure of the development of the vitreous has been reported in mice in association with microphthalmia (Smith, Roderick, Sundberg 1994), it is also possible that development of the primary vitreous may begin, but not be completed. Other potential causes include infectious diseases and toxicities. Experimental exposure to alcohol is a model for fetal alcohol syndrome in which microphthalmia occurs.

Persistent hyaloid vessels (N) (Figure 25) **Vitreous**

Species
Mouse; Rat.

Other Term(s) Used
Persistent primary vitreous.

Pathogenesis/cell of origin
Embryonic hyaloid vessels that fail to completely involute and regress.

Diagnostic Features
- Generally, only small remnants (1-5 arteries) or a single vessel with multiple branches extending from the optic disc into the vitreous cavity are observed.
- Vessels may extend from the optic disc through the vitreous to contact the posterior pole of the lens.
- Hyaloid vessels that extend along the inner surface of the sensory retina from the optic disc to the lens have also been reported (Heywood 1973).
- Hemorrhage in the vitreous may be an associated finding in rats.

Comment

Persistence of a portion of the embryonic hyaloid vessels is a congenital finding reported in rats (Hebel and Stromberg 1976, Taradach, Regnier et al. 1981, Taradach and Greaves 1984, Rubin 1986, Kuno, Usui et al. 1991, Shibuya, Satou et al. 1999, Williams 2002). Hyaloid vasculature gradually undergoes involution, especially during the first 6 weeks; the incidence is less than 1% by the end of one year (Heywood 1973). Mice have a similar hyaloid system as rats do that generally regresses by 30 days (Smith, John, and Nishina 2002). Intravitreal hemorrhage does not appear to be as common in mice as it is in rats (Rubin 1986).

Persistent hyperplastic primary vitreous (N) (Figure 26) **Vitreous**

Species

Mouse; Rat.

Other Term(s) Used

PHPV; persistent fetal vasculature (PFV).

Pathogenesis/cell of origin

Development anomaly that occurs from failure of the embryological vitreous and hyaloid vasculature (used in formation of the fetal eye) to regress.

Diagnostic Features
- Excess mesenchymal tissue; often associated with persistent hyaloid vessels.
- Generally fibrous tissue, but may be cartilaginous tissue.
- Blood vessels and mesenchymal tissue extend from the optic disc to the posterior capsule of the lens near the posterior pole where it blends into the embryonic vessel, the posterior tunic vasculosa lentis (hyperplastic tunica vasculosa lentis).

Comment

Mutations are a common cause of persistent hyperplastic primary vitreous in mice (Smith, John, and Nishina 2002).

Fibroplasia; Fibrosis, vitreous (N) (Figures 27–31) **Vitreous**

Species

Mouse; Rat.

Other Term(s) Used

Vitreal membranes; fibrovascular tissue proliferation.

Pathogenesis/cell of origin

Multiple cell origins have been implicated in the formation of vitreal membranes including hyalocytes, spindle cells associated with zonule fibrils, Müller cells, glial cells, and RPE. Current thinking is that these cells transdifferentiate and acquire phenotypic characteristics of fibroblasts or myofibroblasts with contractile proteins.

Diagnostic Features
- Linear strands of cells with a fibroplastic phenotype located anywhere within the vitreous.
- Linear arrays of fibrillary collagenous tissue strands, often multilayered, that resemble a mat of fibrous connective tissue.
- Fibroplastic strands of tissue frequently tether to fixed structures such as the lens, retina, and optic disc.
- Vitreal fibroplasia is often associated with chronic inflammation, hypertrophic hyalocytes, and pigmented hyalocytes.

Differential Diagnosis

Fibrosis:
- Mature collagen of relatively low cellularity is present; fibrosis is more likely to be observed in end-stage lesions.

Comment

Cell transdifferentiation, proliferation, and migration are thought to occur in the eye in a similar manner to fibrotic reactions that occur systemically. Cytokines, in particular TGBβ, have been ascribed a primary role in the process. Fibroblastic membranes tend to tether to fixed ocular tissues, such as the lens, retina, and optic nerve disc. Because they contain contractile proteins, tension is transferred to these structures, and can result in lens luxation, retinal detachments, and optic nerve prolapse. Vitreal membranes appear as vitreal opacities on ophthalmic examination. In rats, vitreous fibroplasia occurs with or without vessels, and may be accompanied by hemorrhage, pigment-laden macrophages and inflammatory cells (Taradach and Greaves 1984). Fibrovascularization, or organization of the vitreous body, has also been reported in F344 rats with advanced retinal degeneration (Yoshitomi and Boorman 1990), and likely represents a similar pathogenesis. Vitreal fibroplasia tends to be a dynamic and progressive process. The presence of mature collagen may warrant a diagnosis of fibrosis.

Hemorrhage (N) (Figure 29) **Vitreous**

Species

Mouse; Rat.

Other Term(s) Used

None

Histiogenesis/cell of origin
Intraocular blood vessels.

Diagnostic Features
- Presence of erythrocytes, ranging from a population of scattered cells to large aggregates, accompanied by serum.

Differential diagnosis
Erythrocytes, Extravasation
- Breakdown of tight junctions between endothelial cells of retinal blood vessels.

Comment
A common source of spontaneous hemorrhage in young animals is a patent vascular hyaloid. Erythrocytes may be derived from patent hyaloid vessels for 3 weeks or more following birth (Hebel and Stromberg 1976). Small numbers of erythrocytes and small clots that vary in size eventually resolve, generally without sequelae (Rubin, 1986).

Hemosiderin-laden macrophages (N) (Figures 29–31) **Vitreous**

Species
Mouse; Rat.

Other Term(s) Used:
None

Pathogenesis/cell of origin
Hemorrhage from any cause may result in red blood cell engulfment and processing by hyalocytes (resident macrophages) or recruited macrophages (similar to that observed systemically). Patent hyaloid vessels are a potential source of RBCs.

Diagnostic Features
- Hyalocytes and macrophages containing brown pigmented granules are observed, primarily in the cortical vitreous, wherever hyalocytes concentrate (i.e. adjacent to posterior retina and optic disc).

Comment
Because of the slow turnover of fluid and cellular components of the vitreous, cells containing hemosiderin may persist in the vitreous for prolonged periods of time following the occurrence of hemorrhage.

Infiltrate, inflammatory cell (N) **Vitreous**

Species
Mouse; Rat.

Other Term(s) Used
Hyalitis (if limited to increased numbers of hyalocytes) and infiltration, inflammatory cell, if additional leukocytes are present.

Diagnostic Features
- Varies with cell lineage and inciting cause.
- Increased numbers of hyalocytes.
- Leukocytes recruited from the systemic circulation; can be observed near the retinal surface as part of the immune surveillance process of the eye.

Comment
As resident macrophages, hyalocytes are responsible for clearing debris from the vitreous, and are responsive to perturbations within the eye, especially the vitreous. Increased numbers and increased variability in appearance is associated with intravitreal injections in the absence of other inflammatory cell types suggesting that changes in hyalocytes can be sensitive indicator of subtle changes in the eye. Due to the slow turnover rate of the vitreous, hyalocytes and other inflammatory cells tend to have a prolonged presence in the vitreous, lasting well beyond that of the inciting cause.

Inflammation (N) (Figures 27, 30) **Vitreous**

Species
Mouse; Rat.

Other Term(s) Used
Vitritis.

Diagnostic Features
Varies with cell lineage and inciting cause.
- Leukocytes derived from the systemic circulation.
- Leukocytes are most often observed on histopathology at or near the retinal surface, posterior to the lens, or near the optic disc, but can also be observed throughout the vitreous.
- Recruited leukocytes typically result from secondary spread of inflammation from other structures of the globe (Taradach and Greaves 1984).
- Granulomatous inflammation may result in cellular aggregates within the vitreous that appear as opacities on ophthalmic examination.

Comment
Ocular inflammation can occur from a number of inciting causes, including infectious and immune-mediated diseases, metabolic disorders, toxicities, and trauma. Inflammation in the vitreous implies a breach of the BOB, and loss of immune deviation. Cytokine changes to the intraocular environment that are associated with inflammatory conditions can induce transdifferentiation of ocular cells and result in fibroplasia (vitreous or retinal/epiretinal fibroplasia).

Metaplasia, bone or cartilage (N) (Figures 32, 33) **Vitreous**

Species
Mouse; Rat.

Other Term(s) Used
Osseous metaplasia; cartilaginous metaplasia; cellular transdifferentiation.

Pathogenesis/cell of origin
Transdifferentiation of a cell population to bone or cartlilage.

Diagnostic Features
- Presence of bone or cartilage matrix in the vitreous body (Taradach and Greaves 1984).

Differential Diagnosis
Mineralization
- See below.

Comment
Mechanism of intraocular bone or cartilage formation is poorly understood, but may be seen with ocular trauma, or possibly conditions that result in anoxia and degeneration of the vitreous. Cellular transdifferentiation requires the elaboration of appropriate cytokines that favor bone or cartilage production. Both mineralization and bone or cartilage metaplasia result in vitreal opacities on ophthalmic examination.

Mineralization, vitreous (N) **Vitreous**

Species
Mouse; Rat.

Other Term(s) Used
Metastatic mineralization or calcification; dystrophic calcification.

Pathogenesis/cell of origin
Vitreous matrix, or cells within the vitreous. Deposition of calcium salts within the vitreous.

Diagnostic Features
- Irregular deposits of mineral; may be located anywhere within the vitreous.
- May be accompanied by degenerative features in adjacent ocular structures (dystrophic calcification).

Differential Diagnosis
Vitreous metaplasia, Bone or Cartilage
- See above.

Comment
Mineral deposition in the vitreous is similar to that which occurs systemically from two different processes: a) systemic metabolic disorder of calcium regulation resulting in deposition of calcium salts in otherwise normal tissue (metastatic calcification or mineralization), and b) deposition of calcium in tissue as a degenerative process or secondary to trauma (dystrophic calcification). Conditions that favor a dystrophic process include the presence of divitalized cells, and/or conditions that result in anoxia and degeneration of the vitreous.

Retina

Congenital

Retinal rosettes (N) (Figure 34) **Retina**

Species
Mouse; Rat.

Other Term(s) Used
Retinal dysplasia; linear retinopathy; retinochoroidal degeneration; retinal dystrophy; retinal anomaly.

Pathogenesis/cell of origin
Non-specific response to diverse stimuli that affect retinal cell differentiation during development.

Diagnostic Features
- Focal to multifocal rosette-like and tubular structures expanding and distorting the inner and outer nuclear layers.
- Rarely lesions can diffusely affect the retina.
- Rosette-like and tubular structures can present variable morphology with a combination of the following features:
- One to multiple layers of cells with nuclear profiles similar to neurons of the inner and outer nuclear layers.
- Nuclei polarized away from the center or "lumen" of the rosette.
- Eosinophilic linear structures resembling photoreceptors inner segments and/or ciliated cells from primitive neuroepithelial origin may be observed in the inner layer of the rosette.
- Presence of a basement membrane-like structure near the center of the rosette resembling the external limiting membrane of the retina.
- RPE-like cells or macrophages may be in the center of the rosette.

Differential Diagnoses
Retinal folds
- See below.

Artifact of processing:
- Differential-rate fixation of the vitreous and retina can lead to vitreous shrinkage and retinal traction, creating artifact rosettes.

Comment
Retinal rosettes are a focal or multifocal disorganization of the sensory retina due to faulty development. In the rat rosettes appear as unilateral linear elevations of the retina on ophthalmic examination (Hubert, Gillet et al. 1994) and can be induced by the administration of cytosine arabi-

nose, cycasin, N-methyl-N-nitrosurea and trimethyltin (Schafer and Render 2013a). Retinal rosettes (and folds, see below) may not have all layers of the retina intact, often show loss of the outer nuclear layer, and may have direct abutment of the retina onto the choroid or even the sclera (Schafer and Render 2013a).

Retinal folds (N) (Figure 35) **Retina**

Species
Mouse; Rat.

Other Term(s) Used:
None

Pathogenesis/cell of origin
Incidental, spontaneous, or associated with traction from fibroblastic membranes at the retinal surface and subretinal hemorrhage.

Diagnostic Features
- Focal inward projections of the retina with possible separation of the photoreceptor from the retinal pigmented epithelium.
- Less severe lesions affect only the outer retinal layers and present as micro-retinal detachment, with subretinal accumulation of phagocytic cells and do not affect the retinal surface contour.
- More severe folds affect all retinal layers, and can exhibit with subretinal hemorrhage and debris from the photoreceptor outer segments.

Differential Diagnoses
Artifact retinal fold:
- Related to 70% ethanol fixation, and/or relative time differences in tissue fixation. True retinal folds are differentiated from artifact by an association with preretinal traction membranes, sub-retinal deposits, hemorrhage, or aggregates of RPE cells (Render, Schafer et al. 2013).

Comment
Spontaneous retinal folds have been reported in mice and rats (Sprague-Dawley and Wistar) (Hubert, Gillet et al. 1994). Folds found in Sheffield-Wistar rats may be congenital and associated with microphthalmia (Poulsom and Hayes 1988). Artifactual retinal folds (Lange's folds) have been described in the peripheral retina of young animals, and is associated with tissue fixation with 70% ethanol (Gartner and Henkind 1981). When retinal folds are sectioned in a tangential histologic plane they might resemble rosettes.

Acquired

Retinal Atrophy (Figures 36–38) **Retina**

Other Term(s) Used
Decreased cell layers; retina; decreased thickness, retina.

Histiogenesis/cell of origin
Degenerative process of the retina resulting in cell loss and collapse of the retinal layers; atrophy may be specific to the ganglion cell layer and/or inner nuclear layer, or outer retinal layer due to the susceptibility and sensitivity of the cell populations in those areas to the inciting cause, or to both (global). Global atrophy can also be an end-stage lesion associated with secondary degeneration of retinal cells that progresses from one cell layer to the next.

Inner retinal atrophy (N) (Figure 36) **Retina**

Species
Mouse; Rat.

Pathogenesis/cell of origin
Atrophy of the inner retina (inner nuclear, inner plexiform and ganglion cell layers) may be secondary to increased intraocular pressure, compressive lesions of the optic nerve, or direct toxicity resulting in degeneration of retinal cells and eventual cell loss.

Diagnostic Features
- Decreased numbers of ganglion cells.
- Thinning of the nerve fiber and inner plexiform layers.
- Loss of nuclei in the inner nuclear layer.

Comment
The most common causes of loss of ganglion cells and their axon fibers in the nerve fiber layer are 1) an increase intraocular pressure resulting in degeneration of these cells, and subsequent atrophy of the optic nerve and secondary atrophy of the inner nuclear layer, and 2) compressive lesions on the extraocular portion of the optic nerve leading to axonal degeneration and subsequent ganglion cell death. The retinal ganglion cells are target of several known retinal toxicants (e.g. carbon disulfide, doxorubicin, glutamate and lidocaine). A few toxicants, like ethylcholine mustard aziridinium ion (AF64A), preferentially target the cells in the inner nuclear layer (Ramos, Reilly et al. 2011).

Outer retinal atrophy (N) (Figure 37) **Retina**

Species
Mouse; Rat.

Pathogenesis/cell of origin
Conditions resulting in atrophy of the outer retinal layers (outer plexiform and photoreceptor layers) include hereditary or direct photoreceptor injury, and/or RPE toxicity. Atrophy may be incidental following choroidal circular disturbance (Tanaka, Inagaki et al. 1993).

Diagnostic Features
- Decreased numbers of nuclei in the outer nuclear layer, resulting in decreased thickness of the retina.
- Decreased thickness or collapse of the outer plexiform layer with fusion of the inner and outer nuclear layers.

- Loss of inner and outer segments of the photoreceptors.
- Displacement of photoreceptor nuclei to the inner and outer segment layers.
- Hypertrophy of RPE cells, and possible migration of RPE cells and macrophages into the sensory retina.

Comment

Outer retinal atrophy or degeneration is a broad term that indicates loss of photoreceptors from a variety of causes that include hereditary, aging, toxicity, phototoxicity, nutritional deficiencies, retinal detachment, and inflammation. Photoreceptors have high metabolic demands, and thus are susceptible to toxins that interfere with energy metabolism, e.g. nicotinamide phosphoribosyltransferase (NAMPT) inhibitors (Zabka, Singh et al. 2015). Genetic forms of atrophy occur in several strains of mice, including several mutant and transgenic mouse strains and rats. Ocular screening should be conducted prior to study inclusion and animals exhibiting atrophy removed, or equally distributed amongst dose groups. Photoreceptor degeneration may occur with remarkable sparing of the inner retinal layers and RPE. Outer retinal atrophy in rodents is characteristic of senile retinal degeneration, which has a tendency to begin at the peripheral retina (Hockwin, Green et al. 1992). Light-induced retinal atrophy/degeneration (usually RPE cells are not affected) occurs in albino rodents and is caused by prolonged exposure to light or exposure to high intensity light. These lighting conditions may occur if animals are kept in cages on the top of racks close to the room light source (De Vera Mudry, Kronenberg et al. 2013). In contrast, focal atrophy of outer retinal segments following choroidal circular disturbance is always associated with loss of regional RPE cells (Tanaka, Inagaki et al. 1993).

Global retinal atrophy (N) (Figure 38) **Retina**

Species

Mouse; Rat.

Other Term(s) Used

Scar; Glial scar; Diffuse gliosis.

Pathogenesis/cell of origin

Involvement of all cell layers; end stage retinal lesion regardless of the initial cause.

Diagnostic Features

- Decreased numbers of cells in all layers and associated collapse of the plexiform layers.
- Complete collapse of retinal architecture.
- Replacement of the retinal tissue by a fibrous layer with glial cells and occasional neurons.

Comment

Retinal degeneration may occur as a spontaneous (hereditary, aging, exposure to light, nutrient deficiency, inflammatory or trauma) or iatrogenic (e.g. laser treatment, subretinal injection) finding and therefore must be differentiated from treatment-related toxic effects (Schafer and Render 2013a).

Detachment, retina (N) (Figure 39) **Retina**

Species

Mouse; Rat.

Other Term(s) Used:

None

Pathogenesis/cell of origin

Outer retina; associated with trauma, intravitreal injections, chorioretinal inflammation, vitreal degeneration and traction resulting from fibroplasia at the retinal surface (retinal/epiretinal fibroplasia).

Diagnostic Features

- Separation of the photoreceptor outer segment from the retinal pigmented epithelium.
- Subretinal accumulation of fluid, macrophages, red blood cells and cellular debris.
- Secondary hypertrophy of the retinal pigmented epithelium (RPE tombstones).
- Degeneration/atrophy of the photoreceptor outer segments.

Differential Diagnoses

Artifact retinal detachment

Comment

Artifact retinal detachment can be differentiated from true retinal detachment by the lack of subretinal deposits and absence of hypertrophy of the RPE cells. Hypertrophy of the RPE needs to be distinguished from RPE "tenting", an artifact that result from traumatic shearing of the retina during tissue trimming. In contrast to RPE hypertrophy, "tented" RPE cells have angular apices with fragments of photoreceptor outer segments still attached to the surface. Spontaneous retinal detachment is uncommon in laboratory animals, but may occur rarely in B6C3F1 mice and Sprague-Dawley rats (Kuno, Usui et al. 1991).

Displacement, photoreceptor nuclei (N) (Figure 40) **Retina**

Species

Mouse; Rat.

Other Term(s) Used

Photoreceptor displaced nuclei (PDN); subretinal photoreceptor cells; colloquially known as "torpedo" cells.

Pathogenesis/cell of origin

Photoreceptors of the outer nuclear layer; age-related degenerative process of the photoreceptors.

Diagnostic Features
- Photoreceptor cell located external to the retinal outer limiting membrane.
- Cell with scant or no cytoplasm.
- Nuclei morphology very similar to photoreceptor nuclei in the outer nuclear layer; may also be pyknotic.

Differential Diagnoses

Monocytes, (or macrophages):
- Larger cells with cytoplasm; may contain melanin or hemosiderin pigment, and may be associated with inflammation (Lai 1980).

Detached retinal pigment epithelial cells:
- Larger cells with cytoplasm; may contain melanin pigment or other inclusions, and may be associated with detachment of the sensory retina (Lai 1980).

Artifact
- Displacement of photoreceptor nuclei during microtomy.

Comment

Displaced photoreceptor nuclei (PDN) occur in humans and laboratory animals including rats and mice. Both non-pyknotic and pyknotic nuclei may be found in control eyes (Lai 1980; Lai, Masuda et al. 1982), but also in areas of retinal degeneration or inflammation, or both (Saunders and Rubin 1975b; Geiss and Yoshitomi 1999). Displaced nuclei were observed in all strains of rats with a frequency of approximately 50% in normal retinas; they were observed more frequently in very young developing retinas and in aged retinas (Lai 1980).

Fibroplasia, Retinal or epiretinal (N) **Retina**

Species

Mouse; Rat.

Other Term(s) Used

Epiretinal membrane; vitreal traction band

Pathogenesis/cell of origin

Multiple cell origins have been implicated in fibroplasia at the retinal surface, including, hyalocytes, fibroblasts, astrocytes, glial cells, and Müller cells. Cell transdifferntiation occurs as a sequela to disruptions of the vitreous body or internal limiting membrane, retinal or vitreal inflammation, neovascular retinal disease or intraocular surgery.

Diagnostic Features
- A fibrocellular layer carpeting the inner (vitreal) surface of the retina.
- Cellular components may be multiple: fibrocytes, glial cells and retinal pigment epithelial cells.
- Inflammatory cells can be present when associated with ocular or retinal inflammation.
- Small vascular profiles can be present when associated with retinal vascular proliferations (neovascularization).

Special Techniques for Diagnostics
- Histochemical stains for collagen (e.g. Masson's trichrome or Picrosirius red) can be useful to highlight the membranes.
- Immunohistochemistry for cell specific proteins can demonstrate the different origins of cells present in the membranes. GFAP can be useful to highlight the presence of glial cell component.

Differential Diagnoses

Pre-retinal arteriolar loop

Fibrosis (Figure 28)
- Replacement of the retina with fibrous connective tissue; usually observed as a reparative process following tissue injury and necrosis.

Comment

'Epiretinal membrane' is a clinical term for fibroplasia found at, or on the retinal surface. Idiopathic epiretinal membranes (iERM) are characterized by the growth of fibrocellular tissue on the internal limiting membrane (ILM). iERM can range from subtle cellophane-like films without visual consequences to markedly contractile membranes that can cause metamorphopsia and decreased visual acuity. The complete pathogenesis of iERM is unknown, but many theories have been proposed. The most widely accepted theory is that iERM is a consequence of surface breaks in the ILM of the retina and forms within the cortical vitreous, which serves as the structural component and provides a medium upon which glial cells and hyalocytes can proliferate. Impaired vision can result from retinal traction and detachment, or impediment of light transmission.

Increased numbers, glial cells (N) (Figure 41) **Retina**

Species

Mouse; Rat.

Other Term(s) Used

Gliosis.

Pathogenesis/cell of origin

Glial cells; proliferation or migration of glial cells may occur in response to injury or insult, or be incidental.

Diagnostic Features
- Localized to the retina around the optic nerve head in incidental lesions. May occur elsewhere associated with retinal injury.
- Expanded nerve fiber layer containing cells with elongated nuclei, fibrillar eosinophilic cytoplasm and indistinct membranes.

Special Techniques for Diagnostics

The cells are immunohistochemically positive for glial fibrillary acidic protein (GFAP).

Comment

Retinal gliosis is seen in rats as a focal lesion localized in the peripapillary retina (Adams, Auerbach et al. 2011). For diffuse retinal gliosis, refer to Atrophy/degeneration, Global.

Infiltrate, inflammatory cell (N) **Retina**

Species

Mouse; Rat.

Other Term(s) Used:

None

Pathogenesis/cell of origin

Most often lymphoid, but may be myeloid. The pathogenesis is uncertain, but presumably a self-limiting response designed for immune surveillance and minor tissue repair activities. Lymphocyte infiltrates are often observed with immunological responses to delivery of foreign antigens (monoclonal antibodies) to the intraocular space.

Diagnostic Features

- Foci of lymphocytes and rare plasma cells surrounding retinal capillaries within the perivascular space, without other features of inflammation.

Differential Diagnoses

Inflammation:

- Inflammatory cellular infiltrate associated with edema, congestion, hemorrhage, necrosis and increased numbers of glial cells (gliosis) of the retinal tissue.

Comment

The term "infiltrate" is recommended followed by the predominant cell type (neutrophilic, eosinophilic, lymphocytic, plasmacytic or histiocytic) or mixture of different cell types (mixed). The most predominantly and frequently observed inflammatory cell infiltrate in the retina is lymphocytic. Small focal to multifocal lymphocytic infiltrates are thought to be incidental background findings.

Inflammation (N) **Retina**

Species

Mouse; Rat.

Other Term(s) Used

Retinitis.

Pathogenesis/cell of origin

Inflammation can occur in any cell layer. Inflammation may occur from immune-mediated etiologies, infectious agents, trauma, be drug-induced, or experimentally induced.

Diagnostic Features

- Inflammatory cellular infiltrate associated with edema, congestion, hemorrhage and necrosis.
- Evolves to retinal degeneration and glial cell proliferation (gliosis).
- Can be associated with inflammation of the choroid, focal retinal detachment, and loss of photoreceptors.

Differential Diagnoses

Infiltrate, inflammatory cell

Comment

Spontaneous retinal inflammation is rare in the mouse and rat, but can be seen unilaterally secondary to trauma. Retinal inflammation usually occurs secondary to inflammation of the choroid and results in retinal degeneration (Schafer and Render 2013a). Virally induced retinitis and immune-mediated retinitis are well-known disease models in mice (Geiss and Yoshitomi 1999).

Mineralization (N) (Figure 42) **Retina**

Species

Mouse; Rat.

Other Term(s) Used

Calcification.

Pathogenesis/cell of origin

Can occur in any cell layer. Mineralization in the retina is presumed to be associated with a primary vascular wall lesion or be secondary to dystrophic events in necrotic areas (see Mineralization, Vitreous, above).

Diagnostic Features

- Variably sized, often irregular, purple/blue foci in H&E-stained retinal sections.
- Vascular walls are usually involved.
- Laminated appearance (alternating dark and light zones) is typical.

Special Techniques for Diagnostics

Von Kossa stain for calcium may be useful in paraffin sections, though the chelation chemistry (silver nitrate) is not specific for calcium salts; Alizarin red S may also be used. Nonacidic fixatives such as neutral buffered 10% formalin or alcohol are best for tissues containing calcium deposits (Bancroft and Gamble 2002).

Differential Diagnoses

Deposits, subretina (drusen; associated with RPE).

Bone metaplasia

Comment

Mineralization can be an incidental lesion.

Myelin, increased (N) (Figure 43) **Retina**

Species
Mouse; Rat.

Other Term(s) Used
Hypertrophy, myelin.

Pathogenesis/cell of origin
Ganglion cells; developmental anomaly that is generally incidental.

Diagnostic Features
- Presence of myelinated axons in the nerve fiber layer at the central (peri-papillary) retina.
- Myelinated axons form small clusters at the retinal surface, and can cause focal thickening of the retina.

Special Techniques for Diagnostics
LFB will stain myelin blue to green and may be useful for diagnosis.

Comment
Myelinated retinal nerve fibers have been seen more frequently in pigmented rats and had been described in Long-Evans and BW rats (Rubin 1986; Hubert, Gillet et al. 1994). It is suggested to represent a developmental rather than a congenital anomaly (Rubin 1986).

Necrosis; Necrosis, single cell (N) **Retina**

Species
Mouse; Rat.

Other Term(s) Used
Homogenizing cell change; ischemic cell change; metabolic arrest change; oncotic necrosis; colloquially known as "red dead" neurons.

Pathogenesis/cell of origin
Ganglion cell bodies, secondary retinal neurons or photoreceptor cells; recent cell death, typically affecting multiple retinal neurons.

Diagnostic Features
- Shrunken, often angular ganglion cells with hypereosinophilic cytoplasm in H&E-stained paraffin sections.
- Nuclear consolidation, sometimes with shrinkage (early stages).
- Karyorrhexis or karyolysis (later stages).
- May see swollen cells, cytoplasmic vacuoles, or cytoplasmic blebs.
- Necrosis: focal, multifocal or focally extensive regions of the retina containing necrotic cells and cell debris.

Special Techniques for Diagnostics
Necrotic neurons are specifically labeled by:
- Fluorescent stains (e.g., Fluoro-Jade B or Fluoro- Jade C) (Schmued, Stowers et al. 2005) performed on 5- to 10-µm-thick (i.e., routine) perfusion-fixed, paraffin embedded sections. Affected cells appear bright green against a dark field. (Note: erythrocytes that remain in blood vessels of immersion-fixed specimens will autofluoresce, which may make detection of necrotic neurons more difficult.).
- Cupric–silver stains (Switzer 2000) in 30- to 40- mm-thick frozen sections of unfixed tissue. Affected cells are black against a pale-yellow background.
- Electron microscopy: condensed, swollen or ruptured mitochondria; swollen or ruptured lysosomes; disruption of cell membranes.

Differential Diagnoses
Dark neuron artifact:
- Evident as spiky basophilic neurons due to shrinkage of both nucleus and cytoplasm with contracture of the neuronal cell body; often associated with a prominent, tortuous, basophilic apical dendrite.

Comment
Neuronal necrosis is a common end-stage cellular response to irreversible injury. It may be induced by many causes, but the most common are metabolic dysfunction, ischemia, or toxicant exposure (chemicals, drugs, or metals). The intracellular biochemical alterations that ultimately lead to neuron destruction can be triggered by many different mechanisms, but neuronal necrosis in the retina refers to the pathway by which disruption of cellular energy systems results in fluid accumulation within organelles (microvacuolation) and eventually the entire soma (swelling, or oncosis) rather than the apoptotic cascade. (McMartin, O'Donoghue et al. 1997). Necrosis is generally associated with inflammation, but can occasionally precede inflammation such as occurs with a vascular injury (e.g. coagulative necrosis), chronic hypoxia, or cytotoxic cell death.

Pigment, increased (N) **Retina**

Species
Mouse; Rat.

Other Term(s) Used
Lipofuscinosis.

Pathogenesis/cell of origin
Lipofuscin represents residual bodies derived from autophagosomal lysosomes and is composed of polymers of lipid and phospholipid complexed with protein. Lipofuscin accumulates with age in retinal neurons, and is associated with free radical damage.

Diagnostic Features
- Presence of brown pigment granules in neuronal cytoplasm, most evident in ganglion cells, generally of medium-to-large-sized cells.

- The color of pigment granules varies from faint yellow to dark brown; some are eosinophilic (ceroid).

Special Techniques for Diagnostics
- Lipofuscin granules may be detected using several special stains: pink using PAS, pale red to red by Oil Red O, dark blue to purple by LFB, and pale blue to blue by Schmorl's technique for melanin; they are also acid fast by Ziehl-Neelsen.
- Lapham's method (Lapham, Johnstone et al. 1964) is highly specific for neural lipofuscin.
- Autofluorescence can be identified in H&E or unstained slides using a fluorescent microscope.

Comment

Lipofuscin should not form part of the diagnostic term in the absence of a confirmatory stain, although it may be mentioned in discussion. Lipofuscin accumulation results from age-related reductions in the efficiency with which neural cells eliminate degradation by-products (Kreutzberg, Blakemore, and Graeber 1997). Lipofuscin arises in the cell bodies of neurons, astrocytes, and oligodendrocytes by lipid peroxidation in cell membranes. Lipofuscin seems to accumulate without deleterious effects to the retinal neural cells.

Vacuolation, cytoplasmic (N) **Retina**

Species

Mouse; Rat.

Other Term(s) Used:

None

Pathogenesis/cell of origin

Retinal neurons and Müller cells. Vacuolation occurs from either a degenerative or toxic process leading to retention of fluid or metabolic byproducts inside a subcellular compartment, and expansion of intraneuronal cytoplasm or membrane-bound organelles.

Diagnostic Features
- Cytoplasmic vacuolation (usually clear or pale eosinophilic) of ganglion cells, photoreceptors segments or Müller cells.

Special Techniques for Diagnostics

Neuronal vacuoles in some storage diseases or in induced phospholipidosis may be confirmed by electron microscopy or by using special stains (e.g., Luxol fast blue [LFB], periodic acid-Schiff [PAS], or Sudan black) to detect a specific biochemical component within vacuoles.

Differential Diagnoses

Vacuolation of retinal neuropil (extracellular edema)

Vacuolation artifact due to postmortem autolysis:
- Improper collection, handling, or fixation of the globe at the time of necropsy; or prolonged immersion (e.g., over the weekend) in ethanol baths during tissue dehydration. Artifactual vacuolation should not be recorded in the pathology findings data set.

Comment

Hexachlorophene causes vacuolation and degeneration of photoreceptor outer segments, and chloroquine causes vacuolation in neurons and Müller cells.

Vacuolation, extracellular (N) (Figure 44) **Retina**

Species

Mouse; Rat.

Other Term(s) Used

Retinal edema, retinoschisis.

Pathogenesis/cell of origin

Involvement of any retinal layer, often multiple. Degenerative or toxic processes.

Diagnostic Features
- Presence of clear spaces, expanding various retinal layers.
- May be associated with decreased numbers of cells within the affected layer.

Differential Diagnoses

Fixation or handling artifact

cell loss:
- Clear spaces in nuclear layers due to decreased nuclei.
- Clear spaces in plexiform layers due to loss of cell dentrites and axons.

Comment

Extracellular vacuolation in the retina can be observed in multiple degenerative processes and represent reorganization of the retinal parenchyma after cell loss. In detached retinas, extensive clear spaces are commonly seen and may represent tissue edema, which has been erroneously referred to as retinoschisis. Retinoschisis is splitting of the retina between layers to form large spaces and may occur with extensive retinal edema.

Vascular Changes

Arteriolar loop, pre-retinal (N) (Figure 45) **Retina**

Species

Mouse; Rat.

Other Term(s) Used

Vascular anomaly

Pathogenesis/cell of origin
Incidental, abnormal branching of the central retinal artery.

Diagnostic Features
- Arteriole emerging from the central retinal artery, coursing through the posterior vitreous and reconnecting to the inner retina.
- Perivascular intravitreal hemorrhage can occur.

Special Techniques for Diagnostics
Serial sections through the tissue might be necessary to track the progression of the vessel.

Differential Diagnoses
Persistent hyperplastic primary vitreous (PHPV)

Comment
Pre-retinal arteriolar loops are common abnormalities in Sprague-Dawley rats (Tanaka, Inagaki et al. 1994).

Hemorrhage (N) (Figure 46) **Retina**

Species
Mouse; Rat.

Other Term(s) Used
None.

Pathogenesis/cell of origin
Vascular disruption. Depending on size and distribution, either no clinical signs or extension into the subretinal space leading to retinal detachment and blindness.

Diagnostic Features
- Distribution of hemorrhage is usually focal to multifocal but can be extensive when caused by traumatic events.
- Retinal hemorrhage often happens in close proximity to the capillaries.
- Chronic lesions may be associated with hemosiderosis.

Special Techniques for Diagnostics
Special stains for iron accumulation (e.g. Prussian blue and Perl's iron stain) can be used to identify hemosiderin in old sites of hemorrhage.

Differential Diagnoses
Retinal infarcts

Comment
Retinal hemorrhages can occur in a variety of primary clotting disorders, thrombocytopenia of any cause, retinal hypertension, inflammatory retinal conditions, ocular trauma, or from compression to the animal during handling.

Neovascularization (H) **Uvea: Choroid**

Species
Mouse; Rat.

Other Term(s) Used
Choroidal neovascularization (CNV).

Pathogenesis/cell of origin
New vessel growth from pre-existing vasculature, secondary to an ischemic process, and/or release of proangiogenic factors (i.e. VEGF).

Diagnostic Features
- Growth of new blood vessels that originate from the choroid through a break in Bruch's membrane into the space below the retinal pigment epithelium (sub-RPE) or into the subretinal space (between the photoreceptors and RPE).
- Newly formed blood vessels may infiltrate the retina.
- Subretinal, retinal, and vitreal hemorrhages can occur.
- Retinal detachment associated with subretinal hemorrhage.

Special Techniques for Diagnostics
Choroidal and retinal vascular changes are evaluated clinically by vascular angiography; microscopically, via immunohistochemistry or in situ-hybridization for angiogenic and endothelial cell markers (e.g., vascular endothelial growth factor); by microscopic examination of retinal whole mounts, and by transmission electron microscopy.

Differential Diagnoses
Retinal neovascularization:
- Retinal neovascularization is differentiated from CNV by vascular profiles that extend from the IPL and INL into the outer retinal layers, or from the IPL and ganglion cell layers into the inner limiting membrane, or by vascular tufts that project into the vitreous. Neovascular profiles can also contact the RPE cells and colonize the subretinal space similar to CNV. The main differential diagnostic feature is the presence of an intact Bruch's membrane in retinal neovascularization, suggesting retinal origin of the vessels. Transmission electron microscopy might be necessary to confirm the status of Bruch's membrane.

Comment
Neovascularization is spontaneous in the mutant mouse strain JR5558, which exhibits early, reproducible and spontaneous bilateral CNV, accompanied by subsequent retinal anastomosis. In this model, chorioretinal parainflammation is present prior to frank CNV, and is associated with upregulation of VEGF, hyperpermeability of the choriocapillaris, and neuroglial cell loss/dysfunction (Nagai, Izumi-Nagai et al. 2011). CNV may also be induced experimentally, e.g. via laser photocoagulation.

Neovascularization (H) **Retina**

Species
Mouse; Rat.

Other Term(s) Used
New blood vessels, retina
- Intra-retinal neovascularization
- Retinal vascularization proliferation

Pathogenesis/cell of origin
Secondary to ischemic retinal process, intravitreal release of pro-angiogenic factors (i.e. VEGF), and chronic retinal degeneration.

Diagnostic Features
- Presence of vascular profiles extending from the IPL and INL into the outer retinal layers.
- Presence of vascular profiles extending from the IPL and ganglion cell layers into the inner limiting membrane and projecting vascular tufts into the vitreous.
- Neovascular profiles can contact the RPE cells and colonize the subretinal space.
- Subretinal, retinal and vitreal hemorrhages can occur.
- Subretinal hemorrhage can cause retinal detachment.

Special Techniques for Diagnostics
Retinal vascular changes are evaluated clinically by vascular angiography and microscopically by trypsin digestion of retinal whole mounts, immunohistochemistry for endothelial cell markers (e.g., vascular endothelial growth factor) and transmission electron microscopy.

Differential Diagnoses
Choroidal neovascularization:
- Vessels extending from the choroid can breach Bruch's membrane and infiltrate the retina. The main differential diagnostic feature is the presence of an intact Bruch's membrane, suggesting retinal origin of the vessels. TEM might be necessary to confirm the status of Bruch's membrane.

Comment
Retinal neovascular proliferation can be a feature of end-stage retinal degeneration. Retinal neovascularization has been described as a feature of chronic light induced retinopathy in albino rats (Albert, Neekhra et al. 2010). Vitreal or subretinal hemorrhage due to retinal neovascularization can also lead to subretinal or retinal surface fibroplasia, forming membranes.

Optic Nerve

Atrophy (N) (Figure 47) **Optic nerve**

Species
Mouse; Rat.

Other Term(s) Used
Optic atrophy; optic neuropathy (ischemic).

Pathogenesis/cell of origin
Ganglion cell axon; common response to many types of injuries including primary axonal injury, ganglion cell loss, optic neuritis, or hypoxia/ischemia.

Diagnostic Features
- Marked loss of axons with relative increase in the prominence of the remaining pial trabeculae (thin bands of collagen arising from the pia mater that surround the axons).
- Glial proliferation (see gliosis).
- Decrease of optic nerve diameter can be observed in cross sections.
- Posterior bowing of the optic nerve head and lamina cribrosa (cupping of the optic nerve) can be present if atrophy is associated with chronically increased intraocular pressure.

Special Techniques for Diagnostics
Masson's trichrome stain can be used to highlight the collagenous tissue of the pial trabeculae. Luxol fast blue stains myelin blue, and can be used to demonstrate myelin loss in demyelinating injuries.

Differential Diagnoses
Fibrosis of the optic nerve

Comment
Species differences in the structure of the lamina cribrosa are important when interpreting the extent of atrophy near the site where the optic nerve passes through the sclera. Mice have a less robust lamina cribrosa when compared to rats so the accentuation of the collagenous tissue in optic nerve atrophy is less evident (Smith, John, and Nishina 2002). Because optic nerve atrophy is a chronic, irreversible response, it is important to determine the progenitor lesions in toxicological studies (Ramos, Reilly et al. 2011).

Degeneration, axonal (N) **Optic nerve**

Species
Mouse; Rat.

Other Term(s) Used
Axonopathy; dying-back axonopathy; nerve fiber degeneration; Wallerian-type degeneration.

Pathogenesis/cell of origin
Axonal degeneration occurs in several circumstances in the optic nerve. Loss of ganglion cells, and consequently their axons, secondary to glaucoma is likely the most common cause (Teixeira and Dubielzig 2013a). Lesions in the orbital or intracranial portions of the optic nerve can cause Wallerian degeneration with consequent axon loss

and ganglion cell death. Causes for these lesions include trauma leading to optic nerve crush, severance, or avulsion, and compression caused by tumors, periosteal proliferation at the optic foramen (where the nerve enters the calvarium), or granulomatous inflammation (Smith, John, and Nishina 2002).

Diagnostic Features
- Multiple, swollen eosinophilic axons (spheroids) with unaffected myelin sheaths in the early stage (McMartin, O'Donoghue et al. 1997).
- Axonal fragmentation with the formation of digestion chambers containing phagocytic macrophages (gitter cells) and central axonal fragments are characteristics of the late state lesion.
- Lesion progresses to optic nerve atrophy (see above).

Special Techniques for Diagnostics

Detailed evaluation of optic nerve axonal degeneration and axonal loss can be obtained by transmission electron microscopy of optic nerve cross sections (Reynaud, Cull et al. 2012). Faster methods use plastic- or resin-embedded, p-phenylenediamine (PPD) or Toluidine blue-stained optic nerve cross sections, light microscopy and computational image analysis to quantify axon loss (Ebneter, Casson et al. 2012).

Differential Diagnoses

Optic neuritis

Atrophy

Comment

Axonal degeneration associated with ageing has been reported in Sprague-Dawley rats and DBA/2J and AKXD-28/Ty mice (Anderson, Smith et al. 2001; Cavallotti, Cavallotti et al. 2001).

***Demyelination (N)* Optic nerve**

Species

Mouse; Rat.

Other Term(s) Used

Myelinolysis; myelinopathy.

Pathogenesis/cell of origin

Oligodendroglial cell processes. Disintegration of an otherwise normally formed myelin sheath without a primary impact to the ensheathed axon.

Diagnostic Features
- Reduced myelin staining in demyelinated or hypomyelinated fibers.
- Intact denuded axons.
- Formation of myelin ovoids (McMartin, O'Donoghue et al. 1997).

Special Techniques for Diagnostics
- Conventional stains for myelin (paraffin sections):
- Luxol Fast Blue (LFB) or solochrome cyanine for myelin (used independently or in combination with a cresyl violet counterstain for axons), or osmium tetroxide.
- In the later stages of demyelination, macrophages containing recently phagocytosed and partially digested myelin debris may be identified using LFB/PAS (Periodic acid Schiff) staining (Grant Maxie and Youssef 2007).
- Ultrastructural analysis (plastic- or resin-embedded sections), which enables precise identification of the numbers and thicknesses of myelin lamellae that surround axons; EM is particularly useful in the identification of remyelinated axons versus normal axons (McKay, Blakemore et al. 1998; Smith and Jeffery 2006).

Comment

Primary dysmyelination and demyelination affecting the optic nerve are rare in animals, but multiple mouse models have been developed to study human diseases such as Pelizaeus-Merzbacher disease (PMD) and multiple sclerosis (MS) (Smith, John, and Nishina 2002).

Increased number, glial cells (N) (Figure 48) **Optic nerve**

Species

Mouse; Rat.

Other Term(s) Used

Gliosis; reactive glia; glial hyperplasia; glial hypertrophy.

Pathogenesis/cell of origin

Microglial cell tissue repair process. Proliferation and/or hypertrophy of any/or multiple glial cell lineages in response to optic nerve tissue injury.

Diagnostic Features
- Increased numbers and/or size of glial cells; cells are identified as glia (rather than neurons) using cytoarchitectural characteristics and location.
- Increased amount of glial processes.
- Presence of gitter cells (enlarged macrophage-like cells with abundant granular to vacuolated cytoplasm).

Differential Diagnoses

Fibrosis

Inflammation:
- See Inflammation, eye

Comment

Glial cells are identified by their cytoarchitectural characteristics and location. Microglia have a phagocytic role following tissue damage, and are recognized as gitter cells.

***Infiltrate, inflammatory cell (N)* Optic nerve**

Species
Mouse; Rat.

Other Term(s) Used
Infiltration, inflammatory cell.

Histiogenesis/cell of origin
Primarily mononuclear cells; the cause is uncertain, but presumably an incidental, self-limiting response designed for immune surveillance and minor tissue repair activities.

Diagnostic Features
- Foci of leukocytes within the optic nerve or optic disc without other features of inflammation.

Differential Diagnoses
Inflammation:
- Inflammatory cellular infiltrate with associated inflammatory features such as edema, congestion, hemorrhage, necrosis and gliosis of optic nerve neuropil.

Comment
The term "infiltrate" is recommended followed by the predominant cell type (neutrophilic, eosinophilic, lymphocytic, plasmacytic or histiocytic) or mixture of different cell types (mixed). The most predominantly and frequently observed inflammatory cell infiltrate in the optic nerve is lymphocytic. Small, focal to multifocal aggregates of lymphocyte infiltrates are thought to be incidental background findings.

***Inflammation (N)* Optic nerve**

Species
Mouse; Rat.

Other Term(s) Used
Optic neuritis; optic nerve neuritis.

Histiogenesis/cell of origin
Leukocytes of any lineage associated with an inflammatory response.

Diagnostic Features
- Leukocyte infiltration within the optic nerve or optic disc with other features of inflammation.
- Inflammatory features such as edema, congestion, hemorrhage, necrosis and increased numbers of glial cells (gliosis) are also present.

Differential Diagnoses
Infiltrate, inflammatory cell:
- See above.

Comment
Inflammation is the preferred diagnostic term when inflammatory features are present, with the appropriate modifiers used to identify the predominant cell type. Immune-mediated inflammation that is predominantly lymphocytic may be observed in the optic nerve and nerve head following the ocular administration of biologics that are recognized as foreign proteins by the immune system. Optic neuritis is a clinical term designating a swollen optic nerve disc from any cause when viewed on ophthalmoscopy and should not be used as a histological diagnosis.

***Vacuolation (N)* Optic nerve**

Species
Mouse; Rat.

Other Term(s) Used
Myelin splitting; axon swelling; myelin edema; Wallerian degeneration.

Pathogenesis/cell of origin
Separation of myelin sheaths surrounding axons, or cytoplasmic swelling of glial cells.

Diagnostic Features
- Clear spaces within the optic nerve.
- Irregular enlargement of axons observed in longitudinal sections.

Special Techniques for Diagnostics
Myelin defects may be demonstrated using Luxol blue staining.

Differential Diagnoses
Fixation artifact

Demyelination

Comment
Degenerative changes in myelin can occur spontaneously with aging or result from trauma, toxicity, or inflammatory conditions.

Retinal Pigment Epithelium (RPE)

***Atrophy (N)* Retinal pigment epithelium (RPE)**

Species
Mouse; Rat.

Other Term(s) Used
Decreased numbers of RPE cells; RPE cell loss.

Pathogenesis/cell of origin
RPE cell loss often occurs as a generalized aging process that leads to cell degeneration and eventual cell death.

Diagnostic Features
- Regions that exhibit reduced RPE cell count, or areas of Bruch's membrane that may be devoid of overlying RPE.
- Remaining cells may be attenuated, spreading laterally to compensate for any spatial defects in an attempt to maintain the blood-retinal barrier (BRB) and homeostasis.
- Remaining RPE tend to have features of degeneration (cell enlargement and irregular pigmentation).

Comment

Chronic atrophy of RPE is associated with degeneration and atrophy of the adjacent retina. Because the BRB has been breached, there may be associated subretinal edema and inflammation, or subretinal fibroplasia (formation of subretinal membranes).

Deposits, extracellular matrix, subretina (N) **Retinal pigment epithelium (RPE)**

Species

Mouse; Rat.

Other Term(s) Used

Drusen; drusen-like deposits

Pathogenesis/cell of origin

Impaired function of the RPE associated with the metabolism of photoreceptor outer segments.

Diagnostic Features
- Extracellular deposits of irregular, amorphous material located between RPE and Bruch's membrane (Pow and Diaz 2008).
- Often associated with enlarged and/or degenerating RPE containing numerous, prominent pigmented granules.
- May be associated with loss of RPE polarity, RPE and retinal detachment, and/or subretinal or retinal edema.

Differential Diagnoses

RPE degeneration or necrosis

Comment

Drusen are extracellular deposits composed primarily of apolipoproteins derived from RPE metabolism of the outer segments of photoreceptors, and from members of the compliment system (particularly factor H) derived from plasma (Hageman, Luthert et al. 2001). Drusen contain zinc, which is thought to have a role in the precipitation and activation of the complement system (Lengyel, Flinn et al. 2007). These amorphous deposits may accumulate due to impaired transport of the debris through Bruch's membrane into the choroidal circulation. Drusen is a clinical diagnosis that characterizes these findings, and should be avoided as a histological diagnosis. Drusen are associated with age-related macular degeneration, and thus are rarely observed in species other than primates. However, 'hard' drusen (concentric, nodular mass, with well-defined borders; may be mineralized) do occur infrequently in some species other than humans.

Fibroplasia, subretinal (N) (Figure 49) **Retinal pigment epithelium (RPE)**

Species

Mouse; Rat.

Other Term(s) Used

Subretinal membranes; subretinal fibrosis; fibrous metaplasia; RPE migration.

Pathogenesis/cell of origin

Migration, proliferation, and transdifferentiation of RPE in response to injury, and increased production of resident growth factors and cytokines such as TGFβ. Individual RPE cells become fusiform, reminiscent of fibroblasts or myofibroblasts, proliferate, and migrate.

Diagnostic Features
- Linear arrays of fibroblastic-like cells arranged in a membranous mat between the retina and Bruch's membrane.
- Cellular component may be derived from multiple lineages: fibroblasts, hyalocytes, glial cells, Müller cells, and RPE.
- Inflammatory cells are present when there is associated inflammation.
- Small vascular profiles can be present spontaneously, or induced (neovascularization) as in laser models.
- Contraction of membranes can cause buckling of the adjacent retina, and result in retinal detachments.

Special Diagnositic Techniques
- Histochemical stains for collagen (e.g. Masson's trichome or Picrosirius red) can be useful to highlight membranes.
- Immunohistochemistry for GFAP or RPE65 can be used to demonstrate the presence of glial cells and RPE, respectively in the membranes.

Differential Diagnosis

Choroidal Neovascularization
- See retinal neovascularization, below.

Comment

"Subretinal membranes" is a clinical term for fibroplasia occurring in the subretinal space, and in humans they tend to be associated with neovascularization in age-related macular degeneration (AMD). They are rare in non-primate species, but can be experimentally induced using lasers. Membranes may be secondary to subretinal hemorrhage, retinal or choroidal inflammation, neovascular retinal or choroidal disease, or intraocular surgery. Osseous metaplasia (RPE metaplasia to an osseous phenotype) is

a variation and is not well understood (Toyran, Lin et al. 2005). Subretinal membranes can be the cause of retinal detachment or develop secondary to retinal detachment, especially in cases of subretinal hemorrhage. More extensive subretinal fibroplasia that infiltrates and partially replaces the retina (retinal fibrosis) is usually secondary to traumatic inuury, such as scleral rupture.

Hypertrophy, RPE (N) (Figures 49, 50) **Retinal pigment epithelium (RPE)**

Species

Mouse; Rat.

Other Term(s) Used

Enlarged RPE; increased size, RPE.

Pathogenesis/cell of origin

RPE enlargement occurs with cellular disease, toxicity, or aging processes due to increase in size and number of organelles, enlargement of smooth endoplasmic reticulum (increased activity), or accumulation of lipofuscin. Occasional random cells may be enlarged without apparent reason.

Diagnostic Features

- RPE cells are larger than typical on light microscopy and may have unusual pigmentation.
- Melanin may be reduced or irregularly distributed within the cell, or may fuse with lipofuscin to form conjugates with different pigmentation that appears granular.
- On electron microscopy, enlargement of smooth endoplasmic reticulum, and increased numbers of lysosomes or lipofuscin granules may be observed.

Comment

Hypertrophy is often associated with detachment of the retina or photoreceptor death, and may progress to RPE detachment, transdifferentiation, and migration. Drug-induced hypertrophy often presents as uniformly enlarged RPE that are closely apposed to the retina. In some cases, such as with some β-secretase inhibitors, hypertrophied RPE will autofluoresce (Fielden et al 2015).

Inclusions (intracytoplasmic accumulation), RPE (N) (Figure 51) **Retinal pigment epithelium (RPE)**

Species

Mouse; Rat.

Other Term(s) Used

RPE degeneration; vacuolation; lysosomes; lipofuscin or lipofuscinosis; retinal lipidosis (Ivanina, Zueva et al. 1983); myeloid bodies (Peräsalo, Rechardt et al. 1974); residual bodies (DAmico et al. 1984).

Pathogenesis/cell of origin

RPE impaired degradation of shed photoreceptor outer segments is associated with aging processes, but may also occur with enzyme deficiency of some genetic diseases, or with toxicity, such as chloroquine (Ivanina, Zueva et al. 1983) or cationic amphiphilic compounds (DAmico et al. 1984).

Diagnostic Features

- RPE cells are generally enlarged on light microscopy, and have increased numbers of pigmented granules.
- RPE may have loss of polarity, and be detached from Bruch's membrane.
- Abnormal organelles containing concentric membranous whorls can be found in the RPE cytoplasm on electron microscopy (Gregory, Rutty et al. 1970; Matsumura, Yamakawa et al. 1986; Gaafar, Abdel-Khalek et al. 1995); membranes may have lamellated (fingerprint-like) appearance reminiscent of the outer segments of photoreceptors, and are osmophilic due to the phospholipid content of the membranes (Peräsalo, Rechardt, and Palkama 1974).

Differential Diagnoses

Lysosomes:

- Lysosomes containing lipofuscin appear auto-fluorescent on fundic examination, and should be differentiated from drusen (sub-RPE, or Bruch's membrane deposits) that also contain lipofuscin or other autofluorescent pigments.

Comment

Vacuolation may also be associated with abnormal accumulation of lipofuscin or other pigments that are metabolic by-products of RPE processing of shed photoreceptor outer segments. Lipofuscin, and lipofuscin conjugates (i.e. melanolipofuscin) often accumulate in the base of the RPE cytoplasm as granules. These are best observed on fundic examination, and appear as autofluorescent particles. Lipofuscin may not survive routine tissue processing and thus may not be observed on brightfield light microscopy unless associated with other organelles or proteins. Instead, clear vacuoles generally remain, representing the presence of cellular accumulations. Lipofuscin accumulates spontaneously with age, due to impaired ability to properly remove the granules from the cell, and may also occur with toxicities (Brown 1974; Hughes and Coogan 1974; Fox and Chu 1988; Butler, Ford, and Newberne 1987). Occasionally, cytoplasmic crystals may be observed (Caine et al. 1975).

Necrosis (N) (Figure 52) **Retinal pigment epithelium (RPE)**

Species

Mouse; Rat.

Other Term(s) Used

None.

Pathogenesis/cell of origin

RPE cell death can be induced by any number of causes. RPE are subject to light-induced oxidative injury, in addition to chronic oxidative stress related to their metabolic role in photoreceptor maintenance.

Diagnostic Features

- Loss of cell morphology; granular cell debris in absence of RPE, extending into the subretinal space.
- Pyknotic or absent nuclei.
- Retinal detachment; subretinal edema may occur in locations of necrosis, due to loss of blood-retinal barrier.

Comment

RPE degeneration and necrosis can occur spontaneously associated with the accumulation of lipofuscin, vitamin A dimers, and other by-products of the visual cycle that promote free-radical injury. RPE impairment is thought to have a critical role in age-related degeneration of the retina. The RPE contribution to the blood-retinal barrier and transport mechanisms between the vasculature and retina render them vulnerable to toxicities from systemically administered compounds (iodates, L-Ornithine hydrochloride, naphthalene). Free-radical damage can be enhanced through melanin binding, such as occurs with heavy metals and amines. In addition, RPE degeneration and subsequent necrosis can occur secondary to photoreceptor injury.

Pigmentation, decreased (N) (Figure 50) **Retinal pigment epithelium (RPE)**

Species

Mouse; Rat.

Other Term(s) Used

Hypopigmentation; depigmentation; pigmentary incontinence.

Pathogenesis/cell of origin

Reduced pigmentation (reduced numbers of pigment granules) within RPE. Only relevant in pigmented species or strains.

Diagnostic Features

- The number of melanin granules within individual RPE is reduced; RPE are not uniformly affected, but more commonly involve regional or focal changes.
- Melanosomes may assume uncharacteristic shape or size.
- Cytoplasmic distribution of melanin granules may be altered.

Comment

Loss of RPE melanin occurs spontaneously as an age-related change. It may also be associated with some toxicities that result in melanin binding, including some metals and amines (Boulton 1988). Melanin may also be taken up by lysosomes and/or fuse with lipofuscin, resulting in apparent diffusion of pigment. Photobleaching of melanosomes also results in diminished pigmentation, although the granules are still present.

Pigmentation, increased (N) **Retinal pigment epithelium (RPE)**

Species

Mouse; Rat.

Other Term(s) Used

Hyperpigmentation; increased numbers of pigment granules.

Pathogenesis/cell of origin

Melanin gradually decreases as an age-related change. However, lipofuscin accumulates with age, and can fuse with melanin, resulting in the presence of increased numbers of brown, pigmented granules. Lipofuscin is derived from the metabolism of the outer segments shed from photoreceptors (see above), and consists of lipids and fluorescent compounds that impart a yellow-brown auto-fluorescence characteristic to the granules.

Diagnostic Features

- Increased numbers of intracytoplasmic granules that are light brown on light microscopy.
- Pigment may be autofluorescent if lipofuscin remains following processing.
- Cytoplasmic granules may be increased in size and exhibit abnormal distribution throughout the cell.

Comment

Lipofuscin is best visualized on fundic imaging, as it is frequently lost during tissue processing.

Polarity, loss, RPE (N) (Figures 49, 53) **Retinal pigment epithelium (RPE)**

Species

Mouse; Rat.

Other Term(s) Used

Dedifferentiation; detachment/disorganization/degeneration, RPE.

Pathogenesis/cell of origin

In response to cell injury or degeneration (see above), RPE cells lose attachments to adjacent cells and to Bruch's membrane.

Diagnostic Features

- RPE cells are individualized or form aggregates that are separated from Bruch's membrane, residing in the subretinal space.
- RPE cells assume a round to polygonal shape; apical mi-

crovilli and basal infoldings are lacking.
- On electron microscopy, there may be decreased phagosomes observed, but more often, if associated with degeneration, there are numerous lysosomes containing membranes, lipofuscin or melanolipofuscin granules, and decreased or irregular shaped melanosomes.
- Retinal detachment is associated, and eventual retinal atrophy occurs.

Comment

Loss of polarity is associated with loss of integrity of the BRB and retinal homeostasis. Thus, there may be subretinal fluid, retinal edema, and in chronic cases, retinal degeneration and/or atrophy. Loss of polarity is associated with cell migration, however, as this is a primary degenerative process, cellular transdifferentiation does not occur, and subretinal fibroplasia is not a sequela.

Sclera

***Atrophy (N)* Sclera**

Species

Mouse; Rat.

Other Term(s) Used

Staphyloma.

Pathogenesis/cell of origin

Decrease in the amount of scleral connective tissue resulting in sclera thinning; can occur secondary to globe enlargement (inflammation or glaucoma) resulting in stretching of the sclera.

Diagnostic Features
- The sclera is focally or diffusely thinned.
- Connective tissue may have a sclerotic appearance.

Comment

Atrophy of the sclera usually occurs secondary to other changes such as enlargement of the eye due to glaucoma or tumor formation, or as a sequela to inflammation. Atrophy can also occur as a degenerative age-related change. Staphyloma is a clinical term, and consists of a break in the sclera with prolapse of intraocular tissues.

***Infiltrate, inflammatory cell (N)* Sclera**

Species

Mouse; Rat.

Pathogenesis/cell of origin

Generally limited to lymphocytes.

Diagnostic Features
- Loose or scattered infiltrates within the sclera wall, generally oriented in perivascular spaces.

Comment

Occasionally mononuclear cell infiltrates may be observed in the connective tissue surrounding the globe, and extending into the sclera.

***Inflammation (N)* Sclera**

Species

Mouse; Rat.

Other Term(s) Used

Scleritis; scleral inflammation.

Pathogenesis/cell of origin

Depending on the inciting cause, inflammation may be composed of mixed inflammatory cells with neutrophils predominating, mononuclear to histiocytic cells, or granulomatous.

Diagnostic Features
- Infiltrates of inflammatory cells are oriented in the perivascular spaces of vessels that penetrate the sclera.
- Edema, congestion, necrosis and cell debris are associated findings.

Comment

Scleral inflammation does not occur independently, but occurs with inflammation in neighboring areas of the eye. The only known exception is that of toxicity associated with exposure to bisphosphonates which produces scleritis in human patients after intravenous administration. Scleritis may also occur as a manifestation of systemic connective tissue disease (French and Margo 2008). Due to a lack of a primary blood supply, inflammation is slow to resolve and may culminate in necrosis.

Metaplasia, bone or cartilage (N) (Figure 54) **Sclera**

Species

Mouse; Rat.

Other Term(s) Used

Osseous metaplasia; cartilaginous metaplasia, transdifferentiation.

Pathogenesis/cell of origin

Spontaneous formation of bone or cartilage in the sclera.

Diagnostic Features
- Focal or multifocal plaques of immature woven bone or foci of cartilage occurring within the sclera.

Differential Diagnoses

Osteoma; Chondroma;

Mineralization (see Figure 26)

Comment

Osseous metaplasia is a common alteration in aging F344 rats, although cartilaginous metaplasia is rarely observed (Yoshitomi and Boorman 1990). Bone or cartilage formation can also occur secondary to trauma.

Nonneoplastic Proliferative Lesions of the Rat and Mouse Eye: Cornea / Conjunctiva

Dermoid, ocular (H) (Figure 55) **Cornea: Conjunctiva**

Species

Mouse; Rat.

Other Term(s) Used:

None

Pathogenesis/cell of origin

Choriostomatous tissue (normal tissue in abnormal location), presumably arising from an ectodermal anlage.

Diagnostic Features

- Grossly, lesion appears as an elevated white plaque with numerous fine hairs.
- Lesions contain components of skin such as hair follicles, sebaceous glands and fibrous connective tissue beneath a stratified squamous epithelium which covers the lesion.

Differential Diagnoses

Epithelial cyst:

- Lined by stratified squamous epithelium with an innermost layer of keratinizing cells; dermal appendages are not observed in the wall.

Comment

Ocular dermoid is a rare lesion of the cornea and/or conjunctiva of the rat. This lesion is not considered to be a neoplasm.

Hyperplasia/hypertrophy, endothelium (H) (Figure 56)
Cornea: Conjunctiva

Species

Mouse; Rat.

Other Term(s) Used

Endothelialization, associated with production of Descemet's membrane.

Pathogenesis/cell of origin

Abnormal proliferation and migration of corneal endothelial cells over the trabecular meshwork and iris. Compensatory endothelial cell hypertrophy can be observed with endothelial cell loss in attempts to cover spatial defects, particularly in species where hyperplasia is not known to occur.

Diagnostic Features

- Spindle-shaped cells covering the iridocorneal drainage angle and/or anterior surface of the iris.
- Associated with production of thickened Descemet's membrane-like material.
- Enlarged cells, often observed on the peripheral margins of the endothelium.

Comment

In rodents, the corneal endothelium has regenerative capacity throughout life, usually in response to injury. Endothelial cell hypertrophy associated with age-related cellular loss is observed in many species, including mouse and rat. Endothelialization is reported to occur in DBA/2J and AKXD-28/Ty mice (Smith, Sundberg, and John 2002a).

Hyperplasia, squamous cell (H) (Figure 5)
Cornea: Conjunctiva

Species

Mouse; Rat.

Other Term(s) Used:

None

Pathogenesis/cell of origin

Epithelial cells of the cornea, conjunctiva (bulbar and palpebral), or lacrimal duct.

Diagnostic Features

- Increased cell layers of squamous epithelium with exophytic and/or endophytic (rete-peg-like) growth pattern.
- Often associated with epithelial hyperkeratosis.
- Underlying stroma often infiltrated by inflammatory cells (especially in case of reactive hyperplasia).

Differential Diagnoses

Papilloma, squamous cell:

- Characterized by exophytic growth and composed of fronds of squamous epithelium covering a fibrovascular core. Epithelium is retained by a basement membrane.

Carcinoma, squamous cell:

- Malignant neoplasm exhibiting invasion of the underlying stroma, cellular atypia and dysplasia, as well as dyskeratosis, formation of epithelial keratin 'pearls' and mitotic activity.

Comment

Spontaneous corneal and/or conjunctival epithelial hyperplasias are rare lesions. Reactive hyperplasia is more common, resulting from many causes, including topically applied chemical and physical irritants; systemically administered toxins; reduced tear production; bacterial, viral, or fungal infections; nutritional deficiencies; heritable defects; and exophthalmos due to space-occupying orbital masses. In these cases, stromal inflammation, neovascu-

larization, and/or fibrosis are often concurrently present.

Filtration Angle/Trabecular Meshwork

Proliferation, trabecular meshwork (TM) (H) **FA/TM**

Species

Mouse; Rat.

Other Term(s) Used

Migration, TM cell; activation, TM cell.

Pathogenesis/cell of origin

Universal response of TM cells regardless of the injury or irritating stimuli, e.g. laser photocoagulation, phagocytic particle insult, or noxious agents. TM cell activation has been associated with a heightened metabolic state needed for the phagocytosis of debris entering the meshwork (Ramos, Attar et al. 2017).

Diagnostic Features

- Increased numbers of trabecular shaped cells in the filtration angle and overlying the TM.
- TM cells may be linearly arrayed in multiple, irregular layers overlying the trabeculae.

Differential Diagnoses

Mononuclear cell infiltrate:

- Mononuclear leukocytes can be found within the filtration angle.

Comment

TM response to injury is limited. If adequate scaffolding remains following minimal damage (transient elevation in intraocular pressure, mild laser beam application), TM cell migration and proliferation, and reorganization of the trabeculae are possible. Activated TM cells may form distinct spindle shapes expressing α-SMA, synthesize new basement membrane and other collagens, and become phagocytotic (Rohen and van der Zypen 1968; Lütjen-Drecoll 1972; Grierson, Unger et al. 2000).

Uvea

Hyperplasia, melanocyte (H) **Uvea**

Species

Mouse; Rat.

Other Term(s) Used

Ocular melanosis.

Pathogenesis/cell of origin

Neuroectodermal origin, from uveal melanocytes.

Diagnostic Features

- Aggregates of polygonal melanocytes filled with pigment.
- Minimal or no cellular atypia.
- Minimal displacement of normal structures.

Comment

Melanocyte hyperplasia has been reported in the rat (Ackermann et al. 1998).

Lens

Hyperplasia, lens epithelium (H) (Figures 18, 56) **Lens**

Species

Mouse; Rat.

Other Term(s) Used:

None

Pathogenesis/cell of origin

Anterior lenticular epithelium.

Diagnostic Features

- Proliferation of the epithelium (normally a single layer) to form focal or multifocal nodules or aggregates of epithelial cells under the anterior lens capsule.
- Possible migration and proliferation of the epithelium under the posterior portion of the lens capsule.

Differential Diagnoses

Fibroplasia, lens epithelium

- See above. (Figure 19)

Comment

Injury to the lens may result in epithelial cell proliferation and/or transformation to myofibroblasts.

Retinal Pigment Epithelium (RPE)

Hyperplasia, RPE (H) (Figure 49) **Retinal pigment epithelium (RPE)**

Species

Mouse; Rat.

Other Term(s) Used:

RPE proliferation.

Pathogenesis/cell of origin

Hyperplasia occurs as focal populations of RPE that proliferate in response to lost or damaged cells or inflammation (Machemer and Laqua 1975).

Diagnostic Features

- RPE hyperplasia is often observed as focal proliferations of jumbled cell layers that undermine the adjacent retina.
- Involved cells generally lack polarity and may be loosely attached to adjacent cells or to Bruch's membrane.
- On electron microscopy, hyperplastic RPE cells generally have large vesicular nuclei, scant cytoplasmic organelles, few melanosomes, and reduced numbers of apical microvilli (Lee and Valentine 1991).

Comment

RPE hyperplasia may lead to degeneration of the adjacent retina due to impaired capacity to support the metabolic needs of the retina, and subsequent loss of homeostasis. Proliferation of RPE can also be associated with retinal detachment (McMartin et al. 1992).

Neoplastic Proliferative Lesions of the Rat and Mouse Eye

Cornea / Conjunctiva

Papilloma, squamous cell (B) **Cornea: Conjunctiva**

Species

Mouse; Rat.

Other Term(s) Used:

None

Pathogenesis/cell of origin

Epithelial cells of the cornea, conjunctiva (bulbar and palpebral), or the lacrimal duct.

Diagnostic Features

- Exophytic growth with development of multiple branched fronds composed of a lining of variably keratinized squamous epithelium and a variably developed vascular connective tissue core.
- Cells are retained by a basement membrane without invasion into the underlying tissues.
- No cellular dysplasia observed. No or only slight mitotic activity.

Differential Diagnoses

Carcinoma, squamous cell:

- Malignant neoplasm exhibiting invasion of the underlying stroma, cellular atypia and dysplasia as well as dyskeratosis, formation of epithelial keratin 'pearls' and mitotic activity.

Comment

Squamous cell papillomas are rare neoplasms of the cornea and conjunctiva, but have been induced in rats by exposure to vapors of certain carcinogens. A variant of this neoplasm, an inverted mucoepidermoid papilloma, has been reported in a F344/N rat, exhibiting a downward growth pattern of proliferating superficial conjunctival epithelium with prominent squamous metaplasia (Yoshitomi and Boorman 1994).

Carcinoma, squamous cell (M) (Figure 57)
Cornea: Conjunctiva

Species

Mouse; Rat.

Other Term(s) Used:

None

Pathogenesis/cell of origin

Epithelial cells of the cornea, conjunctiva (bulbar and palpebral), or the lacrimal duct.

Diagnostic Features

- Mass composed of cords and nests of neoplastic squamous cells with variable amounts of keratinization.
- Neoplastic cells are large, have abundant eosinophilic cytoplasm, and round to oval vesicular nuclei with prominent nucleoli.
- Neoplastic cells penetrate the basement membrane, invade the underlying corneal stroma and adjacent tissues, and form areas of dyskeratosis and keratin 'pearls'.
- Features of malignancy include lack of differentiation, numerous mitogenic figures, loss of intercellular bridges and metastasis.

Differential Diagnoses

Papilloma, squamous cell:

- Characterized by exophytic growth and composed of fronds of squamous epithelium covering a fibrovascular core. Epithelium is retained by a basement membrane.

Comment

In contrast to domestic animals (cattle, horses, cats), squamous cell carcinoma is a rare neoplasm in the rat.

Uvea

Leiomyoma, uveal (B) (Figure 58) **Uvea**

Species

Mouse; Rat.

Other Term(s) Used:

None

Pathogenesis/cell of origin

Smooth muscle cells of either the iris dilatator or sphincter muscles (neuroectodermal) or from ciliary muscle or muscles of the uveal arterioles (mesodermal).

Diagnostic Features

- The neoplasm is composed of closely packed interlacing bundles and whorls (sometimes around blood vessels) of spindle-shaped cells with eosinophilic granular cytoplasm and elongated to oval nuclei.
- Myofibrils are demonstrated by phosphotungstic/acid hematoxylin stain (PTAH) (Owen and Duprat 1991).

Differential Diagnoses

Melanoma, uveal, malignant:

- Differentiation by light microscopic features may be difficult as both neoplasms are composed of spindle-shaped cells with formation of perivascular whorls. Leiomyoma react positive to desmin on immunohistochemistry, and may be differentiated from melanoma cells, which are negative. Ultrastructurally, leiomyoma cells have cy-

toplasmic myofibrils, focal cytoplasmic densities and surface-connected vesicles, whereas melanoma cells contain stage II melanosomes.

Schwannoma, intraocular, malignant:
- Schannoma cells are negative for desmin on immunohistochemistry and thus may be differentiated from leiomyomas, which are positive. In electron micrographs, Schwannoma cells have partial to complete basal lamina and attenuated cellular processes, whereas the leiomyoma cells have cytoplasmic myofibrils, focal cytoplasmic densities, and surface-connected vesicles.

Comment

Leiomyomas are frequent tumors of the soft tissue, however, few uveal leiomyomas have been reported. Diagnosis should be confirmed by immunohistochemistry and/or electron microscopy.

Melanoma, uveal (M) (Figure 59, 60) **Uvea**

Species

Mouse; Rat.

Other Term(s) Used

Melanoma, amelanotic; Melanoma, intraocular, malignant.

Pathogenesis/cell of origin

Neuroectodermal from uveal melanocytes.

Diagnostic Features
- Generally unilateral lesion of the anterior uvea, but may also be located in the choroid; uveal melanomas may invade the cornea, conjunctiva, sclera, retina and orbit.
- Neoplasms can be composed of spindle-shaped (most common type), epithelioid or mixed cells.
- Spindle-shaped cells arranged in bundles and whorls with perivascular orientation, indistinct cell borders, scant to moderate cytoplasm, fusiform nuclei and indistinct nucleoli.
- Epithelioid cells have ill-defined cell borders, pale-staining cytoplasm, and large oval nuclei with or without nucleoli; large epithelioid cells (rare) have large bizarre nuclei with nucleoli.
- Melanin granules are present in the cytoplasm in varying numbers.
- Necrotic areas may be present.
- Mitotic figures may be numerous in some neoplasms; argyrophilic fibers are present along with a few cells containing yellow-brown pigment.

Differential Diagnoses

(none described in mice).

Leiomyoma, uveal:
- Also composed of spindle-shaped cells with perivascular orientation. Can be differentiated immunohistochemically: leiomyomas are positive for desmin and negative for S-100 protein; melanoma shows opposite immunoreactivity.

Schwannoma, intraocular, malignant:
- Composed of S-100 positive spindle-shaped cells. Differentiation electromicroscopically by demonstration of pericytoplasmic basal lamina, attenuated long cellular processes, and desmosomes.

Comment

Spontaneous melanomas in rodents are apparently extremely rare. There are no reports of benign melanomas in albino or pigmented mice and rats; malignant amelanotic melanomas in albino mice; spontaneous epithelioid anterior uveal melanomas; or uveal melanomas in pigmented strains of rats. However, there are several chemicals known to induce intraocular melanomas in laboratory animals (Ernst et al. 1991). Extraocular metastasis of uveal melanomas is rare. In humans, uveal melanomas are the most common primary intraocular tumors in adults (Everitt and Shadduck 1991).

In rats the diagnosis of uveal melanomas is aided by immunohistochemical demonstration of a positive reaction in the neoplastic cells for S-100 protein and vimentin intermediate filaments and a negative reaction for cytokeratin, desmin and glial fibrillary acid protein (GFAP). Ellipsoid premelanosomes (stage II melanosomes) could be demonstrated in electron micrographs of cells of a rat with amelanotic uveal melanoma. Since the main differential diagnosis is malignant schwannoma, which can be positive for S-100 protein as well, electron microscopy appears to be the best diagnostic method for differentiating these two neoplasms. Schwannomas, especially the "melanotic variant" may contain melanosomes; convoluted, moderately thin cytoplasmic processes lined by a continuous basal lamina are diagnostic for schwannomas.

Schwannoma, intraocular (M) (Figure 61, 62, 63) **Uvea**

Species

Mouse; Rat.

Other Term(s) Used

Neurilemmoma, malignant; neurinoma, malignant.

Pathogenesis/cell of origin

Schwann cells of intraocular ciliary nerves.

Diagnostic Features
- Found in the iris and can involve the ciliary body, and fill the anterior chamber. Local invasion may occur into the cornea. Schwannomas can also be found in the optic nerve.
- Plump spindle-shaped cells with abundant eosinophilic vacuolated cytoplasm; cells are arranged in parallel rows and form palisades around vessels.
- Nuclei are normochromatic oval to short elongate, vary-

ing slightly in size. Some cells have a small eosinophilic nucleolus.
- Mitotic figures may be numerous; may contain multiple areas of necrosis.

Differential Diagnoses

Melanoma, uveal, malignant:
- The spindle shaped cells of the malignant schwannoma are arranged in a perivascular fascicular pattern, whereas the spindle cells of the uveal melanoma are arranged in a perivascular whorl pattern. In electron micrographs melanoma cells contain cytoplasmic stage II premelanosomes.

Leiomyoma, uveal:
- Uveal leiomyoma should have a positive immunoreactivity for desmin and a negative immunoreactivity for S-100 protein (Chandra and Frith 1993). In electron micrographs, cells of uveal leiomyoma have cytoplasmic myofibrosils, focal cytoplasmic densities, and surface-connected vesicles.

Comment

Schwannoma occur frequently in the nervous system of rats and mice. However, they are considered rare spontaneous neoplasms of the globes of rats. Intraocular schwannoma show positive immunoreactivity for S-100 protein. Electromicroscopically, the cells have long thin cellular processes with desmosomes, and a pericytoplasmic partial to complete basal lamina.

Secondary tumors

Pathogenesis/Cell of origin: Dependent on primary neoplasm.

Differential diagnosis: Dependent on primary neoplasm.

Comments: Malignant lymphoma originating in the spleen, lymph nodes and/or thymus has been seen in B6C3F1 mice. Lymphomas are found primarily in the choroid, and can be associated with retinal detachment. Harderian gland carcinomas may also invade the globe, as can fibrosarcoma induced by the injection of 20-methylcholanthrene into the orbit. Secondary hemangiosarcoma has also been reported (Geiss and Yoshitomi 1999).

Optic Nerve

Proliferative lesions of the optic nerve reported in rodents include meningiomas, Schwannomas and gliomas (Ackermann et al. 1998; Fitzgerald et al. 1974; Weisse 1993; Yoshitomi and Boorman 1990; Yoshitomi and Boorman 1991a; Yoshitomi and Boorman 1991b). Although a ganglioneuroma has been reported in rats (Curtis et al. 1931), details of its histologic features were not described, and no instances have been reported since the original reference. Descriptions and terminology for meningiomas, Schwannomas and gliomas can be found in the INHAND committee manuscript on proliferative and nonproliferative lesions of the rat and mouse central and peripheral nervous systems (Kaufmann et al. 2012). The current manuscript will focus on the histologic features of these tumors as they have been reported specifically for the optic nerve.

Meningioma, benign (B) **Optic nerve**

Species

Mouse; Rat.

Pathogenesis/cell of origin

Stromal cells of the meninges.

Comment

Meningiomas that have been reported in rats have exhibited features of malignant meningiomas, as described below.

Meningioma, malignant (M) (Figure 64) **Optic nerve**

Species

Mouse; Rat.

Other Term(s) Used

Meningeal sarcoma.

Pathogenesis/cell of origin

Stromal cells of the meninges.

Comment

Meningiomas of the optic nerve of rats have exhibited characteristics of the malignant form, including local invasion and a high mitotic rate (but without metastasis). They have an epithelioid pattern (meningothelial type), which is rare in the cranial cavity. The epithelioid pattern is characterized by pleomorphic spindle cells with pale eosinophilic cytoplasm, arranged in a whorling pattern, often with perivascular orientation and resembling Hassall's corpuscles of the thymus. Mineralization may be present, but no typical psammoma bodies are observed. Giant cells may be present, some occasionally containing intranuclear cytoplasmic herniations appearing as vacuoles. Foci of necrosis with cholesterol clefts have been seen. Meningiomas of the optic nerve may or may not be S100 positive, and their ultrastructure features consist of interdigitating cellular processes and desmosomes (Yoshitomi and Boorman 1990; Yoshitomi, Everitt, and Boorman 1991).

Schwannoma, benign (B) **Optic nerve**

Species

Mouse; Rat.

Other Term(s) Used

Neurilemmoma; neurinoma.

Pathogenesis/cell of origin

Schwann cells (myelinating cells of peripheral nerves) considered to be of neuroectodermal origin but capable of facultative differentiation to express mesenchymal properties.

Comment

The reported schwannoma in a rat exhibited malignant characteristics, as described below.

Schwannoma, malignant (M) **Optic nerve**

Species

Mouse; Rat.

Other Term(s) Used

Neurilemmoma, malignant; neurinoma, malignant.

Pathogenesis/cell of origin

Schwann cells (myelinating cells of peripheral nerves), considered to be of neuroectodermal origin but capable of facultative differentiation to express mesenchymal properties.

Comment

An orbital malignant Schwannoma of an F344/N NTP rat described was believed to be of optic nerve origin since it was centered on, although obliterated, the optic nerve. Grossly the tumor was cystic. Antoni Type B features were more common than Type A, with well-defined, anaplastic small cells with high nuclear to cytoplasmic ratio, variably-shaped nuclei, and frequent mitoses. There were areas of necrosis, thrombosis and hemorrhage. The cells were S100 negative. Short cell processes, and an incomplete to nearly complete basal lamina investing frequent cells were observed on electron microscopy (Yoshitomi and Boorman 1991b).

Glioma (Astrocytoma), benign (B) **Optic nerve**

Species

Mouse; Rat.

Biological behavior

Minimally aggressive neoplasm.

Other Term(s) Used

Astrocytoma, benign; astrocytoma, low grade; glioma, astrocytic, benign.

Pathogenesis/cell of origin

Resident astrocytes.

Comment

Gliomas of the optic nerve of two rats were characterized by large masses within the bony orbit just posterior to the globe. Histologically, the tumors consisted of numerous, fairly well-differentiated astrocytes with poorly defined borders, elongated nuclei, common mitotic figures, focal cystic degeneration of tumor cells and loosely fibrillar cytoplasm. There was local invasion of adjacent orbital muscles and glandular structures, but no evidence of tumor infiltration into the brain (Fitzgerald et al. 1974). Gliomas of the optic nerve may be caused by injection of nickel compounds (Yoshitomi and Boorman 1990).

II. NONPROLIFERATIVE AND PROLIFERATIVE LESIONS OF THE GLANDS OF THE RAT AND MOUSE EYE

NORMAL ANATOMY AND PHYSIOLOGY OF THE GLANDS OF THE EYE

Harderian Gland

The Harderian gland is a large horseshoe-shaped gland located deep within the orbit of rodents and many other terrestrial vertebrates (Payne 1994). A small superior arm is connected to a large inferior arm by a narrow band medial to the optic nerve. The color of the gland varies from pink to dark grey depending upon the abundance and characteristics of melanocytes in the capsule and interlobar septa (Markert and Silvers 1956). In addition, in rodents the gland is speckled with a pigment identified as a porphyrin that fluoresces under ultraviolet light, which is secreted by the gland, and the amount is said to vary with strain, sex, and age (Figge and Davidheiser 1957). The tubuloalveolar gland is covered by a delicate connective tissue capsule bound loosely to the orbital fascia. Strands from the capsule divide the gland into lobes and lobules. The epithelial cells are pyramidal, their height depending upon the secretory phase. A round nucleus containing two or three nucleoli is located near the base, and the cytoplasm, packed with lipid droplets, appears finely vacuolated or foamy. Myoepithelial cells are present between the epithelial cells and the prominent basement membrane (Chiquoine 1958). The primary glandular secretion are lipids (wax esters), secreted by exocytosis (merocrine-type excretion) and yellow-brown porphyrin pigment, which is not visualized within the cytoplasm but in the acinar and ductal lumina. The ducts are lined by cuboidal epithelium. Alveolar, lobular, and lobar ducts join to form a single excretory duct, which opens at the base of the nictitating membrane.

Lacrimal Glands

There are two pairs of lacrimal glands, the extraorbital (also called exorbital) located subcutaneously, ventral and anterior to the ear (rostral to the parotid gland) and the intraorbital (also called infraorbital) located superficially to the Harderian gland at the outer canthus of the eyelids. The extraorbital gland of the rat is bean shaped (12 x 9 mm) and flat (2 mm thick), whereas the intraorbital gland has an approximate triangular form (major axis of 7.5 mm and 1 mm thickness) (Hebel and Stromberg 1986). In the mouse, the extraorbital gland is approximately 3 mm in diameter and the intraorbital gland can be hardly visualized without magnification (Botts et al. 1999). The excretory ducts of both glands fuse to form a common duct at the temporal angle of the palpebral fissure which opens into the conjunctival sac dorsally. Both lacrimal glands are tubuloacinar and histologically identical. Each is enclosed in a connective tissue capsule and divided by connective tissue septa into lobes and lobules. The serous secretory cells are pyramidal with granular basophilic cytoplasm that stains intensely near the round, basally-located nuclei, and stains much less intensely between the nuclei and the narrow acinar lumen. Myoepithe-

lial cells are found between the epithelium and the basement membrane. The intralobular ducts are lined by cuboidal cells whereas the excretory ducts are lined by stratified columnar epithelium (Krinke et al. 1994; 1996). Histologically, a gender dimorphism of the lacrimal glands can be observed after sexual maturity in rats, which increases with age and is characterized by scattered enlarged acinar epithelial cells containing enlarged nuclei (karyomegaly) in the male. In female rats, the lacrimal gland maintains the normal histological structure with aging, in males the lacrimal gland becomes pleomorphic (see Karyomegaly and Harderian gland alteration).

Nasolacrimal Duct (NLD)

The paired nasolacrimal ducts are the major component of a draining system that carries the lacrimal secretions from the eyes to the nasal cavity. Due to this anatomical and functional relation with the eye and glands of the eye, it is considered to be part of the lacrimal apparatus. The draining system begins with the lacrimal ducts at two puncta lacrimalia in each eye, oval openings located close to the edge of the eyelids lateral to the nasal angle of the palpebral fissure. The lacrimal ducts fuse nasally to form the nasolacrimal duct. In the rat, the paired nasolacrimal ducts are about 22 mm long, 0.5 by 0.2 mm wide in the initial portion and about 0.8 by 0.6 mm in its middle portion. Each nasolacrimal duct as a membranous tube runs along the outer aspect of the lacrimal bone, passes through the infraorbital fissure, and enters the osseous nasolacrimal canal, which crosses the alveolus of the incisor tooth ventrally. Within the region of the nasal cavity it runs in a channel formed by a ventral lamella of the maxilloturbinate and the os incisivum. At the rostral end of the maxilloturbinate it passes to the lateral wall of the nasal cartilage and about 2 mm caudal to the nostril opens ventromedially into the nasal vestibule (Hebel and Stromberg 1986). Since the nasolacrimal duct is visualized when examining the nasal cavity at different section levels, this duct has been referred to as part of the upper respiratory system, or as an accessory structure of the nasal cavity. Depending on the section level of the nasal cavity examined, the nasolacrimal duct can be found dorsolateral to the maxillary sinus at level III (section through the second palatine crest including the first upper molars in the rat); laterally to the root of the incisor tooth at the level II (section at the incisive papilla in rat and mice) or ventromedial to the root of the incisor teeth at level I (section at the posterior part of the upper incisor teeth in rat and mice) (Monticello et al. 1990; Boorman et al. 1990; Uraih and Maronpot 1990; Kittel et al. 2004).The epithelium of the ducts in the mouse varies from slightly keratinized squamous or low cuboidal in levels I and II of the nasal cavity, to non-ciliated pseudostratified cuboidal or columnar epithelium in level III (Herbert and Leininger 1999). According to other authors, stratified squamous epithelium is found at the origin and termination of the nasolacrimal duct. The rest of the duct is lined by pseudostratified non-ciliated columnar epithelium (Uraih and Maronpot 1990). Furthermore, the nasolacrimal duct epithelium has been described as a transitional epithelium (Stewart et al. 1979). Detailed descriptions of the mentioned epithelial types are missing. At level III of the nasal cavity, subepithelial lymphoid cell infiltrates appear to be associated to the initial part of the nasolacrimal duct (Monticello et al. 1990).

TERMINOLOGY AND DESCRIPTIONS

Nonproliferative Lesions of the Glands of the Rat and Mouse Eye

The Harderian and lacrimal glands have similar morphology and function, and develop similar nonproliferative lesions with terminology that is common to both glands. Lacrimal glands, especially the intraorbital gland, are not routinely sampled in toxicity and carcinogenicity studies in rodents. Therefore, most non-neoplastic lesions in the intraorbital lacrimal gland are haphazard findings during the examination of the Harderian gland where lacrimal tissue may be present.

General Terms

***Apoptosis (N)* Harderian gland; Extraorbital lacrimal gland; Intraorbital lacrimal gland**

Refer to general description (see Apoptosis).

Species

Mouse; Rat.

Pathogenesis/cell of origin

Acinar and/or ductal epithelial cells.

Diagnostic Features

- Shrinkage of single, non-contiguous epithelial cells with condensed hypereosinophilic cytoplasm.

Necrosis, single cell; necrosis (N) (Figure 65; Figure 66) **Harderian gland; Extraorbital lacrimal gland; Intraorbital lacrimal gland**

Species

Mouse; Rat.

Pathogenesis/cell of origin

Acinar and/or ductal epithelial cells.

Diagnostic Features

- Cells are swollen and exhibit cytoplasmic eosinophilia affecting groups of epithelial cells or acini (focal, multifocal, diffuse) or individual cells (necrosis, single cell).
- Associated with inflammation.
- Cellular exfoliation/debris.
- Squamous metaplasia and fibrosis may be seen.
- Hemorrhage may be present when necrosis is associated with retro-orbital bleeding procedure.

Differential Diagnoses

None.

Comment

Necrosis is a predominant feature in Rat coronavirus/Sialodacryoadenitis Virus infection. Necrosis may be also observed in xenobiotic induced inflammation (Westwood et al. 1991). Less severe focal necrosis may be observed at the puncture site after retro-orbital blood sampling.

Degeneration (N) (Figure 67, 68) **Harderian gland; Extraorbital lacrimal gland; Intraorbital lacrimal gland**

Species

Mouse; Rat.

Pathogenesis/cell of origin

Acinar and/or ductal epithelial cells.

Diagnostic Features

- Increases or decreases in cytoplasmic vacuolation.
- Swelling of epithelial cells.
- Tubuloacinar architecture is disorganized.

Differential Diagnoses

Atrophy:

- Acinar cells lose secretory differentiation. Irregularly shaped tubular forms with dilated or reduced lumina, lined by cuboidal or flattened epithelium that lack a vacuolated cytoplasm (Harderian gland) or serous (lacrimal gland) aspect.

Comment

Multifocal acinar degeneration resulted from treatment of rats with a phosphodiesterase inhibitor (Westwood et al. 1991).

Regeneration (N) **Harderian gland; Extraorbital lacrimal gland; Intraorbital lacrimal gland**

Species

Mouse; Rat.

Pathogenesis/cell of origin

Acinar and/or ductal epithelial cells.

Diagnostic Features

- Acini and/or ducts with increased cytoplasmic basophilia within or adjacent to areas of degeneration.
- Cells are smaller than typical acinar cells.

Differential Diagnoses

Hyperplasia, acinar:

- Focal non-compressive proliferation or increase in the number of epithelial cells, resulting in pseudostratification or folding of the epithelium with reduction of the lumen.

Comment

Both regeneration and hyperplasia are potential responses to degenerative/necrotic and inflammatory processes.

Hypertrophy (N) **Harderian gland; Extraorbital lacrimal gland; Intraorbital lacrimal gland**

Species

Mouse; Rat.

Pathogenesis/cell of origin

Acinar cells of the Harderian gland.

Diagnostic Features

- Foci of enlarged cells without an increase in cell number
- Reduction of the lumina may ocurr but no compression of adjacent tissue

Differential Diagnoses

Hyperplasia, acinar:

- Focal non-compressive proliferation or increase in the number of acinar/ductal cells, resulting in pseudostratification or folding of the epithelium with reduction of the lumen. Cells exhibiting hypertrophy often have a basophilic tinctorial aspect.

Comment

A clear differentiation between hypertrophy and hyperplasia is often difficult. Hypertrophy may be associated with hyperplasia.

Atrophy (N) (Figure 69) **Harderian gland; Extraorbital lacrimal gland**

Species

Mouse; Rat.

Other Term(s) Used

Atrophy and sclerosis.

Pathogenesis/cell of origin

Acinar and/or ductal epithelial cells.

Diagnostic Features

- Acini/ducts diminished in size.
- Irregularly shaped tubular forms with dilated or reduced lumina, lined by cuboidal or flattened epithelium.
- Acinar epithelial cells lose their serous or vacuolated differentiation. Interstitial fibrosis may be present.
- The lumina of the tubules in the Harderian gland may be filled with porphyrin accretions (masses of solid, brown, laminated porphyrin).

Differential Diagnoses

Dilation:

- Increased size of acinar lumen and/or ducts with reduction of epithelial cell height and maintenance of normal cytoplasmic characteristics and tissue structure.

Porphyrin granuloma of the Harderian gland (also called spontaneous granulomatous dacryoadenitis):

- Multifocal areas of granulomatous inflammation cen-

tered on atrophic acini filled with porphyrin accretions.

Comment

Atrophy may be focal or diffuse. Multifocal atrophy of the Harderian gland is an age-related process that is more prominent in rats than mice (Krinke et al. 1996). Multifocal atrophy is described as a spontaneous finding in the extraorbital gland of B6C3F1 mouse (Botts et al. 1999).

Hemorrhage (N) (Figures 70, 71) **Harderian gland; Extraorbital lacrimal gland; Intraorbital lacrimal gland**

Species

Mouse; Rat.

Pathogenesis/cell of origin

Vascular injury.

Diagnostic Features

- Extravasation of red blood cells in the glandular interstitium.
- Focal degeneration and/or necrosis of glandular and periglandular tissue (ocular muscles) are frequently observed at puncture sites when iatrogenic.
- Inflammation (neutrophilic or mixed cell) may be present in glandular and periglandular tissues near puncture sites.
- Hematoidin/Hemosiderin deposits (golden-yellow to golden-brown iron pigment stored in macrophages due to erythrocyte breakdown) may be observed after blood sampling.

Comment

A common cause of hemorrhage in the Harderian gland is trauma, often resulting from blood sampling from the retro-orbital sinus.

Dilation (N) **Harderian gland; Extraorbital lacrimal gland; Intraorbital lacrimal gland**

Species

Mouse; Rat.

Other Term(s) Used

Ectasia.

Pathogenesis/cell of origin

Acini and/or ducts.

Diagnostic Features

- Increased luminal size of glandular acini and/or ducts.
- Reduction of epithelial cell height.

Differential Diagnoses

Atrophy:

- Irregularly shaped acini/ducts with cuboidal or flat epithelial cells, which have lost the characteristic secretory appearance.

Comment

In mice, dilation of ducts and acini is described in the lacrimal glands as the result of blockage of the duct that drains the secretion to the surface of the eye. The actual blockage cannot usually be demonstrated microscopically (Frith and Ward 1988).

Cyst (N) **Harderian gland; Extraorbital lacrimal gland; Intraorbital lacrimal gland**

Species

Mouse; Rat.

Pathogenesis/cell of origin

Epithelial cells of the nasolacrimal duct.

Diagnostic Features

- Cystic space lined by stratified squamous epithelium.
- Lumen space may contain keratin and cellular debris.

Comment

Cysts are found in the submucosa of the nasolacrimal duct associated with inflammation, and are usually localized laterally to the root of the incisor teeth (Yoshitomi and Boorman 1990).

Inflammatory Changes

Infiltrate, inflammatory cell (N) **Harderian gland; Extraorbital lacrimal gland; Intraorbital lacrimal gland**

Species

Mouse; Rat.

Pathogenesis/cell of origin

Acini and/or ducts and interstitial tissue.

Diagnostic Features

- Foci of a single inflammatory cell type or a mixture of different cell types without other features of inflammation.

Differential Diagnoses

Inflammation:

- Inflammatory cellular infiltrate associated with edema, congestion, degeneration/necrosis and squamous metaplasia of acini /ducts.

Comment

The term “infiltrate” is recommended followed by the predominant cell type present (neutrophilic, eosinophilic, lymphocytic, plasmacytic or histiocytic) or mixture of different cell types (mixed). The most frequent type of inflammatory cell infiltrate observed in the Harderian gland in rat and mouse is lymphocytic (lymphoid aggregates) and occurs spontaneously. In mice, the incidence of lymphocytic infiltrates increase with age and is more common

in male than in female B6C3F1 mice (Botts et al. 1999). Lymphocytic inflammatory cell infiltrates occur spontaneously with advancing age and may or may not be associated with Harderization of the lacrimal gland. It remains unclear whether these lymphocytic infiltrates involve an autoimmune mechanism (Krinke et al. 1996). In the nasolacrimal duct, lymphocytic infiltrates (lymphoid aggregates) predominate (Monticello et al. 1990).

Inflammation (N) (Figure 66) **Harderian gland; Extraorbital lacrimal gland; Intraorbital lacrimal gland**

Species
Mouse; Rat.

Other Term(s) Used
Dacryoadenitis.

Pathogenesis/cell of origin
Acini and/or ducts and interstitial tissue.

Diagnostic Features
- Foci or more extended areas of single or mixed inflammatory cellular types.
- Interstitial edema and/or congestion.
- May be associated with squamous metaplasia of acinar/ductal epithelium or interstitial fibrosis.
- Salivary glands may be involved, in addition to the Harderian and lacrimal glands.
- Porphyrin accretions are associated with granulomatous inflammation in the Harderian gland.
- Inflammation resulting from blood sampling is accompanied by hemorrhage and is localized to the puncture site.
- Inflammation due to viral inflammation tends to be extensive (multilobular).

Differential Diagnoses
Infiltrate, inflammatory cell:
- Foci of single or mixed inflammatory cell types without other features of inflammation.

Comment
Modifiers are recommended in relation to the predominant inflammatory cellular type (neutrophilic, eosinophilic, lymphocytic, plasmacytic or histiocytic) or mixture of different cellular types (mixed). Although uncommon in modern laboratory animal facilities, inflammation caused by Rat coronavirus/Sialodacryoadenitis Virus (SDAV) is multilobular, with degeneration/necrosis as a prominent feature, accompanied by neutrophilic inflammation in early phases. In the late inflammatory phases, lymphocytes and macrophages as well as tubuloacinar squamous metaplasia are the most predominant features (Percy et al. 1989). Chromodacryorrhea (red tears) may be present due to hypersecretion of porphyrin in cases of inflammation in the Harderian gland caused by the SDAV, however no porphyrin accretions are observed in the acini. Xenobiotic induced inflammation may be lymphocytic or mixed (lymphocytes, plasma cells and macrophages). In severe cases epithelial hyperplasia and interstitial fibrosis has been noted (Reuber 1976). Chronic dacryoadenitis with degenerative epithelial changes and increased porphyrin secretion are reported to occur in the Harderian gland after long term treatment with an inotropic phosphodiesterase inhibitor in rats (Westwood et al. 1991).

SDAV also causes inflammation of the nasolacrimal ducts (Bihun and Percy 1995). Inflammation of the nasal cavity is reported to occur with chemical induced inflammation of the ducts (National Toxicology Program 2010; Schoevers et al. 1994; Wagner et al. 2009). Drug-related inflammation needs to be differentiated from degeneration, necrosis and inflammation that is reported in the nasolacrimal duct of aged mice (Herbert and Leininger 1999).

Inflammation, granulomatous (N) **Harderian gland; Extraorbital lacrimal gland; Intraorbital lacrimal gland**

Species
Mouse; Rat.

Other Term(s) Used
Granulomatous dacryoadenitis, foreign body inflammation, porphyrin granuloma (the latter occurs in the Harderian gland; also called atrophy and sclerosis of the Harderian gland in the rat).

Pathogenesis/cell of origin
Acini and/or ducts and interstitial tissue.

Diagnostic Features
- Granulomatous reaction composed of epithelioid macrophages, multinucleated giant cells, lymphocytes and plasma cells.
- May be associated with a foreign body.
- In the case of porphyrin granuloma, granulomatous reaction associated with porphyrin accretions (in the lumen of atrophic acini and/or porphyrin partially engulfed by macrophages).

Comment
Porphyrin granuloma of the Harderian gland is an age-related spontaneous change associated with increased porphyrin secretion and acinar atrophy, which precedes granuloma formation. Abundant deposition of connective tissue fibers may replace the injured acini. Macroscopically, this finding is characterized by the presence of multifocal dark discolorations on the surface of the gland, representing the porphyrin accretions. It appears to be more common in aging rats (from one to three years) than mice. A female sex predilection has been suggested, however, it is questionable whether female rats are more susceptible to porphyrin granulomas than males (Krinke 1991). Rarely, retro-orbital granulomatous inflammation may be associ-

ated with hair shafts in rat and mouse, introduced into the glandular tissues by scratching or by retro-orbital puncture, either which can be associated with fungal hyphae. A granulomatous type of inflammation of the nasolacrimal duct is shown in the "Respiratory System" INHAND (Renne et al. 2009).

Miscellaneous Changes

Porphyrin, increased (N) (Figures 72, 73) **Harderian gland**

Species
Mouse; Rat.

Pathogenesis/cell of origin
Acini

Diagnostic Features
- Normal acini may contain an increased amount of porphyrin (a yellow-brown substance with a fluid appearance). Alternatively, porphrin may appear as solid, laminated brown masses within atrophic acini.

Differential Diagnoses
Granulomatous inflammation
- Porphyrin accretions are accompanied by a granulomatous reaction (epithelioid macrophages, multinucleated giant cells, lymphocytes and plasma cells).

Comment
As a spontaneous change, it is frequently observed in aging rats and mice. Increased porphyrin is also mentioned in inflammation of the Harderian gland caused by phosphodiesterease inhibitors (Westwood et al. 1991).

Karyomegaly (N) **Extraorbital lacrimal gland; Intraorbital lacrimal gland**

Species
Mouse; Rat.

Other Term(s) Used
Cytomegaly; Nuclear pleomorphism; Polyploidy.

Pathogenesis/cell of origin
Acinar epithelial cells of the lacrimal gland

Diagnostic Features
- Acinar epithelial cells with variation in nuclear size and shape (the nuclei may be two to four times the normal size and may be accompanied by increase in cellular size).
- Increased nuclear basophilia.
- Intranuclear eosinophilic inclusions (pseudoinclusions) can be observed.

Comment
Karyomegaly is characteristic of the male rat and mouse lacrimal gland. Increased nuclear size represents polyploidy, whereas the nuclear inclusions represent cytoplasmic invaginations. Karyomegaly is androgen-dependent and is therefore observed in males after sexual maturity (sexual dimorphism) and becomes more prominent with increasing age (Krinke et al. 1994; Krinke et al. 1996; Paulini and Mohr 1975). Karyomegaly may be induced by cytomegalovirus (MCMV) infection.

Alteration, acinar (N) (Figure 74) **Extraorbital lacrimal gland; Intraorbital lacrimal gland**

Species
Mouse; Rat.

Other Term(s) Used
Harderization; Ectopic Harderian gland in the lacrimal gland

Diagnostic Features
- Foci of acini with histological characteristics of Harderian gland (composed of cuboidal to columnar cells with finely vacuolated cytoplasm and distinct alveolar lumen).

Comment
In rats, Harderian gland alteration can be observed in the extraorbital lacrimal gland of male and female rats at three months of age, but increases at six months of age in males only. This process appears to be androgen-dependent but also influenced by the absence of estrogen receptors on lacrimal gland acinar epithelial cells in male rats after six months of age (Ferrara et al. 2004). Conversely in mice, females are more frequently affected than males (Krinke et al. 1996). It remains unclear whether this change reflects a metaplastic or a degenerative change. It appears that the Harderian gland cells develop from undifferentiated basal cells of the lacrimal gland acini and intercalated and excretory ducts (Sashima et al. 1989).

Nonneoplastic Proliferative Lesions of the Glands of the Rat and Mouse Eye

Harderian Gland

Hyperplasia, acinar (H) (Figure 75) **Harderian gland**

Species
Mouse; Rat.

Pathogenesis/cell of origin
Acinar epithelium of the Harderian gland.

Diagnostic Features
- Cellular proliferation confined to solitary or multiple foci.
- There is no evidence of compression of adjacent parenchyma.
- Architecture of the gland is maintained.
- Alveolar pattern is retained, but there is an increased

number of cells lining the acini.
- Epithelium is one layer thick.
- Epithelium may project into the acinar lumen.
- Foci of hyperplasia have an alveolar pattern and an increased number of cells lining the acini. Hyperplastic cells may be larger and tinctorially (basophilic) distinct.

Differential Diagnoses

ADENOMA:
- Adenoma is an expansively enlarging lesion that causes obvious compression and distortion of the architecture of the adjacent gland. Cellular atypia is generally noted.

Comment

Hyperplasia of the Harderian gland occurs in association with adenitis and atrophy of the gland and squamous metaplasia of ducts. This lesion may be a regenerative response to damage to the gland caused by virus-induced sialodacryoadenitis, trauma of orbital bleeding, and other causes. Hyperplasia of the Harderian gland may occur in the absence of adenitis. Primary hyperplasia may be a preneoplastic change.

Lacrimal Gland

Hyperplasia, acinar (H) (Figure 76) **Extraorbital lacrimal gland; Intraorbital lacrimal gland**

Species

Mouse; Rat.

Pathogenesis/cell of origin

Epithelial acinar cells of lacrimal gland.

Diagnostic Features
- Focal non-compressive proliferation of acinar cells is associated with degenerative and inflammatory lesions of the lacrimal gland.
- Squamous cell hyperplasia is observed in the lacrimal duct associated with inflammation.

Differential Diagnoses

ADENOMA:
- Adenoma causes compression and displacement of adjacent non-neoplastic gland, and has distorted arrangement of lobules and acini.

Comment

Hyperplasia of lacrimal glands in the absence of degenerative and inflammatory lesions is exceedingly rare in the rat and has not been reported in the mouse.

Nasolacrimal Duct (NLD)

Hyperplasia, epithelial (H) **Nasolacrimal duct**

Species

Mouse; Rat.

Pathogenesis/cell of origin

Epithelial lining of the NLD (slight to non-keratinized stratified squamous epithelium, pseudostratified cuboidal or columnar epithelium or transitional epithelium).

Diagnostic Features
- Epithelial hyperplasia may be mural, involving a variable expanse of the lining epithelium, or be exophytic (polypoid).

Differential Diagnoses

REACTIVE HYPERPLASIA:
- Signs of inflammation (periductal, intraepithelial and luminal inflammatory cells with accompanying proteinaceous fluid and cellular debris in ductal lumen) in addition to the epithelial hyperplasia.

Comment

Epithelial hyperplasia of the NLD was described in aged mice (158 and 142-week old males) (Leininger et al. 1996).

Neoplastic Proliferative Lesions of the Glands of the Rat and Mouse Eye

Harderian Gland

Adenoma (B) (Figure 77) **Harderian gland**

Species

Mouse; Rat.

Pathogenesis/cell of origin

Acinar epithelium of the Harderian gland.

Diagnostic Features
- Adenomas are usually well demarcated, rarely encapsulated and cause compression of the surrounding gland.
- Architecture of the gland is not maintained within the tumor.
- Piling of cells may be present and clusters of epithelial cells may project into the acinar lumina on the surface of the lining cells.
- The cytoplasm may/may not retain its normal foamy appearance.
- Neoplastic cells are enlarged, the nuclei are fairly uniform, and rarely have mitotic activity (except for acinar type in the mouse).

In the mouse, the following growth patterns can be distinguished: (Krinke et al. 2001)

Papillary:
- Multiple branching papillary projections with a fibrovascular stroma.
- Epithelium is one or occasionally more layers thick but still attached to the basal lamina.

Cystic:
- Multiple distended cystic spaces are lined by epithelium.

- Papillary projections may be present, but are not prominent.
- Mostly large tumors have a prominent capsule.

Cystic-papillary:
- Composed of both papillary and cystic areas.
- Cystic areas appear empty except for cellular debris and remnants of papillary projections.
- The epithelial lining may be flattened.

Acinar:
- Growth pattern resembles acinar glandular architecture despite the marked proliferation of the epithelial cells.
- Encapsulation and compression may be absent.
- Papillary projections are not prominent.
- Cells with single large cytoplasmic vacuoles may be present.
- Cytoplasm may be eosinophilic and homogeneous without foamy appearance.
- Nuclear to cytoplasmic ratio is increased in comparison to the other types.
- Cells are more pleomorphic and mitotic figures are more numerous than in the other types.

Differential Diagnoses

Hyperplasia, acinar:
- In hyperplasia, the architecture of glandular acini is retained without compression of the adjacent gland, whereas in the adenoma the acinar architecture is distorted and compression involves the adjacent gland.

Adenocarcinoma:
- Adenocarcinoma, well differentiated, is distinguished from adenoma by local invasion and cellular atypia; less differentiated adenocarcinoma has a solid growth pattern, cellular pleomorphism, and metastases.

Comment

Spontaneous neoplasms of the Harderian glands are of rare occurrence in rats of various strains, but have been induced by administration of urethane during the neonatal period (Elwell and Boorman 1990). Adenomas of the Harderian gland are common in some mouse strains. In contrast to rats, spontaneous Harderian gland adenomas are frequently observed in old albino and pigmented mice. The incidence varies with strain and significant sex differences have been described. The incidence of spontaneous adenomas given in the literature varies from 0.5 to 14.9% (Krinke et al. 2001).

Adenocarcinoma (M) (Figure 78) **Harderian gland**

Species

Mouse; Rat.

Pathogenesis/cell of origin

Acinar epithelium of the Harderian gland.

Diagnostic Features
- Well differentiated adenocarcinoma is composed of cuboidal to columnar epithelial cells arranged as tubular and acinar structures with solid areas of cells in some neoplasms.
- Poorly differentiated carcinoma is composed of solid sheets of pleomorphic epithelial cells with few tubular and acinar structures.
- Anaplastic carcinoma is composed of solid sheets of pleomorphic epithelial cells without tubular and acinar structures and with numerous mitotic figures (Senoh et al. 2014).
- Invasion of the orbital/periorbital tissues may occur along with foci of necrosis and fibrosis. Adenocarcinomas are frequently associated with exophthalmos. Metastasis to regional lymph nodes and lung has been reported (Carlton and Render 1991).

Differential Diagnoses

Adenoma:
- Well differentiated adenocarcinoma is separated from adenoma by histological evidence of local invasion. In addition, the lack of histological and cellular differentiation distinguishes the poorly differentiated and undifferentiated carcinomas from adenoma.

Comment

Spontaneous adenocarcinomas are rarely described in rats, but adenocarcinomas have been produced by experimental exposure to 2-acetylaminofluorene. In mice, adenocarcinomas also occur less frequently than adenomas.

Lacrimal Gland

Adenoma (B) (Figure 79) **Extraorbital lacrimal gland; Intraorbital lacrimal gland**

Species

Mouse; Rat.

Pathogenesis/cell of origin

Epithelial acinar cells of lacrimal gland.

Diagnostic Features
- Expansive growth causes compression and distortion of adjacent non-neoplastic glandular parenchyma.
- Lobular mass is composed of tubular and acinar structures lined by uniform cuboidal cells with uniform, generally round nuclei.

Differential Diagnoses

Adenocarcinoma:
- Malignant neoplasms have features such as cellular atypia, local invasion, distant metastasis, and mitotic activity. Lobular and acinar arrangements may be absent and the neoplasm is composed of solid areas and clusters of cells.

Comment

Spontaneous neoplasms of the lacrimal glands are rarely reported in rats, although these glands are not routinely examined. Described adenomas have been acinar in type, and ductular adenomas have not been reported.

Adenocarcinoma (M) **Extraorbital lacrimal gland; Intraorbital lacrimal gland**

Species

Mouse; Rat.

Pathogenesis/cell of origin

Acinar epithelial cells of lacrimal gland.

Diagnostic Features

- Expansive mass that causes compression and distortion of adjacent non-neoplastic gland.
- Invasion of adjacent tissues.
- Lobular pattern is obscured and cellular atypia and pleomorphism of varying severity are observed.
- Irregular acinar structures are lined by stratified epithelium and much of the neoplasm may be replaced by solid collections of epithelial cells with round to ovoid, variably-sized nuclei.

Differential Diagnoses

Adenoma:

- The benign neoplasm lacks the cellular atypia and pleomorphism, evidence of local invasion, and poorly developed lobular and acinar patterns of the malignant neoplasm.

Comment

Malignant neoplasms of the lacrimal glands are exceedingly rare in the rat and mouse (Mohr 1994).

Nasolacrimal Duct (NLD)

Papilloma, squamous cell (B) **Nasolacrimal duct**

Species

Mouse; Rat.

Pathogenesis/cell of origin

Epithelial lining of the NLD (slight to non-keratinized stratified squamous epithelium, pseudostratified cuboidal or columnar epithelium).

Diagnostic Features

- Exophytic mass of uniform, regularly arranged squamous cells resting on a stalk of vascularized connective tissue.
- Keratinization may be absent depending on the type of proliferating cell (transitional papilloma).
- Intact basement membrane.

Differential Diagnoses

Polypoid hyperplasia:

- No vascularized stalk of connective tissue.

Carcinoma, squamous cell:

- Cellular atypia.
- Destruction of basement membrane.
- Invasive growth.

Carcinoma, squamous cell (M) **Nasolacrimal duct**

Species

Mouse; Rat.

Pathogenesis/cell of origin

Epithelial lining of the NLD (slight to non-keratinized stratified squamous epithelium, pseudostratified cuboidal or columnar epithelium).

Diagnostic Features

- Irregular cellular and nuclear size and shape (depending on the grade of differentiation).
- Invasion beyond the basement membrane.
- Frequently concurrent with proliferating mass in the nasal cavity and surrounding tissues.

Differential Diagnoses

Papilloma, squamous cell:

- No cellular atypia.
- No invasion beyond basement membrane and into surrounding tissues.

Comment

It is difficult to determine the site of origin of spontaneous squamous cell carcinoma in the nasal cavity. Nasal masses frequently affect secondary paranasal structures such as the incisor tooth or nasolacrimal duct. However, spontaneous carcinomas of the nasal cavity may arise from the nasolacrimal duct and invade adjacent areas (palate, maxillary bone, tooth and nasal cavity) (Maronpot 1990; Schoevers EJ et al. 1994).

III. NONPROLIFERATIVE AND PROLIFERATIVE LESIONS OF THE RAT AND MOUSE OLFACTORY SYSTEM / CHEMOSENSORY STRUCTURES

INTRODUCTION

Standardized nomenclature of nonproliferative and proliferative lesions of the olfactory epithelium is common to the different chemosensory structures in the nasal passages (listed below). Each of these structures is described separately in this manuscript, and there is, therefore, some redundancy of the responses in the different structures. Moreover, the main olfactory epithelium has been described previously under the proliferative and nonproliferative lesions of rat and mouse respiratory tract (Renne et al. 2009); wherever applicable, this section uses identical nomenclature.The chemosensory/olfactory system is represented by a number of structures/organs in the nasal passages (Storan and Key 2006; Ma 2007; Rivière et al. 2009; Silvotti et al. 2011; Barrios et al. 2014),

- Main olfactory epithelium (MOE),
- Vomeronasal organ (VNO)/Jacobson's Organ,
- Septal organ of Masera (SOM)/olfactory septal organ/ organ of Rodolfo-Masera/septal olfactory organ and
- Grueneberg ganglion (GG).

Together these structures function in the special sense of smell or olfaction. All structures connect with areas in the brain via the main (MOE, SOM, GG) or accessory (VNO) olfactory bulb (Jia and Halpern 2003; Restrepo et al. 2004) (Figure 80) via the olfactory nerve (Fuss et al. 2005). MOE is a target of toxicity for several substances, both via air exposure and oral uptake (Harkema 1991; Haschek-Hock and Witschi 2004; Renne et al. 2009; Nyska et al. 2005; Woutersen et al. 2010). Reports on xenobiotic-induced histopathology of the other chemosensory structures are less common (VNO) to very rare (SOM) to absent (GG).

Other neural structures in the nasal passages are

- single receptors/solitary chemosensory cells/'brush' cells and
- free intraepithelial trigeminal nerve branches.

These other neural structures are considered to monitor the inhaled air for flow rate, nociception and thermoperception (Finger et al. 2003; Gulbransen et al. 2008; Tizzano et al. 2011). They connect with the brain via the trigeminal nerve (Figure 80), and stimulation by inhalation of irritating substances may lead to protective reflexes like sneezing. The components are part of the nasal epithelium; one in approximately 100 respiratory epithelial cells, brush cells and free nerve endings are present in the squamous, respiratory and olfactory epithelium (Finger et al. 1990; Spit et al. 1993; Katahashi et al. 1997). Consequently, nasal epithelial toxicants can affect them. However, reports on toxicity to these structures are practically non-existent, and also because they cannot easily be recognized in conventionally-stained sections. Therefore, they are not further addressed here.

There is a close connection of nasal neural structures and the brain. Therefore, the olfactory and trigeminal pathways can act as transport of inhaled substances to the brain, and circumvent the blood-brain barrier. In addition, part of the cerebrospinal fluid drains onto the olfactory nasal mucosa (Brinker et al. 1997). The nose-brain connection should be kept in mind when evaluating histopathology of the nasal neural structures.

The location of lesions is related to the deposition of inhaled or ingested substances and site-specific susceptibility in relation to tissue factors like metabolism, species and sex (Kai et al. 2006). An apparent lack of effects on SOM and GG may also be due to sampling of nasal tissue and selection of levels for microscopic examination.

NORMAL HISTOLOGY AND BIOLOGY

Main olfactory epithelium (MOE)

The MOE covers 50% of the epithelium lining the rat nasal cavity; in the mouse 47% of the nasal epithelium is olfactory (Harkema and Morgan 1996). The MOE covers a small portion of the dorsocranial meatus and contiguous upper one-third of the nasal septum and the majority of the ethmoid turbinates in the posterior nasal cavity. The main olfactory epithelium houses basal (stem) cells, intermediate neuronal precursors, mature sensory neurons and sustentacular/supporting cells. Epithelial degeneration, necrosis and regeneration of the epithelium are often present together, when the tissue is repeatedly exposed to toxic chemicals, resulting in a disorganized morphologic picture (Renne et al. 2009; Hardisty et al. 1999). MOE, olfactory nerve and olfactory bulb have a high regenerative capacity after injury. MOE regenerates from basal cells, Bowman's glands (epithelial or in the submucosa) and duct cells regenerate from progenitor cells within the ducts, whereas sustentacular cells can arise from both cell sources (Huard et al. 1998). However, a certain specificity of odorant perception may not always be restored unless a substantial number of fibers of the same type are spared (Schwob 2002).

Vomeronasal organ (VNO)

The VNO is a bilateral tubular structure located ventrally, within the bone and cartilage at the base of the septum and opening to the nasal cavity. The lumina are lined laterally by respiratory epithelium and medially by neuronal epithelium (Figure 81). Like other olfactory epithelium it houses basal, neurosensory and sustentacular cells. At present, VNO is the only olfactory organ known to connect with the accessory olfactory bulb (Storan and Key 2006). A low number of neutrophils appear to be normal constituents of the non-sensory, respiratory epithelium (Getchell and Kulkarni 1995; Døving and Trotier 1998). The neuronal epithelium is organized into different zones: the marginal zones at the transition/border with the respiratory epithelium; the intermediate zones and the central zone (Brann and Firestein 2010). Vomeronasal glands are found apically of the tubules, within the cartilage that surrounds the VNO (Adams 1992). Its main function is perception of pheromones. VNO is already well-developed at birth (Oikawa et al. 2001), but increases in size postnatally. The

overall volume, neuroepithelial volume, and number of bipolar neurons are larger in males compared to females (Guillamón and Segovia 1997). Mitosis in the adult occurs particularly at the marginal zones of the neural epithelium (Weiler 2005; De La Rosa-Prieto et al. 2009; Martínez-Marcos et al. 2000). Neural turnover in the mouse in the VNO epithelium may occur especially through migration (Halpern and Martínez-Marcos 2003); cells at the edges were found to migrate horizontally very slowly (less than 10% of the distance from the edge to the center of the epithelium per month). Distribution of apoptotic cells indicate that a number of cells in mitosis die before becoming functional neurons. Regeneration of new neurons is preserved even in aged rodents (De La Rosa-Prieto et al. 2010).

Septal organ of Masera (SOM)

The SOM is a bilateral, small island of olfactory cells, surrounded by respiratory ciliated epithelium. The islands are located at the ventral base of the nasal septum, posterior to the opening of the nasopalatine duct. SOM is present at birth, increases in size postnatally till sexual maturity, and declines thereafter, but is still present in aged rats (Breipohl et al. 1989; Weiler and Farbman 2003; Adams 1992). Like other olfactory epithelium it houses basal, neurosensory and sustentacular cells. The SOM is located rostral to the MOE and may serve as a rostral sensor in advance of MOE perception, triggering deeper inhalation (Marshall and Maruniak 1986). Alternatively, SOM olfactory perception may be limited to certain chemical signatures dictated by the limited connection to specific regions within the olfactory bulb. SOM projects mainly to the posterior, ventromedial part of the main olfactory bulb (Ma et al. 2003). Both options are supported by molecular analysis of the receptors present in SOM (Tian and Ma 2004; Su et al. 2009). The sensory neurons in the septal organ and in the MOE share signaling pathways and show similar odorant responses, but some receptors are present in SOM in very high densities. The SOM can serve as an airflow sensor in addition to its chemosensory roles (Ma 2010).

Grueneberg ganglion (GG)

The GG is a bilateral group of ganglion cells and their associated overlying squamous epithelium, located in the dorsal meatus of the vestibulum of the nasal passages (mouse: Grüneberg 1973; Fleischer et al. 2006; Roppolo et al. 2006; mouse and rat: Brechbühl et al. 2014). Ganglion cells are present at birth. GG of neonatal mice most likely has a dual function, namely perception of alarm pheromones (and a few odorous compounds like dimethylpyrazine) and temperatures (Liu et al. 2009; Mamasuew et al. 2008 and 2011; Schmid et al. 2010; Fleischer and Breer 2010). The function of GG appears to decline with age (Fleischer et al. 2006).

Olfactory bulb

The olfactory bulb is part of the brain and receives sensory input via the olfactory nerve (which contains axons from olfactory receptor neurons of the olfactory epithelium), and transmits chemosensory information from the nose to the brain. It is generally assumed that the bulb functions as a filter of chemosensory information (Soucy et al. 2009). The olfactory bulb is reported to also receive inputs from such brain areas as the amygdala, neocortex, hippocampus, locus coeruleus, and substantia nigra (Kang et al. 2009).

The olfactory bulb consists of the main olfactory bulb and the accessory olfactory bulb, both of which have similar histologic structure. The main olfactory bulb is organized into a glomerular layer, external plexiform layer, mitral cell layer, internal plexiform layer and a granule cell layer (Gutman et al. 2013). The glomerular layer receives direct input from the olfactory nerve, and their axons terminate in spherical structures known as glomeruli, where they connect in the external plexiform layer with the apical dendrites of mitral cells. The basal dendrites (internal plexiform layer) of the mitral cells transport the signals further to the olfactory cortex. Mitral cells are connected to interneurons known as granule cells, which are probably involved in inhibition processes. The accessory olfactory bulb, a region located dorsal-posterior to the main olfactory bulb, appears to operate independently from the main olfactory bulb (Yokosuka 2012). It receives input from the vomeronasal organ and connects mainly to the amygdala and hypothalamus (Mucignat-Caretta 2010).

TERMINOLOGY AND DESCRIPTIONS

Nonproliferative Lesions of the Rat and Mouse Olfactory System/Chemosensory Structures

Normal Anatomy (Figures 80–85)

Main Olfactory Epithelium (MOE) - Olfactory Epithelium and Nerves

Congenital Lesions

None.

Degenerative/Epithelial Changes

Atrophy, MOE (N) **Main olfactory epithelium (MOE)**

Species

Mouse; Rat.

Synoymn(s)

Atrophy, olfactory epithelium; atrophy, Bowman's gland.

Pathogenesis/cell of origin

Olfactory epithelium including sustentacular cells; degenerative change.

Diagnostic Features

- Thinning of the affected mucosa.
- Cells are reduced in height (cuboidal to flattened).
- The nuclei appear close together due to reduced cytoplasm.
- Often accompanied by loss of axon bundles in subjacent lamina propria.

- Underlying turbinate bone may also be atrophied (Renne et al. 2009).

Differential Diagnoses

Metaplasia (see Metaplasia, respiratory, MOE and Metaplasia, squamous cell, MOE):
- Change in epithelial cell types present, usually with mixture of cell types in areas of transition.

Degeneration, MOE:
- Loss of cilia and cellular organization but no decrease in thickness of epithelial layer.

Artifacts:
- Postmortem autolysis: Uniform dissolution of entire tissue section with no change in organization or depth of cell layers.
- Tangential section through epithelium: Microscopic evidence of tangential cut in other tissue structures.

Comment

Atrophy is commonly observed as a sequel to degeneration of olfactory epithelium. Atrophy of olfactory epithelium secondary to degeneration of sensory or sustentacular cells has been observed following inhalation of a variety of chemicals (Buckley et al. 1985; Hardisty et al. 1999; Monticello et al. 1990; Leininger et al. 1996).

Degeneration, MOE (N) (Figure 86) **Main olfactory epithelium (MOE)**

Species

Mouse; Rat.

Synoymn(s)

Degeneration, olfactory epithelium; degeneration, Bowman's gland.

Pathogenesis/cell of origin

Olfactory epithelium.

Diagnostic Features

(Renne et al. 2009, see Degeneration).
- Loss of cilia.
- Epithelial vacuolization/bleb formation.
- Increased intercellular spaces.
- Loss of organization of the cell layers.
- Dilatation (ectasia) of Bowman's glands (subepithelial) with accumulation of secretory material.

Differential Diagnoses

Postmortem autolysis:
- Uniform dissolution of entire tissue section with no change in organization or depth of cell layers.

Metaplasia (see Metaplasia, respiratory, MOE and Metaplasia, squamous cell, MOE):
- Change in epithelial cell types present, usually with mixture of cell types in areas of transition.

Comment

Degenerative changes in olfactory epithelium have been reported as sequelae to toxic agent exposure (Harkema 1990; Monticello et al. 1990; Morgan and Haarkema 1996; Maronpot 1990 and as a consequence of aging (St Clair and Morgan 1992). Degeneration of olfactory epithelium may result from primary effects on neurons (Wine 2007), sensory cells or sustentacular cells (Grubb et al. 2007). Severe degeneration may be accompanied by loss of Bowman's glands and nerve bundles (Robinson et al. 2003).

Erosion/ulcer, MOE (N) **Main olfactory epithelium (MOE)**

Species

Mouse; Rat.

Other Term(s) Used

Erosion/ulcer, olfactory epithelium.

Pathogenesis/cell of origin

Olfactory epithelium; caused by tissue injury.

Diagnostic Features

(Renne et al. 2009, see Erosion/ulceration).
- Loss/ablation/sloughing off of nasal epithelium only (erosion).
- Complete loss of the epithelium and underlying basement membrane (ulcer).
- Associated with necrosis and inflammation, usually suppurative or serofibrinous.

Differential Diagnoses

Atrophy, MOE:
- Thinning of mucosa but no inflammation or cell debris.

Necrosis, MOE:
- Pyknosis, karyorrhexis or karyolysis of nuclei, cytoplasmic eosinophilia, cellular swelling or shrinkage, exfoliation of cells.

Degeneration, MOE:
- Loss of cilia and vacuolation but no inflammation or cell debris.

Artifact:
- No evidence of inflammation.

Postmortem autolysis:
- Uniform dissolution of entire tissue section with no change in organization or depth of cell layers.

Comment

Erosion and ulceration are observed in response to a number of inhaled toxicants (Monticello et al. 1990). Care must be taken to distinguish erosion or ulceration from artificial loss of epithelium related to experimental procedures or

autolysis. A serofibrinous or suppurative exudate is usually visible covering areas of ulcerated epithelium in scenarios of non-acute exposure. Metaplasia to squamous or respiratory epithelium may occur following repeated loss of olfactory epithelium. When ulceration is present as part of a necrotic process, recording of both necrosis and ulceration will provide a clear description of the lesion.

Apoptosis, MOE (N) **Main olfactory epithelium (MOE)**

Species

Mouse; Rat.

Other Term(s) Used

Apoptosis, olfactory epithelium; apoptosis, Bowman's gland; degenerative change.

Pathogenesis/cell of origin

Olfactory epithelium.

Diagnostic Features

Apoptosis:

- Single cell death or small clusters of cells.
- Cell shrinkage and convolution.
- Cytoplasmic condensation (hypereosinophilia).
- Chromatin condensation (pyknosis) and peripheralization in early apoptosis.
- Karyorrhexis with fragmentation of condensed chromatin.
- Intact cell membrane.
- Formation of blebs to produce apoptotic bodies.
- Cytoplasm retained in apoptotic bodies.
- Phagocytosis of apoptotic bodies tissue macrophages or other adjacent cells.
- Lack of inflammation.

Special Techniques for Diagnostics

- Terminal TdT-mediated dUTP-Nick-End Labelling (TUNEL) assay, staining for caspases or ultrastructural evaluation can be used to specify apoptosis.

Differential Diagnoses

Necrosis, single cell:

- Often contiguous cells.
- Cell and organelle swelling.
- Pyknosis (nuclear condensation: minor component).
- Karyorrhexis (nuclear fragmentation).
- Karyolysis (degradation of nuclear material).
- Cytoplasmic blebs.
- Plasma membrane rupture.
- Intracellular contents are present in the surrounding tissue.
- Inflammation usually present.

Comment

Apoptosis in the mature and developing olfactory epithelium in rats was described by Cowan and Roskams 2002.

Necrosis, Single cell necrosis, MOE (N) **Main olfactory epithelium (MOE)**

Species

Mouse; Rat.

Other Term(s) Used

Necrosis, olfactory epithelium; necrosis, Bowman's gland.

Pathogenesis/cell of origin

Olfactory epithelium; caused by tissue injury.

Diagnostic Features

(Renne et al. 2009, see Necrosis).

- Pyknosis, karyorrhexis or karyolysis of nuclei.
- Cytoplasmic eosinophilia.
- Cellular swelling or shrinkage.
- Exfoliation of cells.
- May result in erosion or ulceration.
- May be associated with inflammation.
- Luminal accumulations of fibrin and/or cell debris.

Differential Diagnoses

Degeneration, MOE:

- Loss of cilia and vacuolation but no inflammation or cell debris.

Atrophy, MOE:

- Thinning of cell layers but no inflammation or cell debris.

Infiltrate:

- Cellular infiltrates, congestion, and/or edema but no exfoliation or cell debris.

Artifact:

- Postmortem autolysis: Uniform dissolution of entire tissue section with no change in organization or depth of cell layers.

Comment

The most rostral portion of the olfactory epithelium lining the dorsal medial meatus is the area of olfactory epithelium most frequently affected by inhalation of direct-acting gaseous irritants (Buckley et al. 1985; Hardisty et al. 1999). Chemicals that injure the olfactory epithelium that first require metabolism to a toxic intermediate usually induce lesions throughout the olfactory epithelium (Gaskell 1990) and may also induce necrosis in adjacent Bowman's glands (Jensen and Sleight 1987). A frequent sequela to loss of sensory cells (either through aging or toxic injury) is atrophy of nerve bundles within the lamina propria. Conversely, apoptosis of olfactory epithelium can occur with surgical transection of axons or by treatment with antimicrotubule drugs (Levin et al. 1999; Kai et al. 2006). In case necrosis is restricted to a specific cell type, recording of this cell type will provide a clear description of the lesion.

Regenerative Changes

Regeneration, MOE (N) **Main olfactory epithelium (MOE)**

Species
Mouse; Rat.

Other Term(s) Used
Regeneration, olfactory epithelium; regeneration, Bowman's gland.

Pathogenesis/cell of origin
Olfactory epithelium; reparative process.

Diagnostic Features
(Renne et al. 2009, see Regeneration).
- Epithelial cells with basophilic cytoplasm.
- Increased nuclear:cytoplasmic ratio.
- Epithelial architecture may remain irregular.
- Adjacent to or within areas of degenerating, necrotic, hyperplastic or metaplastic epithelium.

Differential Diagnoses
Hyperplasia, MOE:
- Epithelium is thickened due to increased numbers of cells, resulting in an undulating, rugose epithelial surface and irregular arrangement of cell layers (see proliferative lesion section of this document).

Neoplasia:
- Expansile nodule often protruding into nasal cavity, with cellular atypia and compression of adjacent structures (see proliferative lesion section of this document), or invasion of neighboring tissue, for example the olfactory bulb/brain.

Comment
Regeneration is a term indicating the growth of cells and tissues to replace lost or damaged structures, as opposed to hyperplasia, a term denoting an increase in the number of cells beyond normal in a tissue. Irregularity of epithelial cell arrangement is often observed in the olfactory epithelium in the process of regeneration. Degeneration, necrosis, and regeneration are often present together in epithelium that is repeatedly injured by toxicants (see comments in sections on degeneration and necrosis).

Inflammatory Changes

Infiltrate, inflammatory cell, MOE (N) **Main olfactory epithelium (MOE)**

Species
Mouse; Rat.

Other Term(s) Used
Inflammatory cell infiltration.

Pathogenesis/cell of origin
Immune cells within olfactory epithelium.

Diagnostic Features
- Foci of a single inflammatory cell type, or a mixture of different cell types without other features of inflammation.

Differential Diagnoses
Inflammation, MOE:
- Inflammatory cellular infiltrate and additionally edema, congestion, and degeneration/necrosis of the epithelium. Epithelial squamous metaplasia may be a sequela.

Comment
The term "infiltrate" is recommended followed by the predominant cell type (neutrophilic, eosinophilic, lymphocytic, plasmacytic or histiocytic) or mixture of different cell types (mixed).

Inflammation, MOE (N) (Figure 87) **Main olfactory epithelium (MOE)**

Species
Mouse; Rat.

Other Term(s) Used
Rhinitis.

Pathogenesis/cell of origin
Immune cells within olfactory epithelium.

Diagnostic Features
(Renne et al. 2009, see Inflammation, acute).
- Vascular congestion.
- Focal or more extended areas of single (lymphocytes, neutrophils, eosinophils, plasmacytes, or histiocytes) or mixed inflammatory cellular types.
- Interstitial edema and/or congestion.
- Accumulation of serous, mucous, or fibrinous exudate.

Differential Diagnoses
Infiltrate, inflammatory cell, MOE:
- Foci of single or mixed inflammatory cell types without other features of inflammation.

Comment
Modifiers are recommended in relation to the predominant inflammatory cellular type (neutrophilic, eosinophilic, lymphocytic, plasmacytic or histiocytic) or mixture of different cellular types (mixed). Inflammation may be caused by inhaled substances, spontaneous diseases of rats and mice, or can be secondary to reflux following oral dosing. A differentiation into acute, chronic, chronic-active and granulomatous inflammation can also be done.

Vascular changes

Edema, MOE (N) **Main olfactory epithelium (MOE)**

Species
Mouse; Rat.

Other Term(s) Used
Edema, olfactory epithelium

Pathogenesis/cell of origin
Vasculature of lamina propria of the olfactory epithelium; vascular change.

Diagnostic Features
(Renne et al. 2009, see EDEMA).
- Fluid with varying protein content within the lamina propria, olfactory epithelium and/or lumen of the nasal cavity; may result in swelling of the tissue.

Differential Diagnoses
ARTIFACT of postmortem autolysis:
- Uniform dissolution of entire tissue section with lysis of RBCs.

FIBRINOUS EXUDATE:
- Smudged pink exudate with laminar appearance of fibrils within the lumen of the nasal cavity visible at high magnification.

Comment
Congestion, edema, and/or hemorrhage in the nasal mucosa may be the earliest response observed to inhaled toxicants or traumatic injury to the nose. Extensive edema of the lamina propria of the olfactory epithelium was induced by inhalation of acetaldehyde (Woutersen et al. 2010; Gopinath et al. 1987). Chronic edema may result in fibrosis.

Hemorrhage, MOE (N) **Main olfactory epithelium (MOE)**

Species
Mouse; Rat.

Other Term(s) Used
Hemorrhage, olfactory epithelium

Pathogenesis/cell of origin
Vascular injury to vevssels within the lamina propria of the blood vessels of the olfactory epithelium.

Diagnostic Features
(Renne et al. 2009, see HEMORRHAGE).
- Presence of extravascular red blood cells within the lamina propria, olfactory epithelium and/or free in lumen of nasal cavity.

Differential Diagnoses
IATROGENIC BLEEDING:
- Resulting from blood collection via orbital sinus.

Comment
Small amounts of blood may be observed in the nasal passages following ante-mortem blood collection via the orbital sinus (retroorbital plexus at the medial canthus of the eye). Hemorrhage in the nasal cavity may also be a result of trauma, erosion/ulceration, necrosis, or inflammation associated with infection or inhaled irritant chemicals, noxious gases, or vapors.

Thrombus, MOE (N) **Main olfactory epithelium (MOE)**

Species
Mouse; Rat.

Other Term(s) Used
Thrombosis.

Pathogenesis/cell of origin
Vascular injury to vessels in the lamina propria of the olfactory epithelium.

Diagnostic Features
(Renne et al. 2009, see THROMBOSIS).
- Intravascular, amorphous, acellular pink/gray, clearly laminated material.
- May be admixed with leukocytes and/or erythrocytes.
- Attachment to endothelial lining of vessel may be visible on routine sections.

Differential Diagnoses
ARTIFACT of postmortem clot:
- Few or no leukocytes; lamination absent or very fine filaments present.

Comment
Thrombi in the lamina propria of the olfactory epithelium are commonly associated with leukemia in rats, or with generalized debilitation in rats and mice.

Miscellaneous Changes

Eosinophilic globules, MOE (N) (Figure 88) **Main olfactory epithelium (MOE)**

Species
Mouse; Rat.

Other Term(s) Used
Eosinophilic droplets; eosinophilic inclusions; cytoplasmic granularity; degenerative change.

Pathogenesis/cell of origin
Olfactory epithelium.

Diagnostic Features
(Renne et al. 2009, see EOSINOPHILIC GLOBULES (DROPLETS)).
- Accumulation of brightly eosinophilic cytoplasmic inclusions in sustentacular cells of olfactory epithelium.
- Most prominent near the junction of olfactory and respiratory epithelia.

Special Techniques for Diagnostics
- Eosinophilic globules are negative for periodic acid-Schiff (PAS), Alcian Blue, Von Kossa, mucicarmine, phosphotungstic acid hematoxylin (PTAH), Masson's trichrome, Congo red, and toluidine blue stains (Monticello et al. 1990). Ultrastructurally, they present as amorphous flocculent (presumably proteinaceous) material in membrane-bound vesicles. Eosinophilic inclusions in olfactory epithelium of smoke-exposed mice reacted with antibodies for carboxylesterase, an enzyme induced by exposure to some toxic compounds, and with antibodies to the Ym1 sequence of the protein Ym2, a member of the chitinase family (Ward et al. 2001).

Differential Diagnoses

CYTOPLASMIC CHANGES:
- From specific toxic agents.

Comment

Eosinophilic globules are observed occasionally in otherwise normal epithelium of untreated rats, more frequently in aged animals (Boorman et al. 1990; Monticello et al. 1990). They may be seen in association with loss of sensory cells. Increases in the incidence and severity of eosinophilic globules in the olfactory epithelia are frequently observed in inhalation studies and have been observed in rats exposed to dimethylamine (Buckley et al. 1985; Gross et al. 1987) or cigarette smoke (Lewis et al. 1994). They may be restricted to the sustentacular cells (Gopinath et al. 1987).

Corpora amylacea, MOE (N) (Figure 89) **Main olfactory epithelium (MOE)**

Species

Mouse; Rat.

Other Term(s) Used

Corpora amylacea, olfactory epithelium; corpora amylacea, Bowman's gland; degenerative change.

Pathogenesis/cell of origin

Concretions within olfactory epithelium or Bowman's glands.

Diagnostic Features
- Basophilic concretions within epithelium or subepithelial glands.

Vomeronasal Organ (VNO)

Degenerative/Epithelial Changes

Atrophy, VNO (N) (Figure 90) **Vomeronasal organ (VNO)**

Species

Mouse; Rat.

Pathogenesis/cell of origin

Sensory epithelium of the vomeronasal organ; degenerative change.

Diagnostic Features
- Thinning of the sensory epithelium.
- Cells are reduced in height and are cuboidal to flattened.
- The nuclei appear close together due to reduced cytoplasm.

Differential Diagnoses

ARTIFACT of postmortem autolysis:
- Uniform dissolution of entire tissue section with no change in organization or depth of cell layers.

Comments

Atrophy of the VNO was decribed by Sills et al. 1995 and Corps et al. 2010.

Degeneration, VNO (N) (Figure 91) **Vomeronasal organ (VNO)**

Species

Mouse; Rat.

Pathogenesis/cell of origin

Sensory epithelium of the vomeronasal organ.

Diagnostic Features
- Loss of cilia.
- Epithelial vacuolation/bleb formation.
- Increased intercellular spaces.
- Loss of organization of the cell layers.
- Exfoliation of cells.
- Reduction in epithelial thickness by loss of cells.

Differential Diagnoses

None.

Apoptosis, VNO (N) **Vomeronasal organ (VNO)**

Species

Mouse; Rat.

Pathogenesis/cell of origin

Sensory epithelium of the vomeronasal organ; degenerative lesion.

Diagnostic Features
- Cell death of individual or small clusters of cells.
- Cell shrinkage and convolution.
- Cytoplasmic condensation (hypereosinophilia).
- Chromatin condensation and peripheralization in early apoptosis.
- Pyknosis (chromatin condensation).
- Karyorrhexis (nuclear fragmentation).
- Intact cell membrane.
- Formation of blebs to produce apoptotic bodies.

- Cytoplasm retained in apoptotic bodies.
- No inflammation.
- Tingible body macrophages.

Differential Diagnoses

Necrosis, VNO, single cell:

- Single cell necrosis is differentiated from apoptosis by the presence of cell swelling, rupture and inflammation. Consideration to tissue type, location and the physiologic milieu may aid in differentiation from apoptosis.

Comment

Special techniques should be used to differentiate between single cell necrosis and apoptosis. Apoptosis is positive for both Terminal TdT-mediated dUTP-Nick-End Labelling (TUNEL) Caspase-3-immunohistochemistry (Nunez-Parra et al. 2011).

Necrosis; single cell necrosis, VNO (N) (Figure 92) **Vomeronasal organ (VNO)**

Species

Mouse; Rat.

Modifier

Single cell.

Pathogenesis/cell of origin

Sensory epithelium of the vomeronasal organ.

Diagnostic Features

- Minimal nuclear pyknosis and or karyorrhexis of nuclei.
- Cellular swelling or shrinkage.
- Pale eosinophilic cytoplasm.
- Exfoliation of cells.
- Inflammatory cells intermingled.
- Cellular debris in the lumen.
- Detachment of sensory epithelium from the basement membrane.

Necrosis, focal/multifocal/diffuse:

- Affects contiguous cells.

Single cell:

- Affects individual cells.

Differential Diagnoses

Atrophy, VNO:

- No inflammatory cells intermingled. No cellular debris in the lumen. Reduction in epithelial thickness.

Regenerative Changes

Regeneration, VNO (N) (Figure 93) **Vomeronasal organ (VNO)**

Species

Mouse; Rat.

Pathogenesis/cell of origin

Sensory epithelium of the vomeronasal organ.

Diagnostic Features

- Epithelial cells with basophilic cytoplasm.
- Increased nuclear:cytoplasmic ratio.
- Epithelial architecture may be irregular.
- Adjacent to or within areas of degenerating, necrotic, hyperplastic or metaplastic epithelium.

Differential Diagnoses

Hyperplasia, VNO:

- Increase in number of cells and thickening of the sensory epithelial layer.

Comment

Following injury, a large number of neurons can be regenerated in young, but also in aged rodents. Adult stem cells (basal cells) of the olfactory epithelium retain the capacity to regenerate new neurons (mice up to 24 months; Brann and Firestein 2010). Neurogenesis in the process of regeneration was described in rats (Matsuoka et al. 2002; Martínez-Marcos et al. 2000) and mice (Suzuki 1998; Martínez-Marcos et al. 2000).

Regeneration of neuroepithelium, VNO (N) (Figure 94) **Vomeronasal organ (VNO)**

Species

Mouse; Rat.

Pathogenesis/cell of origin

Sensory epithelium of the vomeronasal organ.

Diagnostic Features

- Abnormalities in the shape of cells.
- Abnormalities in the cellular layers.
- Disturbance of the architecture.

Inflammatory Changes

Infiltrate, inflammatory cell, VNO (N) (Figure 95) **Vomeronasal organ (VNO)**

Species

Mouse; Rat.

Other Term(s) Used

Inflammatory cell infiltration.

Pathogenesis/cell of origin

Sensory epithelium of the vomeronasal organ and immune cells.

Diagnostic Features

- Infiltration and transmigration of immune cells, lymphocytes and/or neutrophils, of the epithelium.

Differential Diagnoses

Normal tissue with GRANULOCYTES:

- Can be a background finding, with granulocytes that may transmigrate the epithelium.

INFLAMMATION:

- Salient features of inflammation are present.

Comment

The term "infiltrate" is recommended followed by the predominant cell type (neutrophilic, eosinophilic, lymphocytic, plasmacytic or histiocytic) or mixture of different cell types (mixed).

Inflammation, VNO (N) (Figure 96) **Vomeronasal organ (VNO)**

Species

Mouse; Rat.

Other Term(s) Used

(none)

Pathogenesis/cell of origin

Sensory epithelium of the vomeronasal organ and immune cells.

Diagnostic Features

- Infiltration and transmigration of immune cells, lymphocytes and/or neutrophils, of the epithelium.
- May be associated with vascular injury resulting in hemorrhage and/or edema.
- Evidence of cell necrosis.

Differential Diagnoses

INFILTRATE, INFLAMMATORY CELL:

- Salient features of inflammation are absent.

Comment

The term "inflammation" is recommended followed by the predominant cell type (neutrophilic, eosinophilic, lymphocytic, plasmacytic or histiocytic) or mixture of different cell types (mixed).

Vascular Changes

Edema, VNO (N) (Figure 96) **Vomeronasal organ (VNO)**

Species

Mouse; Rat.

Pathogenesis/cell of origin

Vasculature within connective tissue supporting the sensory epithelium of the vomeronasal organ; increased permeability of vasculature.

Diagnostic Features

- Proteinaceous fluid around vessels and free in lumen of vomeronasal organ.

Differential Diagnoses

POSTMORTEM AUTOLYSIS:

- Uniform dissolution of entire tissue section with lysis of red blood cells.

Comment

Interstitial edema and necrosis of the supporting cells of the vomeronasal organ was observed in rats infected by sialodacryoadenitis virus (Bihun and Percy 1995).

Miscellaneous Changes

Dilation/"diverticulum", VNO (N) (Figure 97) **Vomeronasal organ (VNO)**

Species

Mouse; Rat.

Pathogenesis/cell of origin

Sensory epithelium of the vomeronasal organ.

Diagnostic Features

- Downgrowth of epithelial lined out-pocketings into supporting soft tissue with or without continuity to the VMO.
- Normal appearing epithelial cells.
- Normal nucleus to cytoplasm ratio.
- Proteinaceous material may fill the lumen.

Differential Diagnoses

CARCINOMA, NEUROEPITHELIAL, VNO:

- Anaplastic cells or epithelial cells with abnormal nucleus to cytoplasm ratio.

Septal Organ of Masera (SOM)

Remarks: Principally, all histopathological changes observed in the MOE, as described by Renne et al. (2009; see Nasal cavity) can potentially be observed in SOM. Observation of effects in SOM is hampered by the lack of sampling; SOM is often not included in the selection of slides to be examined. Even if SOM is potentially included, 'Metaplasia, respiratory cell', will often go unnoticed, because of similarity with surrounding tissue. Even changes like necrosis/ulceration can go unnoticed or ascribed to respiratory epithelium, especially in cases where the change is not restricted to SOM (see Figure, normal anatomy, Septal Organ of Masera) but includes/affects surrounding respiratory epithelium as well.

Degenerative Changes/Epithelial Changes

Atrophy, SOM (N) **Septal organ of Masera (SOM)**

Species

Mouse; Rat.

Pathogenesis/cell of origin

Olfactory epithelium; degenerative lesion.

Diagnostic Features
- Expected to be similar to those of MOE and VNO.

Differential Diagnoses
- Expected to be similar to those of MOE and VNO.

Comment
SOM represents only a small area of the septal epithelium and may not be included in the section; therefore degeneration may go unnoticed. Alternatively, degeneration may be ascribed to the respiratory epithelium rather than the SOM. Degeneration can occur unilaterally.

Degeneration, SOM (N) (Figures 98, 99) **Septal organ of Masera (SOM)**

Species
Mouse; Rat.

Pathogenesis/cell of origin
Olfactory epithelium.

Diagnostic Features
- Expected to be similar to those of MOE and VNO.

Differential Diagnoses
- Expected to be similar to those of MOE and VNO.

Comment
SOM represents only a small area of the septal epithelium and may not be included in the section; therefore degeneration may go unnoticed. Alternatively, degeneration may be ascribed to the respiratory epithelium rather than the SOM. Degeneration can occur unilaterally.

Apoptosis, SOM (N) **Septal organ of Masera (SOM)**

Species
Mouse; Rat.

Pathogenesis/cell of origin
Sensory epithelium of the septal organ; degenerative lesion.

Diagnostic Features
- Pyknosis and or karyorrhexis of single cells.
- Cell shrinkage.
- Nuclear shrinkage.
- Hypereosinophilic cytoplasm.
- Apoptotic bodies.

Comment
Special techniques should be used to differentiate between single cell necrosis and apoptosis. Apoptosis is positive in both Terminal TdT-mediated dUTP-Nick-End Labelling (TUNEL) assay and Caspase-3-immunohistochemistry.

Grueneberg Ganglion (GG)

Degenerative Changes/Epithelial Changes

Degeneration/necrosis, ganglion cells (GG) (N) **Grueneberg ganglion (GG)**

Species
Mouse; Rat.

Pathogenesis/cell of origin
Ganglion cells.

Diagnostic Features
- Decrease in number.
- Cytoplasmic changes.
- Nuclear pyknosis.

Differential Diagnoses
None.

Comment
The diagnostic features are hypothetical, because reports on degeneration of the Grueneberg ganglion cells are lacking. Ganglion cell loss can be determined only in serial sections as the distribution of ganglion cells is variable, ranging from clusters to a single row to clusters aligned adjacent to the epithelium. Additionally, their number may show inter-individual variation.

Degeneration, epithelium (GG) (N) **Grueneberg ganglion (GG)**

Species
Mouse; Rat.

Pathogenesis/cell of origin
Squamous epithelium covering the ganglion cells.

Diagnostic Features
- Cytoplasmic vacuolation.
- Desquamation of cells/ Sloughing of affected cells into the lumen.
- Thinning of epithelium.
- Increase in keratin.

Differential Diagnoses
- None.

Comment
The exact interaction between the overlying nasal epithelium and the ganglion cells is unknown. Degeneration of the epithelium could lead to damage of the ganglion cells, however, reports on ganglion cell damage are lacking.

Erosion/ulcer, epithelium (GG) (N) **Grueneberg ganglion (GG)**

Species
Mouse; Rat.

Pathogenesis/cell of origin
Squamous epithelium covering the ganglion cells.

Diagnostic Features
- Loss of cells.
- Desquamation of cells/ sloughing of affected cells into the lumen.
- Infiltration of granulocytes.

Differential Diagnoses
None.

Comment
The exact interaction between the overlying nasal epithelium and the ganglion cells is unknown. Ulceration of the epithelium could lead to damage of the ganglion cells and ganglion cell loss. Reports on ganglion cell damage and loss are lacking.

Inflammatory Changes

Inflammatory cell infiltrate (GG) (N) (Figures 100, 101) **Grueneberg ganglion (GG)**

Species
Mouse; Rat.

Pathogenesis/cell of origin
Gangion cells and leukocytes.

Diagnostic Features
- Presence of granulocytes in the overlying epithelium and around the ganglion cells.

Differential Diagnoses
Inflammation
- Salient features of inflammation are present.

Inflammation (GG) (N) **Grueneberg ganglion (GG)**

Species
Mouse; Rat.

Pathogenesis/cell of origin
Ganglion cells and leukocytes.

Diagnostic Features
- Presence of granulocytes in the overlying epithelium and around the ganglion cells.
- Additional features of inflammation, such as edema, hemorrhage, cell necrosis.

Differential Diagnoses
Inflammatory cell infiltrate
- Salient features of inflammation are absent.

Olfactory Bulb

For general lesions of the CNS see Kaufmann et al. 2012 (see Introduction).

Degenerative Changes/Epithelial Changes

Degeneration/vacuolation, olfactory bulb (N) **Olfactory bulb**

Species
Mouse; Rat.

Pathogenesis/cell of origin
Neurons of the olfactory bulb (brain).

Diagnostic Features
- Cytoplasmic vacuolation (usually clear or pale eosinophilic) of neurons in CNS.

Differential Diagnoses
None.

Apoptosis, olfactory bulb (N) **Olfactory bulb**

Species
Mouse; Rat.

Biological behavior
Degenerative lesion.

Pathogenesis/cell of origin
Neurons of the olfactory bulb (brain).

Diagnostic Features
- Pyknosis and or karyorrhexis of single or scattered nuclei.
- Cell shrinkage.
- Nuclear shrinkage.
- Hypereosinophilic cytoplasm.
- Apoptotic bodies.

Comment
Special techniques should be used to differentiate between necrosis, single cell and apoptosis. Apoptosis is positive for Terminal TdT-mediated dUTP-Nick-End Labelling (TUNEL) and Caspase-3-immunohistochemistry.

Inflammatory Changes

Infiltrate, inflammatory cell, olfactory bulb (N) (Figure 102) **Olfactory bulb**

Species
Mouse; Rat.

Other Term(s) Used
Inflammatory cell infiltration.

Pathogenesis/cell of origin
Immune cells and olfactory bulb neurons.

Diagnostic Features
- Infiltration of the olfactory bulb by immune cells, macrophages/monocytes, lymphocytes and/or neutrophils.

Differential Diagnoses
Lymphoma, malignant, infiltrated site

Comment
Inflammatory cell infiltrates were observed after intranasal instillation of Satratoxin G in mice (Islam et al. 2006).

Inflammation, olfactory bulb (N) **Olfactory bulb**

Species
Mouse; Rat.

Other Term(s) Used
(none)

Pathogenesis/cell of origin
Immune cells and olfactory bulb neurons.

Diagnostic Features
- Infiltration of the olfactory bulb by immune cells, macrophages/monocytes, lymphocytes and/or neutrophils.
- Associated with other features of inflammation, such as edema, hemorrhage, and cell necrosis.

Differential Diagnoses
Infiltrate, inflammatory cell
- Salient features of inflammation are lacking.

Nonneoplastic Proliferative Lesions of the Rat and Mouse Olfactory System / Chemosensory Structures

Main Olfactory Epithelium (MOE) - Olfactory Epithelium and Nerves

Hyperplasia, MOE (H) (Figure 103) **Main olfactory epithelium (MOE)**

Species
Mouse; Rat.

Biological behavior
Proliferative, non-neoplastic lesion.

Other Term(s) Used
Hyperplasia, olfactory epithelium; Hyperplasia, Bowman's gland

Pathogenesis/cell of origin
Proliferation of precursors of olfactory sensory neurons, sustentacular cells, basal cells of olfactory epithelium or of Bowman's glands.

Diagnostic Features
(Renne et al. 2009, see Hyperplasia, olfactory epithelium).
- Increased thickness of the epithelium resulting from an increase in the number of sustentacular, olfactory sensory precursor basal cells.

Differential Diagnoses
Adenoma:
- An expansile nodular mass that may protrude into the nasal or paranasal cavities. Cellular atypia is common in the case of endophytic growth. Adenoma of the subepithelial glands causes compression of the adjacent structures.

Papilloma, squamous cell:
- A papillary projection above the surface of the epithelium or extension into the lumen of the ducts of the submucosal glands. Delicate vascular mesenchymal stroma and marked proliferative epithelial thickening is present.

Carcinoma, neuroepithelial, MOE:
- Epithelial hyperplasia with cellular atypia might progress to adenocarcinoma, squamous carcinoma or neuroepithelial carcinoma (depending on site in the nasal epithelium and principal cell involved). Diagnosis of a malignant tumor is based on one or more features including overall size, loss of polarity of epithelium, a high degree of atypia, increased numbers of mitoses, or invasive growth.

Comment
Hyperplasia of the main olfactory epithelium may result from chronic changes that are degenerative, inflammatory or vascular in nature. Regenerative neuroepithelial cell proliferation was described in young mice after injury (Suzukawa et al. 2011).

Metaplasia, respiratory, MOE (H) (Figure 104) **Main olfactory epithelium (MOE)**

Species
Mouse; Rat.

Biological behavior
Proliferative non-neoplastic lesion.

Other Term(s) Used
Metaplasia, respiratory, olfactory epithelium; Metaplasia, respiratory, Bowman's gland

Pathogenesis/cell of origin
Metaplasia of cells of olfactory epithelium and/or cells of Bowman's glands underneath the olfactory epithelium.

Diagnostic Features
(Renne et al. 2009, see Metaplasia, respiratory, olfactory/glandular epithelium).
- Respiratory epithelial metaplasia of olfactory epithelium is most common in the epithelium lining the dorsal medial meatus.
- Characterized by loss of sensory and sustentacular neuroepithelial cells, which may be associated with focal atrophy and degeneration.
- Replacement is by ciliated or nonciliated simple colum-

nar epithelium that resembles respiratory epithelium.
- Frequently, respiratory epithelial metaplasia extends into the submucosal glands of the affected segments of olfactory epithelium.

Differential Diagnoses

Hyperplasia, MOE:
- Increased thickness of the epithelium due to proliferation of sustentacular, precursor olfactory sensory, and/or basal cells. Proliferating cells are disorganized and usually not ciliated.

Comment:

This change is occasionally seen spontaneously in aged rats and mice or may be a response to an irritant. The spontaneous lesion tends to affect one side more than the other and is associated with slightly dilated Bowman's glands, possibly containing neutrophils and/or eosinophilic granular debris. However, induced lesions may also be restricted to or be more pronounced unilaterally, because of differences in air flow between the two passages. There is no evidence that respiratory epithelial metaplasia is preneoplastic. The normal extension of olfactory epithelium into the anterior region of the dorsal meatus may vary with age and can be possibly strain dependent. Precise anatomic localization and comparison with controls are necessary to ensure proper diagnosis of the epithelium involved.

Metaplasia, squamous cell, MOE (H) **Main olfactory epithelium (MOE)**

Species

Mouse; Rat.

Biological behavior

Proliferative non-neoplastic lesion.

Other Term(s) Used

Metaplasia, squamous cell, olfactory epithelium; metaplasia, squamous cell, Bowman's gland.

Pathogenesis/cell of origin

Metaplasia of cells of olfactory epithelium and/or cells of submucosal glands in the lamina propria.

Diagnostic Features

(Renne et al. 2009, see Metaplasia, squamous cell).
- Characterized by replacement of olfactory or ductal cells of Bowman's glands by squamous epithelium.
- Where the squamous epithelium is stratified, epithelial cells and their nuclei are increasingly flattened superficially.
- Compact or large epithelial cells with complete loss of cilia.
- Sometimes slight nuclear polymorphism and cellular atypia.
- Surface cells might contain only keratohyaline granules, or they might be excessively keratinized.
- Often desquamation of surface cells.

Differential Diagnoses

Papilloma, squamous cell:
- A papillary projection above the surface of the epithelium or extension into the lumen of the ducts of the submucosal glands. Delicate vascular mesenchymal stroma and marked proliferative epithelial thickening is present.

Carcinoma, squamous cell:
- Characterized by destruction of the basement membrane; cellular atypia and disorientation; frequent mitoses; or presence of other signs of malignancy, such as invasive growth or metastases.

Regeneration, MOE:
- Usually follows acute injury. Cells are one or possibly two layers thick, with increased basophilia; slight karyomegaly, but there is no horizontal layering (stratification) of flattened cells as in squamous metaplasia.

Comment

Squamous metaplasia sometimes occurs in association with chronic inflammation or following the process of regeneration. Squamous metaplasia with a normal maturation pattern may be reversible under some experimental circumstances (e.g., depending on nature of inhaled irritant and duration of exposure) but in other situations may eventually give rise to squamous cell papilloma or squamous cell carcinoma.

Vomeronasal organ (VNO)

Hyperplasia, VNO (H) (Figure 105) **Vomeronasal organ (VNO)**

Species

Mouse; Rat.

Biological behavior

Proliferative non-neoplastic lesion.

Pathogenesis/cell of origin

Proliferation of precursors of sensory epithelial cells of the vomeronasal organ.

Diagnostic Features
- Increased thickness of the epithelium resulting from an increase in the number of sustentacular, sensory precursor, and/or basal cells.

Differential Diagnoses

Regeneration, VNO:
- Changed nucleus to cytoplasm ration, increased basophilia, but no increase in the number of cells.

Carcinoma, neuroepithelial, VNO:
- Rosette formation and invasive growth or anaplasia or

destructive growth.

Septal Organ of Masera (SOM)

Remarks: Principally, all histopathological changes observed in the MOE, as described by Renne et al. (2009; see Nasal cavity) can potentially be observed in SOM. Observation of effects in SOM is hampered by the lack of sampling, as SOM is often not included in the section of slides to be examined. Even when present, changes to SOM are often overlooked, or they are ascribed solely to the respiratory epithelium, especially when findings are not restricted to SOM (normal anatomy, Septal Organ of Masera).

Metaplasia, squamous cell, SOM (H) (Figure 106) **Septal Organ of Masera (SOM)**

Species
Mouse; Rat.

Biological behavior
Proliferative non-neoplastic lesion.

Pathogenesis/cell of origin
Olfactory epithelium.

Diagnostic Features
- Characterized by replacement of olfactory epithelium by squamous epithelium.
- Layers of stratified epithelial cells, with flattening of the superficial cells.
- Surface area may be excessively keratinized.
- Covers small area at the location of the VNO.

Differential Diagnoses
Carcinoma, squamous cell:
- Characterized by destruction of the basement membrane.

Neoplastic Proliferative Lesions of the olfactory system/ chemosensory structures

Main Olfactory Epithelium (MOE)

Carcinoma, neuroepithelial, MOE (M) (Figure 107) **Main Olfactory Epithelium (MOE)**

Species
Mouse; Rat.

Biological behavior
Proliferative neoplastic lesion.

Pathogenesis/cell of origin
Malignant transformation of olfactory epithelium (sustentacular cells, basal cells, immature sensory cells, and possibly ductal cells of Bowman's glands).

Diagnostic Features
(Dungworth et al. 1992; Dungworth et al. 2001; Renne et al. 2009, see Carcinoma, neuroepithelial).
- Arises from the olfactory epithelium.
- Frequently there is compartmentalization of sheets of neoplastic cells into lobules by fibrovascular septa.
- Small round or columnar cells with poorly defined, pale-staining cytoplasm.
- Round to oval, basally located nuclei that do not display marked atypia.
- Distinct, sharply defined nuclear chromatin.
- True (Flexner-Wintersteiner) rosettes (tumor cells surround an open central lumen bounded by distinct cell membranes, mimicking glandular structures) or pseudo (Homer-Wright) rosettes (tumor cells arranged in a circle around a small central lumen, which is filled with amorphous or tangled fibrillary material) may be present. Frequency and morphology of rosette structures are highly variable.
- Plexiform intercellular fibrils.
- Areas of anaplastic cells may be present.

Differential Diagnoses
Adenocarcinoma:
- Absence of rosettes or plexiform intercellular fibrils. A useful distinguishing feature between true rosettes sometimes present in neuroepithelial carcinomas and the acinar spaces in adenocarcinomas is that in neuroepithelial carcinomas, the nuclei of cells forming the rosettes blend peripherally with the uniform population forming the rest of the tumor.

Comment
Neuroepithelial carcinoma often invades the ethmoid bone and olfactory bulb/brain. Whether tumors arising from olfactory epithelium are more appropriately classified under the term neuroepithelial carcinoma or olfactory neuroblastoma cannot be resolved on the basis of current information, and they are considered synonyms in this manuscript. The general term neuroepithelial carcinoma is used here because it allows for origin of neoplasms from sensory or sustentacular cells, whereas olfactory neuroblastoma implies origin only from neurogenic components. There is clearly a need to develop procedures to distinguish neuroepithelial tumors of neurogenic origin (neuroblastoma, esthesioneuroblastoma), from those of nonneurogenic cell types, especially sustentacular cells and their precursors. When neither rosettes (true or pseudo) nor plexiform intercellular fibrils are demonstrable, a diagnosis of adenocarcinoma is preferable. Ultrastructural analysis of a neuroepithelial carcinoma should reveal some clear characteristics of olfactory epithelium such as olfactory vesicles, cilia, and microtubules. The histogenic relationship of Bowman's glands to the other components of the nasal epithelium has not been clearly defined, but their origin is most likely not neurogenic. Therefore, carcinomas origi-

nating from Bowman's glands should be classified with adenocarcinomas. Most cases of neuroepithelial carcinoma are negative for immunohistochemical reactions with antibodies against intermediate filaments.

VOM or SOM could be the site of origin of neuroepithelial carcinomas however it could be difficult to allocate their origin to these miniature sites. For cases where the main olfactory epithelium is still intact this question should be raised.

Vomeronasal Organ (VNO)

Carcinoma, neuroepithelial, VNO (M) **Vomeronasal Organ (VNO)**

See comment under Carcinoma, neuroepithelial, MOE

Species

Mouse; Rat.

IV. NONPROLIFERATIVE AND PROLIFERATIVE LESIONS OF THE RAT AND MOUSE OTIC SYSTEM

INTRODUCTION

The ear is the sensory organ of hearing and balance. The ear can be divided into three segments, the external, middle, and inner ear. The middle and inner ear are only infrequently assessed either grossly or microscopically in preclinical toxicity and carcinogenicity studies with rodents used for safety assessment. However, the external ear is easily assessed during macroscopic examination, and is often sampled in carcinogenicity studies when grossly identified masses are examined. The lesions of the external ear are largely those of the skin and are reported with the integumentary system.

This INHAND document serves as a framework that can be used for the harmonization of diagnostic criteria of otic lesions in laboratory rats and mice. These recommendations for diagnostic criteria and preferred terminology should not be considered mandatory; proper diagnoses are ultimately based on the discretion of the toxicologic study pathologist.

This document is organized to provide introductory material that reviews comparative interspecies differences in anatomy and otic function, followed by a listing of middle and inner ear lesions in a standardized format. The otic lesion descriptions include differential diagnoses to aid in distinguishing primary diagnoses from similar appearing lesions. It should be noted that the preferred diagnostic terminology for some lesions in this document might represent departures from traditional nomenclature schemes found in standard textbooks. Furthermore, illustrative photomicrographs for a given diagnostic entity may occasionally depict additional tissue changes as this reflects actual situations observed in evaluation of toxicity studies. In addition, for the complex structures of the middle and inner ear, diagnostic terms should include anatomic locators whenever possible (e.g., tympanic membrane, ossicles, round window niche, etc.).

NORMAL ANATOMY, HISTOMORPHOMETRY AND PHYSIOLOGY OF THE EAR

In laboratory animal species, the ear can be divided into three compartments. The external ear includes the pinna and external ear canal. The tympanic membrane ("ear drum") is the barrier between the external ear canal and the middle ear. The middle ear consists of the tympanic cavity largely formed by the tympanic bulla and contains the three ossicles, the incus, malleus, and stapes. The inner ear is comprised of the cochlea (engaged in hearing) and the vestibular apparatus (for balance). The vestibular apparatus includes the bony and membranous labyrinths of the semicircular canals, the utricle, and the saccule. The utricle and saccule are the otolith organs.

The acoustic meatus is the ear canal. The pinna makes up the external acoustic meatus. It is the outermost portion of the ear and is lined on the external surface by haired skin, and, on

the internal surface, by sparsely haired to hairless skin. The pinna in some species such as rabbits or pigs has readily observable large veins, which are often used for blood collection or even drug or test article administration. It has a supporting cartilage, which helps to maintain its shape. The internal acoustic meatus is the portion of the ear canal lined by the bony collar of the temporal bone. The ear canal in most species has an obtuse-angle turn external to this bony collar. The tympanic membrane is the innermost margin of the ear canal. The pinna is easily assessed macroscopically at necropsy, and the tympanic membrane also can be assessed reliably at necropsy with an otoscope. The pinna and ear canal funnel sound waves to the tympanic membrane.

The middle and inner ear are not readily evaluated macroscopically, and therefore generally are not examined at necropsy in routine toxicology studies. The tympanic cavity is an air-filled space that extends into a ventral osseous expansion, the tympanic bulla, and contains the auditory ossicles (malleus, incus and stapes). The malleus ("hammer") is embedded broadly in the tympanic membrane and articulates with the incus ("anvil"). The malleus has muscular attachments to the wall of the tympanic wall. The incus articulates in turn with the stapes ("stirrup"); the footplate of the stapes lies in the oval window. Sound waves that cause vibration of the tympanic membrane are transmitted to the oval window by the bridging middle ear ossicles. This mechanical apparatus amplifies the transmitted vibrations, possibly providing an increase in magnitude of as much as 20-fold. Tension on the muscular attachments to the malleus can be lessened by feedback innervation in response to high ambient noise levels, thereby dampening this amplification as a protective mechanism. With a bit of patience and dissection, the ossicles can be evaluated grossly, and their articulations and movement tested at necropsy. The auditory (pharyngotympanic or Eustachian) tube originates at the rostral (anterior) wall of the tympanic cavity and extends to the nasopharynx. It allows for drainage of fluid and normalization of pressure across the tympanic membrane.

The cochlea lies on and is embedded in the petrous portion of the temporal bone which is on the medial wall of the tympanic cavity. It is more prominent and projects into the tympanic cavity to a greater degree in chinchillas and guinea pigs than in rats or dogs, and is almost entirely contained within the temporal bone in primates. It appears as a spiral or "beehive" in chinchillas and guinea pigs. The otic capsule is the bony external frame of the cochlea and is part of the temporal bone. The cochlea has the stapes footplate embedded in the oval window, and the round window is readily visible as an adjacent, membrane-lined structure. The semicircular canals, utricle, and saccule are all contained within temporal bone and so are not readily visible during gross examination.

The pinna has a cutaneous lining on both the external and internal surfaces. In either case, the dermis is thin. The auricular cartilage of the pinna is comprised of a fibrocartilaginous core. The lining of the ear canal changes as microscopic examination progresses from the external areas toward the tympanic membrane. For example, in the rabbit, the more external areas have a thin epidermis and dermis with a paucity of hair follicles. In the external ear canal just outside of the bony collar (i.e., at about the level of the obtuse-angle turn), the ear canal retains the thin epidermis but has a circumferential zone containing sebaceous glands (ceruminous glands) but lacking hair follicles. Within the internal acoustic meatus, defined by the presence of the bony collar, the dermis is very thin to nonexistent with the epidermis almost lying upon the temporal bone. However, a dermis of sorts is still present, and it can be expanded greatly when injured by congestion, hemorrhage, edema, and/or inflammation. The dermis and epidermis of the internal auditory meatus lack any adnexal structures. The epidermis continues seamlessly as the external squamous epithelial lining of the tympanic membrane.

Rodents do not have multiple small ceruminous glands, which are simple sebaceous glands as observed in the rabbit, but instead have a relatively large compound sebaceous gland, the Zymbal's or auditory sebaceous gland. This latter gland is located rostral and ventral to the ear, medial to the temporal bone. Like the ceruminous glands, it secretes sebaceous material ("ear wax"), which often also is referred to as cerumin.

The tympanic membrane is lined externally and internally by a thin, simple squamous epithelium. The stroma of the tympanic membrane has areas that are thin, fibrous and tightly stretched (typically found centrally) as well as areas closer to the periphery which are fleshy and highly vascularized. When conducting a histologic evaluation of the tympanic membrane in cross-section, these distinct areas should be recognized as normal. The air-filled tympanic bulla is lined by a mucous membrane with epithelium varying from tall columnar with goblet cells to a thin squamous epithelium. The tall columnar regions tend to be in ventral areas and adjacent to the auditory tube. These epithelial cells line all surfaces, including the surfaces of the auditory ossicles. The auditory tube is lined by a columnar ciliated respiratory epithelium with goblet cells. The auditory tube is supported by either bone, in segments extending from the tympanic cavity, to a cartilaginous collar as it nears the nasopharynx. In some species, there are bony "struts" within the tympanic bulla that partially subdivide it. These are more prominent in chinchillas, which have large tympanic bullae, than in rats or dogs.

The inner ear (cochlea and vestibular apparatus) is composed of an osseous labyrinth, a part of the petrous portion of the temporal bone, which contains perilymph that surrounds the membranous labyrinth. The stapes footplate rests within the oval window with cartilaginous surfaces forming a seal (oval window ligament). Movement of the oval window causes movement of perilymph. The round window membrane is the "relief valve" that allows the fluid waves to be propagated. Perilymph is exterior to the membranous labyrinth and movement of perilymph causes movement of structures of the membranous labyrinth and the endolymph within the membranous labyrinth.

The inner ear begins with the vestibule which has further openings into the cochlea as well as vestibular structures (the semicircular canals, utricle and saccule). The various elements

of the vestibulocochlear apparatus of the inner ear serve three distinct sensory functions: the organ of Corti within the cochlea is integral to the sense of hearing, the semicircular canals detect rotational motion via changes in fluid inertia, and the utricle and saccule detect linear motion via the effect of gravity on the otoliths embedded in an otolithic membrane overlying sensory hair cells. The membranous labyrinth is contained within the encasing bony labyrinth.

The cochlea is a spiral-shaped structure that has 2.5 to 3.5 turns, depending on the mammalian species. Humans and rats have 2.5 turns, while chinchillas and guinea pigs have 3.5 turns. The 3.5 turns are often referred to as apical, middle, and basal turns, while the most basal part, the "hook", extends away from the spiral and into the vestibule and toward the round window. The cochlear or otic capsule is part of the osseous labyrinth of the inner ear. It is the hard external supporting structure of the cochlea and is part of the temporal bone. The membranous labyrinth also continues within the inner ear as the cochlear duct and other cellular constituents.

When histologically examined, the cochlea is normally sectioned in a mid-modiolar plane. This is a longitudinal orientation containing the central supporting bony structures (modiolus) and cochlear nerve. When viewing the cochlea in cross-section in this mid-modiolar plane, there are three fluid-filled spaces in each turn: the scala tympani, scala vestibuli, and scala media (also known as the cochlear duct). The scala tympani and scala vestibuli are continuous, meeting at the most apical turn of the spiral at the helicotrema. They both contain perilymph, which is similar to serum and cerebrospinal fluid in composition in that it is high in sodium (Na^+) and low in potassium (K^+). The scala media is located between the scala tympani and scala vestibuli and is separated from them apically by the Reissner's membrane and basally by the organ of Corti and its cellular constituents. The scala media contains endolymph, which is high in K^+ and low in Na^+. The chemical potential (endocochlear potential), formed by the differential electrolyte concentrations between the continuous canals of the scala vestibuli and scala tympani and the separate scala media, is essential for the function of the hair cells.

Within the scala media, on the basal membrane, lies the organ of Corti. This structure consists of the inner and outer sensory hair cells and the associated supporting cells and matrix. The inner hair cells normally occur as a single row running the length of the spiral of the scala media on the medial side. The outer hair cells occur as three rows located more laterally on the basilar membrane. Hair cells have arrays of stereocilia on their apical surfaces.

The inner hair cell is the true otic sensory cell. Deflection of the inner hair cell's stereocilia by sound-induced fluid waves traveling in the endolymph opens transduction ion channels in the apical cell surface that allow influx of K^+ ions into the cell from the endolymph and activates voltage-sensitive calcium (Ca^{++}) channels and Ca^{++}-activated K^+ channels in the lateral and basal membranes, in turn causing release of neurotransmitters at the base of the inner hair cell. The nerve fibers which synapse with the inner hair cell are bipolar neurons of the cochlear (auditory) nerve. The soma of each neuron is located in the spiral ganglion.

The outer hair cells also have arrays of stereocilia on their apical surfaces. Deflection of these stereocilia also causes ion channel opening and closing. The opening of ion channels in these cells results in rapid changes in length and stiffening of the outer hair cell via the cytoskeleton and a prestin motor. These changes in the outer hair cells amplify the extent of transduction at the inner hair cells. Inner and outer hair cells are terminally differentiated in mammals and thus do not proliferate and are not regenerated.

Within the scala media on the lateral wall is the stria vascularis and the spiral ligament. The stria vascularis consists of three layers of cells, marginal cells, intermediate cells, and basal cells. The marginal cells have apical tight junctions, adherens junctions, and desmosomes, and are atypical for epithelial cells in that they lack a basement membrane. The marginal cells have membrane ion pumps and channels; in particular, they pump Na^+ out of the endolymph via Na^+/K^+-ATPases. Intermediate cells contain melanin, are derived from the neural crest, and are sometimes referred to as melanocytes. Basal cells are adjacent to the more laterally located spiral ligament. These flat cells form a continuous layer. They also have a dense network of junctional complexes, but lack Na^+/K^+-ATPases. Embedded within the stria vascularis is a prominent capillary bed. The stria vascularis is an important component of the blood-labyrinth barrier. The spiral ligament is a fibrous cushion located between the stria vascularis and the bony otic capsule. This ligament is primarily composed of connective tissue, especially extracellular matrix and cells of mesodermal origin. The basilar membrane is anchored laterally by the spiral ligament, and this anchoring may not be passive in that the ligament contains tension fibroblasts. These cells have contractile proteins and may either generate or regulate the tension of the basilar membrane.

The dorsal (superior) aspect of the scala media is bounded by the Reissner's membrane, which completes the triangular borders of the scala media.

Specific sound frequencies are detected in particular portions of the organ of Corti. The basal turns detect high frequency sounds, while the apical turns detect low frequency sounds.

The spiral ganglion is embedded within the modiolus and extends centrally as the cochlear nerve, which is a branch of the cranial nerve VIII. Each afferent nerve fiber synapses with only one inner hair cell. However, each inner hair cell will synapse with multiple afferent nerve fibers. Also passing through the cochlear nerves are unmyelinated or poorly myelinated efferent nerve fibers from the central auditory centers that synapse at inner and outer hair cells. Auditory pathways in the brain that may be of interest when investigating apparent deficits in hearing are the auditory nucleus and 8th cranial nerve roots in the brainstem as well as the caudal (inferior) colliculi and the medial geniculate nuclei in the midbrain.

The saccule and utricle (otolith organs) of the vestibular apparatus are located within the vestibule of the inner ear. These sac-like membranes are important for sensing location rather

than appreciating sound. The saccule and utricle each have a placode of tissue located on one wall, referred to as the macula or otolith membrane. This macula is lined by hair cells and other supporting epithelial cells. Hair cells are innervated by fibers of the vestibular nerve (a branch of cranial nerve VIII), the neurons of which are located in the vestibular ganglion with projections to the vestibular nuclei and cerebellum. The surface of the macula has an adherent viscous gel in which the hair cells are embedded. Microliths (otoliths) are also entrapped within this gel. Being denser than the surrounding gel and fluid, the microliths respond to gravity causing the stereocilia on the hair cells to deflect and allows for sensation of vertical (saccule) or horizontal (utricle) motion.

The semicircular canals of the vestibular apparatus are membrane-lined bony canals. The membranes have a single crista ampullaris in each canal that protrudes into the lumen. These cristae ampullaris are mounds of loose connective tissue with overlying hair cells and supporting cells. The semicircular canals are roughly oriented in three distinct planes representing unique X, Y, and Z axes, which allows for rotational sensation in all directions. Nerve fibers of the vestibular nerve extend up through the loose connective tissue to synapse with the basal cytoplasm of the hair cells. The cupola is the gel-like material on the luminal surface of the cristae in which the stereocilia of the hair cells are embedded. As the head is turned, inertia of the fluid within the semicircular canals causes the stereocilia of the hair cells to flex, thereby allowing the detection of motion.

TERMINOLOGY AND DESCRIPTIONS

Nonproliferative Lesions of the Rat and Mouse Ear

Normal Anatomy (Internal Ear) (Figure 108)

External Ear

Many of these changes of the external ear involve the skin of the pinna, and so the integumentary system nomenclature (Mecklenburg et al. 2013, see Introduction) can be relied upon for these diagnoses. These include changes such as erosions and ulcers, hemorrhage, edema, necrosis, and congestion of the tissues of the external ear. Terms for lesions of the integument lining the external ear are described in the publication of the integumentary system and are not unique to the ear. Terms for Zymbal's glands are described in the publication of Proliferative and Nonproliferative Lesions of the Rat and Mouse Mammary, Zymbal's, Preputial, and Clitoral Glands (see Introduction, Rudmann et al. 2012).

Those terms that may be considered specific for the external ear are presented below.

Degenerative Changes

Perforation, tympanic membrane (N) (Figure 109) **Ear, external**

Species
Mouse; Rat.

Other Term(s) Used
Rupture, typmpanic membrane.

Pathogenesis/cell of origin
Perforation of the tympanic membrane may be traumatic from a penetrating foreign object or may follow necrosis of the tympanic membrane.

Diagnostic Features
- The tympanic membrane is discontinuous, which must be differentiated from artifact of sectioning or histologic processing.
- If a true perforation, depending on chronicity, there may be hemorrhage, inflammation, hyperplasia of tympanic membrane epithelium, hemosiderin deposition, or fibrosis.

Differential Diagnoses
Artifact of sectioning or histologic processing

Comment
Perforation of the tympanic membrane may be due to multiple causes. Often it is due to trauma or inflammation or both. Some locally administered test articles may inhibit healing such that transtympanic injections may be slow to heal or fail to heal.

Inflammatory Changes

Inflammation, auricular cartilage (N) (Figures 110, 111) **Ear, external**

Species
Mouse; Rat.

Pathogenesis/cell of origin
There are several causes of inflammatory conditions affecting chondrocytes of the pinna (see comments below).

Diagnostic Features
- Granulomatous inflammation is centered on cartilage of the pinna.
- Cartilage may have regenerative hyperplasia.
- Bone formation within the cartilage may occur.

Differential Diagnoses
- Chondroma; Osteoma
- Otitis externa

Comment
Auricular cartilage inflammation is both a naturally occurring and inducible condition. Spontaneous auricular cartilage inflammation occurs in various rat strains, including Sprague-Dawley and fawn-hooded rats. Induction of auricular cartilage inflammation may be achieved by intradermal injection of type II collagen, suggesting that it is an autoimmune disease (Chiu 1991; Kitagaki et al. 2003).

Inflammation, external ear canal (N) (Figures 112, 113***)***
Ear, external

Species
Mouse; Rat.

Pathogenesis/cell of origin
There are several causes of inflammatory conditions affecting the epithelium of the epidermis or adnexa (see comments below).

Diagnostic Features
- Inflammation is centered on the epithelium or adnexa of the external ear canal as part of an irritant process in response to locally administered test articles.

Differential Diagnoses
Inflammation, auricular cartilage

Comment
Many of the changes of the external ear canal (spontaneous or test article induced) are similar to that of the skin. Readers are recommended to review the INHAND monograph on the skin and associated glands and structures (see Introduction, Mecklenburg et al. 2013).

Debris, external ear canal (N) **Ear, external**

Species
Mouse; Rat.

Pathogenesis/cell of origin
Proteinaceous material, sebum, exfoliated cells, and infllammatory cells may accumulate in the external ear canal.

Diagnostic Features
- Amorphous eosinophilic material, degenerating cells, cell fragments, lipid clefts, and other material accumulates in the external ear, often gravitating to the tympanic membrane, where the greatest amount of this material is often found.

Differential Diagnoses
Inflammation, External ear canal

Comment
Debris accumulations can be a spontaneous, background finding, but may occur with transtympanic injection or ear canal instillation of an irritating material.

Miscellaneous Changes

Cyst, tympanic membrane (N) (Figure 114) **Ear, external**

Species
Mouse; Rat.

Pathogenesis/cell of origin
External tympanic membrane epithelium.

Diagnostic Features
- The tympanic membrane has the formation of a spherical cyst lined by squamous epithelium with an internal core of effete squames.
- This change may progress to a cholesteatoma.

Differential Diagnoses
Cholesteatoma

Comment
Cysts occur within the tympanic membrane proper or on the lateral side of the tympanic membrane.

Middle Ear

Degenerative Changes

Mineralization (N) **Ear, middle**

Species
Mouse; Rat.

Other Term(s) Used
Calcification.

Pathogenesis/cell of origin
Mineral deposition in the lining of the tympanic bulla is frequently observed as a spontaneous, background change, but may be increased in frequency and extent with administrations of test articles or vehicle into the tympanic bulla.

Diagnostic Features
- Mineralization occurs in the subepithelial region of the tympanic membrane, appearing as basophilic plaques. Mineralization may be confirmed with von Kossa stain.
- May be associated with epithelial necrosis, foreign body reaction and scarring.

Ulcer (N) (Figure 115) **Ear, middle**

Species
Mouse; Rat.

Pathogenesis/cell of origin
Epithelium lining the tympanic bulla.

Diagnostic Features
- Cells are necrotic and slough into the lumen with exposure of the underlying propria.
- Secondary changes like inflammation, hyperplasia, fibroplasia, etc. may be present.

Differential Diagnoses
None.

Comment
An irritant in the tympanic bulla may produce necrosis of the epithelium. Since it is normally a single layer thick, it may be considered an ulcer (Schafer and Bolon 2013).

Necrosis, bone (N) (Figure 116) **Ear, middle**

Species
Mouse; Rat.

Other Term(s) Used
Osteonecrosis.

Pathogenesis/cell of origin
Osteocytes of the tympanic bulla.

Diagnostic Features
- Nuclei in the lacuna of the bones of the tympanic bulla are absent.

Differential Diagnoses
None.

Comment
Severe irritants instilled into the external ear canal or into the middle ear can produce necrosis of the bone.

Necrosis, tympanic membrane (N) (Figure 117) **Ear, middle**

Species
Mouse; Rat.

Other Term(s) Used
Coagulative necrosis.

Pathogenesis/cell of origin
All layers of the tympanic membrane.

Diagnostic Features
- The tympanic membrane is diffusely eosinophilic consistent with coagulative necrosis.

Differential Diagnoses
None.

Comment
Severe irritants instilled into the external ear canal or into the middle ear can produce necrosis of the tympanic membrane. Necrosis is often accompanied by inflammation.

Inflammatory Changes

Infiltrate, inflammatory cell (N) **Ear, middle**

Species
Mouse; Rat.

Pathogenesis/cell of origin
Leukocytes recruited from the systemic circulation. The pathogenesis is uncertain, but presumably a self-limiting response designed for immune surveillance and minor tissue repair activities.

Diagnostic Features
- Foci of single inflammatory cell type or a mixture of different cell types without other features of inflammation.
- Infiltrates may be neutrophil, macrophage, foamy macrophage, mononuclear cell, or mixed cell populations.

Differential Diagnoses
Inflammation:
- Inflammatory cellular infiltrate with possible edema, congestion, hemorrhage, and/or necrosis.

Comment
'Infiltrate' is the preferred term, followed by the predominant cell type (neutrophilic, eosinophilic, lymphocytic, plasmacytic, histiocytic, or foamy macrophages) or mixture of different cell types (mixed). Infiltrates resolve without residual damage to the otic tissues. Foamy macrophages in small numbers may be observed as a spontaneous background change in the tympanic bulla lumen, but will be increased in number and more prominent with transtympanically injected drug and/or vehicle.

Inflammation, middle ear (N) (Figure 118) **Ear, middle**

Species
Mouse; Rat.

Other Term(s) Used
Otitis media.

Pathogenesis/cell of origin
The inflammation affects the mucosa lining the tympanic bulla. Neutrophils, lymphocytes, and/or macrophages infiltrate into tissues or spaces in response to an irritant or infectious process.

Diagnostic Features
- The propria of the mucosa of the tympanic bulla is expanded by edema and/or infiltrating inflammatory cells.
- Migration of inflammatory cells into the bulla lumen may occur.

Differential Diagnoses
None.

Comment
May have necrosis of associated tissues. Inflammation of the middle ear may be induced by instillation of irritating substances, but also occur spontaneously (Verdaguer et al. 2006). Inflammation in the middle ear is often due to a breach or compromise in the natural barriers of the middle ear, although spontaneous infections are relatively frequent. The specific location within the middle ear should be designated with anatomic locators whenever possible (e.g., tympanic membrane, ossicles, round window niche, etc.).

Inflammation, middle ear, catarrhal (N) **Ear, middle**

Species
Mouse; Rat.

Other Term(s) Used
Otitis media, catarrhal; mucous hyperplasia/metaplasia.

Pathogenesis/cell of origin
Mucus production by the epithelium lining the tympanic bulla.

Diagnostic Features
- Accumulation of relatively cell-free fluid and mucous material is present in the tympanic bulla space.

Differential Diagnoses
Edema

Inflammation, middle ear

Comment
Catarrhal inflammation is usually accompanied by metaplasia of the epithelium of the tympanic bulla to include numerous goblet cells. Low numbers of exfoliated epithelial cells may be part of the alteration (Schafer and Bolon 2013).

Metaplasia, squamous cell (N) (Figure 119) **Ear, middle**

Species
Mouse; Rat.

Other Term(s) Used
Epithelial hyperplasia, tympanic bulla mucosa.

Pathogenesis/cell of origin
Epithelium lining the tympanic bulla.

Diagnostic Features
- The epithelium lining the tympanic bulla has a stratified squamous morphology.
- The epithelium may or may not be keratinizing.

Differential Diagnoses
None.

Comment
The epithelium lining the tympanic bulla is a simple squamous epithelium in most areas with simple cuboidal to simple columnar epithelium in the most dependent areas (ventral). The epithelium can undergo squamous metaplasia as an adaptive, protective change in response to an irritant or infectious process and may be associated with inflammation.

Metaplasia, tall cuboidal to columnar (N) **Ear, middle**

Species
Mouse; Rat.

Pathogenesis/cell of origin
Epithelium lining the tympanic bulla.

Diagnostic Features
- The epithelium lining the tympanic bulla consists of tall cuboidal to columnar cells.
- May include numerous goblet cells.

Differential Diagnoses
None.

Comment
The epithelium lining the tympanic bulla is normally a simple squamous epithelium in most areas with simple cuboidal to simple columnar epithelium in the most dependent areas (ventral). Alterations may be induced by a mild irritant in the inner ear, e.g. slightly acidic solutions. The epithelium can undergo cuboidal or columnar metaplasia as an adaptive, protective change in response to an irritant or infectious process and may be associated with inflammation. The most ventral aspect of the tympanic bulla will often have cuboidal to columnar epithelium normally.

Fibrosis (N) (Figures 120, 121) **Ear, middle**

Species
Mouse; Rat.

Pathogenesis/cell of origin
Proliferation of fibroblasts and deposition of loose connective tissue in the propria of the mucosa of the tympanic bulla.

Diagnostic Features
- The tympanic bulla propria is expanded by loose connective tissue with minimal collagen production.

Differential Diagnoses
Edema

Comment
Fibrosis is usually accompanied by inflammation and represents a protective mechanism.

Granulation tissue (N) **Ear, middle**

Species
Mouse; Rat.

Pathogenesis/cell of origin
Proliferation of fibroblasts and deposition of loose connective tissue in the propria of the mucosa of the tympanic bulla in combination with edema, vascular proliferation, and sometimes new bone formation. The mucosa of the

typamic bulla may be expanded by pseudoglands.

Diagnostic Features
- The tympanic bulla propria is expanded by loose connective tissue with minimal collagen production, edema, and vascular proliferation.

Differential Diagnoses
Edema, Fibrosis

Comment
Granulation tissue is usually accompanied by inflammation and represents a protective mechanism, often in reaction to a chronic irritant in the middle ear.

Inflammation, granulomatous (N) (Figure 122) **Ear, middle**

Species
Mouse; Rat.

Pathogenesis/cell of origin
Reaction of mucosa to foreign material in the tympanic bulla.

Diagnostic Features
- Infiltrates consist of epithelioid macrophages, multinucleated giant cells and lymphocytes.
- May have abundant necrotic cells and debris and neutrophils.
- May fill large portions of the tympanic bulla.

Differential Diagnoses
Inflammation, middle ear

Cholesteatoma

Comment
Often occurs as a response to foreign body gaining entry via a ruptured tympanic membrane or as a reaction against materials administered via a cannula. Inert material may result in accumulation of foamy macrophages.

Vascular Changes

Hemorrhage (N) (Figure 123) **Ear, middle**

Species
Mouse; Rat.

Pathogenesis/cell of origin
Ulceration or necrosis of the mucosa may expose the underlying propria and result in bleeding into the lumen. Rupture of the tympanic membrane may disrupt the vessels of the membrane and produce hemorrhage as well. Severe irritants may produce hemorrhage of the propria of the tympanic bulla.

Diagnostic Features
- Blood is present in the tympanic bulla space or in the propria of the tympanic bulla.
- Secondary changes of pigment deposition, fibroplasia etc. may be present.

Differential Diagnoses
None.

Edema (N) (Figure 123) **Ear, middle**

Species
Mouse; Rat.

Pathogenesis/cell of origin
Leakage of fluid into the propria.

Diagnostic Features
- The propria of the middle ear is expanded by pale staining fluid.

Differential Diagnoses
Hemorrhage

Comment
Edema is usually accompanied by epithelial and inflammatory changes. It may occur with administration of saline alone.

Miscellaneous Changes

Cyst (N) **Ear, middle**

Species
Mouse; Rat.

Pathogenesis/cell of origin
Epithelium lining the tympanic bulla.

Diagnostic Features
- The epithelium forms cystic structures.
- Cysts contain nonstaining fluid or mucoid material and cell debris.
- Cysts most likely occur in the ventral aspects of the tympanic bulla.

Differential Diagnoses
Cholesteatoma

Comment
None.

Cholesteatoma (N) **Ear, middle**

Species
Mouse; Rat.

Pathogenesis/cell of origin
The tympanic membrane squamous epithelium forms an expansive mass. It may be the result of a trauma.

Diagnostic Features
- A squamous cyst is present in the tympanic bulla.
- May contain cholesterol clefts from the degenerating cell membranes or previous hemorrhage.
- May be associated with granulomatous inflammation.

Differential Diagnoses
Tympanic membrane Cyst

Comment
Cholesteatomas occur on the medial side of the tympanic membrane. They may be pedunculated or occur as a polyp-like structure, and may progressively enlarge with time. Cholesteatomas can be induced by irritants or surgical ligation of the external ear canal (Hottendorf 1991; McGinn et al. 1982, Steinbach and Grüninger 1980).

Atrophy, bone (N) **Ear, middle**

Species
Mouse; Rat.

Sublocation
Tympanic bulla or middle ear ossicles.

Other Term(s) Used
Osteopenia.

Pathogenesis/cell of origin
Osteoclasts.

Diagnostic Features
- The tympanic bulla or middle ear ossicles have scalloping of margins and thinning of the bone.

Differential Diagnoses
None.

Comment
The atrophy of the bone may be the consequence of an inflammatory process that encapsulates the ossicles as a reaction to a nonspecific irritant.

New bone formation (N) (Figure 124) **Ear, middle**

Species
Mouse; Rat.

Other Term(s) Used
Hyperostosis; Osteosclerosis.

Pathogenesis/cell of origin
Osteoblasts.

Diagnostic Features
- The tympanic bulla is thickened, often with a prominent "watermark" delineating the newly deposited woven bone.
- In some instances, there may be sharp spicules of new bone formation that extends into exudates in the tympanic bulla.

Differential Diagnoses
None.

Comment
The new bone formation is usually the consequence of an irritant that induces a chronic-active inflammatory process that results in persistent exudate in the tympanic bulla.

Inner Ear

Degenerative Changes

Degeneration, hair cells and/or epithelium (N) (Figure 125) **Ear, inner**

Species
Mouse; Rat.

Sublocation
Crista ampullaris.

Synonym
Decreased number, hair cell

Pathogenesis/cell of origin
Hair cells of crista ampullaris.

Diagnostic Features
- The surface epithelium is disorganized and may show vacuolation.
- Pyknotic debris may be visible within the epithelium.

Differential Diagnoses
Hair cell necrosis

Comment
Often there is evidence of both degeneration and necrosis present in the epithelium of the crista ampullaris. Alterations may be induced by macrolide antibiotics and other intoxicants (Ibrahim et al. 2014; Schafer & Bolon 2013).

Decreased Number, Hair cell (N) (Figure 126; 127 [normal]) **Ear, inner**

Species
Mouse; Rat.

Sublocation
Cochlea or cristae ampullaris.

Pathogenesis/cell of origin
Injury to the outer or inner hair cells of the organ of Corti or cristae ampullaris.

Diagnostic Features
- Hair cells are absent and replaced by large, non-descript, swollen cells.
- In more chronic instances, these large cells will shrink and form a low cuboidal layer lining the scala media where the inner and outer hair cells should be in the organ of Corti.

Differential Diagnoses
Hair cell necrosis

Degeneration, hair cells (cochlea or crista ampullaris)

Comment
Hair cell necrosis, depending on the insult, may occur fairly rapidly in the course of a toxicology study such that the process of hair cell necrosis is not observed, only the end result (hair cell loss is no longer active). Because the hair cell necrosis appears to be an apoptotic process, there is generally not residual inflammation present unless the test article applied to the middle/inner ear was a severe irritant producing generalized inflammation and necrosis of the tissues of the cochlea. (Schafer & Bolon 2013).

Necrosis, Hair cell (N) (Figure 128) **Ear, inner**

Species
Mouse; Rat.

Sublocation
Cochlea or cristae ampullaris.

Pathogenesis/cell of origin
Injury to the outer or inner hair cells of the organ of Corti or the hair cells at the apex of the crista ampullaris.

Diagnostic Features
- Cells are shrunken with eosinophilic cytoplasm and pyknotic, karyorrhectic, or karyolytic nuclei (consistent with apoptosis).

Differential Diagnoses
Hair cell loss

Comment
Hair cell necrosis due to specific ototoxicants (in contrast to non-specific irritants) tends to be apoptotic necrosis. Macrolide antibiotics such as gentamicin will produce this change (Schafer & Bolon 2013).

Necrosis, cartilage (N) (Figure 129) **Ear, inner**

Species
Mouse; Rat.

Sublocation
Oval window footplates.

Other Term(s) Used
Chondronecrosis.

Pathogenesis/cell of origin
Chondrocytes.

Diagnostic Features
- Nuclei in the lacuna of the cartilage of the footplates of the stapes and the corresponding rim of the oval window are absent.

Differential Diagnoses
None.

Comment
Severe irritants instilled into the middle ear can produce necrosis of the cartilage of the stapes and round window.

Necrosis, vestibular organ (N) (Figure 130) **Ear, inner**

Species
Mouse; Rat.

Pathogenesis/cell of origin
Vestibular organ hair cells/epithelium or entire organ.

Diagnostic Features
- With specific ototoxicants, there may be shrunken, eosinophilic epithelial cells with pyknotic, karyorrhectic, karyolytic nuclei.
- With nonspecific irritants, there may be coagulative necrosis of all cells of the vestibular organ.

Differential Diagnoses

Degeneration of vestibular organ

Necrosis, neuronal (N) (Figure 131) **Ear, inner**

Species
Mouse; Rat.

Pathogenesis/cell of origin
Neuronal cell bodies of spiral or vestibular ganglion.

Diagnostic Features
- The neurons of the ganglia are shrunken and with hypereosinophilic cytoplasm.

Differential Diagnoses
Dark neuron artifact

Comment
With sufficient time, a dying back process due to loss of hair cells of the organ of Corti, the crista ampullaris, or the vestibular organ will result in loss of connections and loss of neurons. Due to the normal variability of density of ganglion cells in the spiral ganglion, it is difficult to diag-

nose loss of ganglion cells without observation of active necrosis. Further details can be found in proliferative and nonproliferative lesions of the rat and mouse central and peripheral nervous system (Kaufmann et al. 2012, see Introduction).

Degeneration, axonal, vestibulo-cochlear nerve (N) (Figure 132) **Ear, inner**

Species
Mouse; Rat.

Pathogenesis/cell of origin
Vestibular nerve, cochlear nerve, or vestibulocochlear nerve (CN VIII).

Diagnostic Features
- Early stage lesions include axonal swelling and eosinophilia.
- Late stage lesions include axonal fragmentation and formation of digestion chambers within the nerve.

Differential Diagnoses
None.

Comment
With sufficient time, a dying back process due to loss of hair cells of the organ of Corti, the crista ampullaris, or the vestibular organ will result in loss of connections and loss of neurons and subsequent loss of axons that extend to the brain. Further details can be found in proliferative and nonproliferative lesions of the rat and mouse central and peripheral nervous system (Kaufmann et al. 2012, see Introduction).

Decreased cellularity, spiral limbus, spiral ligament, and/or stria vascularis (N) (Figure 133) **Ear, inner**

Species
Mouse; Rat.

Pathogenesis/cell of origin
Fibrocytes of the spiral limbus, fibrocytes of the spiral ligament, epithelial cells of the stria vascularis.

Diagnostic Features
- The cell density is decreased when compared to concurrent controls.

Differential Diagnoses
Necrosis, neuronal

Degeneration, axonal, vestibulo-cochlear nerve

Comment
Loss of cellularity of the spiral limbus will often follow hair cell loss, presumably by a feedback mechanism, although of currently unknown mechanism. The loss of cells of the spiral ligament may be a specific toxicity or may be a consequence of injury to the overlying stria vascularis. The stria vascularis may be injured by various toxicants and have loss of cells of the inner, intermediate, or outer layers (Schafer and Bolon 2013).

Decreased cellularity, spiral ganglion (N) **Ear, inner**

Species
Mouse; Rat.

Pathogenesis/cell of origin
Ganglion cells, spiral ganglion.

Diagnostic Features
- The cell density is decreased when compared to concurrent controls.

Differential Diagnoses
Necrosis, neuronal

Comment
Loss of cellularity of the spiral ganglion should be made with extreme caution. The spiral ganglion has wide variability in cellular density from the apex to the base. This variability makes identification of cell loss difficult in the absence of other markers of change (ganglion cell necrosis or axonal degeneration of the cochlear nerve. Careful comparison of the same areas of the spiral ganglion between controls and treated animals need to be done to make this diagnosis (Schafer and Bolon 2013).

Vacuolation, hair cell/supporting cell (N) **Ear, inner**

Species
Mouse; Rat.

Pathogenesis/cell of origin
Hair cell or supporting cell injury in the organ of Corti.

Diagnostic Features
- Hair cells or supporting cells are vacuolated.
- Loss of hair cells with replacement by supporting cells may have pallor, hydropic change, or vacuolation of the supporting cells.

Differential Diagnoses
Hair cell necrosis

Hair cell loss

Degeneration, hair cells

Comment
Histologic processing will often produce an artifactual vacuolation of the supporting cells of the organ of Corti, including cells of Hensen, cells of Boettcher, and others that must be distinguished from a toxic insult (Schafer and Bolon 2013).

Vacuolation, stria vascularis (N) (Figure 134) **Ear, inner**

Species
Mouse; Rat.

Pathogenesis/cell of origin
Epithelial cells of the stria vascularis.

Diagnostic Features
- Swelling and vacuolation is present in individual cells of the stria vascularis.

Differential Diagnoses
None.

Comment
Injury to the stria vascularis, which is critical in maintaining an electropotential across the inner ear, will often manifest by swelling. This may be intracellular (hydropic change) or extracellular (edema) (Schafer & Bolon 2013).

Inflammatory Changes

Inflammation, inner ear (N) (Figures 135, 136) **Ear, inner**

Species
Mouse; Rat.

Other Term(s) Used
Otitis interna.

Pathogenesis/cell of origin
Infiltrates of inflammatory cells are present in various spaces of the inner ear. This may be accompanied by readily apparent proteinaceous exudates, or the exudate may be the sole change.

Diagnostic Features
- Inflammatory cells (often neutrophils, but may include macrophages, giant cells, and lymphocytes) accumulate in the fluid spaces of the scala vestibuli, scala tympani, and/or scala media or within the soft tissues lining the cochlea (spiral ligament, stria vascularis, etc).

Differential Diagnoses
Serous exudation

Suppurative inflammation

Pyogranulomatous inflammation

Granulomatous inflammation

Comment
Infiltrates of inflammatory cells are usually a reflection of injury by a nonspecific irritant. The inflammation can secondarily injure important structural components of the inner ear such as the hair cells and stria vascularis. The inflammation could potentially be due to infectious agents, which need to be distinguished from an injury by a toxic insult.

Fibrosis (N) (Figure 137***)*** **Ear, inner**

Species
Mouse; Rat.

Sublocation
Round window, scala vestibuli, scala media, and/or scala tympani.

Pathogenesis/cell of origin
Fibroblasts of the membranes.

Diagnostic Features
- The membranes may be thickened by loose connective tissue and have epithelium that is folded due to the irregularity of the membranes.

Differential Diagnoses
None.

Comment
The fibrosis of these membranes is usually due to nonspecific irritants; this change would be anticipated to deaden vibrations.

Otolith loss, disorganization, or disruption (N) **Ear, inner**

Species
Mouse; Rat.

Sublocation
Vestibular organ.

Pathogenesis/cell of origin
Otolith epithelium.

Diagnostic Features
- Otoliths contained within the gel lining the surface of the vestibular organ are misaligned, disrupted, or absent.

Differential Diagnoses
None.

Comment
The loss of otoliths is likely an effect on the underlying epithelium that maintains the gel matrix.

Vascular Changes

Edema (N) **Ear, inner**

Species
Mouse; Rat.

Sublocation
Round window membrane, scala vestibuli, scala media, and or scala tympani.

Pathogenesis/cell of origin
Injury to the lining epithelium of the various tissues.

Diagnostic Features
- Loose expansion of the mucosa of the spaces adjacent to the otic capsule or modiolus is present.

Differential Diagnoses
Fibrosis

Comment
With an irritant, the submembranous spaces adjacent to the bone are expanded by fluid, likely as a consequence of injury to the lining epithelium.

***Hemorrhage (N)* Ear, inner**

Species
Mouse; Rat.

Pathogenesis/cell of origin
Hemorrhage likely arises from the stria vascularis, if in the scala media, and from the mucosa lining the wall, if in the scala tympani and/or scala vestibuli.

Diagnostic Features
- Blood is present within the scala vestibuli, scala tympani, and/or scala media.

Differential Diagnoses
Artifactual spillage of blood during sectioning or trimming.

***New bone formation (N)* Ear, inner**

Species
Mouse; Rat.

Other Term(s) Used
Hyperostosis; Osteoscerosis.

Pathogenesis/cell of origin
Osteoblasts.

Diagnostic Features
- The cochlea has increased bone formation of the internal surfaces.

Differential Diagnoses
None.

Comment
New bone formation is usually the consequence of a chronic irritant or severe toxicity to the inner ear.

Proliferative Lesions of the Rat and Mouse Ear

There are no proliferative lesions that are unique to the external ear. Terms for the integument lining the external ear are described in the publication of proliferative and nonproliferative lesions of the rat and mouse integument (see Introduction, Mecklenburg et al. 2013).

Terms for Zymbal's glands are described in the publication of Proliferative and Nonproliferative Lesions of the Rat and Mouse Mammary, Zymbal's, Preputial, and Clitoral Glands (see Introduction, Rudmann et al. 2012).

Proliferative lesions of the middle ear are largely a response to irritants or associated with inflammation and are described in the preceding sections on nonproliferative lesions. Neoplastic lesions of the middle ear are not described in the literature for rodents, and any neoplastic changes observed there would be anticipated to resemble those described for soft tissues (see Introduction, Greaves et al. 2013) or bone and are described in those respective publications.

Proliferative lesions of the inner ear are not described in the literature for rodents. However, tumors that might be anticipated to occur would likely arise from the neural or soft tissues and would be consistent with those described in those respective publications (see Introduction, Kaufmann et al. 2012; see Introduction, Greaves et al. 2013).

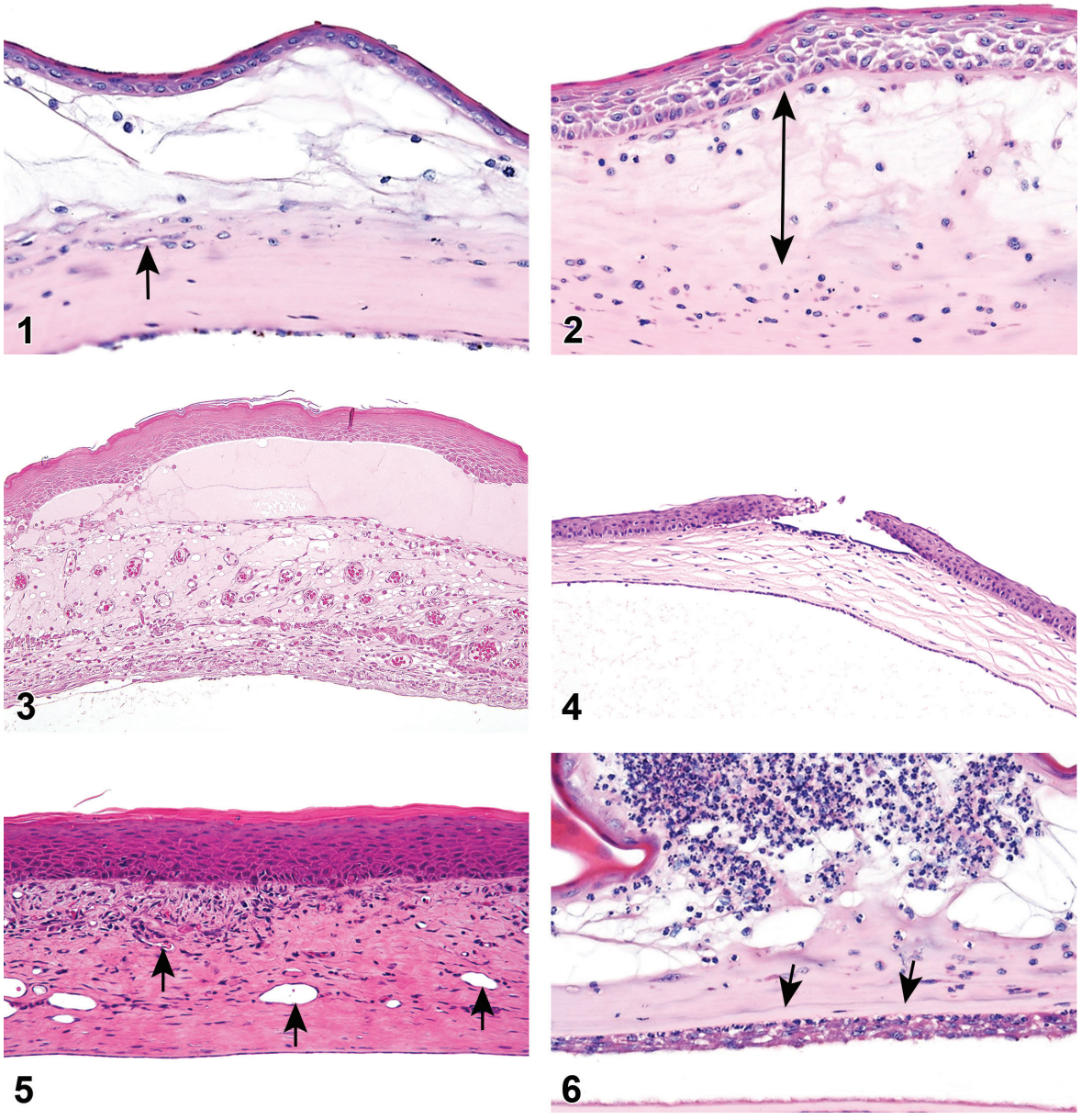

FIGURE 1.——Atrophy, epithelium; Edema, subepithelial; Neovascularization, stroma; cornea; rat. The epithelium has been reduced to a single layer of basal cells that is undermined by subepithelial edema containing scattered inflammatory cells. Profiles of blood vessels (neovascularization) are present in stroma (arrow).

FIGURE 2.——Edema, epithelium and stroma; Inflammation, mixed cell, stroma; cornea; rat. Epithelial cells are separated by clear spaces characteristic of extracellular edema. The epithelium is undermined by proteinaceous fluid (double headed arrow) containing scattered inflammatory cells.

FIGURE 3.——Edema, transmural; Keratinization, epithelium; Inflammation, mixed cells, stroma; Neovascularization, stroma; cornea; rat. Proteinaceous fluid undermines the epithelium and expands all layers of the cornea. The surface of the cornea is covered by a layer of keratin (keratinization), and the stroma contains the profiles of numerous congested blood vessels (neovascularization).

FIGURE 4.——Ulcer, epithelium; Inflammation, mixed cell; cornea; rat. Focal epithelial loss and detachment, with inflammatory cells at base of ulcer and scattered in adjacent corneal stroma.

FIGURE 5.——Fibroplasia, stroma; Inflammation, mixed cell; Hyperplasia, squamous cell, epithelium; Keratinization, epithelium; Neovascularization, stroma; cornea; rat. A population of fusiform, collagen-producing cells is subjacent to the epithelium. The epithelium is thickened by the presence of several extra rows of epithelial cells (hyperplasia) and a superficial layer of keratin. Blood vessels (arrows) are present in the cornea stroma (neovascularization).

FIGURE 6.——Hypertrophy, Descemet's membrane; Hyperplasia/Hypertrophy, endothelium; Inflammation, neutrophils; cornea; rat. Descemet's membrane is expanded by an eosinophilic matrix (arrows). The adjacent corneal endothelium contains multiple layers of prominent endothelial cells. An aggregate of neutrophils undermines an atrophic epithelium.

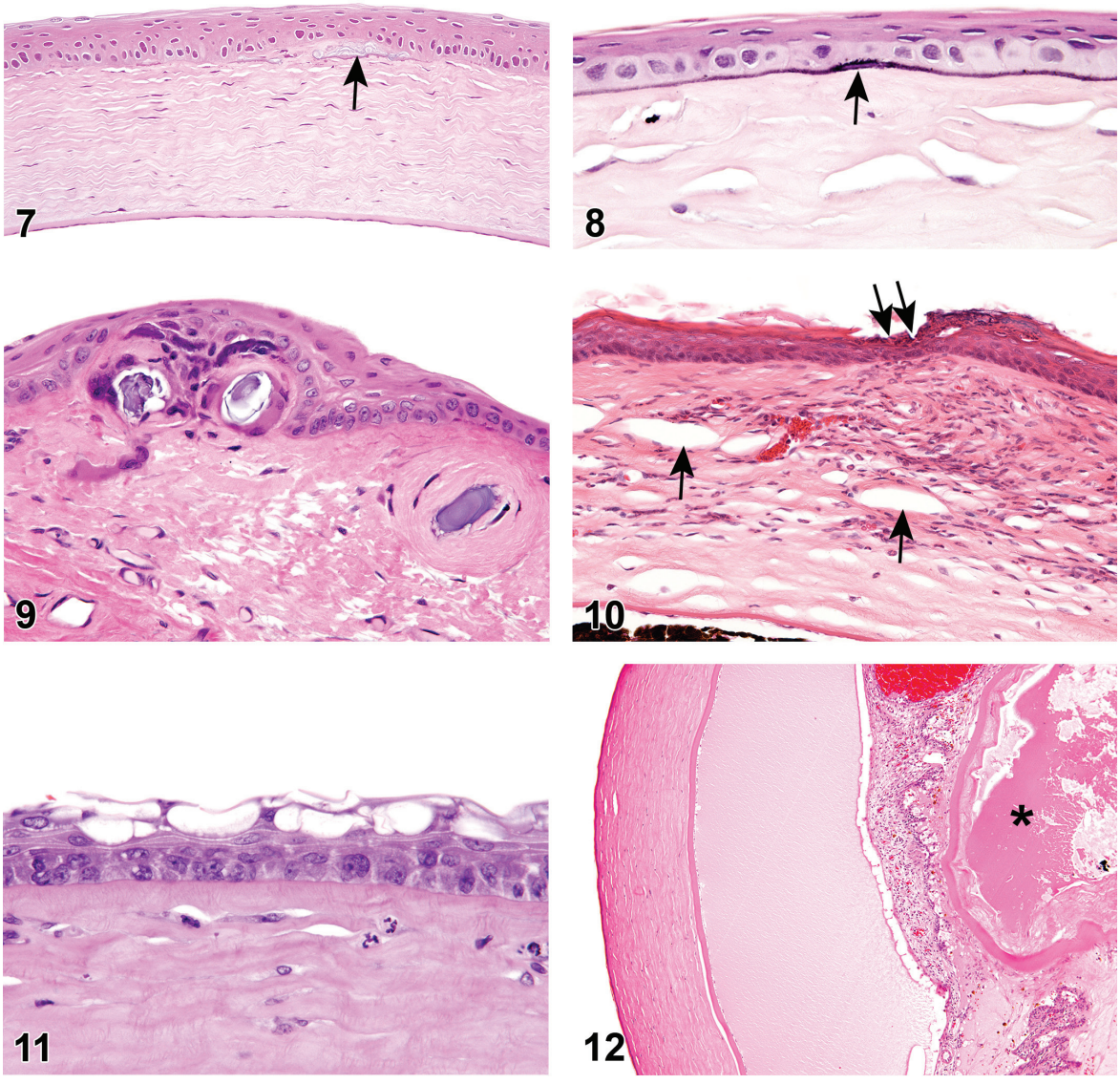

FIGURE 7.—Mineralization, subepithelium, cornea; rat. Linear, basophilic deposits are located parallel and adjacent to the epithelium (arrow), a common location.

FIGURE 8.—Mineralization, epithelium, cornea; F344/N rat. The basement membrane of the epithelium is accentuated by linear basophilic deposits of mineral. NTP archives.

FIGURE 9.—Mineralization, epithelium and stroma; Fibrosis, stroma; cornea; F344/N rat. Several aggregates of basophilic mineral are located in the epithelium and subjacent stroma. A concentric mass of collagen (fibrosis) isolates a mineral aggregate from the rest of the stroma in the far right. NTP archives.

FIGURE 10.—Neovascularization, stroma; Inflammation, stroma, neutrophils; Erosion, epithelium; Keratinization, epithelium; cornea; rat. Profiles of blood vessels (arrows) are present in the stroma, which contains an inflammatory infiltrate. A superficial layer of keratin is present on the epithelium which is focally eroded (double arrow). NTP archives.

FIGURE 11.—Vacuolation, epithelium; Infiltrates, stroma, neutrophils; cornea; F344/N rat. Prominent clear cytoplasmic vacuoles are present in the superficial layer of the epithelium. NTP archives.

FIGURE 12.—Vacuolation, endothelium, cornea; F344/N rat. Clear vacuoles are present in the corneal endothelial cells. The anterior chamber contains proteinaceous fluid, the iris and ciliary process are congested and expanded by inflammation and edema, and the lens is degenerated and distorted (*). NTP archives.

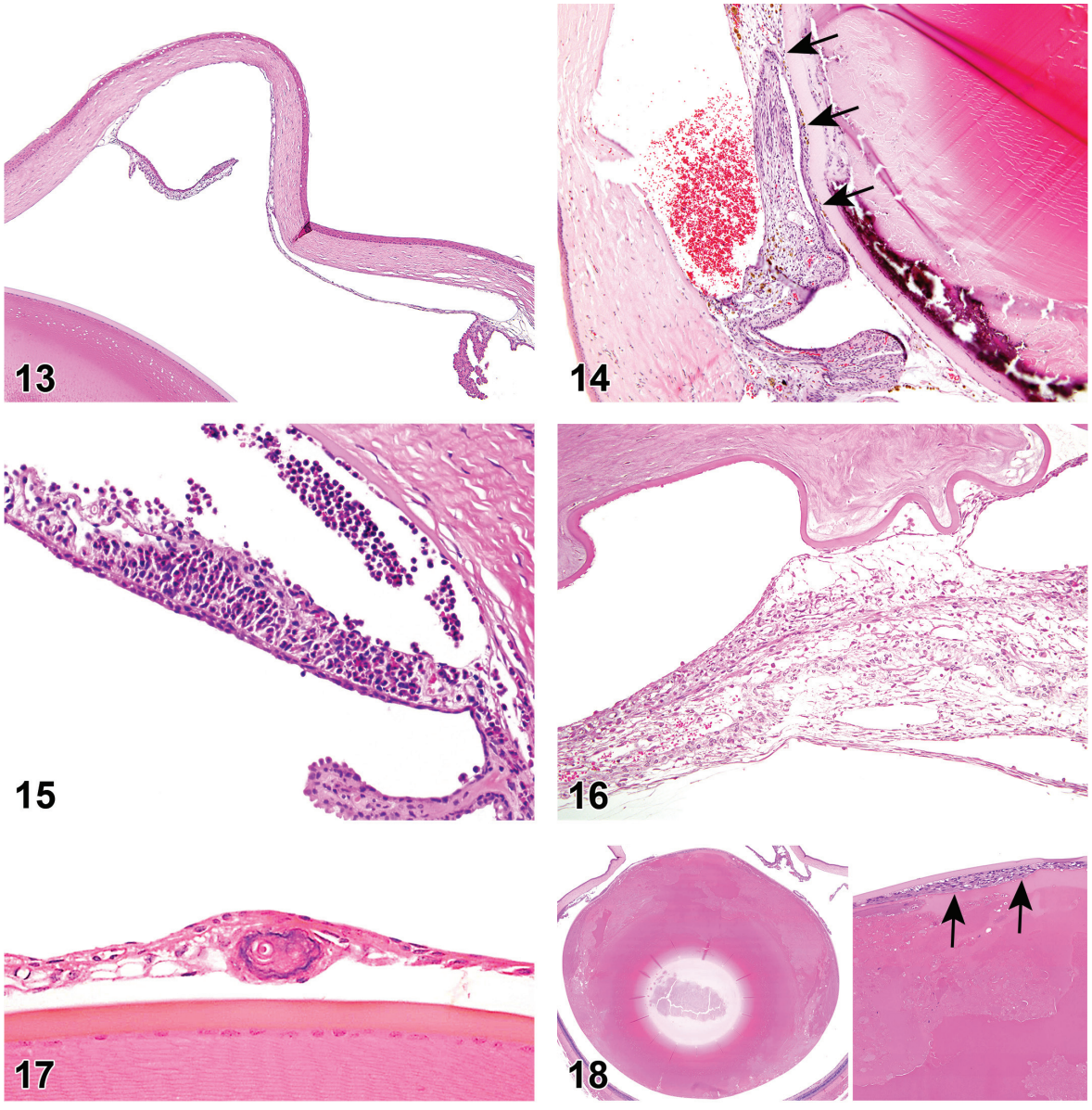

FIGURE 13.—Adhesion, anterior (cornea), iris; rat. Iris is displaced anterior and attached to the cornea endothelium (arrow).

FIGURE 14.—Adhesion, posterior (lens), iris; Hemorrhage, anterior chamber, iris, and ciliary body; Degeneration (with mineralization), lens; F344/N rat. Iris is displaced posterior and attached to the anterior surface of the lens (arrows). Lens fibers subjacent to the anterior lens capsule are basophilic and fragmented, characteristic of mineralization. NTP archives.

FIGURE 15.—Infiltrate, neutrophils, iris and ciliary body; rat. The stroma of the iris is expanded by a neutrophilic infiltrate, which is also present in the filtration angle. Note the lack of other findings characteristic of inflammation.

FIGURE 16.—Fibroplasia; Adhesion, anterior (cornea), iris; rat. Note the buckling of the cornea associated with the adhesion of the iris to the inner surface of the cornea. A mixed cell infiltrate is present within the iris stroma.

FIGURE 17.—Vacuolation, cytoplasmic, posterior epithelium; Mineralization, iris; rat. Variably sized clear vacuoles are present in the posterior epithelium of the iris, which also contains a concentric mass that is mineralized (note basophilic rim).

FIGURE 18.—Degeneration, lens fiber (left and right image); Hyperplasia, lens epithelium (right image); lens; SDT rat. Diabetic –associated lens degeneration. Loss of lens fiber morphology with collection of eosinophilic fluid in the lens cortex. A focal area of epithelial cell proliferation subjacent to the anterior lens capsule is depicted in the higher magnification image on the right (arrows).

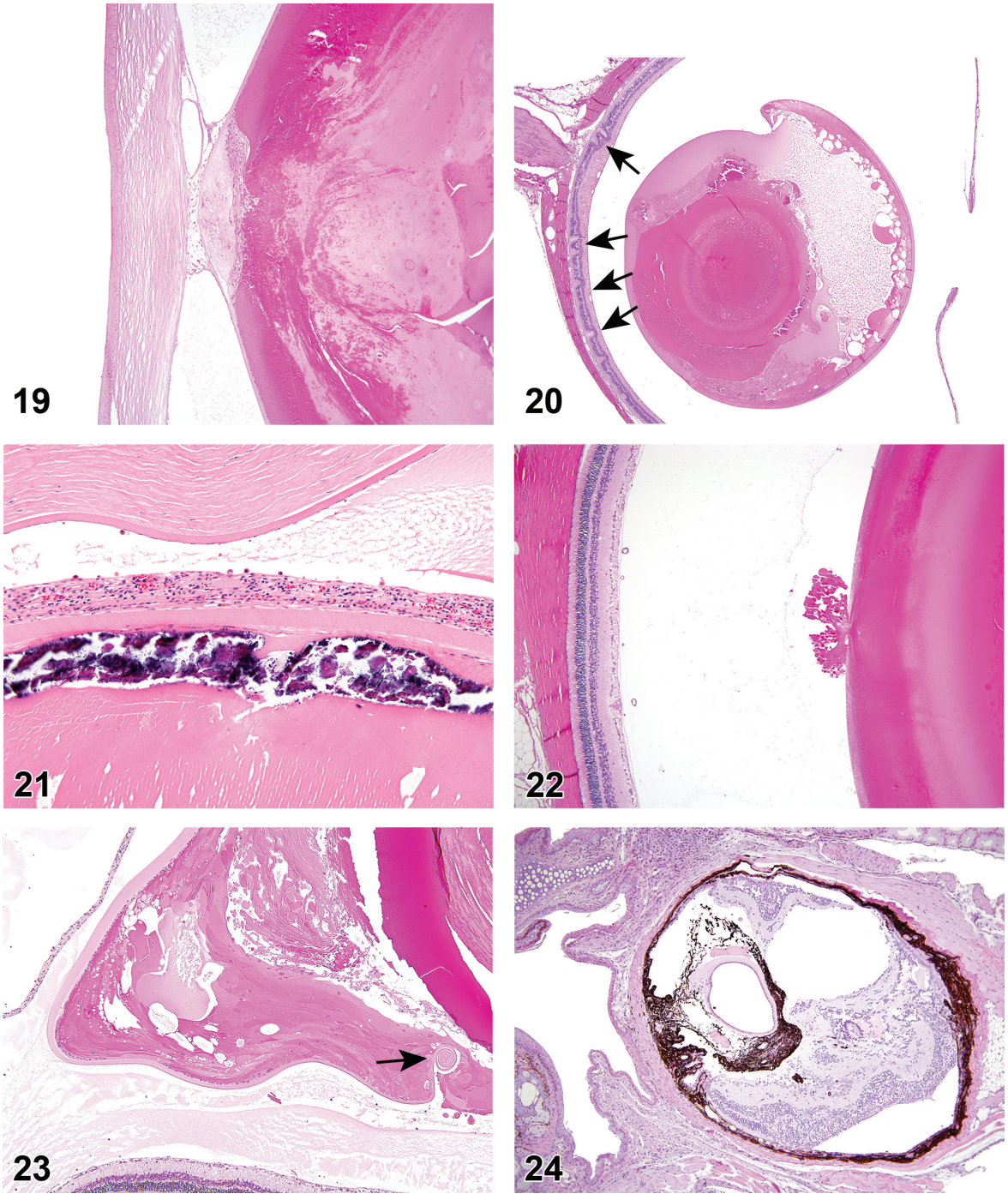

FIGURE 19.—Dislocation, anterior, lens; Fibroplasia, capsular and subcapsular, anterior lens, with corneal adhesion; Degeneration, lens fiber, lens; rat. The lens is displaced into the anterior chamber and adhered to the cornea by fibroblastic strands of connective tissue. A dome-shape mound of bland fibrous connective tissue resides in the adjacent, anterior subscapular region of the lens. Degenerative features in the lens include globular enlargement, fragmentation, and dissolution of lens fibers and collection of eosinophilic fluid.

FIGURE 20.—Dislocation, posterior, lens; Degeneration, lens fiber, lens; Retinal folds; rat. The lens is posteriorly displaced (note that lens is completely posterior to the ciliary body, which is not included in this image). Several features of lens degeneration are present and the retina has several folds within the outer nuclear layer (arrows).

FIGURE 21.—Mineralization, lens fiber, lens; Proteinaceous fluid, anterior chamber; F344/N rat. Associated with tetrafluroethylene administration. NTP archives.

FIGURE 22.—Rupture, posterior lens capsule; SD rat. Extruded lens fibers at the posterior surface of the lens.

FIGURE 23.—Rupture, posterior lens capsule; Degeneration, lens fiber; SD rat. Note the curled lens capsule (arrow) and features of lens degeneration. Increased protein is present in both the anterior chamber and vitreous (granular eosinophilic matrix).

FIGURE 24.—Microphthalmia; Agenesis, vitreous; rat. Vitreous agenesis is associated with microphthalmia. In this example the retina is detached and resides within the vitreous cavity as a consequence of vitreous agenesis, and the cell layers of the retina are in disarray. Note the lack of lens development and overall malformation.

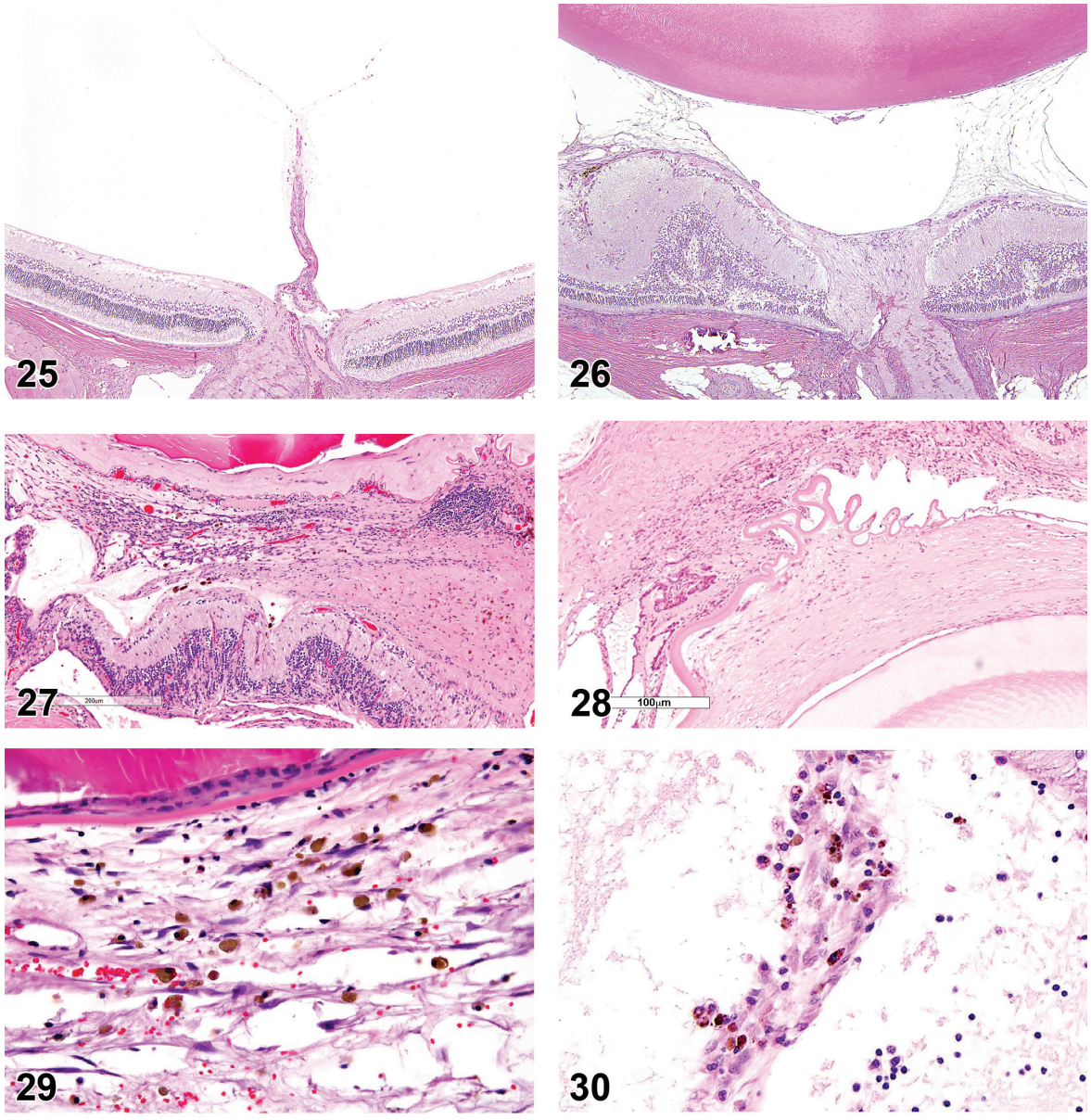

FIGURE 25.—Persistent hyaloid vessel, vitreous, rat. A remnant of fibrovascular tissue extends from the optic nerve head into the body of the vitreous.

FIGURE 26.—Persistent hyperplastic primary vitreous, vitreous; Detachment, retina; Mineralization, sclera; rat. Delicate strands of fibroblastic tissue extend between the posterior lens and the retina. The resultant tension placed on the retina has caused buckling and distortion of the retina with focal detachment. Basophilic spicules of mineralized collagen are present within the sclera.

FIGURE 27.—Fibrosis; Inflammation, mononuclear; vitreous; F344/N rat. The posterior lens capsule is rimmed by a layer of fibrovascular tissue containing inflammatory infiltrates, while a dense band of fibrotic tissue resides between the lens and retina. Note the retinal detachment resulting from tension placed on the retina at areas of attachment. NTP archives.

FIGURE 28.—Fibrosis, vitreous, retina, and lens; F344/N rat. A dense layer of fibrous connective tissue is subjacent to the folded posterior lens capsule. The retina is nearly obliterated by fibrovascular tissue which spans the vitreous and connects to the folded lens capsule. NTP archives.

FIGURE 29.—Hemorrhage; Fibroplasia; Neovascularization; vitreous; F344/N rat. Fibrovascular tissue containing red blood cells and infiltrates of macrophages that contain brown pigment (hemosiderin) is adherent to the lens capsule. NTP archives.

FIGURE 30.—Hemosiderin-laden macrophages; Fibroplasia; Inflammation, mixed cell; vitreous; F344/N rat. NTP archives.

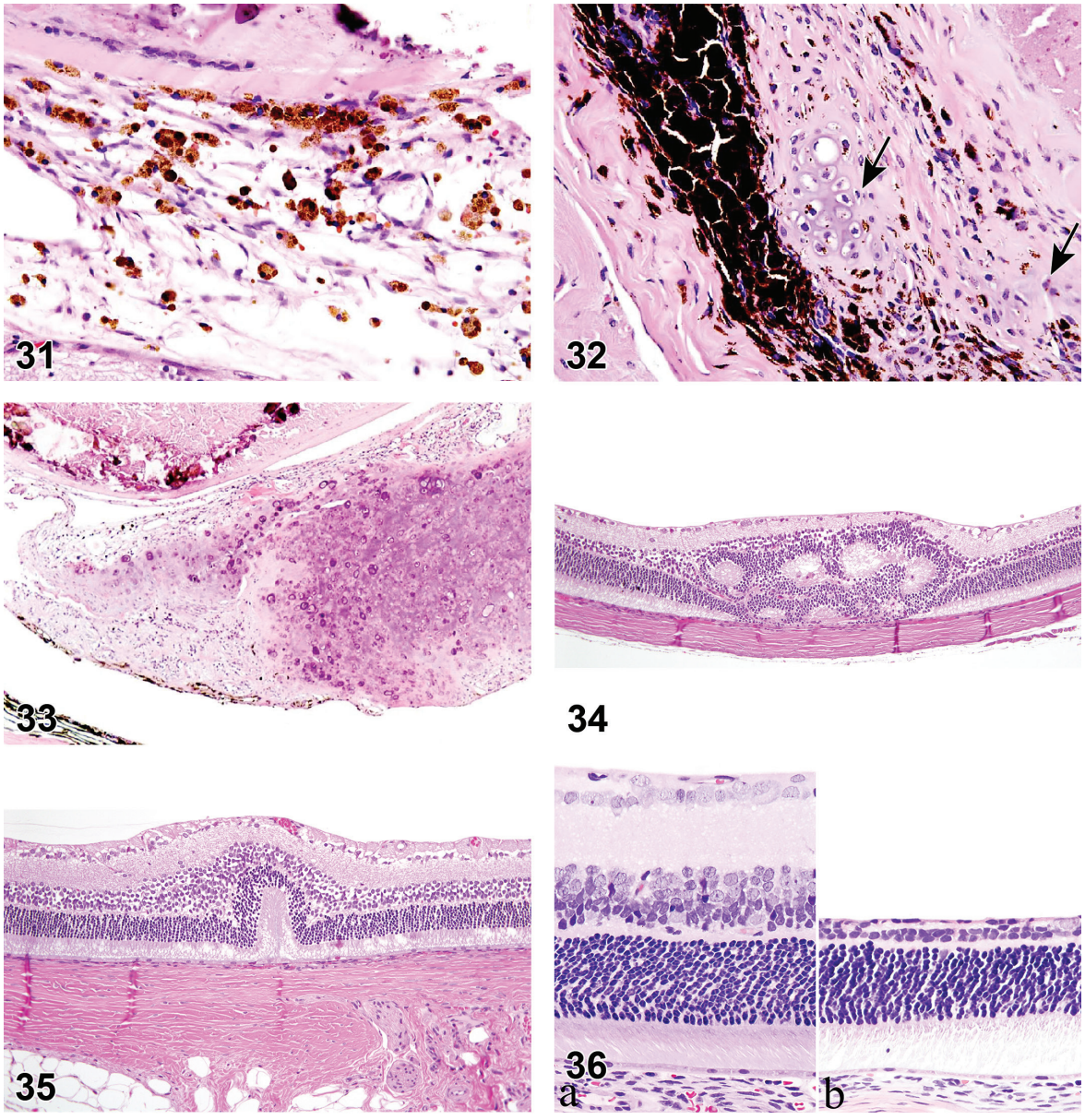

FIGURE 31.—Hemosiderin-laden macrophages; Fibroplasia; Inflammation, mixed cell; vitreous; F344/N rat. Higher magnification; NTP archives

FIGURE 32.—Metaplasia, cartilage; vitreous; B6C3F1 mouse. Fibrotic tissue within the vitreous containing areas of cartilaginous metaplasia (arrows). NTP archives

FIGURE 33.—Metaplasia, cartilage; vitreous; F344/N rat. Concentric mass of cartilaginous and connective tissue within the vitreous. The lens has degenerative changes including a band of mineralization. NTP archives.

FIGURE 34.—Rosettes, retina; rat. Multiple rosettes resulting in disorganization of both the inner and outer nuclear layers of the retina.

FIGURE 35.—Fold, retina; rat.

FIGURE 36.—Atrophy, inner retina; rat. Normal retinal anatomy of control rat (a), compared to retina with atrophy (b). Diffuse atrophy of nerve fiber, ganglion cell, inner plexiform and inner nuclear layers is depicted. Note sparing of outer nuclear layer.

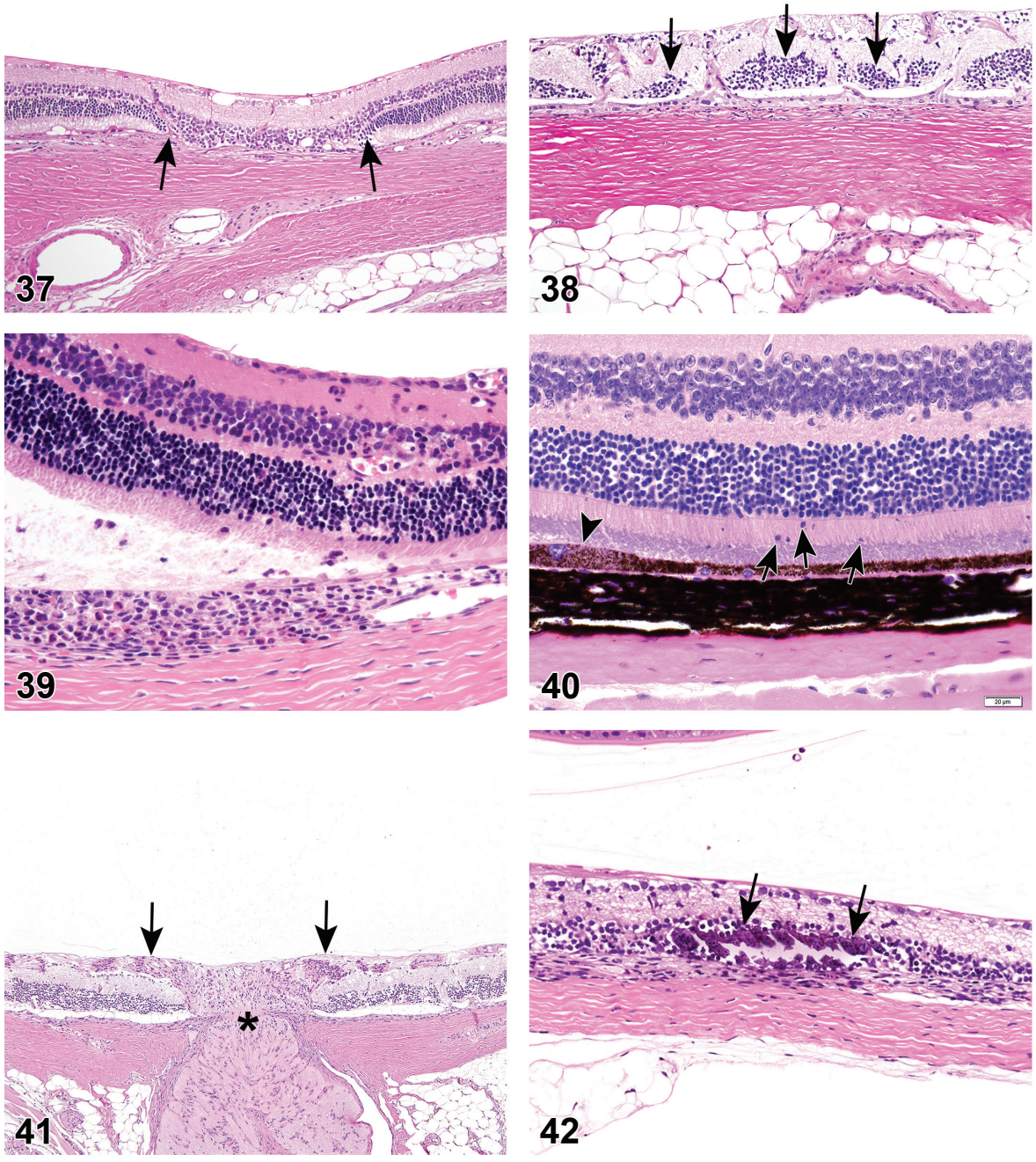

FIGURE 37.—Atrophy, outer retina; rat. Focal area of the outer nuclear and photoreceptor segment layers depicts atrophy, and is associated with loss of adjacent RPE (between arrows). Note sparing of the nerve fiber, ganglion cells and inner nuclear layers at the affected region, and the normal morphology of the retina on either side of the lesion.

FIGURE 38.—Atrophy, global retina; rat. Diffuse retinal atrophy involving all layers, with multifocal remnants of outer nuclear layer neuronal bodies remaining (arrows).

FIGURE 39.—Detachment, retina; Inflammation, mixed cell, choroid and retina; rat. Focally extensive separation between the retinal photoreceptor outer segment layer and the RPE, associated with subretinal fluid and macrophage infiltrate. Also note a lymphoplasmacytic and neutrophilic infiltrate in the inner retina and accumulation within the choroid.

FIGURE 40.—Displacement, photoreceptor nuclei, retina; Hypertrophy, RPE; mouse. Pyknotic photoreceptor nuclei (arrows) located external to the retinal outer limiting membrane. Minimal displacement of the photoreceptor layer is associated with an enlarged RPE cell (arrowhead).

FIGURE 41.—Increased numbers ("gliosis"), glial cell, retina and optic nerve; rat. Multifocal clusters of elongated and hypereosinophilic glial cells expand the nerve fiber layer (arrows) and optic nerve head (arrowhead).

FIGURE 42.—Mineralization; Atrophy, outer nuclear/global; retina; rat. Focal accumulation of deep basophilic mineral (arrow) replacing the inner and outer nuclear layers of the retina, associated with MNU administration. Note outer to global retinal atrophy.

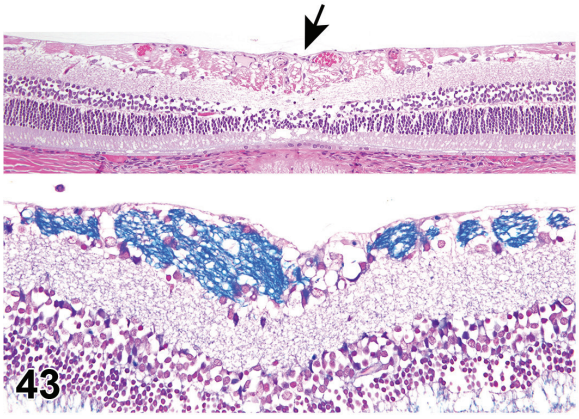

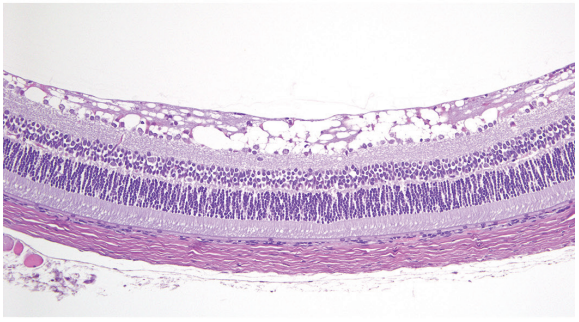

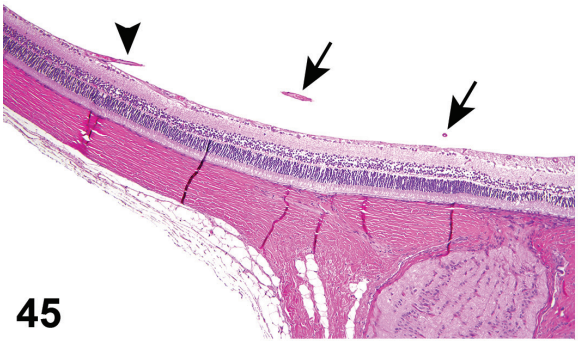

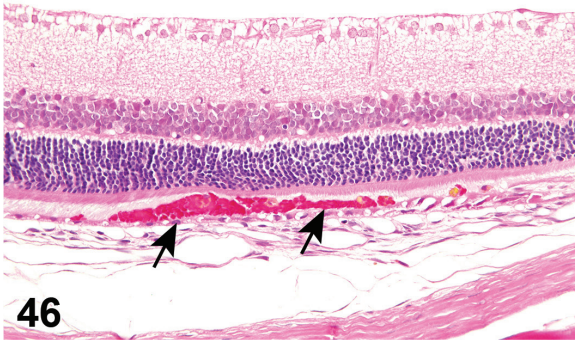

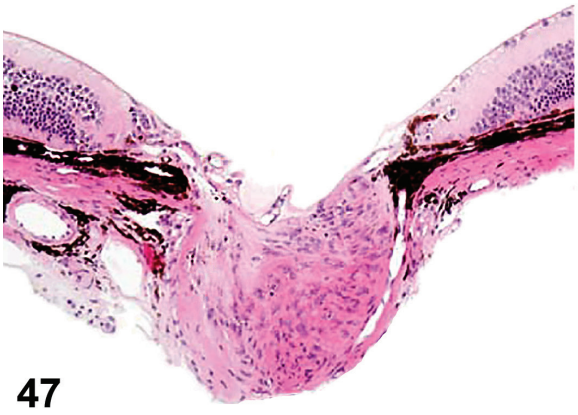

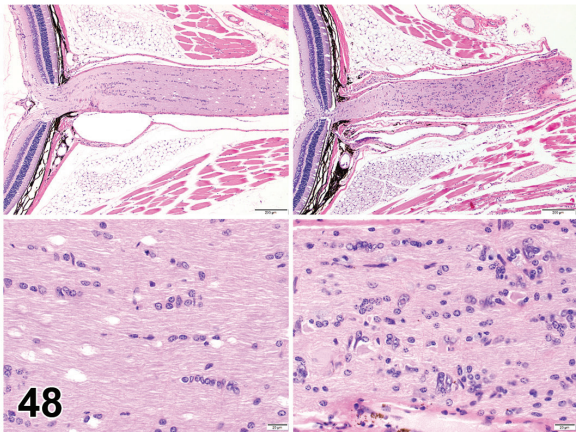

FIGURE 43.—Increased myelin; retina; rat. Clusters of myelinated axons are present in the nerve fiber layer of the central (peri-papillary) retina (arrow) in the top image. A higher magnification of the myelinated fibers stained with luxol fast blue is shown in the bottom image.

FIGURE 44.—Vacuolation, extracellular, retina; rat. The nerve fiber layer is expanded by numerous vacuoles appearing as clear spaces.

FIGURE 45.—Pre-retinal arteriolar loop; retina; rat. Note an arteriole emerging from the central retinal artery (arrow), coursing through the posterior vitreous, and reconnecting to the inner retina (arrowhead).

FIGURE 46.—Hemorrhage, subretina; rat. Accumulation of red blood cells in the subretinal space (arrows).

FIGURE 47.—Atrophy, optic nerve; mouse. Loss of axons associated with glial cell proliferation ("gliosis") and posterior bowing of the optic nerve head and lamina cribosa (cupping of the optic nerve).

FIGURE 48.—Increased numbers ("gliosis"), glial cell; optic nerve; mouse. The top and bottom (higher magnification) images on the right depict an increase in numbers of glial cell nuclei dispersed throughout the optic nerve neuropil. Compare to normal optic nerve shown in the top and bottom images to the left.

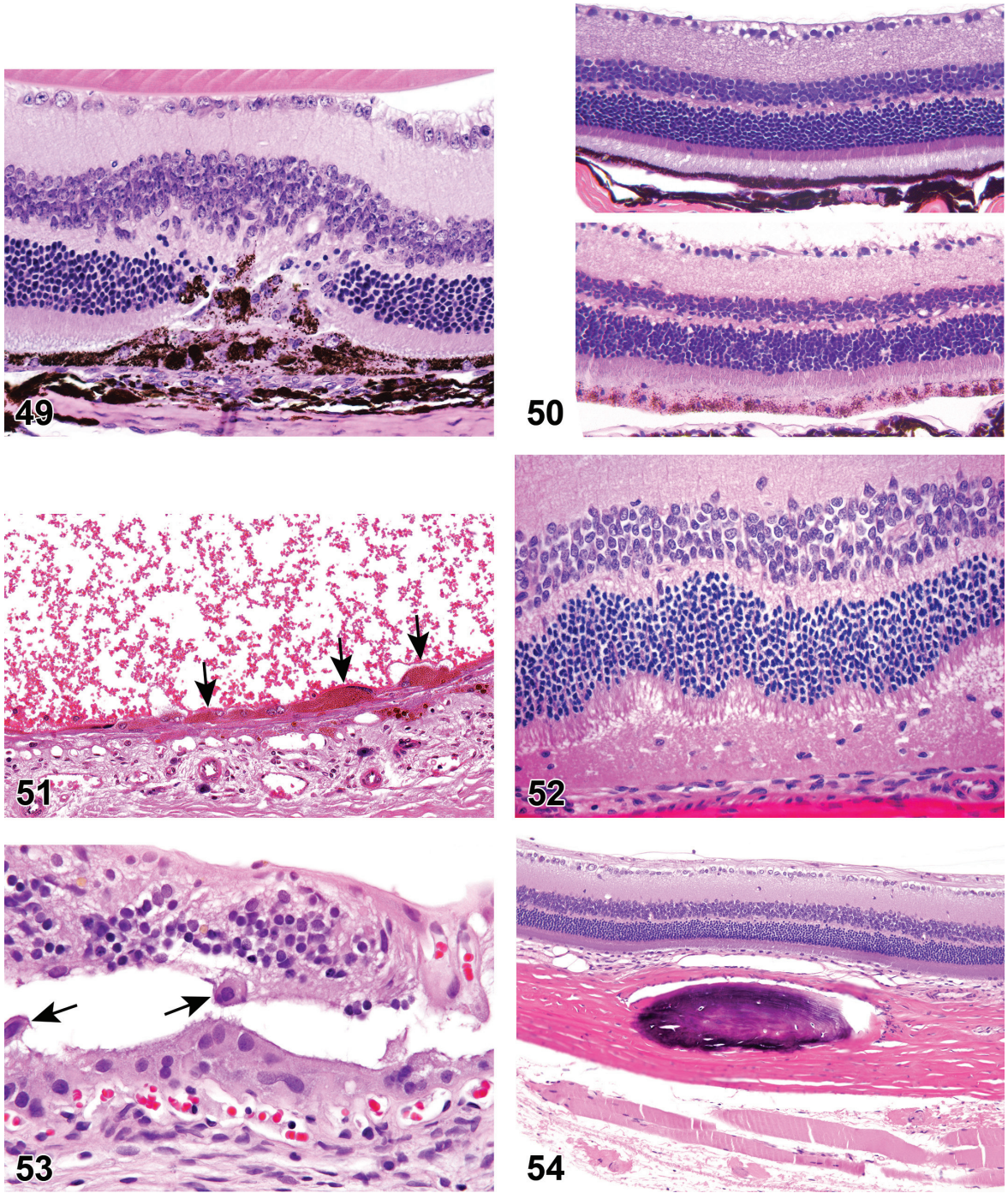

FIGURE 49.—Fibroplasia, sub-retinal; Hypertrophy and Hyperplasia, RPE; C57BL/6 mouse. The RPE layer is focally replaced by a linear array of fibrovascular tissue that extends into the subretinal space and adjacent retina. There is enlargement, proliferation and migration of RPE with pigment dispersion within the lesion. Also note the presence of glial cells within the retina and atrophy of the outer nuclear layer. [used with permission: Int. J. Mol. Sci. 2014, 15(6), 9372-9385; doi:10.3390/ijms15069372]

FIGURE 50.—Hypertrophy; Pigmentation, decreased; RPE; mouse. Enlarged RPE are depicted in the bottom image. Note the lighter cytoplasmic pigmentation compared to the normal RPE shown in the top image.

FIGURE 51.—Inclusions (hemosiderin), RPE; Hypertrophy, RPE; Hemorrhage, sub-retinal; rat. RPE are distended by the cytoplasmic accumulation of hemosiderin (arrows). Note the presence of RBCs in the sub-retinal space.

FIGURE 52.—Necrosis, RPE; rat. Necrotic debris and pyknotic nuclei are all that remain of the RPE following necrosis associated with administration of sodium iodate. Note retinal detachment, and cell debris in the subretinal space.

FIGURE 53.—Polarity loss, RPE; detachment and atrophy, retina; rat. Disorganized layers of enlarged, rounded RPE and a few detached cells free-floating (arrows) in the sub-retinal space. Note the detachment and atrophy of the retina. Associated with C1 pigment red administration. NTP archives.

FIGURE 54.—Metaplasia, osseous, sclera; F344/N rat. Ovoid basophilic mass containing lacunae found in the sclera. Associated with alpha-methylstyrene administration. NTP archives.

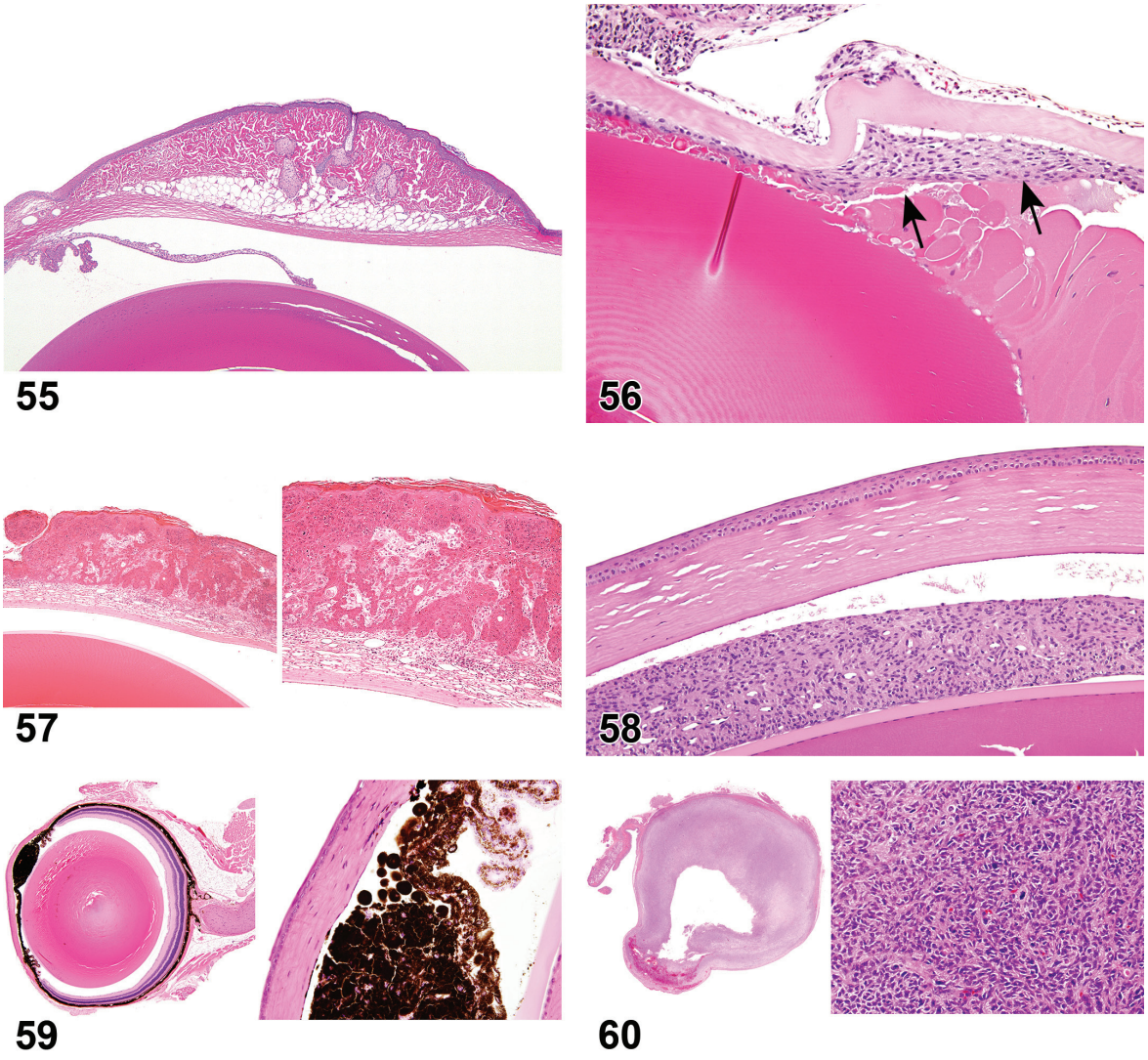

FIGURE 55.—Dermoid, ocular, cornea; rat. Note the mound of dermis containing sebaceous glands and adipose located within the cornea.

FIGURE 56.—Hyperplasia, lens epithelium; Degeneration; lens; F344/N rat. Subcapsular proliferation of epithelial cells (arrow) adjacent to region of lens degeneration (swollen fibers, eosinophilic globules, granular debris).

FIGURE 57.—Carcinoma, squamous cell, cornea, rat. Marked expansion of the cornea epithelium by islands of neoplastic epithelial cells. Note the neovascularization of the adjacent cornea stroma. (Image courtesy of Dr. Frederic Schorsch)

FIGURE 58.—Leiomyoma, uvea, iris; rat. Benign expansion of the iris stroma with bundles of spindle cells of smooth muscle origin. NTP archives

FIGURE 59.—Melanoma, uvea, iris; B6C3F1 Mouse. Malignant proliferation of melanocytes replacing the iris. NTP archives.

FIGURE 60.—Melanoma, uvea; rat. Ocular tissues have been obliterated by an amelanotic melanoma. Note the densely cellular mass depicted in the high magnification image to the right, composed of nests of spindle and epitheloid cells lacking pigment granules.

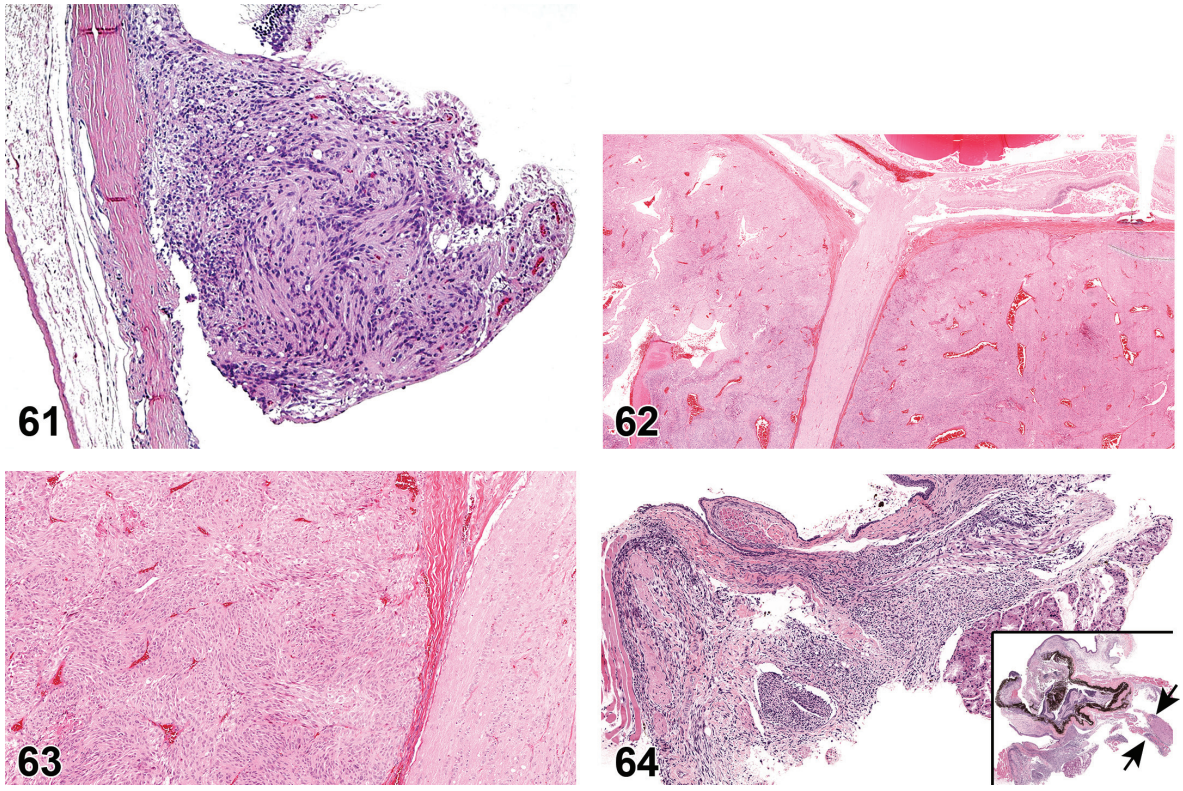

FIGURE 61.—Schwannoma, uvea, iris; rat. Malignant bundles of Schwann cells expand and replace the iris.
FIGURE 62.—Schwannoma, optic nerve; F344/N rat. Malignant bundles of Schwann cells surround the optic nerve. NTP archives
FIGURE 63.—Schwannoma, optic nerve; F344/N rat. Higher magnification depicting interlacing bundles of Schwann cells. NTP archives
FIGURE 64.—Meningioma, optic nerve, extra-ocular orbital space; C57BL/6 mouse. Spindloid cells form interlacing bundles situated between the Harderian gland and the sclera (high magnification). Note the invasiveness of this tumor on low magnification (inset; overview of the eye). Tumor cells can be seen infiltrating the sclera, cornea, uvea, and retina. Tumor cells also surround the optic nerve and adjacent muscles (arrows). Associated with bromodichloromethane administration; NTP archives.

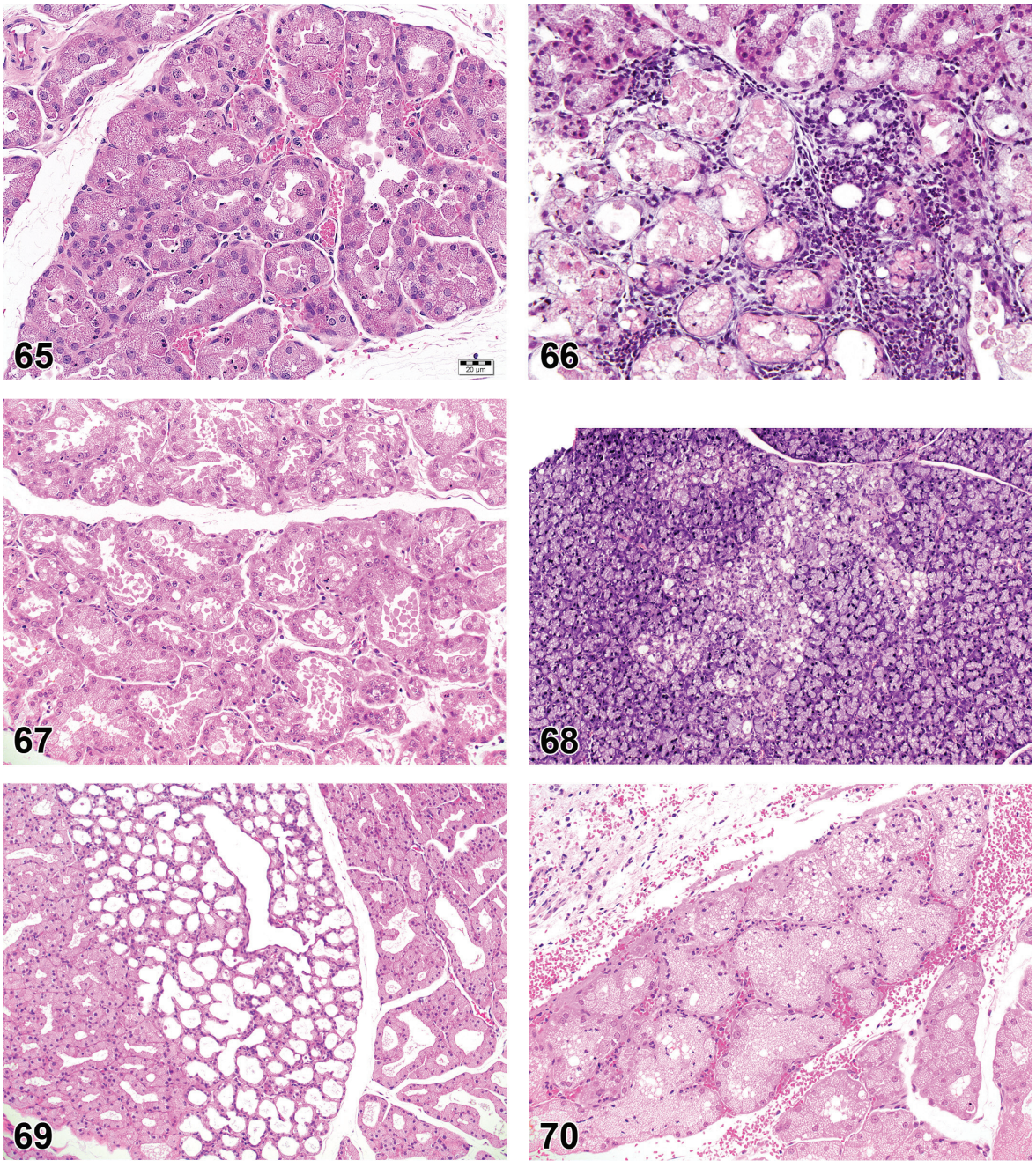

FIGURE 65.—Necrosis, single cell, Harderian gland; rat. Note the pyknotic nuclei, and exfoliation of epithelial cells.
FIGURE 66.—Necrosis; Inflammation, granulocytic; Harderian gland; rat. Loss of cell morphology and acinar debris. An inflammatory infiltrate surrounds the necrotic acini.
FIGURE 67.—Degeneration, epithelial cell, Harderian gland; rat. Note the exfoliation of epithelial cells.
FIGURE 68.—Degeneration, epithelial cell, lacrimal gland; rat. NIEHS
FIGURE 69.—Atrophy, Harderian gland; rat. Note the acini lined by flattened epithelial cells.
FIGURE 70.—Hemorrhage, Harderian gland; rat. Traumatic injury of acini associated with blood sampling immediately prior to sacrifice.

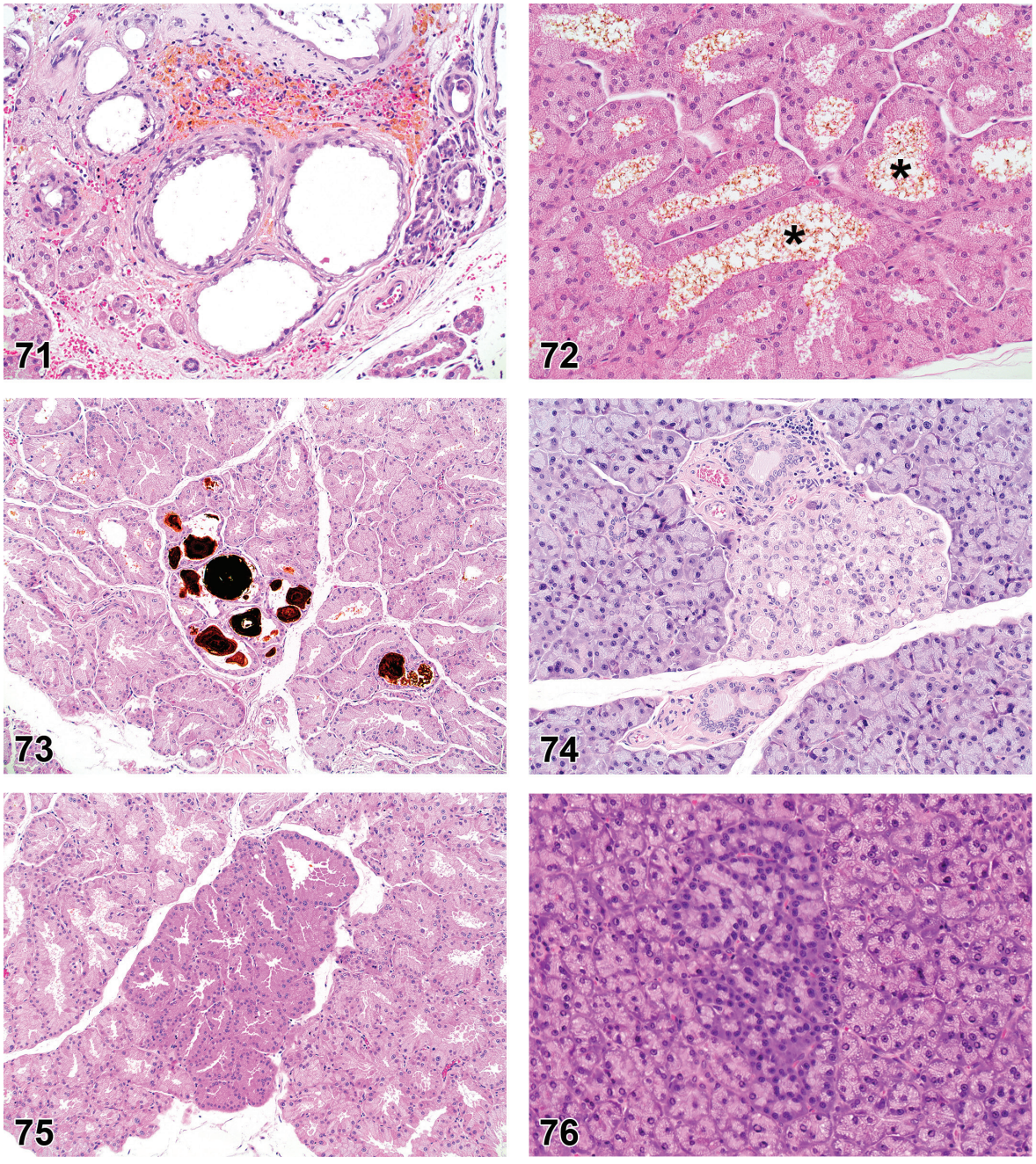

FIGURE 71.—Hemorrhage; Fibrosis, Harderian gland; rat. Hemorrhage with hemosiderin deposits, fibrosis and atrophy of acini after repeated blood sampling.

FIGURE 72.—Porphyrin, increased, Harderian gland; rat. Fibrillar appearance of prophyrin located within the acinar lumina (*).

FIGURE 73.—Porphyrin, increased, Harderian gland; rat. Prophyrin is present as solid accretions within the acinar lumina.

FIGURE 74.—Alteration, Harderian gland in the lacrimal gland; rat. Focal region of paler staining epithelial cells representing Harderian gland acini.

FIGURE 75.—Hyperplasia, acinar, Harderian gland; rat. Focal region of densely populated acini composed of epithelial cells tinctorially different than that of surrounding acini.

FIGURE 76.—Hyperplasia, acinar, lacrimal gland; rat. Focal region of densely populated acini composed of darker staining epithelial cells than that of surrounding acini. RITA

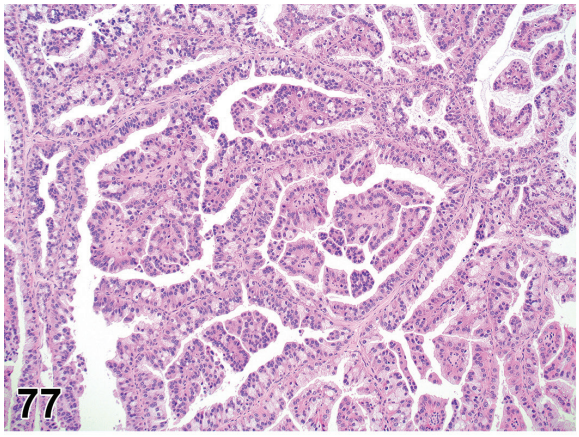

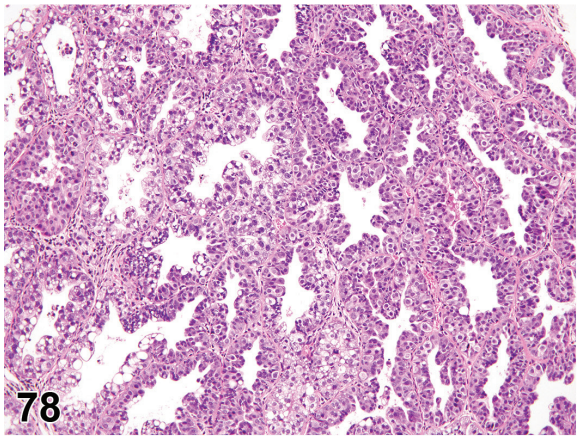

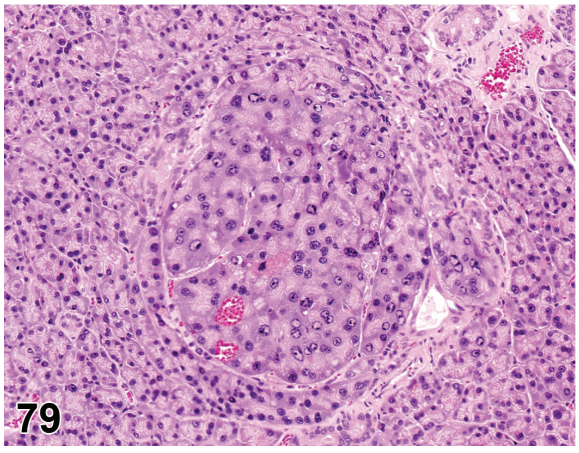

FIGURE 77.—Adenoma, Harderian gland; mouse. Benign, papillary fronds of epithelial cells.

FIGURE 78.—Adenocarcinoma, Harderian gland; mouse. Malignant epithelial cells align enlarged acinar structures supported by a network of thin fibrovascular tissue. NIEHS

FIGURE 79.—Adenoma, lacrimal gland; rat. Concentric aggregate of enlarged epithelial cells with displacement and compression of adjacent, normal acinar tissue. RITA

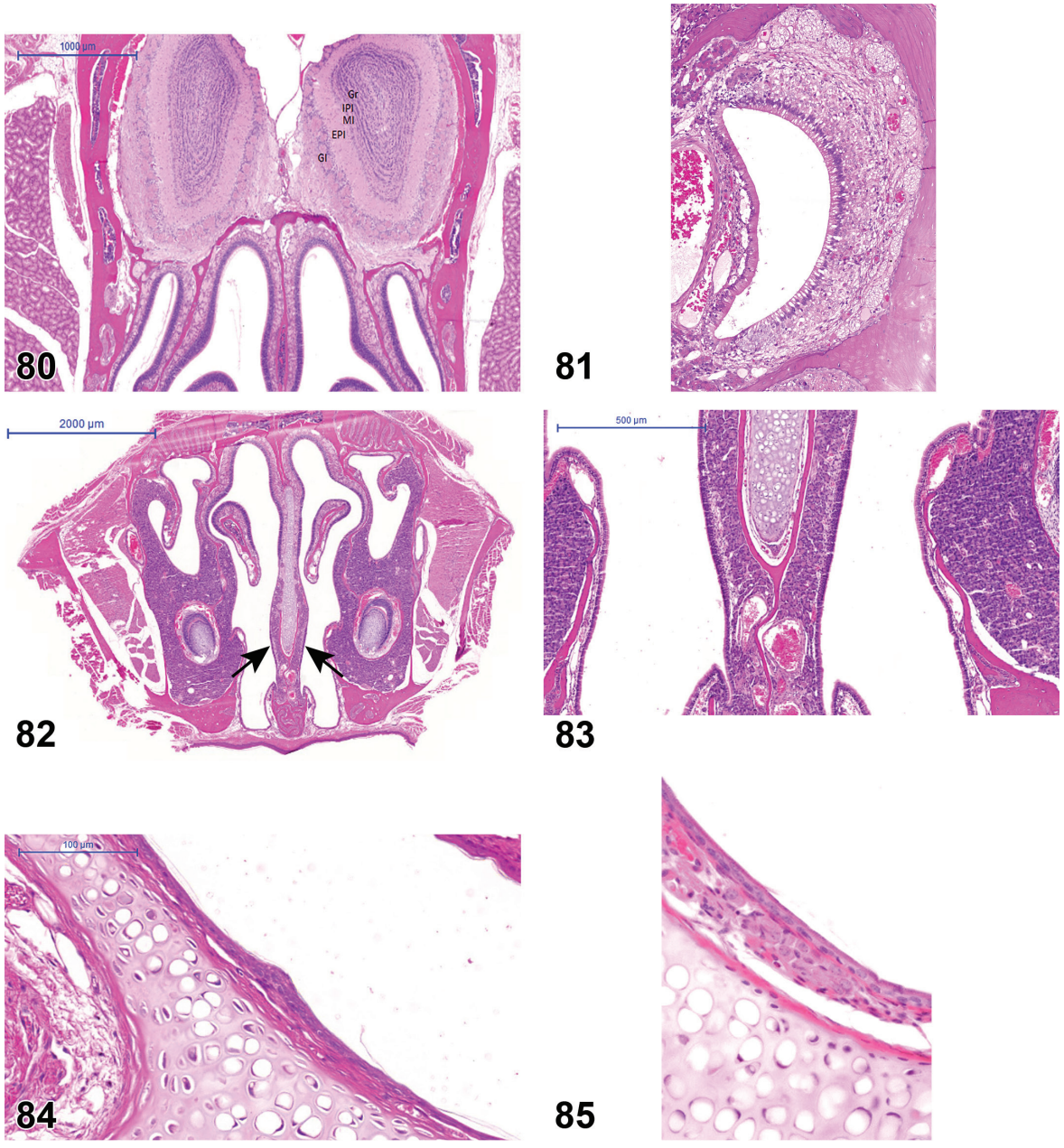

FIGURE 80.—Normal anatomy; nasal passage and olfactory bulb; rat. Cross section through the posterior region of the nasal passage lined by olfactory epithelium (main olfactory epithelium; MOE) and dorsally, the main olfactory bulb with its micro-anatomical features: GI = Glomerular layer; EPI = external plexiform layer; MI = mitral cell layer; IPI = internal plexiform layer; GR = granular layer. The accessory olfactory bulb is not included at this level.

FIGURE 81.—Normal anatomy, Vomeronasal organ; rat.

FIGURE 82.—Normal anatomy, Septal Organ of Masera (SOM); rat. Arrows indicate the position of the SOM on either side of the septum.

FIGURE 83.—Normal anatomy, Septal Organ of Masera (SOM); rat. Higher magnification of Figure 82, depicting the normal anatomy of the SOM as an island of olfactory cells amidst respiratory epithelium.

FIGURE 84.—Normal anatomy, Grueneberg ganglion; rat.

FIGURE 85.—Normal anatomy, Grueneberg ganglion; rat. Higher magnification of Figure 84, depicting the normal anatomy of the Grueneberg ganglion.

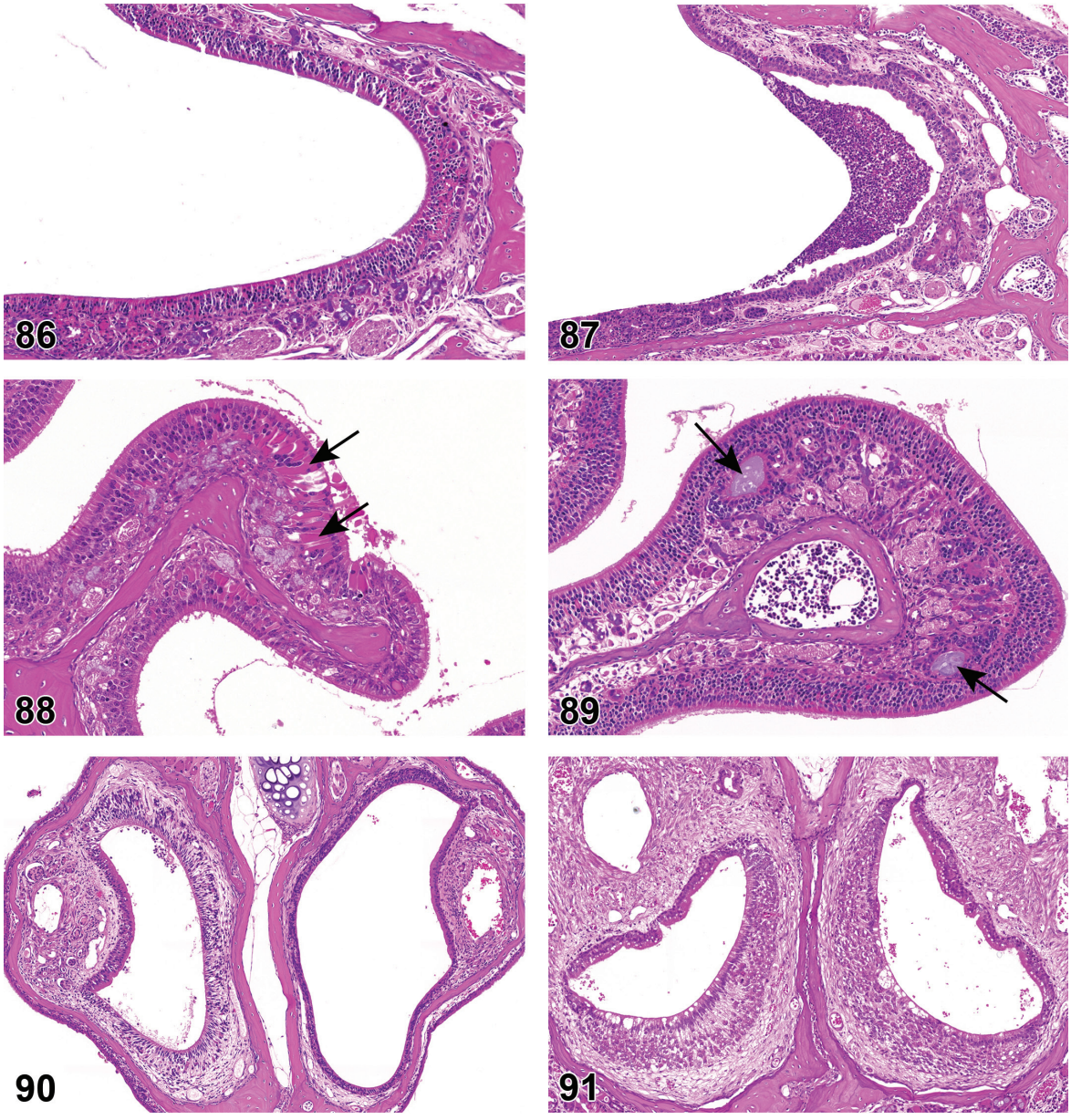

Figure 86.—Degeneration, main olfactory epithelium (MOE); mouse. Degeneration and disorganization of olfactory epithelium.

Figure 87.—Inflammation, granulocytic (neutrophils), main olfactory epithelium (MOE); mouse. Inflammation of the olfactory epithelium in the nose. In addition to an infiltration of neutrophils, there is disorganization of the epithelium.

Figure 88.—Eosinophilic globules, main olfactory epithelium (MOE); mouse. Eosinophilic globules are present in the epithelium (arrows) of the MOE.

Figure 89.—Corpora amylacea; Hyperplasia; main olfactory epithelium (MOE); mouse. Corpora amylacea (basophilic aggregates, arrows) and hyperplasia of Bowman's gland within the subepithelial region of the olfactory epithelium.

Figure 90.—Atrophy, Vomeronasal Organ (VNO), mouse. Normal anatomy is depicted in the left VNO; compare to the VNO located on the right side, which depicts atrophy.

Figure 91.—Degeneration, Vomeronasal Organ (VNO); mouse. Bilateral epithelial degeneration of the VNO, with desquamation and an inflammatory cell infiltrate.

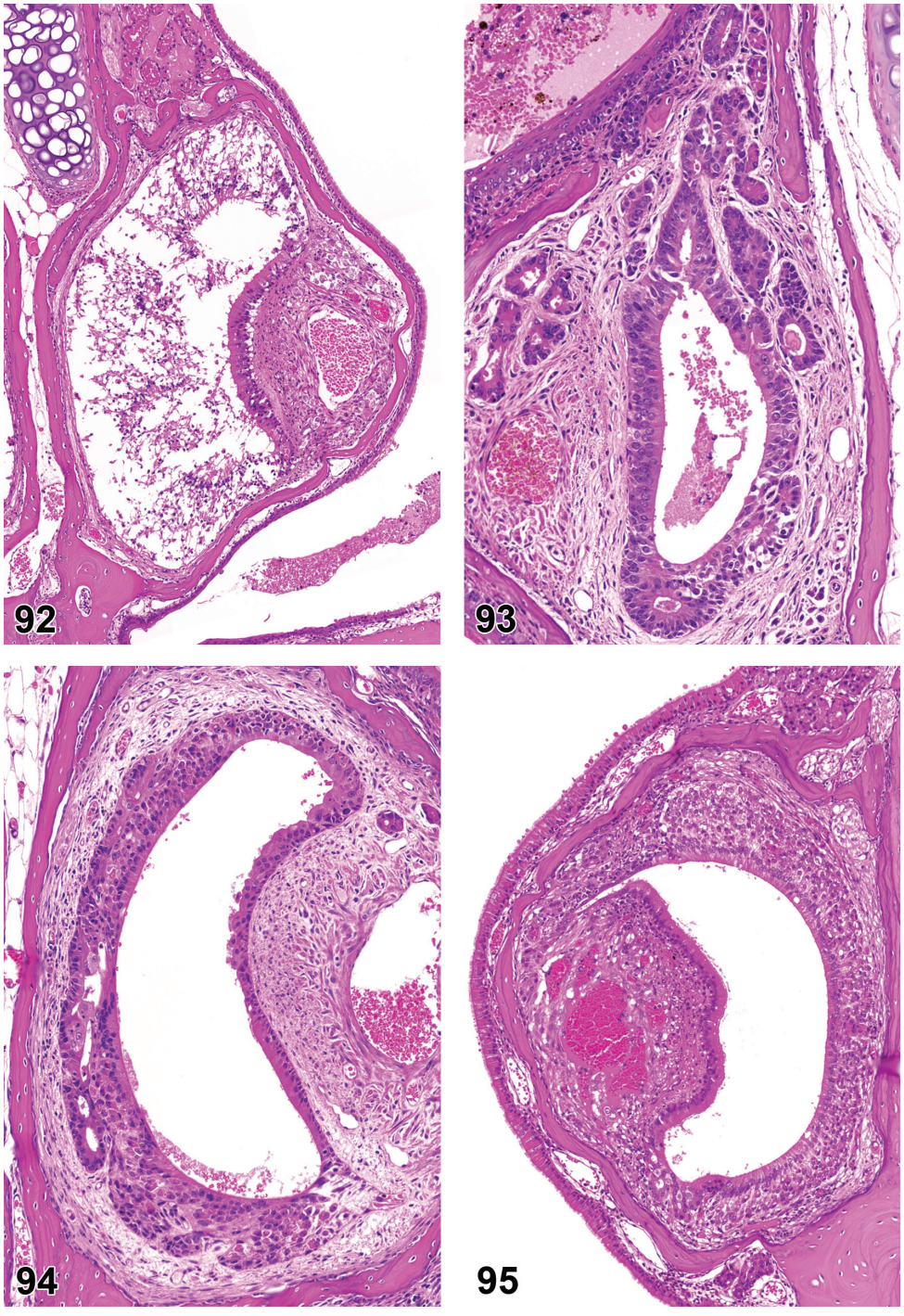

FIGURE 92.—Necrosis, epithelium, Vomeronasal Organ (VNO); mouse. Extensive necrosis of the VNO epithelium, with cellular debris in lumen.
FIGURE 93.—Regeneration, epithelium, Vomeronasal Organ (VNO); mouse. Proliferation/re-population of epithelium lining the VNO following injury. Note residual debris and RBC in lumen.
FIGURE 94.—Regeneration, neuroepithelium, Vomeronasal Organ (VNO); mouse. Regeneration and disorganization of the VNO neuroepithelium.
FIGURE 95.—Infiltrate, inflammatory cell (mixed cell), Vomeronasal Organ (VNO); mouse.

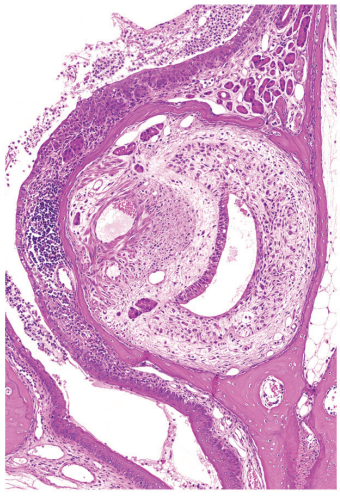

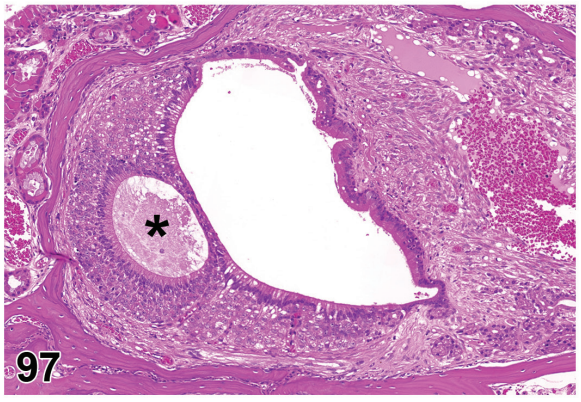

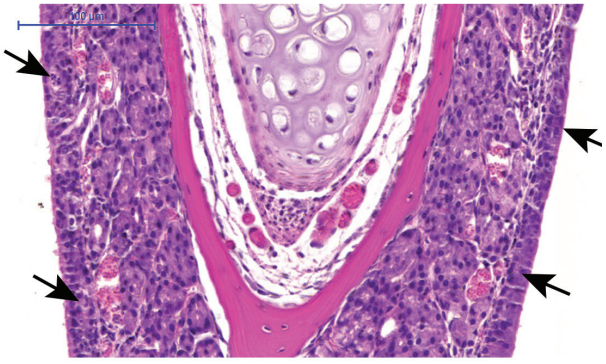

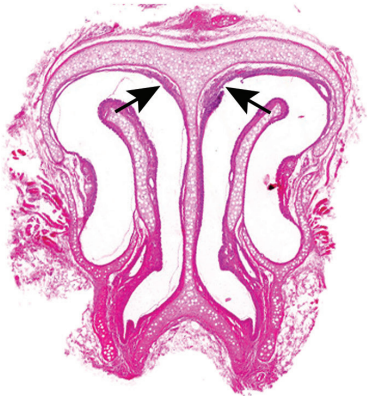

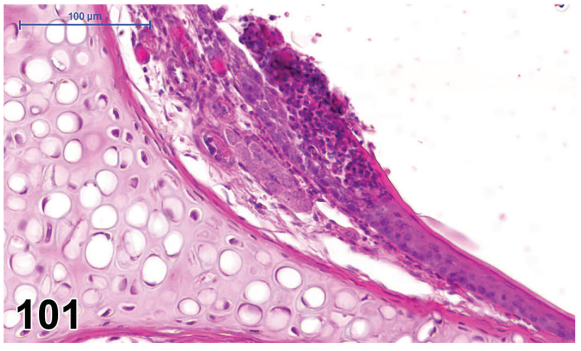

FIGURE 96.—Edema; Inflammation, mixed cell; Degeneration, epithelium; Vomeronasal Organ (VNO); mouse. Note the edema expanding the tissues of the VNO, which contains an inflammatory cell infiltrate.

FIGURE 97.—Dilation/ Diverticulum, Vomeronasal organ (VNO); mouse. A small lumen encircled by epithelium (*) is present adjacent to the primary lumen of the VNO.

FIGURE 98.—Degeneration, epithelium, Septal organ of Masera (SOM); mouse. Degeneration of olfactory epithelium (affected olfactory epithelium indicated by brackets; adjacent respiratory epithelium is not affected)

FIGURE 99.—Degeneration, epithelium, Septal organ of Masera (SOM); mouse. Higher magnification of Figure 98, depicting degeneration of olfactory epithelium and loss of sensory cells (arrows). Compare to Figure 83, with normal anatomy.

FIGURE 100.—Infiltrate, inflammatory cell, Grueneberg ganglion (GG). Glutaraldehyde effect. Location of ganglion indicated by arrows.

FIGURE 101.—Infiltrate, inflammatory cell, Grueneberg ganglion (GG).Higher magnification of figure 100. Primarily neutrophilic infiltration, with thickening of epithelium.

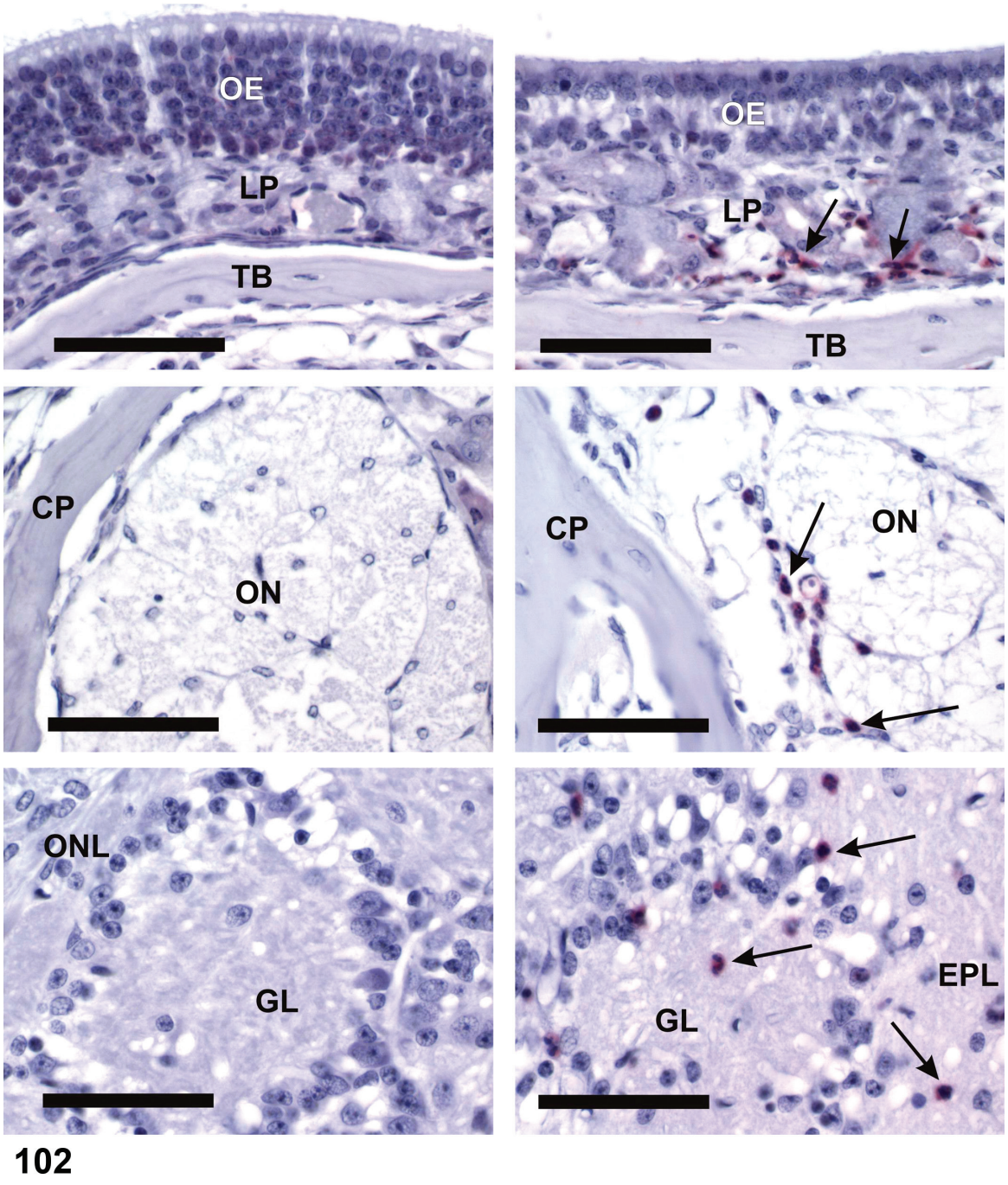

FIGURE 102.—Infiltrate, Inflammatory cell, neutrophilic, olfactory bulb (OB); mouse. Immunohistochemical detection of neutrophils (red stained cells indicated by arrows). Images on left from mouse treated with saline; images on right from an animal exposed to a mycotoxin (satratoxin G). Top images = olfactory epithelium (OE); middle images, olfactory nerve bundles (ON) passing through cribiform plate (CP) from nose to OB; bottom images, olfactory nerve layer (ONL), glomerular layer (GL), and external plexiform layer (EPL) of the OB. LP = lamina propria; TB = turbinate bone. [Image courtesy of Dr. Jack Harkema; in EnvironmentalHealth Perspectives 114:1099-1107 (2006), doi: 10.1289/ehp.8854]

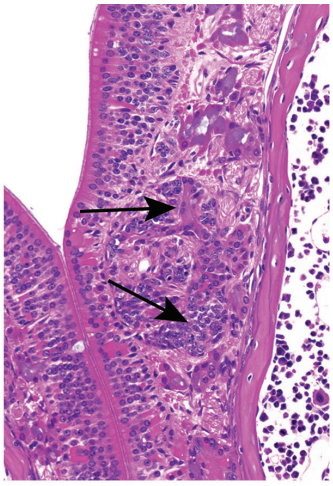

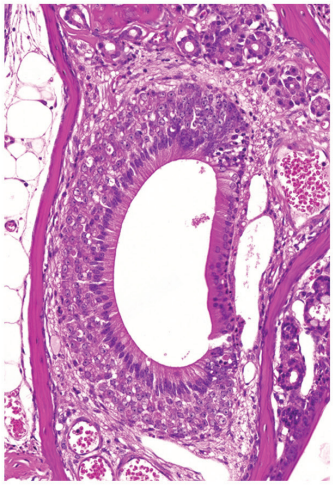

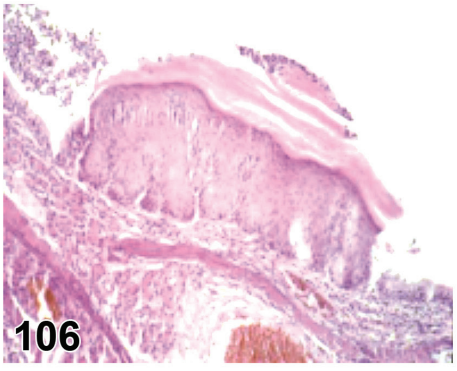

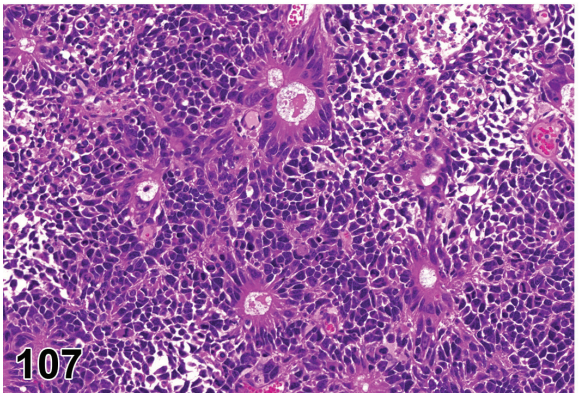

FIGURE 103.—Hyperplasia, Main olfactory epithelium (MOE); mouse. Hyperplasia of Bowman's glands in the subepithelial region of the olfactory epithelium (arrows).

FIGURE 104.—Metaplasia, respiratory, Main olfactory epithelium (MOE); mouse. Respiratory metaplasia of the olfactory epithelium with downgrowth (arrow) to Bowman's glands.

FIGURE 105.—Hyperplasia, Vomeronasal organ (VNO); mouse. Hyperplasia of the respiratory epithelium of the VNO.

FIGURE 106.—Metaplasia, Squamous cell, Vomeronasal organ (VNO); mouse. Note that the respiratory epithelium has been focally replaced by a region of hyperplastic squamous epithelium. [Image courtesy of Prof. Dr. V.J.Feron]

FIGURE 107.—Carcinoma, neuroepithelial, Main olfactory epithelium (MOE); mouse. Neuroepithelial carcinoma with true rosettes and pseudorosettes.

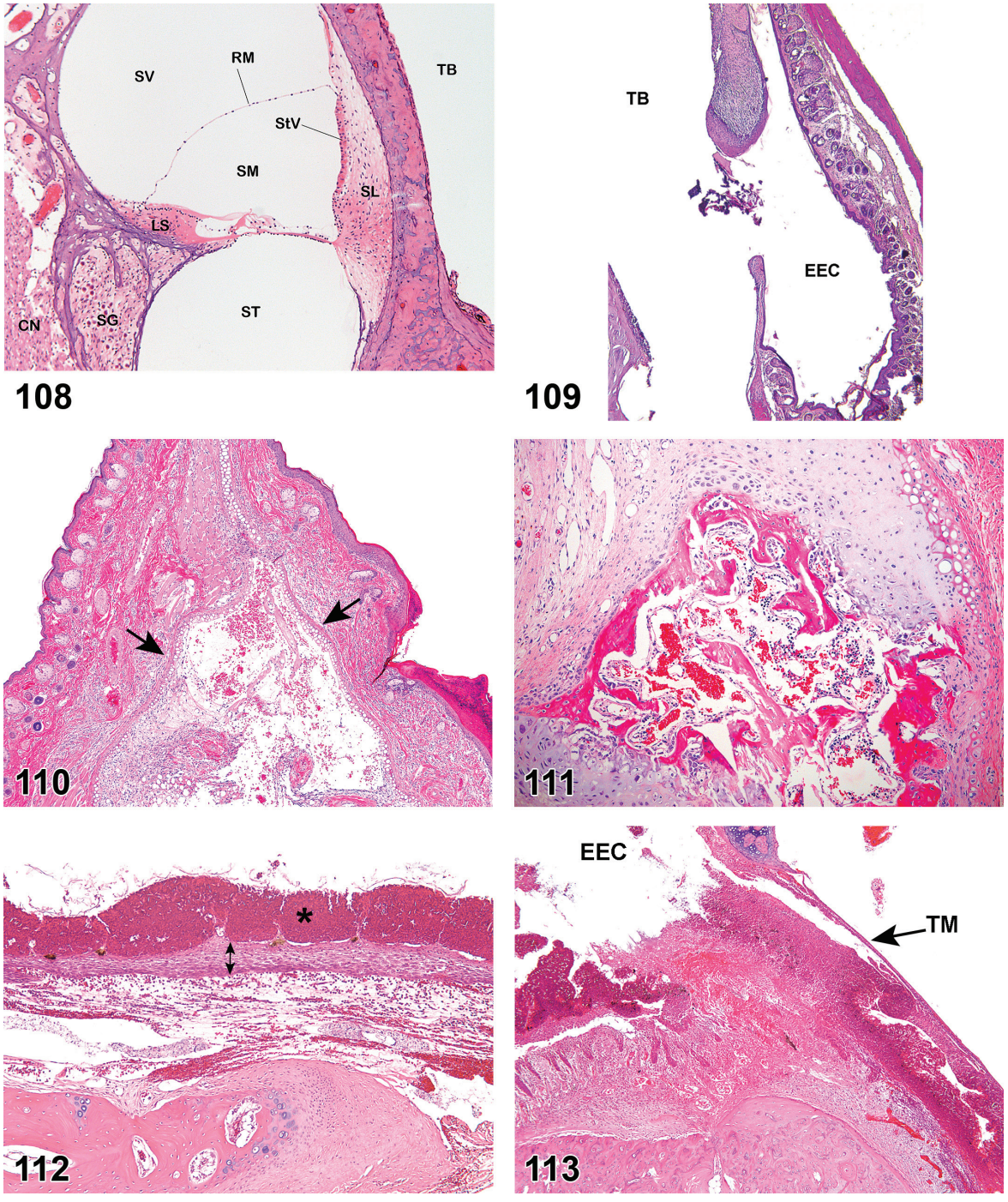

FIGURE 108.—Normal anatomy of the Otic system. Normal histology of one turn of a midmodiolar section of the chinchilla cochlea. SV = Scala vestibuli; ST = Scala tympani; SM = Scala media; SL = Spiral ligament; LS = Limbus spiralis; StV = Stria vascularis; RM = Reissner's membrane; SG = Spiral ganglion; CN = Cochlear nerve; TB = Tympanic bulla lumen. The scala vestibuli and scala tympani contain perilymph and are continuous with each other at the apex of the cochlea. The scala media contains endolymph. The tympanic bulla space is normally air-filled. The hair cells (see Figure 127 for higher magnification) are located in the center of the field to the right of the limbus spiralis.

FIGURE 109.—Perforation, tympanic membrane, external ear; rat. The tympanic membrane is ruptured, and there is thickening of the stroma and growth of lining epithelium from the external surface onto the internal surface in a rat that received a trans-tympanic injection. The opening has keratinized cells and debris. EEC = External ear canal; TB = Tympanic bulla lumen.

FIGURE 110.—Inflammation, auricular cartilage, external ear; rat. The pinna is expanded by inflammation typical of "auricular chondritis". Note that the cartilage of the pinna has split (arrows) and contains fibrin, edema, and inflammatory cells.

FIGURE 111.—Inflammation, auricular cartilage, external ear; rat. Pinna with inflammation of the cartilage. Note focal area of osseous metaplasia within the cartilage.

FIGURE 112.—Inflammation, external ear canal; rabbit. The superficial epidermis (asterisk) is expanded by numerous heterophils forming pustules. At this low magnification, the heterophils appear as hemorrhage. The deeper layers of the epidermis (double arrow) are expanded by intercellular edema. The dermis is expanded by edema and heterophilic infiltrates. The bone below the dermis at the left of the image is the bony collar of the external ear canal as it approaches the tympanic membrane.

FIGURE 113.—Inflammation, external ear canal; rabbit. There is necrosis and loss of the epidermis with extensive heterophilic infiltrates and hemorrhage of the dermis. EEC = External ear canal; TM = Tympanic membrane.

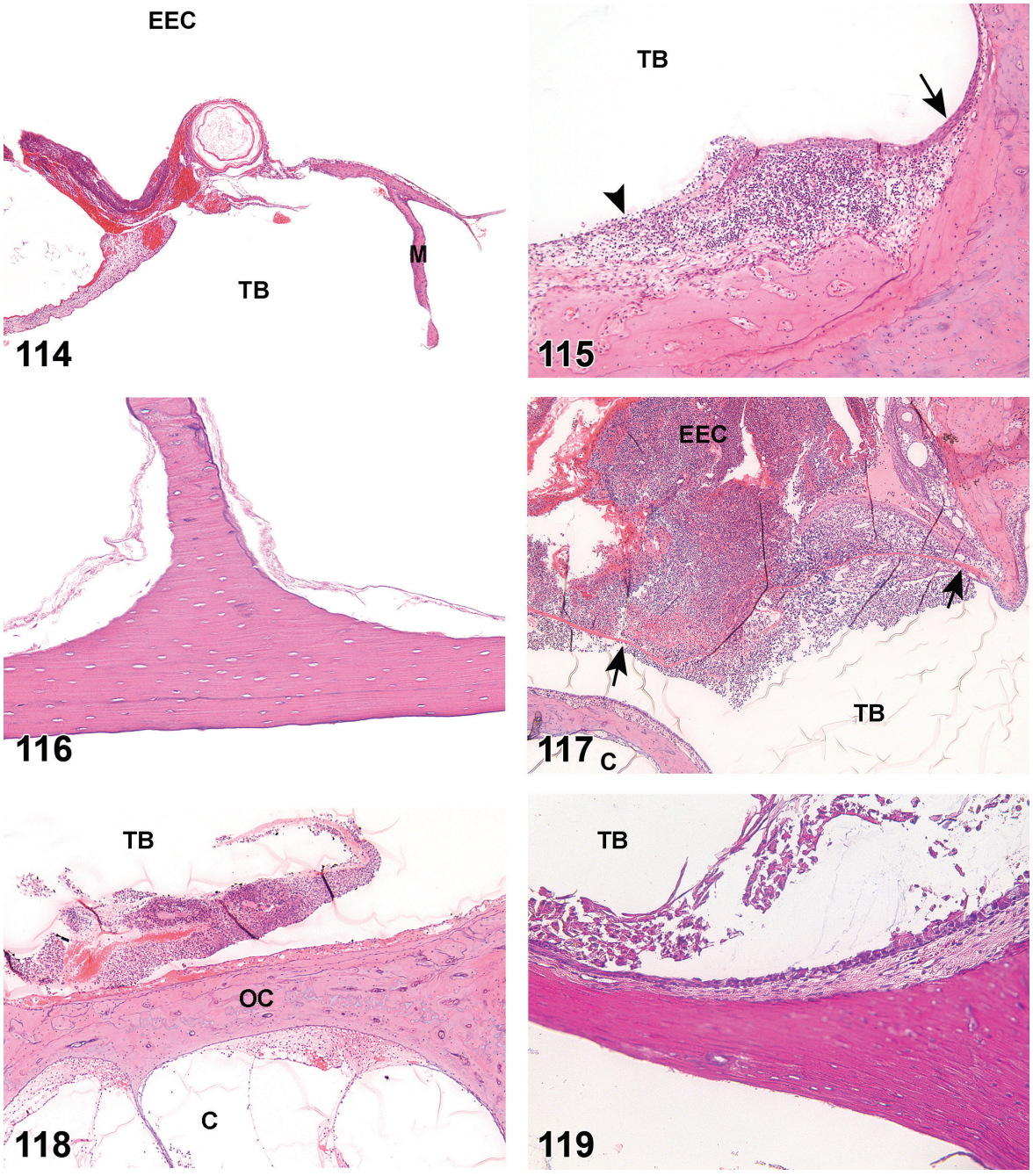

FIGURE 114.—Cyst, tympanic membrane, external ear; rabbit. Squamous cyst in the tympanic membrane. This was an incidental finding. EEC = External ear canal; TB = Tympanic bulla lumen; M = Malleus. Blood observed in the tympanic membrane is normal congestion and pooling that can occur at necropsy and during histological processing.

FIGURE 115.—Ulcer (double arrow); Metaplasia, squamous; middle ear; guinea pig. The lining epithelium of the tympanic bulla is normally a simple squamous or simple cuboidal epithelium, but can be columnar with goblet cells in ventral areas. The epithelium in this animal has undergone squamous metaplasia (nonkeratinizing). The mucosa is expanded by inflammatory cell infiltrates.

FIGURE 116.—Necrosis, bone, middle ear; chinchilla. Necrosis of the bone of the tympanic bulla in a chinchilla treated with a strong irritant. Note the absence of osteocyte nuclei within lacunae and the absence of cellular detail in the mucosal lining (upper left and right chambers).

FIGURE 117.—Necrosis, tympanic membrane; middle ear; guinea pig. Coagulative necrosis of the tympanic membrane in a guinea pig. The tympanic membrane (arrows) is homogeneously eosinophilic and surrounded by intense inflammatory infiltrates on both the external and internal sides. TB = Tympanic bulla lumen; EEC = External ear canal; C = Cochlea. Wrinkles in section are artifact of the GMA sectioning and placement on water bath.

FIGURE 118.—Inflammation; middle ear; guinea pig. The lumen of the tympanic bulla (TB) has inflammatory cell aggregates and admixed hemorrhage. The otic capsule of the cochlea has a thickened, congested mucosa. OC = otic capsule; C = Cochlea; TB = Tympanic bulla lumen.

FIGURE 119.—Metaplasia, squamous; middle ear; rat. Squamous metaplasia of the lining epithelium of the internal surface of the tympanic bulla in a rat ear with sloughing of epithelial cells into the lumen. Compare with Figure 115. TB = Tympanic bulla lumen.

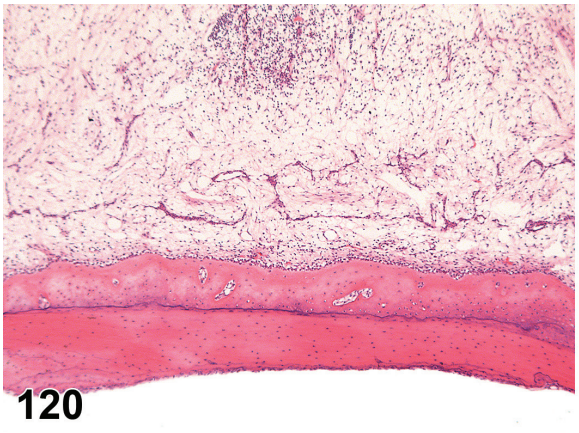

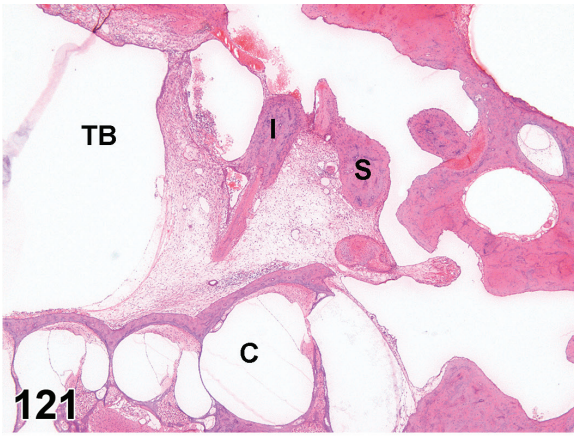

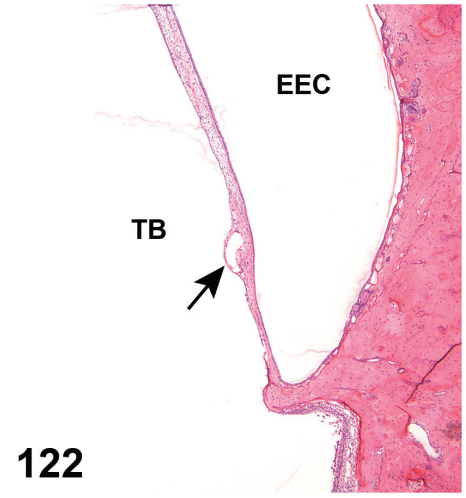

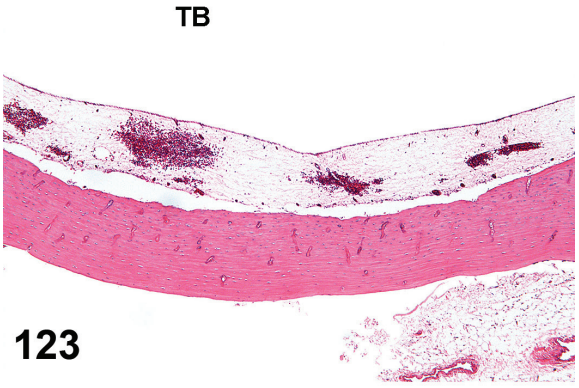

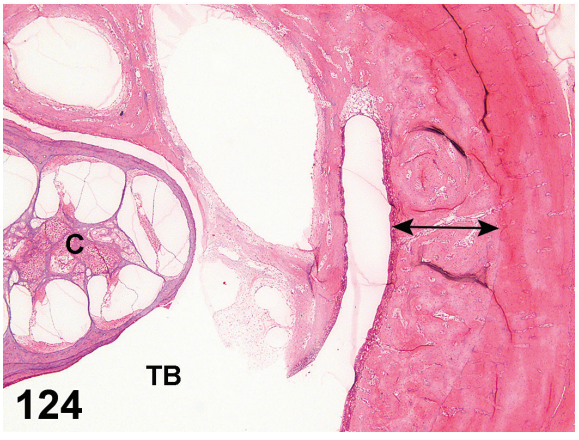

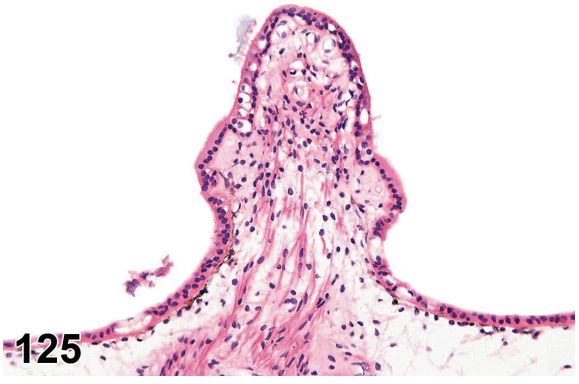

FIGURE 120.—Fibrosis; Edema; middle ear; chinchilla. Fibrosis and edema of the mucosal lining of the tympanic bulla. The expansion of the mucosa is sufficient at this low magnification that the entire width could not be captured in section. Admixed are inflammatory cells.

FIGURE 121.—Fibrosis; middle ear; guinea pig. Fibrosis from the capsule of the cochlea (C) extends into the tympanic bulla lumen (TB) and encompasses the middle ear ossicles. I = Incus; S = Stapes.

FIGURE 122.—Inflammation, granulomatous; middle ear; guinea pig. Granulomatous inflammatory reaction against a spicule (nonstaining cleft, arrow) of tissue glue embedded in the tympanic membrane. This guinea pig had placement of a tympanic bulla cannula that was secured with tissue glue and suture. Note the macrophage associated with the spicule. TB = Tympanic bulla lumen; EEC External ear canal.

FIGURE 123.—Hemorrhage; Edema; middle ear; rabbit. Mucosa of the tympanic bulla of a rabbit with multifocal hemorrhage and edema. TB = Tympanic bulla lumen.

FIGURE 124.—New bone formation; middle ear; guinea pig. A watermark delineates the new bone (double headed arrow) from the existing tympanic bulla. TB = Tympanic bulla lumen; C = Cochlea.

FIGURE 125.—Degeneration, epithelium; inner ear; chinchilla. Crista ampullaris from a chinchilla with degeneration of the epithelium. The epithelium is variably vacuolated with intra-epithelial cell debris.

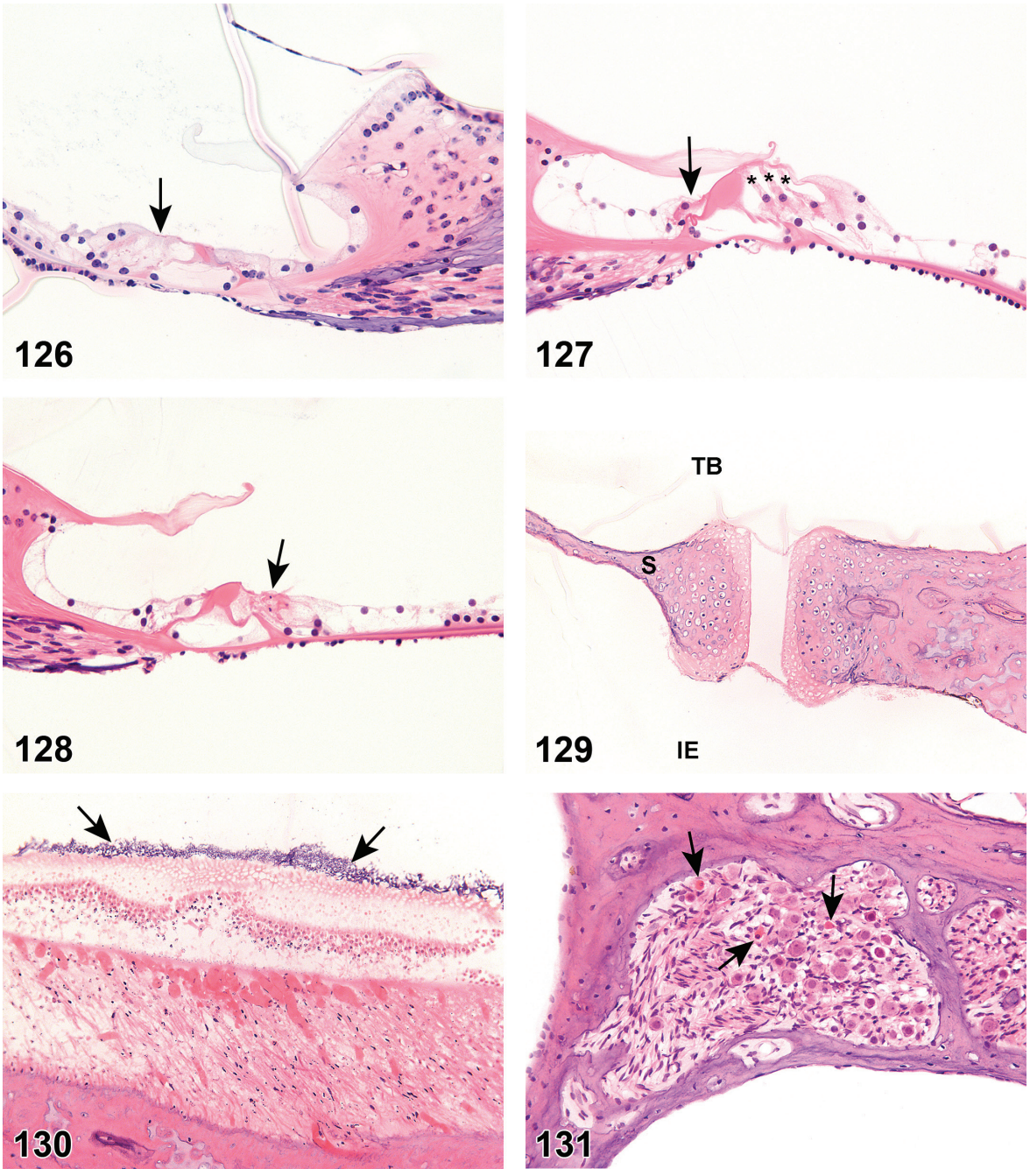

Figure 126.—Decreased number, hair cell (loss); inner ear; chinchilla. Organ of Corti from a chinchilla. Arrow marks the location where the three outer hair cells were. Compare with normal anatomy of Organ of Corti, Figure 127. Wrinkle in section is an artifact of the GMA sectioning and placement on water bath.

Figure 127.—Normal Organ of Corti; inner ear; chinchilla. (Asterisks = Three outer hair cells. Arrow = Inner hair cell.)

Figure 128.—Necrosis, hair cell; inner ear; chinchilla. Single cell necrosis of the outer hair cells of the Organ of Corti. Positive control animal that received gentamicin four days prior. Compare with normal anatomy of Organ of Corti, Figure 127. Arrow = single cell necrosis.

Figure 129.—Necrosis, cartilage; inner ear; chinchilla. Footplate of the stapes resting in the oval window in a chinchilla. The chondrocytes of the stapes footplate and the oval window are necrotic as demonstrated by the absence of basophilic staining nuclei in chondrocyte lacunae. TB = Tympanic bulla lumen; S = Stapes; IE = Inner ear.

Figure 130.—Necrosis, vestibular organ; inner ear; chinchilla. Coagulative necrosis of the otolith organ from a chinchilla. Arrows indicate otoliths on the surface. The entire thickness of the organ is eosinophihlic with nuclear pkynosis.

Figure 131.—Necrosis, neuronal; inner ear; chinchilla. Neuron necrosis in the spiral ganglion of a chinchilla given gentamicin as a positive control. Note the few, hypereosinophilic neurons (arrows).

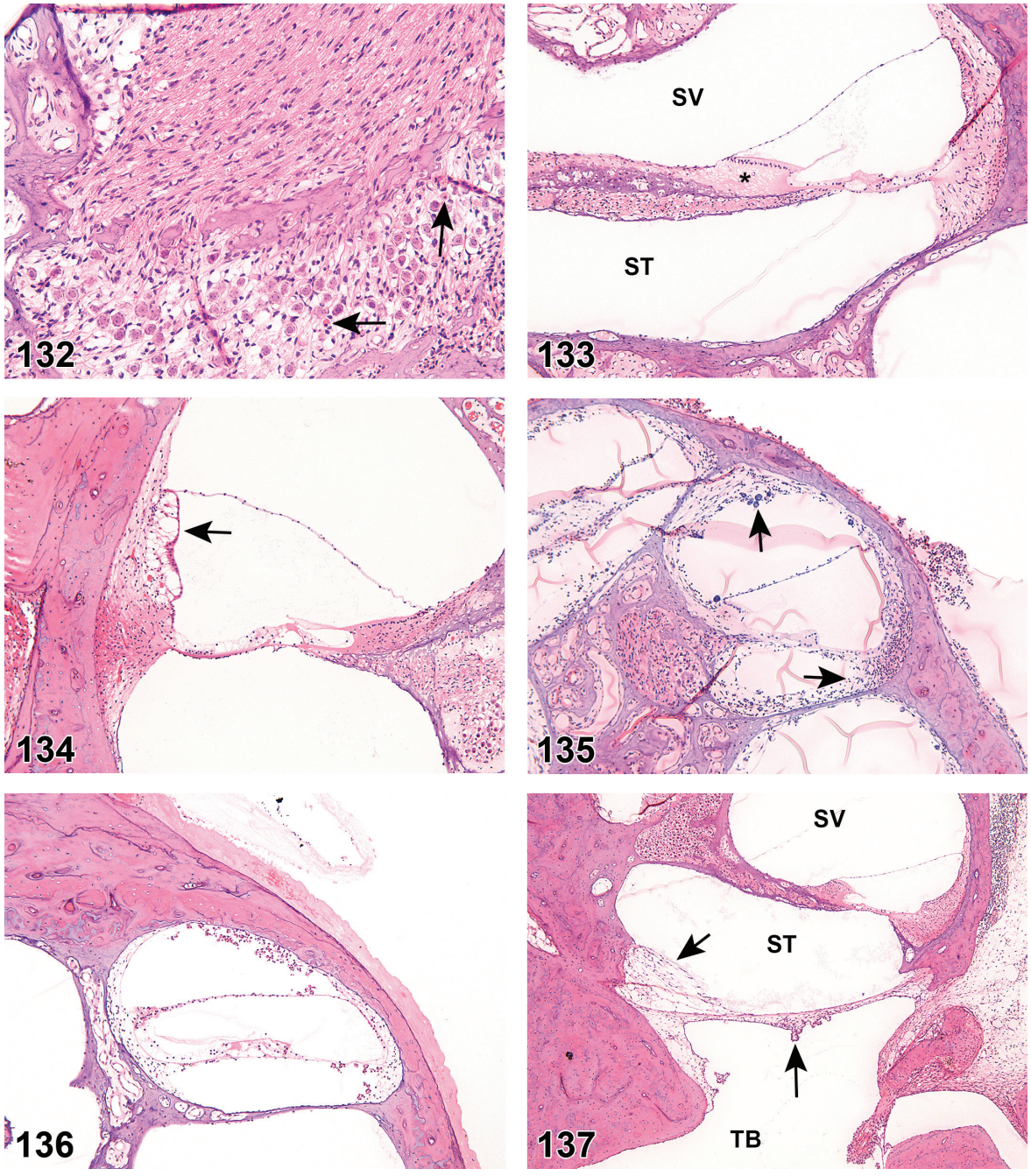

FIGURE 132.—Degeneration, axonal, vestibulo-cochlear nerve; inner ear; chinchilla. Cochlear nerve (upper half of image) from a chinchilla has degeneration of axons due to dying back from the spiral ganglion. Infrequent spiral ganglion neurons are necrotic (arrows).

FIGURE 133.—Decreased cellularity, spiral limbus; inner ear; guinea pig. Limbus spiralis from a guinea pig with decreased cellularity. This guinea pig was given a single dose of gentamicin as a positive control one month prior. Asterisk = Limbus spiralis. SV = Scala vestibuli; ST = Scala tympani. Compare with Figures 134 and 137.

FIGURE 134.—Vacuolation, stria vascularis (arrow); inner ear; chinchilla. Compare with Figure 108.

FIGURE 135.—Inflammation; inner ear; guinea pig. Inflammation and edema is expanding the lining of the cochlea. Arrows indicate inflammatory infiltrates. Guinea pig was given neomycin as a positive control. Note that inflammation also affects the external surface of the cochlea. Wrinkles in section are artifact of the GMA sectioning and placement on water bath.

FIGURE 136.—Inflammation; inner ear; guinea pig. Note that the inflammatory cells are largely free-floating in the scala vestibuli and scala tympani with only minor expansion of the lining by edema.

FIGURE 137.—Fibrosis; Edema; inner ear; guinea pig. The round window membrane is thickened by fibrosis and edema (arrows). SV = Scala vestibuli; ST = Scala tympani; TB = Tympanic bulla lumen.

References

Ackermann LJ, Yoshitomi K, Fix AS, Render JA (1998) Proliferative lesions of the eye in rats, OSS. In: Guides for Toxicologic Pathology, STP/ARP/AFIP, Washington, DC.

Adams DR. Fine structure of the vomeronasal and septal olfactory epithelia and of glandular structures. *Microsc Res Tech*. **23**: 86–97. 1992. [Medline] [CrossRef]

Adams ET, Auerbach S, Blackshear PE, Bradley A, Gruebbel MM, Little PB, Malarkey D, Maronpot R, McKay JS, Miller RA, Moore RR, Morrison JP, Nyska A, Ramot Y, Rao D, Suttie A, Wells MY, Willson GA, and Elmore SA. Proceedings of the 2010 National Toxicology Program Satellite Symposium. *Toxicol Pathol*. **39**: 240–266. 2011. [Medline] [CrossRef]

Agardh CD, Agardh E, Zhang H, and Ostenson CG. Altered endothelial/pericyte ratio in Goto-Kakizaki rat retina. *J Diabetes Complications*. **11**: 158–162. 1997. [Medline] [CrossRef]

Albert DM, Neekhra A, Wang S, Darjatmoko SR, Sorenson CM, Dubielzig RR, and Sheibani N. Development of choroidal neovascularization in rats with advanced intense cyclic light-induced retinal degeneration. *Arch Ophthalmol*. **128**: 212–222. 2010. [Medline] [CrossRef]

Anderson MG, Smith RS, Savinova OV, Hawes NL, Chang B, Zabaleta A, Wilpan R, Heckenlively JR, Davisson M, and John SW. Genetic modification of glaucoma associated phenotypes between AKXD-28/Ty and DBA/2J mice. *BMC Genet*. **2**: 1-12. 2001. [Medline] [CrossRef]

Atsumi I, Kurata M, Sakaki H. Comparative study on ocular anatomical features among rabbits, beagle dogs and cynomolgus monkeys. *Animal Eye Research*. 2013; 32: 35-41.

Balazs EA, Toth LZJ, Eckl EA, and Mitchell AP. Studies on the structure of the vitreous body. *Exp Eye Res*. **3**: 57–71. 1964. [Medline] [CrossRef]

Bancroft JD, Gamble M. (2002) Chapter 13. Pigments and minerals. In: Theory and Practice of Histological Techniques. Harcourt Publishers Limited. 258–256.

Barrios AW, Núñez G, Sánchez Quinteiro P, and Salazar I. Anatomy, histochemistry, and immunohistochemistry of the olfactory subsystems in mice. *Front Neuroanat*. **8**: 63-73. 2014. [Medline] [CrossRef]

Barskey D. (2006) Anatomy of the Uveal Tract. In: Tasman W, Jaeger EA (eds) Duane's Ophthalomology. Lippincott, Williams, & Wilkens, Philadelphia, PA. 1–11.

Bihun CGD, and Percy DH. Morphologic changes in the nasal cavity associated with sialodacryoadenitis virus infection in the Wistar rat. *Vet Pathol*. **32**: 1–10. 1995. [Medline] [CrossRef]

Bishop PN. (2014) Biochemistry. In: Vitreous in Health and Disease. J Sebag (ed). Springer Science and Business Media, New York, 3–12.

Bobu C, Lahmam M, Vuillez P, Ouarour A, and Hicks D. Photoreceptor organisation and phenotypic characterization in retinas of two diurnal rodent species: potential use as experimental animal models for human vision research. *Vision Res*. **48**: 424–432. 2008. [Medline] [CrossRef]

Bok D. The retinal pigment epithelium: a versatile partner in vision. *J Cell Sci Suppl*. **17:** 189–195. 1993. [Medline] [CrossRef]

Boorman GA, Morgan KT, Uriah LC. (1990) Nose, larynx, and trachea. In: Pathology of the Fischer rat. Reference and atlas. GA Boorman, SL Eustis, MR Elwell, CA Montgomer, Jr, WF MacKenzie (eds). Academic Press, San Diego New York London, 295–337.

Botts S, Jokinen M, Gaillard ET, *et al.* (1999) Salivary, Harderian and lacrimal glands. In: Pathology of the mouse. RR Maronpot, GA Boorman, BW Gaul (eds). Cache River Press, USA, 49–79.

Boulton M. (1988) Melanin and the retinal pigment epithelium. In: Retinal Pigment Epithelium. MF Marmor, TW Wolfensberger (eds). Oxford University Press, New York, 68–85.

Bourne WM. Biology of the corneal endothelium in health and disease. *Eye (Lond)*. **17**: 912–918. 2003. [Medline] [CrossRef]

Boycott B, and Wässle H. Parallel processing in the mammalian retina: the Proctor Lecture. *Invest Ophthalmol Vis Sci*. **40**: 1313–1327. 1999. [Medline]

Brann JH, and Firestein S. Regeneration of new neurons is preserved in aged vomeronasal epithelia. *J Neurosci*. **30**: 15686–15694. 2010. [CrossRef]

Brechbühl J, Klaey M, Moine F, Bovay E, Hurni N, Nenniger-Tosato M, and Broillet MC. Morphological and physiological species-dependent characteristics of the rodent Grueneberg ganglion. *Front Neuroanat*. **8**: 87-101. 2014. [Medline]

Breipohl W, Naguro T, Walker DG. The postnatal development of Masera's organ in the rat. *Chem Senses*. 1989; 14: 649-662. [CrossRef]

Bredow L, Schwartzkopff J, and Reinhard T. Regeneration of corneal endothelial cells following keratoplasty in rats with bullous keratopathy. *Mol Vis*. **20**: 683–690. 2014. [Medline]

Brinker T, Lüdemann W, Berens von Rautenfeld D, and Samii M. Dynamic properties of lymphatic pathways for the absorption of cerebrospinal fluid. *Acta Neuropathol*. **94**: 493–498. 1997. [Medline] [CrossRef]

Brown DV. Reaction of the rabbit retinal pigment ipithelium to systemic lead poisoning. *Trans Am Ophthalmol Soc*. **72**: 404–447. 1974. [Medline]

Buckley LA, Morgan KT, Swenberg JA, James RA, Hamm TE Jr, and Barrow CS. The toxicity of dimethylamine in F-344 rats and B6C3F1 mice following a 1-year inhalation exposure. *Fundam Appl Toxicol*. **5**: 341–352. 1985. [Medline] [CrossRef]

Butler WH, Ford GP, and Newberne JW. A study of the effects of vigabatrin on the central nervous system and retina of Sprague Dawley and Lister-Hooded rats. *Toxicol Pathol*. **15**: 143–148. 1987. [Medline] [CrossRef]

Caine R, Albert DM, Lahav M, and Bullock J. Oxalate retinopathy: an experimental model of a flecked retina. *Invest Ophthalmol*. **14**: 359–363. 1975. [Medline]

Carlton WW, Render JA. (1991) Adenoma and adenocarcinoma, Harderian gland, mouse, rat, hamster. In: Monographs on Pathology of Laboratory Animals. Eye and Ear. TC Jones, U Mohr, RD Hunt (eds). Springer, Berlin Heidelberg New York Tokyo, 33–137.

Cavallotti D, Cavallotti C, Pescosolido N, Iannetti GD, and Pacella E. A morphometric study of age changes in the rat optic nerve. *Ophthalmologica*. **215**: 366–371. 2001. [Medline] [CrossRef]

Chandra M, and Frith CH. Histopathologic and immunohistochemical features of two spontaneously generated ocular schwannomas in Sprague Dawley rats. *Lab Anim Sci*. **43**: 500–502. 1993. [Medline]

Chiquoine AD. The identification and electron microscopy of myoepithelial cells in the Harderian gland. *Anat Rec*. **132**: 569–583. 1958. [Medline] [CrossRef]

Chiu T. (1991) Auricular Chondritis, Rat. In: Monographs on Pathology of Laboratory Animals: Eye and Ear. TC Jones, U Mohr, RD Hunt (eds). Springer-Verlag, Berlin.

Choi SO, Jeon HS, Hyon JY, Oh YJ, Wee WR, Chung TY, Shin YJ, and Kim JW. Recovery of corneal endothelial cells from periphery after injury. *PLoS ONE*. **10**: e0138076. 2015. [Medline] [CrossRef]

Chung EH, Bukusoglu G, and Zieske JD. Localization of corneal epithelial stem cells in the developing rat. *Invest Ophthalmol Vis Sci*. **33**: 2199–2206. 1992. [Medline]

Coca-Prados M. The blood-aqueous barrier in health and disease. *J Glaucoma*. **23**(Suppl 1): S36–S38. 2014. [Medline] [CrossRef]

Collinson JM, Hill RE, and West JD. Different roles for Pax6 in the optic vesicle and facial epithelium mediate early morphogenesis of the murine eye. *Development*. **127**: 945–956. 2000. [Medline]

Corps KN, Islam Z, Pestka JJ, and Harkema JR. Neurotoxic, inflammatory, and mucosecretory responses in the nasal airways of mice repeatedly exposed to the macrocyclic trichothecene mycotoxin roridin A: dose-response and persistence of injury. *Toxicol Pathol*. **38**: 429–451. 2010. [Medline] [CrossRef]

Cowan CM, and Roskams AJ. Apoptosis in the mature and developing olfactory neuroepithelium. *Microsc Res Tech*. **58**: 204–215. 2002. [Medline] [CrossRef]

Crafoord S, Ghosh F, Sebag J. (2014) Vitreous Biochemistry and Artificial Vitreous. In: Vitreous in Health and Disease. J Sebag (ed). Springer Science and Business Media, New York, 13–20.

Cursiefen C, Chen L, Saint-Geniez M, Hamrah P, Jin Y, Rashid S, Pytowski B, Persaud K, Wu Y, Streilein JW, and Dana R. Nonvascular VEGF receptor 3 expression by corneal epithelium maintains avascularity and vision. *Proc Natl Acad Sci USA*. **103**: 11405–11410. 2006. [Medline] [CrossRef]

Curtis MR, Bullock FD, Dunning WF. A statistical study of the occurrence

of spontaneous tumors in a large colony of rats. *Amer Assoc Canc Res*. 1931; 15: 67-121.

DAmico DJ, Libert J, Kenyon KR, Hanninen LA, and Caspers-Velu L. Retinal toxicity of intravitreal gentamicin. An electron microscopic study. *Invest Ophthalmol Vis Sci*. **25**: 564–572. 1984. [Medline]

Døving KB, and Trotier D. Structure and function of the vomeronasal organ. *J Exp Biol*. **201**: 2913–2925. 1998. [Medline]

Dawes LJ, Sugiyama Y, Lovicu FJ, Harris CG, Shelley EJ, and McAvoy JW. Interactions between lens epithelial and fiber cells reveal an intrinsic self-assembly mechanism. *Dev Biol*. **385**: 291–303. 2014. [Medline] [CrossRef]

De La Rosa-Prieto C, Saiz-Sanchez D, Ubeda-Bañon I, Argandoña-Palacios L, Garcia-Muñozguren S, and Martinez-Marcos A. Fate of marginal neuroblasts in the vomeronasal epithelium of adult mice. *J Comp Neurol*. **517**: 723–736. 2009. [Medline] [CrossRef]

De la Rosa-Prieto C, Saiz-Sanchez D, Ubeda-Bañon I, Argandoña-Palacios L, Garcia-Muñozguren S, and Martinez-Marcos A. Neurogenesis in subclasses of vomeronasal sensory neurons in adult mice. *Dev Neurobiol*. **70**: 961–970. 2010. [Medline] [CrossRef]

De Vera Mudry MC, Kronenberg S, Komatsu S, and Aguirre GD. Blinded by the light: retinal phototoxicity in the context of safety studies. *Toxicol Pathol*. **41**: 813–825. 2013. [Medline] [CrossRef]

Denlinger JL, Balaz EA. (2014) Hyaluronan and Other Carbohydrates in the Vitreus. In: Vitreous in Health and Disease. J Sebag (ed). Springer Science and Business Media, New York, 13–20.

Dungworth DL, Hahn FF, Hayashi Y, Keean K, Mohr U, Rittinghausen S, Schwartz L (1992) 1. Respiratory system. In: International Classification of Rodent Tumours. Part I: The Rat. U Mohr, CC Capen, DL Dungworth, RA Griesemer, N Ito, VS Turusov (eds). IARC Scientific Publications No. 122, Lyon, 1–57.

Dungworth DL, Rittinghausen S, Schwartz L, *et al.* (2001) Respiratory system and mesothelium. In: International classification of rodent tumors: The mouse. U Mohr (ed). Springer, Berlin Heidelberg New York, 87–137.

Ebneter A, Casson RJ, Wood JPM, and Chidlow G. Estimation of axon counts in a rat model of glaucoma: comparison of fixed-pattern sampling with targeted sampling. *Clin Experiment Ophthalmol*. **40**: 626–633. 2012. [Medline] [CrossRef]

Eiben R, and Liebich HG. Detection and evaluation of lesions in the retina, optic nerve and ciliary muscle of old rats using a electron microscope. *Lens Eye Toxic Res*. **6**: 269–287. 1989. [Medline]

Elmore SA, Dixon D, Hailey JR, Harada T, Herbert RA, Maronpot RR, Nolte T, Rehg JE, Rittinghausen S, Rosol TJ, Satoh H, Vidal JD, Willard-Mack CL, and Creasy DM. Recommendations from the INHAND Apoptosis/Necrosis Working Group. *Toxicol Pathol*. **44**: 173–188. 2016. [Medline] [CrossRef]

Elwell MR, Boorman GA. (1990) Tumours of the Harderian gland. In: Pathology of Tumours in Laboratory Animals. Vol I. Tumours of the Rat, 2nd edition. VS Turusov, U Mohr U (eds). IARC Scientific Publications No. 99, Lyon, 79–88.

Ernst H, Rittinghausen S, Mohr U. (1991) Melanoma of the eye, mouse. In: Monographs on Pathology of Laboratory Animals. Eye and Ear. TC Jones, U Mohr, RD Hunt (eds). Springer, Berlin Heidelberg New York Tokyo, 44–47.

Everitt JF, Shadduck JA. (1991) Melanoma of the uvea, rat. In: Monographs on Pathology of Laboratory Animals. Eye and Ear. TC Jones, U Mohr, RD Hunt (eds).Springer, Berlin Heidelberg New York Tokyo, 40–43.

Ferrara D, Monteforte R, Baccari GC, Minucci S, and Chieffi G. Androgen and estrogen receptors expression in the rat exorbital lacrimal gland in relation to "harderization". J Exp Zool A Comp. *Exp Biol*. **301**: 297–306. 2004.

Fielden MR, Werner J, Jamison JA, Coppi A, Hickman D, Dunn RT 2nd, Trueblood E, Zhou L, Afshari CA, Lightfoot-Dunn R. Retinal toxicity induced by a novel β-secretase inhibitor in the Sprague-Dawley rat. *Toxicol Pathol*. **43**: 581–592. 2015. [Medline] [CrossRef]

Figge FHJ, and Davidheiser RH. Prophyrin synthesis by mouse harderian gland extracts: sex, age, and strain variation. *Proc Soc Exp Biol Med*. **96**: 437–439. 1957. [Medline] [CrossRef]

Finger TE, Böttger B, Hansen A, Anderson KT, Alimohammadi H, and Silver WL. Solitary chemoreceptor cells in the nasal cavity serve as sentinels of respiration. *Proc Natl Acad Sci USA*. **100**: 8981–8986. 2003. [Medline] [CrossRef]

Finger TE, St Jeor VL, Kinnamon JC, and Silver WL. Ultrastructure of substance P- and CGRP-immunoreactive nerve fibers in the nasal epithelium of rodents. *J Comp Neurol*. **294**: 293–305. 1990. [Medline] [CrossRef]

Fitzgerald JE, Schardein JL, and Kurtz SM. Spontaneous tumors of the nervous system in albino rats. *J Natl Cancer Inst*. **52**: 265–273. 1974. [Medline] [CrossRef]

Fleischer J, and Breer H. The Grueneberg ganglion: a novel sensory system in the nose. *Histol Histopathol*. **25**: 909–915. 2010. [Medline]

Fleischer J, Schwarzenbacher K, Besser S, Hass N, and Breer H. Olfactory receptors and signalling elements in the Grueneberg ganglion. *J Neurochem*. **98**: 543–554. 2006. [Medline] [CrossRef]

Foster HL. Purulent keratoconjunctivitis in laboratory rats, caused by Micrococcus pyogenes var. aureus. *J Am Vet Med Assoc*. **133**: 201. 1958. [Medline]

Fox DA, and Chu LWF. Rods are selectively altered by lead: II. Ultrastructure and quantitative histology. *Exp Eye Res*. **46**: 613–625. 1988. [Medline] [CrossRef]

French DD, and Margo CE. Postmarketing surveillance rates of uveitis and scleritis with bisphosphonates among a national veteran cohort. *Retina*. **28**: 889–893. 2008. [Medline] [CrossRef]

Frith CH, Ward JM. (1988) Eye and adnexal glands. In: Color atlas of Neoplastic and Non-neoplastic Lesions in Aging Mice. Elsevier, Amsterdam.

Fuss SH, Omura M, and Mombaerts P. The Grueneberg ganglion of the mouse projects axons to glomeruli in the olfactory bulb. *Eur J Neurosci*. **22**: 2649–2654. 2005. [Medline] [CrossRef]

Gaafar KM, Abdel-Khalek LR, el-Sayed NK, and Ramadan GA. Lipidemic effect as a manifestation of chloroquine retinotoxicity. *Arzneimittelforschung*. **45**: 1231–1235. 1995. [Medline]

Gartner S, and Henkind P. Langes Folds. *Ophthalmology*. **88**: 1307–1310. 1981. [Medline] [CrossRef]

Gaskell BA. Nonneoplastic changes in the olfactory epitheliumexperimental studies. *Environ Health Perspect*. **85**: 275–289. 1990. [Medline] [CrossRef]

Geiss V, Yoshitomi K. (1999) Eyes. In: Pathology of the Mouse. Reference and Atlas. RR Maronpot, GA Boorman, BW Gaul (eds). Cache River Press, Vienna, pp 471–489.

Getchell ML, and Kulkarni AP. Identification of neutrophils in the nonsensory epithelium of the vomeronasal organ in virus-antibody-free rats. *Cell Tissue Res*. **280**: 139–151. 1995. [Medline] [CrossRef]

Gopinath C, Prentice DE, Lewis DJ. (1987) Atlas of Experimental Toxicological Pathology. MTP Press limited, Norwell, MA USA.

Grüneberg H. A ganglion probably belonging to the N. terminalis system in the nasal mucosa of the mouse. *Z Anat Entwicklungsgesch*. **140**: 39–52. 1973. [Medline] [CrossRef]

Grant Maxie M, Youssef S. (2007) Chapter 3. Nervous System In: Jubb, Kennedy and Palmer's Pathology of Domestic Animals. 5th ed. Volume 1. M Grant Maxie (ed). Saunders Elsevier. 287–295; 454.

Greaves P. (2000) Histopathology of Preclinical Toxicity Studies: Nervous system and special sense organs. Elsevier, Amsterdam, 2nd ed. 823–883.

Greaves P, Chouinard L, Ernst H, Mecklenburg L, Pruimboom-Brees IM, Rinke M, Rittinghausen S, Thibault S, Von Erichsen J, and Yoshida T. Proliferative and non-proliferative lesions of the rat and mouse soft tissue, skeletal muscle and mesothelium. *J Toxicol Pathol*. **26**(Suppl): 1S–26S. 2013. [Medline] [CrossRef]

Gregory MH, Rutty DA, and Wood RD. Differences in the retinotoxic action of chloroquine and phenothiazine derivatives. *J Pathol*. **102**: 139–150. 1970. [Medline] [CrossRef]

Grierson I, Unger W, Webster L, and Hogg P. Repair in the rabbit outflow system. *Eye (Lond)*. **14**(Pt 3B): 492–502. 2000. [Medline] [CrossRef]

Gross EA, Patterson DL, and Morgan KT. Effects of acute and chronic dimethylamine exposure on the nasal mucociliary apparatus of F-344 rats. *Toxicol Appl Pharmacol*. **90**: 359–376. 1987. [Medline] [CrossRef]

Grubb BR, Rogers TD, Kulaga HM, Burns KA, Wonsetler RL, Reed RR,

and Ostrowski LE. Olfactory epithelia exhibit progressive functional and morphological defects in CF mice. *Am J Physiol Cell Physiol*. **293**: C574–C583. 2007. [Medline] [CrossRef]

Gruebbel MM (2014) Special Senses System. NTP. Nonneoplastic Lesion Atlas. Research Triangle Park, NC: National Toxicology Program, National Institute of Environmental Health Sciences, National Institutes of Health. http://ntp.niehs.nih.gov/nnl/ (accessed 11 February 2014).

Guillamón A, and Segovia S. Sex differences in the vomeronasal system. *Brain Res Bull*. **44**: 377–382. 1997. [Medline] [CrossRef]

Gulbransen BD, Clapp TR, Finger TE, and Kinnamon SC. Nasal solitary chemoreceptor cell responses to bitter and trigeminal stimulants in vitro. *J Neurophysiol*. **99**: 2929–2937. 2008. [Medline] [CrossRef]

Gutman DA, Magnuson M, Majeed W, Keifer OP Jr, Davis M, Ressler KJ, and Keilholz S. Mapping of the mouse olfactory system with manganese-enhanced magnetic resonance imaging and diffusion tensor imaging. *Brain Struct Funct*. **218**: 527–537. 2013. [Medline] [CrossRef]

Hageman GS, Luthert PJ, Victor Chong NH, Johnson LV, Anderson DH, and Mullins RF. An integrated hypothesis that considers drusen as biomarkers of immune-mediated processes at the RPE-Bruchs membrane interface in aging and age-related macular degeneration. *Prog Retin Eye Res*. **20**: 705–732. 2001. [Medline] [CrossRef]

Halfter W, Sebag J, Cunningham ETJ. (2014) Vitreoretinal Interface and Inner Limiting Membrane. In: Vitreous in Health and Disease. J Sebag (ed). Springer Science and Business Media, New York. 165–191.

Halpern M, and Martínez-Marcos A. Structure and function of the vomeronasal system: an update. *Prog Neurobiol*. **70**: 245–318. 2003. [Medline] [CrossRef]

Hardisty JF, Garman RH, Harkema JR, Lomax LG, and Morgan KT. Histopathology of nasal olfactory mucosa from selected inhalation toxicity studies conducted with volatile chemicals. *Toxicol Pathol*. **27**: 618–627. 1999. [Medline] [CrossRef]

Harkema JR. Comparative pathology of nasal mucosa in laboratory animals exposed to inhaled irritants. *Environ Health Perspect*. **85**: 231–238. 1990

Harkema JR. Comparative aspects of nasal airway anatomy: relevance to inhalation toxicology. *Toxicol Pathol*. **19**: 321–336. 1991. [Medline] [CrossRef]

Harkema JR, and Morgan KT. (1996) Histology, ultrastructure, embryol-ogy, function: normal morphology of the nasal passages. In: Monographs on Pathology of Laboratory Animals: Respiratory System. TC Jones, DL Dungworth, U Mohr (eds). Springer-Verlag, New York. 3–17.

Haschek-Hock WM, Witschi HP. (2004) Chapter 22, Respiratory system. In: Handbook of Toxicologic Pathology. WN Haschek-Hock, CG Rousseaux CG (eds). Academic Press, San Diego, CA. 761–827.

Hassell JR, and Birk DE. The molecular basis of corneal transparency. *Exp Eye Res*. **91**: 326–335. 2010. [Medline] [CrossRef]

Hebel R, Stromberg MW. (1976) In: Anatomy of the Laboratory Rat. R Hebel, MW Stromberg (eds). Baltimore, MD, Williams and Wilkins.

Hebel R, Stromberg MW. (1986) Sensory organs. In: Anatomy and Embryology of the Laboratory Rat. Biomedical Verlag Wörthsee, Germany, 218–224.

Henriksson JT, McDermott AM, and Bergmanson JPG. Dimensions and morphology of the cornea in three strains of mice. *Invest Ophthalmol Vis Sci*. **50**: 3648–3654. 2009. [Medline] [CrossRef]

Herbert RA, Leininger JR. (1999) Nose, larynx and trachea. In: Pathology of the Mouse. Reference and Atlas. RR Maronpot, GA Boorman, BW Gaul (eds). Cache River press, Vienna, IL. 259–292.

Heywood R. Some clinical observations on the eyes of Sprague-Dawley rats. *Lab Anim*. **7**: 19–27. 1973. [Medline] [CrossRef]

Hogan MJ, Zimmerman LE. (1962) Ophthalmic Pathology, An Atlas and Textbook, 2nd ed. W. Saunders Company. 58–61.

Hockwin O, Green K, Rubin LF. (1992) Manual of Oculotoxicity Testing of Drugs. New York, Fischer.

Hottendorf GH. (1991) Cholesteatoma, aural, gerbil. In: Monographs on Pathology of Laboratory Animals: Eye and Ear. TC Jones, U Mohr, RD Hunt (eds). Springer-Verlag, Berlin. 156–158.

Huard JMT, Youngentob SL, Goldstein BJ, Luskin MB, and Schwob JE. Adult olfactory epithelium contains multipotent progenitors that give rise to neurons and non-neural cells. *J Comp Neurol*. **400**: 469–486. 1998. [Medline] [CrossRef]

Hubert MF, Gillet JP, and Durand-Cavagna G. Spontaneous retinal changes in Sprague Dawley rats. *Lab Anim Sci*. **44**: 561–567. 1994. [Medline]

Hughes WF, and Coogan PS. Pathology of the pigment epithelium and retina in rabbits poisoned with lead. *Am J Pathol*. **77**: 237–254. 1974. [Medline]

Hughs BA. (1998) Transport Mechanisms in the Retinal Pigment Epithelium. In: The Retinal Pigment Epithelium. MF Marmor, TW Wolfensberger (eds). Oxford University Press, New York.103–134.

Ibrahim KE, Khan HA, and Omer FA. Histological insights in iminodipropionitrile-induced toxicity in rats. *Exp Toxicol Pathol*. **66**: 89–96. 2014. [Medline] [CrossRef]

Islam Z, Harkema JR, and Pestka JJ. Satratoxin G from the black mold Stachybotrys chartarum evokes olfactory sensory neuron loss and inflammation in the murine nose and brain. *Environ Health Perspect*. **114**: 1099–1107. 2006. [Medline] [CrossRef]

Ivanina TA, Zueva MV, Lebedeva MN, Bogoslovsky AI, and Bunin AJ. Ultrastructural alterations in rat and cat retina and pigment epithelium induced by chloroquine. *Graefes Arch Clin Exp Ophthalmol*. **220**: 32–38. 1983. [Medline] [CrossRef]

Jensen RK, and Sleight SD. Toxic effects of N-nitrosodiethylamine on nasal tissues of Sprague-Dawley rats and golden Syrian hamsters. *Fundam Appl Toxicol*. **8**: 217–229. 1987. [Medline] [CrossRef]

Jeon CJ, Strettoi E, and Masland RH. The major cell populations of the mouse retina. *J Neurosci*. **18**: 8936–8946. 1998. [Medline]

Jester JV, Nicolaides N, and Smith RE. Meibomian gland studies: histologic and ultrastructural investigations. *Invest Ophthalmol Vis Sci*. **20**: 537–547. 1981. [Medline]

Jia C, and Halpern M. Calbindin D28K immunoreactive neurons in vomeronasal organ and their projections to the accessory olfactory bulb in the rat. *Brain Res*. **977**: 261–269. 2003. [Medline] [CrossRef]

Joshi M, Agrawal S, and Christoforidis JB. Inflammatory mechanisms of idiopathic epiretinal membrane formation. *Mediators Inflamm*. **2013**: 192582. 2013. [Medline] [CrossRef]

Jun AS, Chakravarti S, Edelhauser HF, and Kimos M. Aging changes of mouse corneal endothelium and Descemets membrane. *Exp Eye Res*. **83**: 890–896. 2006. [Medline] [CrossRef]

Kai K, Sahto H, Yoshida M, Suzuki T, Shikanai Y, Kajimura T, and Furuhama K. Species and sex differences in susceptibility to olfactory lesions among the mouse, rat and monkey following an intravenous injection of vincristine sulphate. *Toxicol Pathol*. **34**: 223–231. 2006. [Medline] [CrossRef]

Kalatzis V, Serratrice N, Hippert C, Payet O, Arndt C, Cazevieille C, Maurice T, Hamel C, Malecaze F, Antignac C, Müller A, and Kremer EJ. The ocular anomalies in a cystinosis animal model mimic disease pathogenesis. *Pediatr Res*. **62**: 156–162. 2007. [Medline] [CrossRef]

Kang N, Baum MJ, and Cherry JA. A direct main olfactory bulb projection to the vomeronasal amygdala in female mice selectively responds to volatile pheromones from males. *Eur J Neurosci*. **29**: 624–634. 2009. [Medline] [CrossRef]

Katahashi T, Kanda T, Konno A. Distribution of choline acetyltransferase (ChAT) immunoreacive nerve fibers in the nasal mucosa; especially in the repiratory epithelium. *Auris Nasus Larynx*. **24**: 271–277. 1997.

Kaufmann W, Bolon B, Bradley A, Butt M, Czasch S, Garman RH, George C, Gröters S, Krinke G, Little P, McKay J, Narama I, Rao D, Shibutani M, and Sills R. Proliferative and nonproliferative lesions of the rat and mouse central and peripheral nervous systems. *Toxicol Pathol*. **40**(Suppl): 87S–157S. 2012. [Medline] [CrossRef]

Kingston ZS, Provis JM, Madigan MC. (2014) Development and Development Disorders of the Vitreous In: Vitreous in Health and Disease. J Sebag (ed). Springer Science and Business Media, New York. 95-112.

Kita T, Sakamoto T, Ishibashi T. (2014) Hyalocytes: Essential Vitreous Cells. In: Vitreoretinal Health and Disease. J Sebag (ed). Springer, New York. 151–164.

Kitagaki M, Suwa T, Yanagi M, and Shiratori K. Auricular chondritis in young ear-tagged Crj:CD(SD)IGS rats. *Lab Anim*. **37**: 249–253. 2003. [Medline] [CrossRef]

Kittel B, Ruehl-Fehlert C, Morawietz G, Klapwijk J, Elwell MR, Lenz B, OSullivan MG, Roth DR, Wadsworth PF. RITA Group NACAD Group. Revised guides for organ sampling and trimming in rats and mice – Part 2. *Exp Toxicol Pathol*. **55**: 413–431. 2004. [Medline] [CrossRef]

Kowalczuk L, Latour G, Bourges JL, Savoldelli M, Jeanny JC, Plamann K, Schanne-Klein MC, and Behar-Cohen F. Multimodal highlighting of structural abnormalities in diabetic rat and human corneas. *Transl Vis Sci Technol*. **2**: 3-18. 2013. [Medline] [CrossRef]

Kreutzberg GW, Blakemore WF, Graeber MB. (1997) Cellular pathology of the central nervous system. In: Greenfield's Neuropathology. DI Graham, PL Lantos (eds). 6th ed. Arnold, London, Sydney, Auckland. Volume 1. 85–140.

Krinke AL, Schaetti P, Krinke GJ. (1994) Changes in the major ocular glands. In: Pathobiology of the Aging Rat. U Mohr, DL Dungworth, CC Capen (eds). Vol 2, ILSI Press, Washington. 109–119.

Krinke G, Fix A, Jacobs M, *et al.* (2001) Eye and Harderian Gland. In: International Classification of Rodent Tumors. The Mouse. U Mohr (ed). Springer-Verlag Heidelberg Berlin New York. 347–359.

Krinke GJ, Schaetti PR, and Krinke AL (1996) Nonneoplastic and neoplastic changes in the Harderian and lacrimal glands. In: Pathobiology of the Aging Mouse. U Mohr, DL Dungworth, CC Capen, WW Carlton, JP Sundberg, JM Ward (eds). Vol. 2, ILSI Press, Washington. 139–152.

Krinke GK. (1991) Atrophy and Sclerosis, Harderian Gland, Rat. In: Monographs on Pathology of Laboratory Animals: Eye and Ear. TC Jones, U Mohr, RD Hunt (eds). Springer Verlag, Berlin. 137–140.

Kuno H, Usui T, Eydelloth RS, and Wolf ED. Spontaneous ophthalmic lesions in young Sprague-Dawley rats. *J Vet Med Sci*. **53**: 607–614. 1991. [Medline] [CrossRef]

Lütjen-Drecoll E. Electron microscopic studies on reactive changes of the trabecular meshwork in human eyes after microsurgery. *Albrecht Von Graefes Arch Klin Exp Ophthalmol*. **183**: 267–285. 1972. [Medline] [CrossRef]

Lai YL. Outward movement of photoreceptor cells in normal rat retina. *Invest Ophthalmol Vis Sci*. **19**: 849–856. 1980. [Medline]

Lai YL, Masuda K, Mangum MD, Lug R, Macrae DW, Fletcher G, and Liu YP. Subretinal displacement of photoreceptor nuclei in human retina. *Exp Eye Res*. **34**: 219–228. 1982. [Medline] [CrossRef]

Lapham LW, Johnstone MA, and Brundjar KH. A new paraffin method for the combined staining of myelin and glial fibers. *J Neuropathol Exp Neurol*. **23**: 156–160. 1964. [Medline] [CrossRef]

Lee KP, and Valentine R. Pathogenesis and reversibility of retinopathy induced by 1,4-bis (4-aminophenoxy)-2-phenylbenzene (2-phenyl-APB-144) in pigmented rats. *Arch Toxicol*. **65**: 292–303. 1991. [Medline] [CrossRef]

Lei Y, Overby DR, Boussommier-Calleja A, Stamer WD, and Ethier CR. Outflow physiology of the mouse eye: pressure dependence and washout. *Invest Ophthalmol Vis Sci*. **52**: 1865–1871. 2011. [Medline] [CrossRef]

Leininger JR, Herbert RA, Morgan KT. (1996) Aging changes in the upper respiratory tract. In: Pathobiology of the Aging Mouse. U Mohr, DL Dungworth, CC Capen, WW Carlton, JP Sundberg, JM Ward (eds). Vol. 1, ILSI Press, Washington. 247–260.

Lengyel I, Flinn JM, Pető T, Linkous DH, Cano K, Bird AC, Lanzirotti A, Frederickson CJ, and van Kuijk FJ. High concentration of zinc in sub-retinal pigment epithelial deposits. *Exp Eye Res*. **84**: 772–780. 2007. [Medline] [CrossRef]

Levin S, Bucci TJ, Cohen SM, Fix AS, Hardisty JF, LeGrand EK, Maronpot RR, Trump BF. The nomenclature of cell death: recommendations of an ad hoc Committee of the Society of Toxicologic Pathologists. *Toxicol Pathol*. **27**: 484–490. 1999.

Levkovitch-Verbin H, Quigley HA, Martin KR, Valenta D, Baumrind LA, and Pease ME. Translimbal laser photocoagulation to the trabecular meshwork as a model of glaucoma in rats. *Invest Ophthalmol Vis Sci*. **43**: 402–410. 2002. [Medline]

Lewis JL, Nikula KJ, Sachetti LA (1994) Induced xenobiotic-metabolizing enzymes localized to eosinophilic globules in olfactory epithelium of toxicant-exposed F344 rats. Inhal Toxicol. 6(S): 422–425.

Liu CY, Fraser SE, and Koos DS. Grueneberg ganglion olfactory subsystem employs a cGMP signaling pathway. *J Comp Neurol*. **516**: 36–48. 2009. [Medline] [CrossRef]

Los LI. The rabbit as an animal model for post-natal vitreous matrix differentiation and degeneration. *Eye (Lond)*. **22**: 1223–1232. 2008. [Medline] [CrossRef]

Ma M. Encoding olfactory signals via multiple chemosensory systems. *Crit Rev Biochem Mol Biol*. **42**: 463–480. 2007. [Medline] [CrossRef]

Ma M, Grosmaitre X, Iwema CL, Baker H, Greer CA, and Shepherd GM. Olfactory signal transduction in the mouse septal organ. *J Neurosci*. **23**: 317–324. 2003. [Medline]

Ma M. (2010) Multiple Olfactory Subsystems Convey Various Sensory Signals. In: The Neurobiology of Olfaction. A Menini (ed). CRC Press/Taylor & Francis. Boca Raton (FL). Chapter 9.

Machemer R, and Laqua H. Pigment epithelium proliferation in retinal detachment (massive periretinal proliferation). *Am J Ophthalmol*. **80**: 1–23. 1975. [Medline] [CrossRef]

Mamasuew K, Breer H, and Fleischer J. Grueneberg ganglion neurons respond to cool ambient temperatures. *Eur J Neurosci*. **28**: 1775–1785. 2008. [Medline] [CrossRef]

Mamasuew K, Hofmann N, Breer H, and Fleischer J. Grueneberg ganglion neurons are activated by a defined set of odorants. *Chem Senses*. **36**: 271–282. 2011. [Medline] [CrossRef]

Markert CL, and Silvers WK. The effects of genotype and cell environment on melanoblast differentiation in the house mouse. *Genetics*. **41**: 429–450. 1956. [Medline]

Marmor MF. (1998) Structure, Function and Disease of the Retinal Pigment Epithelium. In: The Retinal Pigment Epithelium: Function and Disease. MF Marmor, TW Wolfensberger (eds). Oxford University Press, New York. 3–9.

Maronpot RR. Pathology Working Group review of selected upper respiratory tract lesions in rats and mice. *Environ Health Perspect*. **85**: 331–352. 1990. [Medline] [CrossRef]

Marshall DA, and Maruniak JA. Maseras organ responds to odorants. *Brain Res*. **366**: 329–332. 1986. [Medline] [CrossRef]

Martínez-Marcos A, Ubeda-Bañón I, Deng L, and Halpern M. Neurogenesis in the vomeronasal epithelium of adult rats: evidence for different mechanisms for growth and neuronal turnover. *J Neurobiol*. **44**: 423–435. 2000. [Medline] [CrossRef]

Masland RH. The fundamental plan of the retina. *Nat Neurosci*. **4**: 877–886. 2001. [Medline] [CrossRef]

Masli S, Vega JL. (2011) Ocular Immune Privilege Sites. In: Methods in Molecular Biology. MC Cuturi, I Anegon (eds). Vol. 677, Springer Science and Business Media. 449–458.

Massof RW, and Chang FW. A revision of the rat schematic eye. *Vision Res*. **12**: 793–796. 1972. [Medline] [CrossRef]

Matsumura M, Yamakawa R, Shirakawa H, and Ogino N. Effects of phenothiazines on cultured retinal pigment epithelial cells. *Ophthalmic Res*. **18**: 47–54. 1986. [Medline] [CrossRef]

Matsuoka M, Osada T, Yoshida-Matsuoka J, Ikai A, Ichikawa M, Norita M, and Costanzo RM. A comparative immunocytochemical study of development and regeneration of chemosensory neurons in the rat vomeronasal system. *Brain Res*. **946**: 52–63. 2002. [Medline] [CrossRef]

Maurer JK, and Parker RD. Light microscopic comparison of surfactant-induced eye irritation in rabbits and rats at three hours and recovery/day 35. *Toxicol Pathol*. **24**: 403–411. 1996. [Medline] [CrossRef]

Maurer JK, Parker RD, and Carr GJ. Ocular irritation: microscopic changes occurring over time in the rat with surfactants of known irritancy. *Toxicol Pathol*. **26**: 217–225. 1998. [Medline] [CrossRef]

McCracken JS, and Klintworth GK. Ultrastructural observations on experimentally produced melanin pigmentation of the corneal epithelium. *Am J Pathol*. **85**: 167–182. 1976. [Medline]

McGinn MD, Chole RA, and Henry KR. Cholesteatoma. Experimental induction in the Mongolian gerbil, Meriones unguiculaus. *Acta Otolaryngol*. **93**: 61–67. 1982. [Medline] [CrossRef]

McKay JS, Blakemore WF, and Franklin RJ. Trapidil-mediated inhibition of CNS remyelination results from reduced numbers and impaired differentiation of oligodendrocytes. *Neuropathol Appl Neurobiol*. **24**: 498–506. 1998. [Medline] [CrossRef]

McMartin DN, O'Donoghue JL, Morrissey R, *et al.* (1997) Non-proliferative lesions of the nervous system in rats. NS-1. In: Guides for Toxicologic Pathology. STP/ARP/AFIP, Washington DC.

McMartin DN, Sahota PS, Gunson DE, Hsu HH, and Spaet RH. Neoplasms and related proliferative lesions in control Sprague-Dawley rats from carcinogenicity studies. Historical data and diagnostic considerations. *Toxicol Pathol*. **20**: 212–225. 1992. [Medline] [CrossRef]

Mecklenburg L, Kusewitt D, Kolly C, Treumann S, Adams ET, Diegel K, Yamate J, Kaufmann W, Müller S, Danilenko D, and Bradley A. Proliferative and non-proliferative lesions of the rat and mouse integument. *J Toxicol Pathol*. **26**(Suppl): 27S–57S. 2013. [Medline] [CrossRef]

Mecklenburg L, and Schraermeyer U. An overview on the toxic morphological changes in the retinal pigment epithelium after systemic compound administration. *Toxicol Pathol*. **35**: 252–267. 2007. [Medline] [CrossRef]

Mehta S, Zhang R, Grossniklaus HE. (2014) Cell Proliferation at the Vitreoretinal Interface in Proliferative Vitreoretinopathy and Related Disorders. In: Vitreous in Health and Disease. J Sebag (ed). Springer, New York. 395–405.

Miyazaki M, Man WC, and Ntambi JM. Targeted disruption of stearoyl-CoA desaturase1 gene in mice causes atrophy of sebaceous and meibomian glands and depletion of wax esters in the eyelid. *J Nutr*. **131**: 2260–2268. 2001. [Medline] [CrossRef]

Morgan KT, Haarkema JR. (1996) Nonneoplastic Lesions of the Olfactory Mucosa. In: Monographs on Pathology of Laboratoy Animals: Respiratory System. TC Jones, DL Dungworth, U Mohr (eds). Springer, New York. 28-43.

Mohr U. (1994) International Classification of Rodent Tumours. Part I, The Rat, 7. Central Nervous System; Heart; Eye; Mesothelium. IARC Publication No.122. Lyon. 34–51.

Monticello TM, Morgan KT, and Uraih L. Nonneoplastic nasal lesions in rats and mice. *Environ Health Perspect*. **85**: 249–274. 1990. [Medline] [CrossRef]

Morrison JC, Fraunfelder FW, Milne ST, and Moore CG. Limbal microvasculature of the rat eye. *Invest Ophthalmol Vis Sci*. **36**: 751–756. 1995. [Medline]

Morrison JC, Johnson EC, Cepurna WO, and Funk RH. Microvasculature of the rat optic nerve head. *Invest Ophthalmol Vis Sci*. **40**: 1702–1709. 1999. [Medline]

Mucignat-Caretta C. The rodent accessory olfactory system. *J Comp Physiol A Neuroethol Sens Neural Behav Physiol*. **196**: 767–777. 2010. [Medline] [CrossRef]

Nagai N, Izumi-Nagai K, Robbie S, *et al.* (2011) Spontaneous CNV in a Novel Mutant Mouse is associated with early Chorio-Retinal Para-Inflammation and Vegf Driven Angiogenesis. ARVO.

National Toxicology Program. NTP toxicology and carcinogenesis studies of 5-(Hydroxymethyl)-2-furfural (CAS No. 67470) in F344/N rats and B6C3F1 mice (gavage studies). *Natl Toxicol Program Tech Rep Ser*. **554**: 7–13, 15–19, 21–31 passim. 2010. [Medline]

Nunez-Parra A, Pugh V, and Araneda RC. Regulation of adult neurogenesis by behavior and age in the accessory olfactory bulb. *Mol Cell Neurosci*. **47**: 274–285. 2011. [Medline] [CrossRef]

Nyska A, Yoshizawa K, Jokinen MP, Brix AE, Sells DM, Wyde ME, Orzech DP, Kissling GE, and Walker NJ. Olfactory epithelial metaplasia and hyperplasia in female Harlan Sprague-Dawley rats following chronic treatment with polychlorinated biphenyls. *Toxicol Pathol*. **33**: 371–377. 2005. [Medline] [CrossRef]

Oikawa T, Saito H, Taniguchi K, and Taniguchi K. Immunohistochemical studies on the differential maturation of three types of olfactory organs in the rats. *J Vet Med Sci*. **63**: 759–765. 2001. [Medline] [CrossRef]

Owen RA, Duprat P. (1991) Leiomyoma of the iris, Sprague-Dawley rat. In: Monographs on Pathology of Laboratory Animals. Eye and Ear. TC Jones, U Mohr, RD Hunt (eds). Springer, Berlin Heidelberg New York Tokyo. 47–49.

Palczewski K. Chemistry and biology of the initial steps in vision: the Friedenwald lecture. *Invest Ophthalmol Vis Sci*. **55**: 6651–6672. 2014. [Medline] [CrossRef]

Paulini K, and Mohr W. Hormone-dependent Polyploidy in the glandula orbitalis externa and glandula infraorbitalis of animals of different age. *Beitr Pathol*. **156**: 65–74. 1975. [Medline] [CrossRef]

Payne AP. The harderian gland: a tercentennial review. *J Anat*. **185**: 1–49. 1994. [Medline]

Peichl L. Diversity of mammalian photoreceptor properties: adaptations to habitat and lifestyle? *Anat Rec A Discov Mol Cell Evol Biol*. **287A**: 1001–1012. 2005. [Medline] [CrossRef]

Peräsalo R, Rechardt L, and Palkama A. Chloroquine-induced ultrastructural changes in the pigment epithelium of the albino rat. *Acta Ophthalmol Suppl*. **123**: 94–98. 1974. [Medline]

Percy DH, Wojcinski ZW, and Schunk MK. Sequential changes in the harderian and exorbital lacrimal glands in Wistar rats infected with sialodacryoadenitis virus. *Vet Pathol*. **26**: 238–245. 1989. [Medline] [CrossRef]

Poulsom R, and Hayes B. Congenital retinal folds in Sheffield-Wistar rats. *Graefes Arch Clin Exp Ophthalmol*. **226**: 31–33. 1988. [Medline] [CrossRef]

Pow DV, and Diaz CM. AMD-like lesions in the rat retina: a latent consequence of perinatal hemorrhage. *Invest Ophthalmol Vis Sci*. **49**: 2790–2798. 2008. [Medline] [CrossRef]

Protti DA, Flores-Herr N, Li W, Massey SC, and Wässle H. Light signaling in scotopic conditions in the rabbit, mouse and rat retina: a physiological and anatomical study. *J Neurophysiol*. **93**: 3479–3488. 2005. [Medline] [CrossRef]

Quantock AJ, and Young RD. Development of the corneal stroma, and the collagen-proteoglycan associations that help define its structure and function. *Dev Dyn*. **237**: 2607–2621. 2008. [Medline] [CrossRef]

Ramos M, Reilly CM, Bolon B. (2011) Toxicological pathology of the retina and optic nerve. In: Fundamental Neuropathology for Pathologists and Toxicologists: Principles and Techniques. B Bolon, MT Butt (eds). John Wiley & Sons, Inc, New Jersey. 385–412.

Ramos MF, Attar M, Stern ME, *et al.* (2017) Safety Evaluation of Ocular Drugs, in A Comprehensive Guide to Toxicology in Nonclinical Drug Development, 2nd ed. AS Faqi (ed). Academic Press.

Remtulla S, and Hallett PE. A schematic eye for the mouse, and comparisons with the rat. *Vision Res*. **25**: 21–31. 1985. [Medline] [CrossRef]

Render JA, Schafer KA, Altschuler RA. (2013) Special Senses: Eye and Ear. In: Toxicologic Pathology Nonclinical Safety Assessment. PS Sahota, JA Popp, JF Hardisty, C Gopinath (eds). Boca Raton, Florida, CRC Press. 931–968.

Renne R, Brix A, Harkema J, Herbert R, Kittel B, Lewis D, March T, Nagano K, Pino M, Rittinghausen S, Rosenbruch M, Tellier P, and Wohrmann T. Proliferative and nonproliferative lesions of the rat and mouse respiratory tract. *Toxicol Pathol*. **37**(Suppl): 5S–73S. 2009. [Medline] [CrossRef]

Restrepo D, Arellano J, Oliva AM, Schaefer ML, and Lin W. Emerging views on the distinct but related roles of the main and accessory olfactory systems in responsiveness to chemosensory signals in mice. *Horm Behav*. **46**: 247–256. 2004. [Medline] [CrossRef]

Reuber MD. Chronic Dacryoadenitis Involving the Harderian Gland in Buffalo-Strain Rats Ingesting 3′-Methyl-4-Dimethylaminoazobenzene. *Toxicol Pathol*. 1976; 4: 5-8.

Reynaud J, Cull G, Wang L, Fortune B, Gardiner S, Burgoyne CF, and Cioffi GA. Automated quantification of optic nerve axons in primate glaucomatous and normal eyesmethod and comparison to semi-automated manual quantification. *Invest Ophthalmol Vis Sci*. **53**: 2951–2959. 2012. [Medline] [CrossRef]

Riordan-Eva P. (2011) Anatomy and Embryology of the Eye. In: Vaughan and Ashbury's General Ophthalmology. P Riordan-Eva, ET Cunningham (eds). McGraw-Hill, New York.

Rivière S, Challet L, Fluegge D, Spehr M, and Rodriguez I. Formyl peptide receptor-like proteins are a novel family of vomeronasal chemosensors. *Nature*. **459**: 574–577. 2009. [Medline] [CrossRef]

Robinson DA, Foster JR, Nash JA, and Reed CJ. Three-dimensional mapping of the lesions induced by beta-beta-iminodiproprionitrile, methyl iodide and methyl methacrylate in the rat nasal cavity. *Toxicol Pathol*. **31**: 340–347. 2003. [Medline]

Rodriguez-Ramos Fernandez J, and Dubielzig RR. Ocular comparative anatomy of the family Rodentia. *Vet Ophthalmol*. **16**(Suppl 1): 94–99. 2013.

[Medline] [CrossRef]
Roe FJC, Millican D, and Mallett JM. Induction of melanotic lesions of the iris in rats by urethan given during the neonatal period. *Nature*. **199**: 1201–1202. 1963. [Medline] [CrossRef]
Rohen JW, and van der Zypen E. The phagocytic activity of the trabecularmeshwork endothelium. An electron-microscopic study of the vervet (Cercopithecus aethiops). *Albrecht Von Graefes Arch Klin Exp Ophthalmol*. **175**: 143–160. 1968. [Medline] [CrossRef]
Roppolo D, Ribaud V, Jungo VP, Lüscher C, and Rodriguez I. Projection of the Grüneberg ganglion to the mouse olfactory bulb. *Eur J Neurosci*. **23**: 2887–2894. 2006. [Medline] [CrossRef]
Rosolen SG, Kolomiets B, Varela O, and Picaud S. Retinal electrophysiology for toxicology studies: applications and limits of ERG in animals and ex vivo recordings. *Exp Toxicol Pathol*. **60**: 17–32. 2008. [Medline] [CrossRef]
Rubin LF. (1974) Atlas of Veterinary Ophthalmoscopy. Lea and Febiger, Philadelphia, PA.
Rubin LF. Ocular abnormalities in rats and mice: A survey of commonly occurring conditions. *Animal Eye Research*. 1986; 5: 15-30.
Rubin LF, and Daly IW. Ectopic pupil in mice. *Lab Anim Sci*. **32**: 64–65. 1982. [Medline]
Rudmann D, Cardiff R, Chouinard L, Goodman D, Küttler K, Marxfeld H, Molinolo A, Treumann S, Yoshizawa K. INHAND Mammary, Zymbals, Preputial, and Clitoral Gland Organ Working Group. Proliferative and nonproliferative lesions of the rat and mouse mammary, Zymbals, preputial, and clitoral glands. *Toxicol Pathol*. **40**(Suppl): 7S–39S. 2012. [Medline] [CrossRef]
Ruggeri M, Wehbe H, Jiao S, Gregori G, Jockovich ME, Hackam A, Duan Y, and Puliafito CA. In vivo three-dimensional high-resolution imaging of rodent retina with spectral-domain optical coherence tomography. *Invest Ophthalmol Vis Sci*. **48**: 1808–1814. 2007. [Medline] [CrossRef]
Saïdi T, Mbarek S, Chaouacha-Chekir RB, and Hicks D. Diurnal rodents as animal models of human central vision: characterisation of the retina of the sand rat Psammomys obsesus. *Graefes Arch Clin Exp Ophthalmol*. **249**: 1029–1037. 2011. [Medline] [CrossRef]
Sakamoto T, and Ishibashi T. Hyalocytes: essential cells of the vitreous cavity in vitreoretinal pathophysiology? *Retina*. **31**: 222–228. 2011. [Medline] [CrossRef]
Samuelson DA. (2007) Ophthalmic anatomy: The Uvea. In: Veterinary Ophthalmology. KN Gelatt (ed). Blackwell Publishing, Ames, Iowa. 62–98.
Sashima M, Hatakeyama S, Satoh M, and Suzuki A. Harderianization is another sexual dimorphism of rat exorbital lacrimal gland. *Acta Anat (Basel)*. **135**: 303–306. 1989. [Medline] [CrossRef]
Saunders LZ, Rubin LF. (1975b) The Retina. In: Ophthalmic Pathology of Animals. An Atlas and Reference Book. Basel, S. Karger. 122–123.
Schafer KA, Bolon B. (2013) Chapter 54. Ear. In: Haschek and Rousseaux's Handbook of Toxicologic Pathology, 3rd ed. WM Haschek, CG Rousseaux, MA Wallig (eds). Elsevier, Amsterdam.
Schafer KA, Render JA. (2013a) Toxicologic Pathology of the Eye: Alterations of the Lens and Posterior Segment. In: Assessing Ocular Toxicology in Laboratory Animals. AB Weir, MJ Collins (eds). New York, Humana Press. 219–257.
Schafer KA, Render JA. (2013b) Toxicologic Pathology of the Eye: Histologic Preparation and Alterations of the Anterior Segment. Uvea. In: Assessing Ocular Toxicity in Laboratory Animals. AB Weir, MJ Collins (eds). New York, Humana Press. 159–217.
Schmid A, Pyrski M, Biel M, Leinders-Zufall T, and Zufall F. Grueneberg ganglion neurons are finely tuned cold sensors. *J Neurosci*. **30**: 7563–7568. 2010. [Medline] [CrossRef]
Schmued LC, Stowers CC, Scallet AC, and Xu L. Fluoro-Jade C results in ultra high resolution and contrast labeling of degenerating neurons. *Brain Res*. **1035**: 24–31. 2005. [Medline] [CrossRef]
Schoevers EJ, Kuijpers MH, Woutersen RA, and Feron VJ. Spontaneous squamous cell carcinoma of nasal and paranasal structures in the Cpb:WU (Wistar random) rat: nasolachrymal duct as major site of origin. *J Environ Pathol Toxicol Oncol*. **13**: 49–57. 1994. [Medline]
Schulz D, Iliev ME, Frueh BE, and Goldblum D. In vivo pachymetry in normal eyes of rats, mice and rabbits with the optical low coherence reflectometer. *Vision Res*. **43**: 723–728. 2003. [Medline] [CrossRef]
Schwob JE. Neural regeneration and the peripheral olfactory system. *Anat Rec*. **269**: 33–49. 2002. [Medline] [CrossRef]
Sebag J. (1989) The Vitreous, Structure, Function, and Pathobiology. Springer-Verlag, New York.
Sebag J. Anatomy and pathology of the vitreo-retinal interface. *Eye (Lond)*. **6**: 541–552. 1992. [Medline] [CrossRef]
Secker GA, Daniels JT. (2009) Limbal Epithelial Stem Cells of the Cornea. In: StemBook. L Girard, E Board (eds). Harvard Stem Cell Institute, Cambridge, MA.
Senoh H, Katagiri T, Takanobu K, Umeda Y, Aiso S, and Fukushima S. Spontaneous harderian gland adenocarcinoma in a female f344 rat: a case report. *J Toxicol Pathol*. **27**: 139–142. 2014. [Medline] [CrossRef]
Sha O, Kwong WH. Postnatal developmental changes of vitreous and lens volumes in Sprague-Dawley rats. *Neuroembryology Aging*. 2006; 4: 183-188. [CrossRef]
Shi Y, Tu Y, De Maria A, Mecham RP, and Bassnett S. Development, composition, and structural arrangements of the ciliary zonule of the mouse. *Invest Ophthalmol Vis Sci*. **54**: 2504–2515. 2013a. [Medline] [CrossRef]
Shi Y, Tu Y, Mecham RP, and Bassnett S. Ocular phenotype of Fbn2-null mice. *Invest Ophthalmol Vis Sci*. **54**: 7163–7173. 2013b. [Medline] [CrossRef]
Shibuya K, Satou K, Sugimoto K, *et al.* (1999) Background data on spontaneous ophthalmic lesions in Crj:CD(SD)IGS rats. In: Biological Reference Data on CD(SD) IGS Rats. T Matsuzawa, H Inoue (eds). Tokyo, Best Printing Company. 60–62.
Silvotti L, Cavalca E, Gatti R, Percudani R, and Tirindelli R. A recent class of chemosensory neurons developed in mouse and rat. *PLoS ONE*. **6**: e24462. 2011. [Medline] [CrossRef]
Smith PM, and Jeffery ND. Histological and ultrastructural analysis of white matter damage after naturally-occurring spinal cord injury. *Brain Pathol*. **16**: 99–109. 2006. [Medline] [CrossRef]
Smith RS, Hawes NL, Kuhlmann SD, Heckenlively JR, Chang B, Roderick TH, and Sundberg JP. Corn1: a mouse model for corneal surface disease and neovascularization. *Invest Ophthalmol Vis Sci*. **37**: 397–404. 1996a. [Medline]
Smith RS, John SWM, Nishina PM. (2002). Posterior segment and orbit. In: Systematic Evaluation of the Mouse Eye: Anatomy, Pathology, and Biomethods. RS Smith, SWM John, PM Nishina, JP Sundberg (eds). Boca Raton, Florida, CRC Press.
Smith RS, Montagutelli X, Sundberg JP. (1996b) Ulcerative blepharitis in aging inbred mice. In: Pathobiology of the Aging Mouse. U Moh, DL Dungworth, CC Capen, WW Carlton, JP Sundberg, JM Ward (eds). Vol. 2, ILSI Press, Washington. 139–152.
Smith RS, Sundberg JP, John SWM. (2002a) Cornea of the Mouse. In: Systematic Evaluation of the Mouse Eye: Anatomy, Pathology, and Biomethods. RS Smith, SWM John, PM Nishina, JP Sundberg (eds). CRC Press, Boca Raton, Florida. 3–21.
Smith RS, Sundberg JP, John SWM. (2002b) The Anterior Segment. In: Systematic Evaluation of the Mouse Eye: Anatomy, Pathology, and Biomethods. RS Smith, SWM John, PM Nishina, JP Sundberg (eds). CRC Press, Boca Raton, Florida. 111–159.
Smith RS, Roderick TH, and Sundberg JP. Microphthalmia and associated abnormalities in inbred black mice. *Lab Anim Sci*. **44**: 551–560. 1994. [Medline] [CrossRef]
Song JY, Park R, Kim JY, Hughes L, Lu L, Kim S, Johnson RL, and Cho SH. Dual function of Yap in the regulation of lens progenitor cells and cellular polarity. *Dev Biol*. **386**: 281–290. 2014. [Medline] [CrossRef]
Sonoda KH, Sakamoto T, Qiao H, Hisatomi T, Oshima T, Tsutsumi-Miyahara C, Exley M, Balk SP, Taniguchi M, and Ishibashi T. The analysis of systemic tolerance elicited by antigen inoculation into the vitreous cavity: vitreous cavity-associated immune deviation. *Immunology*. **116**: 390–399. 2005. [Medline] [CrossRef]
Soucy ER, Albeanu DF, Fantana AL, Murthy VN, and Meister M. Precision and diversity in an odor map on the olfactory bulb. *Nat Neurosci*. **12**: 210–220. 2009. [Medline] [CrossRef]

Spit BJ, Bretschneider F, Hendriksen EGJ, and Kuper CF. Ultrastructure of free nerve endings in respiratory and squamous epithelium on the rat nasal septum. *Cell Tissue Res*. **274**: 329–335. 1993. [Medline] [CrossRef]

St Clair MGB, and Morgan KT. (1992) Changes in the upper respiratory tract. In: Pathology of the Aging Rat. U Mohr, DL Dungworth, CC Capen (eds). International Life Sciences Institute Press, Washington, DC. 111-127.

Stahl A, Connor KM, Sapieha P, Chen J, Dennison RJ, Krah NM, Seaward MR, Willett KL, Aderman CM, Guerin KI, Hua J, Löfqvist C, Hellström A, and Smith LE. The mouse retina as an angiogenesis model. *Invest Ophthalmol Vis Sci*. **51**: 2813–2826. 2010. [Medline] [CrossRef]

Steinbach E, and Grüninger G. Experimental production of cholesteatoma in rabbits by using non-irritants (skin tolerants). *J Laryngol Otol*. **94**: 269–279. 1980. [Medline] [CrossRef]

Stewart HL, Dunn TB, Snell KC, *et al.* (1979) Tumors of the respiratory tract. In: Pathology of Tumors in Laboratory Animals. VS Turusov (ed). Vol. II, IARC Scientific Publication, Lyon. 251–252.

Storan MJ, and Key B. Septal organ of Grüneberg is part of the olfactory system. *J Comp Neurol*. **494**: 834–844. 2006. [Medline] [CrossRef]

Streilein JW. Ocular immune privilege: therapeutic opportunities from an experiment of nature. *Nat Rev Immunol*. **3**: 879–889. 2003. [Medline] [CrossRef]

Su CY, Menuz K, and Carlson JR. Olfactory perception: receptors, cells, and circuits. *Cell*. **139**: 45–59. 2009. [Medline] [CrossRef]

Suzukawa K, Kondo K, Kanaya K, Sakamoto T, Watanabe K, Ushio M, Kaga K, and Yamasoba T. Age-related changes of the regeneration mode in the mouse peripheral olfactory system following olfactotoxic drug methimazole-induced damage. *J Comp Neurol*. **519**: 2154–2174. 2011. [Medline] [CrossRef]

Suzuki Y. Cell death, phagocytosis, and neurogenesis in mouse olfactory epithelium and vomeronasal organ after colchicine treatment. *Ann N Y Acad Sci*. **855**: 252–254. 1998. [Medline] [CrossRef]

Switzer 3rd RC. Application of silver degeneration stains for neurotoxicity testing. *Toxicol Pathol*. **28**: 70–83. 2000. [Medline] [CrossRef]

Tanaka K, Inagaki S, and Doi K. Preretinal arteriolar loops in rats. *Lab Anim Sci*. **44**: 71–72. 1994. [Medline]

Tanaka K, Inagaki S, Kemi M, *et al.* Lens Luxation in Rats. *J Toxicol Pathol*. 1995; 8: 161-163. [CrossRef]

Tanaka K, Inagaki S, Matsumoto H, Ikemoto F, and Doi K. Posterior lens rupture in rats. *Toxicol Pathol*. **24**: 639–641. 1996. [Medline] [CrossRef]

Tanaka K, Inagaki S, Ohmori R, *et al.* Focal chorioretinal atrophy in rats. *J Toxicol Pathol*. 1993; 6: 205-211. [CrossRef]

Taradach C, Greaves P. Spontaneous eye lesions in laboratory animals: incidence in relation to age. *Crit Rev Toxicol*. **12**: 121–147. 1984. [Medline] [CrossRef]

Taradach C, Regnier B, and Perraud J. Eye lesions in Sprague-Dawley rats: type and incidence in relation to age. *Lab Anim*. **15**: 285–287. 1981. [Medline] [CrossRef]

Taylor AW. Ocular immune privilege. *Eye (Lond)*. **23**: 1885–1889. 2009. [Medline] [CrossRef]

Taylor AW, and Kaplan HJ. Ocular immune privilege in the year 2010: ocular immune privilege and uveitis. *Ocul Immunol Inflamm*. **18**: 488–492. 2010. [Medline] [CrossRef]

Teixeira LBC, Dubielzig RR. (2013a) The Eye. In: Haschek and Rousseaux's Handbook of Toxicologic Pathology. WM Haschek, CG Rousseaux, AA Walling (eds). Elsevier, London, UK. 2095–2185.

Teixeira LBC, Dubielzig RR. (2013b) Uvea and Filtration Apparatus. In: Haschek and Rousseaux's Handbook of Toxicologic Pathology. WM Haschek, CG Rousseaux, AA Walling (eds). Elsevier, London, UK. 2135–2143.

Tian H, and Ma M. Molecular organization of the olfactory septal organ. *J Neurosci*. **24**: 8383–8390. 2004. [Medline] [CrossRef]

Tizzano M, Cristofoletti M, Sbarbati A, and Finger TE. Expression of taste receptors in solitary chemosensory cells of rodent airways. *BMC Pulm Med*. **11**: 3. 2011. [Medline] [CrossRef]

Toyran S, Lin AY, and Edward DP. Expression of growth differentiation factor-5 and bone morphogenic protein-7 in intraocular osseous metaplasia. *Br J Ophthalmol*. **89**: 885–890. 2005. [Medline] [CrossRef]

Ueda J, Sawaguchi S, Hanyu T, Yaoeda K, Fukuchi T, Abe H, and Ozawa H. Experimental glaucoma model in the rat induced by laser trabecular photocoagulation after an intracameral injection of India ink. *Jpn J Ophthalmol*. **42**: 337–344. 1998. [Medline] [CrossRef]

Uraih LC, and Maronpot RR. Normal histology of the nasal cavity and application of special techniques. *Environ Health Perspect*. **85**: 187–208. 1990. [Medline] [CrossRef]

Van Winkle TJ. (1991) Cornea Opacities, Spontaneous, Mouse. In: Monographs on Pathology of Laboratory Animals. TC Jones, U Mohr, RD Hunt (eds). Berlin, Springer-Verlag. 21–25.

Verdaguer JM, Trinidad A, González-García JA, García-Berrocal JR, and Ramírez-Camacho R. Spontaneous otitis media in Wistar rats: an overlooked pathology in otological research. *Lab Anim (NY)*. **35**: 40–44. 2006. [Medline] [CrossRef]

Wässle H, and Boycott BB. Functional architecture of the mammalian retina. *Physiol Rev*. **71**: 447–480. 1991. [Medline] [CrossRef]

Wagner JG, Harkema JR, Jiang Q, Illek B, Ames BN, and Peden DB. Gamma-tocopherol attenuates ozone-induced exacerbation of allergic rhinosinusitis in rats. *Toxicol Pathol*. **37**: 481–491. 2009. [Medline] [CrossRef]

Ward JM, Yoon M, Anver MR, Haines DC, Kudo G, Gonzalez FJ, and Kimura S. Hyalinosis and Ym1/Ym2 gene expression in the stomach and respiratory tract of 129S4/SvJae and wild-type and CYP1A2-null B6, 129 mice. *Am J Pathol*. **158**: 323–332. 2001. [Medline] [CrossRef]

Weiler E. Postnatal development of the rat vomeronasal organ. *Chem Senses*. **30**(Suppl 1): i127–i128. 2005. [Medline] [CrossRef]

Weiler E, and Farbman AI. The septal organ of the rat during postnatal development. *Chem Senses*. **28**: 581–593. 2003. [Medline] [CrossRef]

Weisse I. (1993) Aging and ocular changes. In: Pathogiology of the Aging Rat. U Mohr, DL Dunworth, CC Capen (eds). Vol. 2, ILSI press, Washington, DC. 65–89.

Westwood FR, Iswaran TJ, and Greaves P. Long-term effects of an inotropic phosphodiesterase inhibitor (ICI 153,110) on the rat salivary gland, harderian gland, and intestinal mucosa. *Toxicol Pathol*. **19**: 214–223. 1991. [Medline] [CrossRef]

Wilkerson CL, Syed NA, Fisher MR, Robinson NL, Wallow IH, and Albert DM. Melanocytes and iris color. Light microscopic findings. *Arch Ophthalmol*. **114**: 437–442. 1996. [Medline] [CrossRef]

Williams D. Rabbit and Rodent Ophthalmology. *Eur J Companion Anim Pract*. 2007; 17: 242-252.

Williams DL. Ocular disease in rats: a review. *Vet Ophthalmol*. **5**: 183–191. 2002. [Medline] [CrossRef]

Wine JJ. *The inexhaustible mouse nose*. Focus on olfactory epithelia exhibit progressive functional and morphological defects in CF mice. *Am J Physiol Cell Physiol*. **293**: C537–C539. 2007; . [Medline] [CrossRef]

Worst JGF, and Los LI. Comparative anatomy of the vitreous body in rhesus monkeys and man. *Doc Ophthalmol*. **82**: 169–178. 1992. [Medline] [CrossRef]

Woutersen RA, Kuper CF, Slootweg PJ. (2010) Chronic tissue changes and carcinogenesis in the upper airway. Chapter 18. In: Toxicology of the Nose and Upper Airways. JB Morris, DJ Shusterman (eds). Informa Health Care. 272–297.

Yokosuka M. Histological properties of the glomerular layer in the mouse accessory olfactory bulb. *Exp Anim*. **61**: 13–24. 2012. [Medline] [CrossRef]

Yoshitomi K, Boorman GA. (1990) Eye and associated glands. In: Pathology of the Fischer Rat. Reference and Atlas. GA Boorman, SL Eustis, MR Elwell, CA Montgomery, Jr, WF MacKenzie (eds). Academic Press, San Diego New York London. 239–260.

Yoshitomi K, and Boorman GA. Intraocular and orbital malignant schwannomas in F344 rats. *Vet Pathol*. **28**: 457–466. 1991a. [Medline] [CrossRef]

Yoshitomi K, and Boorman GA. Spontaneous amelanotic melanomas of the uveal tract in F344 rats. *Vet Pathol*. **28**: 403–409. 1991b. [Medline] [CrossRef]

Yoshitomi K, and Boorman GA. Inverted mucoepidermoid papilloma and mucous cell adenocarcinoma of the palpebral conjunctiva in two F344 rats. *Vet Pathol*. **31**: 254–258. 1994. [Medline] [CrossRef]

Yoshitomi K, Everitt JI, and Boorman GA. Primary optic nerve meningiomas in F344 rats. *Vet Pathol*. **28**: 79–81. 1991. [Medline] [CrossRef]

Young C, Festing MF, and Barnett KC. Buphthalmos (congenital glaucoma)

in the rat. *Lab Anim*. **8**: 21–31. 1974. [Medline] [CrossRef]

Zabka TS, Singh J, Dhawan P, Liederer BM, Oeh J, Kauss MA, Xiao Y, Zak M, Lin T, McCray B, La N, Nguyen T, Beyer J, Farman C, Uppal H, Dragovich PS, OBrien T, Sampath D, and Misner DL. Retinal toxicity, in vivo and in vitro, associated with inhibition of nicotinamide phosphoribosyltransferase. *Toxicol Sci*. **144**: 163–172. 2015. [Medline] [CrossRef]

Zampighi GA, Zampighi L, and Lanzavecchia S. The three-dimensional distribution of αA-crystalline in rat lenses and its possible relation to transparency. *PLoS ONE*. **6**: e23753. 2011. [Medline] [CrossRef]

Zeiss CJ. Animals as models of age-related macular degeneration: an imperfect measure of the truth. *Vet Pathol*. **47**: 396–413. 2010. [Medline] [CrossRef]

Zhao F, Gandorfer A, Haritoglou C, Scheler R, Schaumberger MM, Kampik A, and Schumann RG. Epiretinal cell proliferation in macular pucker and vitreomacular traction syndrome: analysis of flat-mounted internal limiting membrane specimens. *Retina*. **33**: 77–88. 2013; . [Medline] [CrossRef]

Zieske JD. Corneal development associated with eyelid opening. *Int J Dev Biol*. **48**: 903–911. 2004. [Medline] [CrossRef]